School of Molecular and Cell Biology
University of the Witwatersrand
Johannesburg

MICRO ANALYTICAL OBSERVATION OF ELEMENTAL DISTRIBUTION IN ARBUSCULAR MYCORRHIZAL (AM) ROOTS FROM MINING SITES IN SOUTH AFRICA AND IDENTIFICATION OF THEIR AM FUNGI

BY

MTUTUZELI ZAMXAKA

Submitted: **10 August 2016**

A thesis submitted to the Faculty of Science, University of the Witwatersrand, Johannesburg,
in fulfilment of the requirements for the degree of
Doctor of Philosophy
Johannesburg, 2016

Declaration

I, **MTHUTHUZELI ZAMXAKA**, am a student registered for the degree of Doctor of Philosophy to the University of the Witwatersrand, Johannesburg in the academic year 2016.

I hereby declare the following:

- I am aware that plagiarism (the use of someone else's work without their permission and/or without acknowledging the original source) is wrong.
- I confirm that the work submitted for assessment for the above degree is my own unaided work except where explicitly indicated otherwise and acknowledged.
- I have not submitted this work before for any other degree or examination at this or any other University.
- The information used in the Thesis **HAS** been obtained by me while employed by, or working under the aegis of, any person or organisation other than the University.
- I have followed the required conventions in referencing the thoughts and ideas of others.
- I understand that the University of the Witwatersrand may take disciplinary action against me if there is a belief that this is not my own unaided work or that I have failed to acknowledge the source of the ideas or words in my writing.

……..……

(Signature of candidate)

10th day of August 2016

Abstract

South Africa, as one of the leaders in mining industry, due to the variety and quantity of minerals produced, has been and is still producing a number of mine tailings which are contaminated by heavy metals. Heavy metals are very harmful to plants and especially to human beings and animals due to their non-biodegradable nature. The problem of environmental metal pollution could be combated by the establishment of Arbuscular Mycorrhiza (AM) vegetation on the surface of mine tailings. Besides the toxicity of the substrate, such areas usually lack essential nutrients (mainly N, P, and K) and organic matter. AM fungi contribute to soil structure by forming micro- and macro- soil aggregates within the net of external hyphae. Their presence may reduce stress caused by lack of nutrients or organic matter and increase plant resistance to pathogens, drought and heavy metals. Therefore, mycorrhizal fungi may become the key factor in successful plant revegetation of heavy-metal-polluted areas by promoting the success of plant establishment and increasing soil fertility and quality.

The aim of this project was to identify AM fungi from a number of heavy metal sites in South Africa using both morphological and molecular techniques, followed by the evaluation of heavy metal distribution and localisation in mycorrhizal roots. Soil samples were collected from three different provinces, namely: Gauteng, Mpumalanga and North West provinces. The sites were selected based on their historical and current heavy metal contamination. Indigenous AM fungal isolates (which are adapted to local soil conditions) can stimulate plant growth better than non-indigenous isolates. AM fungal spores were isolated from 100g of representative soil sample by the wet sieving and decanting method, followed by assessment of spore numbers and infective propagules. The spores of a subset of the pot samples were mounted on microscope slides in polyvinyl lactic acid glycerol and identified by morphological characteristics to the level of genus or species. Most of the spores counted were observed in a 45 µm sieve. These spores were tiny and had different sizes, colours and shapes. The majority of the observed spores were small, brown

and oval in shape. For morphological identification, plant roots were stained and hyphae were found to be the most abundant in roots.

For molecular identification, two sets of nested PCR primers, namely NS1 & NS4 coupled with AML1 & AML2, were employed in this study due to their ability to amplify all subgroups of arbuscular mycorrhizal fungi (AM fungal, Glomeromycota), while excluding sequences from other organisms. Through both morphological characteristics and molecular identification, the following fungal genera were identified for the first time in the studied sites in South Africa. The study identified a total of 14 AM fungal genera and 55 AM fungal species, which are: *Glomus (15), Acaulospora (11), Scutellospora (6), Gigaspora (6), Rhizophagus (3), Funneliformis (3), Archaeospora (2), Claroideoglomus (2), Ambispora (2), Sclerocystis (1), Fuscutata (1), Entrophospora (1), Diversispora (1), Paraglomus (1).* Both *Glomus* and *Acualospora* have been observed to be the highest occurring genera in the analysed soil samples, followed by *Scutellospora* and *Gigaspora* and others mentioned.

PIXE technique was successful in localising elemental concentration in both plant roots and AM fungal structures, as well as in indicating the large vesicles in root tissue. AM fungal structures in the outer cortex or outer epidermal layer of the root cross-sections were observable, as shown by the more significantly enriched Si in the vesicles and arbuscules. Distinctive elemental maps can be used to localise sites of colonisation and verification of the symbiotic nature of the tissue. This indicates that a range of metals can be sequestered in AM fungal structures above levels in surrounding host root tissue, and demonstrates the potential of Micro-PIXE to determine metal accumulation and elemental distribution in mycorrhizal plant roots and inter-and intracellular AM fungal structures.

This research highlights the potential of AM fungi for inoculation of plants as a prerequisite for successful restoration of heavy metal contaminated soils. It also illustrates the importance of AM fungal diversity in selected high heavy metal

(HM) sites in RSA, particularly in the North West and the Gauteng gold mining slime dams. Therefore, phytoremediation of mine tailings by mycorrhizal plants seems to be one of the most promising lines of research on mine tailings contamination by heavy metals. The strategies which evolved during this project have great potential for phytoremediation of toxic mining sites, and thus can help mitigate the environmental problems, especially in the mining waste sites.

Dedication

I lovingly dedicate my thesis to my Heavenly Father, my Creator, for making all things possible for me; my family especially my wife, Vathiswa Papu-Zamxaka for her love and encouragement and support; my beautiful daughters, Kungawo Dioko and Bulumko Angel Zamxaka for their help in sorting Daddy's study room;

My parents, starting with my late father Mzimkhulu Zamxaka who passed away waiting for the degree and my mother, Nozuku Zamxaka for her continuous love and dedication to our family.

Acknowledgements

Firstly, I must give my sincere gratitude to the Almighty God for having given me the wisdom, courage and strength to see this study into completion. I thank my Lord Jesus Christ for his grace that kept me in faith despite the storms of life. To my Heavenly Father be the glory, for the great things he has done and he keeps doing.

Special thanks go to my wife, children, family and friends, their love, prayers and unending support that kept me going through the hardest of times. I promise that the sleeping in the lab is now over.

I would like to extend my sincere gratitude to Prof. Colin Straker, my supervisor for his advice, encouragement, patience and support throughout this long journey and for giving me the opportunity to improve my scientific knowledge through workshops, seminars and conferences.

My gratitude also goes to Dr Wojciech J. Przybylowicz and Dr Jolanta Mesjasz-Przybylowicz from iThemba LABS for their assistance during the Micro-PIXE measurements and analysis.

Many thanks also go to Ms Isabel Weiersbye (APES, Wits University) for the valuable information provided, for her contribution during the different sampling

campaigns and for the financial support. Not to forget Ms Alexandra Wald, Shena Kennedy and Dr Sashnee Raja also from APES, Wits University, for thier great assistance in the preparation of the thesis before it was printed and submitted. I would like to also thank my high school teachers from Tyali Senior Secondary School, Mr. S Ntakana (Principal) Mr and Mrs Babushe (Maths, Physics and Biology) as well as Ms Qaba (isiXhosa) for seeing potential in me while I was still at High School.

Special thanks go to Prof Helder M Marques, the Dean of the Faculty of Science for allowing my PhD to be submitted for examination.

I am grateful to the Ford Foundation for providing the funds for this study. I am also thankful to the National Research Foundation (NRF), THRIP and Wits Post Grad Award for funding as well as AngloGold Ashanti Limited for allowing us to access their mining sites for sampling. Lastly, I would like to thank the South African Agency for Science and Technology Advancement (SAASTA) for offering me with study leaves to conduct my laboratory experiments and write up.

Key words: arbuscular mycorrhiza, evolutionary history, ribosomal DNA, ribosomal RNA genes, RNA polymerase genes, morphological identification, molecular identification, colonisation, abundance, AM fungal diversity, phytoremediation, Nested PCR, Micro-PIXE, spores, AM fungi, sample sites, mine dumps, mine tailings, Heavy Metal, PIXE, ICPMS, PCA and Shannon-Weaver.

Table of contents

List of Figures

List of Tables

Abbreviation and Glossary:

Background AM fungi plus additional mixture of indigenous AM fungal spore inoculum: This is an experimental pot with slime soil samples that has been treated with Previcur® N aqueous fungicide (AgrEvo South Africa) and with the addition of indigenous AM fungal spore inoculum.

Background arbuscular mycorrhizal fungi only: This is an experimental pot with slime soil samples that has been treated with the Previcur® N aqueous fungicide (AgrEvo South Africa) with no additional spores.

Biogenic metals: Substances produced by living organisms or biological processes.

Bushveld Igneous Complex: The Bushveld Igneous Complex is a large layered igneous intrusion within the Earth's crust which has been tilted and eroded and now outcrops around what appears to be the edge of a great geological basin, the Transvaal Basin.

Chalcophilic: Sulphur-Loving.

Control 1 – Plants were grown in nutrient solution and Zeolite + Sand

Control 2 – Plants were grown in nutrient solution and Zeolite + Sand and Mycoroot.

Detrital bonds: Loose fragments or grains that have been worn away from the rock.

Dolomite /ˈdɒləmaɪt/ is an anhydrous carbonate mineral composed of calcium magnesium carbonate, ideally $CaMg(CO_3)_2$. The word **dolomite** is also used to describe the sedimentary carbonate rock, which is composed predominantly of the mineral **dolomite** (also known as dolostone).

DRDGOLD: It is a gold tailings retreatment company with a huge footprint. DRDGOLD Limited (DRDGOLD) is a medium-sized, unhedged gold producer with investments in South Africa and Australia. More gold ‘factory’ than mining company, a rising gold price and advances in technology over the years has made the extraction of smaller and smaller particles of gold viable. Until recently, DRDGOLD operated four metallurgical plants, two of which were approaching maturity. The flagship plant in Brakpan, possibly the largest in the world and with

the required treatment capacity, was well-positioned to take over but was located up to 50km from many of the slime dams and sand dumps in the west, earmarked for future retreatment.

Environmental pollutant: It is a substance or energy introduced into the **environment** that has undesired effects, or adversely affects the usefulness of a resource.

Exchangeable concentration of the element: is the process whereby elemental ions buffer the medium, solution or refers to elements that can be used interchangeable between the objects such as plants and fungi**.**

Extractable concentration of the element: refers to elements that can be extracted or assimilated or absorbed by plants from the soil. It is an available concentration of the element to the plant.

Gabbro: (Geology) A dark, coarse-grained igneous rock, consisting of the mineral calcium-feldspar and crystals of the pyroxene group (olivine may be present). It is the plutonic equivalent of basalt and dolerite.

Heavy Metals (HM): The term heavy metal in the context of this thesis is appropriate and refers to any metallic chemical element that has a relatively high density and is toxic or poisonous at low concentrations. However, we are aware of the definition heavy metals given by Duffus (2002).

INVAM: International Culture Collection of Arbuscular and (Vesicular) Arbuscular Mycorrhizal Fungi) website, which was created by Professor J. B. Morton of West Virginia University, USA (INVAM). This germplasm resource provides researchers with sets of voucher specimens, namely photographs, slides, vials of intact spores (Pfleger and Linderman, 1994) and this is particularly important for researchers that do not have the facilities or the time to carry out these analyses. As well as vouchers, INVAM maintains a large number of isolates, including those not described (INVAM).

Lithophylic: Rock-loving.

Live root pictures – Are pictures of roots taken by light microscope before treatment, either before the roots were dried or stained.

Mafic: (Geology) pertaining to ferromagnesium minerals (rich in iron and magnesium). It is often used to describe rocks rich in these minerals although, sticky, melanocratic is the correct term (Whitten & Brooks 1972).

Monoxenically: Relating to or being a culture in which one organism is grown or contaminated with only one other organism.

Morphotypes - A group of different types of individuals of the same species in a population.

Murographs: Illustrate organization of discrete morphological characters such as Spore wall (sw), first inner wall (iwl), germinal layer (gl), germ tube (gt), germination shield (gs).

Mycoroot: A commercial inoculum of mycorrhizal seeds manufactured by Mycoroot (Pty.) Ltd. SA (http://www.mycoroot.com).

Ontogeny (also ontogenesis or morphogenesis): is the origination and development of an organism, usually from the time of fertilization of the egg (Embryo) to the organism's mature form (adult). Yet, the term can be used to refer to the study of the entirety of an organism's lifespan.

Previcur® N aqueous fungicide (AgrEvo South Africa): A commercial fungicide for removing non-AMF fungal contamination from the mixture. **Previcur** (active ingredient Propamocarb-HCl): Active against soil parasites such as *Pythium* but affects AMF minimally.

Propagule: A portion of a plant or fungus, such as a seed or spore, from which a new individual may develop. It is any material that is used for the purpose of propagating an organism to the next stage in their life cycle, such as by dispersal.

Serpentine: (Geology) a group of ultramafic rocks (including Hartzburgite, peridotite, phonolite, gabbro and norite) characterized by high magnesium-to-calcium ratios and often high concentration of heavy metals (nickel, chromium, copper).

Siderophilic: Iron-loving.

Ultramafic: - Ultramafic (also referred to as ultrabasic rocks, although the terms are not wholly equivalent) are igneous and meta-igneous rocks with a very low silica content (less than 45%), generally >18% MgO, high FeO, low potassium,

and are composed of usually greater than 90% mafic minerals (dark coloured, high magnesium and iron content). The Earth's mantle is composed of ultramafic rocks. Ultrabasic is a more inclusive term that includes igneous rocks with low silica content that may not be extremely enriched in Fe and Mg, such as carbonatites and ultrapotassic igneous rocks.

List of Acronyms

<	Less than
°E	Degrees East
°S	Degrees South
AC	Arbuscular Colonisation
AM	Arbuscular Mycorrhizal
AML	Primers discovered by *Lee at al.*, 2008.
ANOVA	Analysis of Variance
APS	Ammonium Persulphate
ARD	Acid rock drainage
BLAST	Basic Local Alignment Search Tool
BP	Base Pairs
BS	Backscattering
BSA	Bovine Serum Albumin
C	Carbon
CEC	Cation Exchange Capacity
cm	Centimetre
CRF	Carbon Leader Reef
CTAB	Hexadecyltrimethyl Ammonium Bromide
DGGE	Denaturing Gradient Gel Electrophoresis
dH2O	Distilled And Deionized Water
DMSO	Dimethyl Sulfoxide
DNA	Deoxyribonucleic Acid
dNTP	Deoxyribose Nucleotide Triphosphate
e.g.	For Example
EDTA	Ethylene Diamine Tetra Acetic Acid
ERH	Extraradical Hyphae
FAME	Fatty Acid Methyl Ester
g	Gram
Gd	Gadolinium
HC	Hyphal Colonisation

hr(s)	Hour(s)
i.e.	That is
IAA	Indole Acetic Acid
Ir	Iridium
IRH	Intraradical Hyphae
ITS	Internal Transcribed Spacer
Kb	Kilobase
l/L	Litre
La	Lanthanium
LB	Luria Bertani
M	Micron (10-6)
Mg	Milligram
mg/ml	Milligram/Millilitre
MHB	Mycorrhizal Helper Bacteria
Min(s)	Minute(s)
mM	Milli (10-3) Molar
MPN	Most Probable Number
N	Nitrogen
NCBI	National Centre for Biotechnology Information
nd	Not Detected.
nm	Nanometer
O	Oxygen
P	Phosphorus
Pb	Lead
PCR	Polymerase Chain Reaction
PGPR	Plant Growth Promoting Bacteria
PIXE	Particle-induced x-ray emission
PLFA	Phospholipid Fatty Acid
ppm	Part Per Million
PSB	Phosphate Solubilising Bacteria
R	Correlation coefficients

rDNA	Ribosomal Deoxynucleic Acid
RFLP	Restriction Fragment Length Polymorphism
Rh	Rhodium
RNA	Ribose Nucleic Acid
rpm	Rotation Per Minute
rRNA	Ribosomal Ribonucleic Acid
RSA	Republic of South Africa
SA	South Africa
SDS	Sodium Dodecyl Sulphate
Sec	Seconds
SEM	Standard Error of the Mean
SOM	Soil Organic Matter
sp.	Species (Singular)
spp.	Species (Plural)
SSU	Small Subunit
TAE	Tris-Acetic Acid-EDTA
TBE	Tris-borate-EDTA Buffer
Te	Tellurium
TE	Tris-HCl EDTA
TEMED	Tetramethylethylenediamine
Th	Thorium
Tm	Melting Temperature
T-RFLP	Terminal Restriction Fragment Length Polymorphism
V	Volts
VC	Vesicular Colonisation
VCR	Ventersdorp Contact Reef
Vol/Vol	Volume / Volume
VR	Vaal River
Wt/Vol	Weight / Volume
WW	West Wits
Y	Yttrium

CHAPTER 1

1 INTRODUCTION

Ecosystems have been contaminated with heavy metals (HM) and toxic metals, metalloids and radionuclides such as Arsenic (As), Cadmium (Cd), Chromium (Cr), Copper (Cu), Gold (Au), Lead (Pb), Nickel (Ni), Platinum (Pt), Radon (Ra), Titanium (Ti) Uranium (U), and Zinc (Zn), throughout the world largely by various anthropogenic activities. These metals are commonly called heavy metals, although this term strictly refers to metallic elements with a specific mass higher than 5 g cm^{-3}; which is able to form sulphides (Suruchi and Khanna, 2011; Adriano, 1986). Heavy metals are very harmful to plants and especially to human beings and animals due to their non-biodegradable nature, long biological half lives and their potential to accumulate in different body parts since there is no proper mechanism for their elimination from the body (Suruchi and Khanna, 2011).

In non Heavy Metal (HM) contaminated soils, the concentrations of Zn, Cu, Pb, Ni, Cd and Cr range between 0.0001 and 0.065%, whereas Mn and Fe can reach 0.002% and 10.0%, respectively. With the exception of iron, all heavy metals above a concentration of 0.1% in the soil become toxic to plants and therefore change the community structure of plants in a polluted habitat (Bothe *et al*., 2010). Soils that carry metallophytes (HM resistant plants) can be classified by the content of their main heavy metal. For example, serpentine soils are rich in Ni, seleniferous soils carry Se, calamine soils have Zn as major contaminant and soils of the African copper belt are rich in Cu, Co, Cr, Ni, and Zn (Alford *et al.*, 2010). Some of these metals such as Zn, Cu, Iron (Fe), Manganese (Mn), Cobalt (Co) and Cr are essential elements for many plants, animals and man but at trace levels. At high concentrations, they are all potentially toxic (Nyriagu, 1988; Goyer, 1996). Pb and Cd are generally regarded as toxic elements even at trace levels (Jarup, 2003; Goyer, 1996). Monitoring of these metals in the environment is therefore critical as it gives vital information as to whether exposure concentrations can cause adverse effects especially to humans (Odiyo *et al*., 2005).

The sources of metals in the soil are diverse, including burning of fossil fuels, mining and smelting of metalliferous ores, municipal wastes, fertilizers, pesticides, sewage sludge amendments, the use of pigments and batteries. A large number of these metals come from mining operations, industrial manufacturing facilities, recycling plants, and solid waste disposal sites. Military munitions are also major worldwide sources of groundwater and soil heavy metal contaminants, which wind or rain can sometimes disperse great distances from their point of use or disposal (Song *et al.*, 2003).

Heavy metals cannot be chemically degraded and need to be physically removed or be immobilized (Kroopnick, 1994). Traditional methods of removing heavy metals from soil and water are expensive and laborious, and often disrupt the environment. Remediation of heavy metal contaminated soils involves either on-site management or excavation, and subsequent disposal to a landfill site (Parker, 1994). However, this method of disposal merely shifts the contamination problem elsewhere along with the hazards associated with transportation of contaminated soil and migration of contaminants from landfill into an adjacent environment (Williams, 1998). Therefore, sustainable on-site techniques for remediation of heavy metal contaminated sites need to be developed. South Africa is a developing country with intensive mining and agricultural activities and the concomitant production of toxic wastes in the form of tailings and contaminated ground water. Hence legislation requires the rehabilitation of mine wastes primarily through revegetation (Fourie *et al*., 2008).

The most effective suggested approach to reclaim the land contaminated by heavy metal concentrations is the use of vegetation for landscaping, stabilization and pollution control (Robinson *et al*., 2007; Bolan *et al*., 2011). An emerging technology that should be considered for remediation of contaminated sites because of its cost effectiveness, aesthetic advantages, and long-term applicability is phytoremediation (Kumar *et al*., 1995; Meier *et al.*, 2011). Phytoremediation, the use of plants to remediate or clean-up contaminated soils can be used as a

promising method to remove and/or stabilize soils contaminated with heavy metals (Zak and Parkinson, 1982; Lone *et al*., 2008). Phytoremediation can be further developed by utilizing mycorrhizal fungi since they can bind metals and reduce their translocation to the shoots (Gohre and Paszkowski, 2006).

Arbuscular mycorrhizal (AM) fungi occur in almost all habitats and form mycorrhizas with plant roots thereby contributing positively to plant growth. A number of research findings have been reported to demonstrate the potential use of AM fungi in improving agricultural yield and in the remediation of heavy metal contaminated mining sites. Wang *et al*. (2011) for instance, showed a promising potential of AM fungi for enhancing vegetable production and reducing organophosphorus pesticide residues in plant tissues and their growth media, as well as for the phytoremediation of organophosphorus pesticide-contaminated soils. Furthermore, the fungi can accelerate the revegetation of severely degraded lands such as coal mines or waste sites containing high levels of heavy metals (Marx and Altman, 1979; Meier *et al*., 2012). Their diversity and abundance is affected by heavy metal concentrations in soil, but they in turn influence the availability of metals in soil either directly by uptake or indirectly through their effect on plant growth, root exudation, and rhizosphere chemistry (Hetrick *et al*., 1994). Moreover, the contribution of mycorrhizal symbionts to soil productivity and enhanced heavy metal uptake has not been seriously investigated in developing countries and there is a vast potential to utilize mycorrhizal plants to rehabilitate polluted sites.

The present study is focused on the mechanisms of tolerance and accumulation of toxic and heavy metals/metalloids/radionuclides in roots of plants growing on mining waste sites. More specifically the study is looking at the ability of the AM fungi growing in the plant roots to tolerate and accumulate these metals. The study attempts to localise heavy metals such as Cr, Ti, Ni, U, Pt, Cu, Zn and other elements such as K, P, S, and Ca in plant root samples colonised by AM fungi by microanalytical techniques, and to identify the fungi from spore samples.

CHAPTER 2

2 LITERATURE REVIEW

2.1 Methods of toxic and heavy metal remediation using plants

Remediation is a process that is taking action to reduce, isolate, or remove contamination from an environment with the goal of preventing exposure to people, animals and plants (Mulligan *et al.,* 2001). Examples include dredging to remove contaminated sediment, or capping to prevent contaminated sediment from contacting benthic (Sea or Lake Bottom) organisms. Most of the conventional remedial technologies such as leaching of pollutant, electrokinetical treatment (Gonzini *et al.,* 2010), excavation and off-site treatment are expensive and technically limited to relatively small areas (Barceló and Poschenrieder, 2003). Each of the conventional remediation technology has both benefits and limitations (EPA, 1997; MADEP, 1993). Bioremediation is one of the remediation processes which is difined as the use of living organisms such as micro-organism or plants for the recovery/ cleaning up of a contaminated medium like soil, sediment, air and water. The process of bioremediation might involve introduction of new organisms to a site, or the adjustment of environmental conditions to enhance degradation rates of indigenous species.

Phytoremediation is the use of vegetation for *in-situ* treatment of contaminated soils, sediments, and water. It is best applied at sites with shallow contamination of organic, nutrient, or metal pollutants (Meier *et al.,* 2011). It is an emerging technology that should be considered for remediation of contaminated sites because of its cost effectiveness, aesthetic advantages, and long-term applicability (Kumar *et al*., 1995). Phytoremediation makes use of the unique, selective and inherent capabilities of plant root systems, including the translocation, bioaccumulation and pollutant storage/degradation abilities of the entire plant body (Hooda *et al*., 2007).

Some plants which grow on metalliferous soils have developed the ability to accumulate massive amounts of the indigenous metals in their tissues (shoots and

roots) without exhibiting symptoms of toxicity (Baker *et al.,* 1991; Entry *et al.,* 1999). Chaney (1983) was the first to suggest using these "hyperaccumulators" for the phytoremediation of metal polluted sites. However, hyperaccumulators were later believed to have limited potential in this area because of their small size and slow growth, which limit the speed of metal removal (Cunningham *et al.,* 1995).

Phytoremediation is well-suited for use at very large field sites where other methods of remediation are not cost-effective or practicable (Das and Maiti, 2008) at sites with low concentrations of contaminants where only "polishing treatment" is required over long periods of time; and in conjunction with other technologies where vegetation is used as a final cap and closure of the site. There are limitations to the technology that need to be considered carefully before it is selected for site remediation. These include limited regulatory acceptance, long duration of time sometimes required for clean-up to below action levels, potential contamination of the vegetation and food chain, and difficulty establishing and maintaining vegetation at some toxic waste sites (Kumar *et al*., 1995). However, as phytoremediation is a slow process, improvement of efficiency and thus increased stabilization or removal of heavy metals (HM)s from soils is an important goal (Prasad and Freitas, 2003). Phytoremediation is a type of bioremediation that uses plants and is often proposed for bioaccumulation of metals, although there are many other different types. About four types of phytoremediation namely: Phytoextraction, Rhizofiltration, Phytostabilization and Phytotransformation are discussed below.

2.1.1 Phytoextraction

Phytoextraction is defined as the uptake and concentration of substances from the environment into the plant biomass. Phytoextraction is also known as phytoaccumulation, phytoabsorption and phytosequestration (Mukhopadhyay *et al.,* 2010). It can be categorized into two types, namely continuous and induced phytoextraction (Salt *et al.,* 1998). Continuous phytoextraction makes use of plant hyperaccumulators, which accumulate high levels of the toxic contaminants

throughout their lifetime, while induced phytoextraction is activated by the addition of chelators or accelerants to the soil which in turn enhances the toxin accumulation at a single time point (Mukhopadhyay *et al.,* 2010).

The objective of this approach is to use a metal-accumulating plant producing enough biomass in the field to remove metals from the soil (Evangelou *et al.*, 2007). Most of the wild metal accumulators belong to the family Brassicaceae, such as *Thlaspi caerulescens*, which are non-mycorrhizal plants. However, since these plants produce little biomass, other plants like *Larix* have been considered (Landberg and Greger, 1997). A good example is the use of the nickel hyperaccumulator *Berkheya coddii* to decontaminate land near the Rustenburg smelter (South Africa) in the late 1990s. The nickel uptake was 2-3% by mass of dried plant. Ashes of dried plants, containing about 15% by mass, were added to the bulk metal ore and returned to the smelter (Landberg and Greger, 1997).

2.1.2 Rhizofiltration

Rhizofiltration, also known as phytofiltration refers to the use of plant roots to absorb, concentrate, and precipitate toxic metals from contaminated groundwater (Ignatius *et al.,* 2014). Initially, suitable plants with stable root systems are supplied with metal contaminated water to acclimate the plants. These plants are then transferred to the contaminated site to collect the contaminants, and once the roots are saturated, they are harvested (Salt *et al*., 1995). Rhizofiltration allows *in-situ* treatment, minimizing disturbance to the environment (Raskin *et al*., 1994). Rhizofiltration has been reported to be cost-competitive technology in the treatment of surface water or groundwater containing low, but significant concentrations of heavy metals such as Cr, Pb, and Zn (Kumar *et al.,* 1995b; Ensley, 2000), therefore making it a promising alternative amongst the conventional clean-up methods (Prasad and Freitas, 2003).

2.1.3 Phytostabilization

Phytostabilization is a process which reduces the mobility of substances in the environment, for example by limiting the leaching of substances from the soil. The principle of the phytostabilization method is to promote plant growth to reduce or eliminate the bioavailability of metals, minimize wind and water erosion, improve soil quality (organic matter content in particular) and to reduce leaching of metals. Unlike other phytoremediative techniques, the goal of phytostabilization is not to remove metal contaminants from a site, but rather to stabilize them and reduce the risk to human health and the environment (Prasad and Freitas, 2003). Treatments include appropriate fertilization, either a reduction of metal availability using different amendments and/or using metal-tolerant plant species. Various grasses such as *Agrostis tenuis* and *Festuca rubra* have been used commercially (Salt *et al*., 1995; Van Tichelen *et al*., 1996). Phytostabilization is, however, a temporary solution, since the metals are not eliminated and there is a risk, increasing with time, of metal mobilization in the rhizosphere and of metal transfer from plants to animals. For these reasons, phytostabilizing plants should also immobilize metals in the roots and have low shoot accumulation (Berti and Cunningham, 2000).

2.1.4 Phytotransformation

Phytotransformation is defined as a chemical modification of environmental pollutants as a direct result of plant metabolism, often resulting in their inactivation, degradation (phytodegradation) or immobilization (phytostabilization) (Gao *et al.*, 2000). In the case of organic pollutants, such as pesticides, explosives, solvents, industrial chemicals, and other xenobiotic substances, certain plants, such as Cannas, render these substances non-toxic by their metabolism. In other cases, microorganisms living in association with plant roots may metabolize these substances in soil or water (Nzengung *et al*., 1999).

2.2 Mycorrhizal fungi

Mycorrhizal fungi are soil microorganisms that establish mutual symbioses with the majority of higher plants, providing a direct physical link between soil and plant roots (Barea and Jeffries, 1995). They establish an intimate association with the roots of most land plants in which the fungi supply mineral nutrients from the soil while acquiring carbon compounds from the photosynthetic host (Smith and Smith, 2011). About seven kinds of mycorrhiza are recognized in the scientific literature. The type of mycorrhiza formed can be influenced by the identity of both plant and fungus. For example, the same fungus can form arbutoid (monotropoid) and ectomycorrhizas, or ecto and ectondomycorrhizas, or ecto- and orchid mycorrhizas, depending on the identity of the plant associate, so that there is a plexus of behaviour amongst the species of plant and the septate fungi with regard to mycorrhizal structures that they produce (Izzo *et al*., 2005).

A most familiar type of mycorrhiza is the ectomycorrhiza (ECM) in which the fungus penetrates the root but not the root cells. Ectomycorrhizas also called ectotrophic mycorrhizas are characteristic of mainly forest trees in the cooler parts of the world, such as, pines, spruces, firs, oaks, birches in the Northern Hemisphere and eucalypts in Australia and in South Africa (Roman *et al*., 2005). The fungi are commonly known to form mushrooms or truffles. Ectendomycorrhiza is one type that is closely related to ECM, in which the fungus enters the root cells. Ectendomycorrhizas usually possess a well-developed Hartig net with the sheath being reduced or absent, but hyphae penetrate into the cells of the plant (Read, 1998).

Arbutoid mycorrhizas are formed in association with manzanita, madrone, and some other plants. Arbutoid mycorrhizas possess a sheath, external hyphae and usually, a well-developed Hartig net. In addition, there is extensive intracellular development of hyphal coils in the plant cells. These look like ECM and have similar fungi, but are technically endomycorrhizas. A separate but apparently related category is monotropoid, found on certain plants without chlorophyll.

While these traditionally have been called "saprophytic," it turns out that they share a mycorrhizal fungus with a nearby tree, and they are in effect parasites of the tree by way of the mycorrhizal fungus. The Ectomycorrhizas, Ectondomycorrhizas and Arbutoid mycorrhizas have several features in common (Smith and Read, 1997).

Ericoid mycorrhizas are found in blueberries and in related plants. Many autotrophic members of the ericaceae and related families have no sheath formed but possess the hair-like roots enmeshed in an extensive weft of hyphae, which penetrate the root cells. The fungi identified as forming ericoid mycorrhizas are mainly ascomycetes while some are basidiomycetes and they probably evolved from saprotrophic fungi when organic matter began to accumulate in certain soils 200 million years ago (Cairney, 2000). Many ericaceous species colonise as pioneer plants substrates ranging from arid sandy soils to moist or humus, in association with their mycorrhizal fungi. Due to the symbiosis with ericoid mycorrhizal fungi, ericaceous plants are also able to grow in highly polluted environments, where metal ions can reach toxic levels in the soil substrate (Perotto1 *et al*., 2002).

Orchid mycorrhizas are unique in that they are required for seed germination. In the Orchidaceae, the plants are partially or wholly achlorophyllous for some part of their life. The Orchidaceae is one of the largest plant families, including almost 10% of all flowering plant species (Jones, 2006). The orchid family's unique characteristics and much of its diversity may be attributable to its distinctive relationship with mycorrhizal fungi (Benzing, 1981; Zettler *et al.*, 2004). Some kinds of orchids never photosynthesize, but instead parasitize the mycorrhizal fungi. They form mycorrhizas with basidiomycetes of various affinities. Some of these are highly effective saprophytes or parasites of other plants which facilitate the transfer of organic C and minerals to orchids (Tao *et al.*, 2008). There is increasing evidence that some orchids are dependent on fungi that are mycorrhizal

with autotrophic plants obtaining organic C from them, as well as mineral nutrients derived from the soil (McCormick *et al.*, 2004).

2.3 Arbuscular mycorrhizal (AM) fungi

Arbuscular is the most common type of mycorrhiza which is named after its internal structures called arbuscules or vesicular-arbuscular. Arbuscular mycorrhiza possess both arbuscules and another structure called vesicles. This is also called an endomycorrhiza, because the fungus enters the cells of the root. AM fungi are found in almost all habitats and climates (Barea *et al*., 1997) such as on grasses, most crop plants, many trees, shrubs, flowers, and in about 80 to 95% of the world's plant species (Lanfranco and Young, 2012). Fossil records of AM fungi as proposed by Redecker *et al*. (2000) demonstrate that the AM fungal symbiosis points back to the Ordovician age, 460 million years ago. These fossils suggest that Glomeromycota-like fungi may have played a significant role in facilitating the colonisation of land by plants. The symbiosis is generally mutualistic and based on bi-directional nutrient transfer between the symbionts. AM fungi are obligate symbionts, thus they are not yet successfully cultured in the absence of plant root. However, the mycorrhizal association may vary along a symbiotic gradient ranging from strong mutualism to antagonism (Howeler *et al*., 1987; Johnson *et al*., 1997).

Arbuscular mycorrhizal fungi were previously classified in the phylum Zygomycota under the family Endogonaceae because of their resemblance with *Endogone* species. However this was later revised when it was discovered that AM fungi produced asexual spores instead of sexual spores like other *Endogone* species. The relationship between AM fungi and other fungi as detected by molecular analysis elevated the group to the phylum Glomeromycota (Koide and Mosse, 2004). The phylum Glomeromycota comprises approximately 150 described species distributed among ten genera, defined primarily by spore development and morphology. DNA sequences have also been used recently to circumscribe taxa, although the latest molecular analyses indicate that the definite

number of AM fungal taxa may be much higher (Daniell *et al*., 2001; Vandenkoornhuyse *et al*., 2002). It has been reported that almost all members of the AM fungi are asexual and their vegetative mycelium and intraradical structures are aseptate and multinucleate. Spores may be formed singly, in clusters or in morphologically distinct "fruit bodies" called sporocarps. Glomeromycotan fungi produce relatively large spores which are between 40 and 800 μm in diameter depending on the species (Bécard and Pfeffer, 1993).

2.3.1 Colonisation of plant roots by AM fungi

There are three important components of the mycorrhizal root system namely, the root itself, the intraradical mycelium (the fungi within the root) and the extraradical mycelium (the fungi within the soil). Root colonisation by AM fungi can arise from spores, infected root fragments and/or hyphae. The spores are formed on the extraradical hyphae, but some species also may form spores inside the roots. Upon root colonisation, mycorrhizal fungi develop an external mycelium which is a bridge connecting the root with the surrounding soil (Toro *et al*., 1997). One of the most notable effects of colonisation by mycorrhizal fungi on the host plant is the increase in phosphorus (P) uptake mainly due to the capacity of the mycorrhizal fungi to absorb phosphate from soil and transfer it to the host roots (Asimi *et al*., 1980). As reported by Birhane *et al.* (2012) in their study, AM fungi can enhance photosynthesis, efficiency of water usage and growth of frankincense seedlings under pulsed water availability. Elias and Safir (1987) also reported that the growth and branching of mycelium growing from spores are stimulated by soluble exudates or extracts from the roots of host species, whereas the exudates from a nonhost had no effect (Gianinazzi-Pearson *et al*., 1989). Hyphal contact with the root is followed by adhesion and formation of swollen appressoria preceding the penetration (Giovannetti *et al*., 1993b). There is evidence that the host plant recognises the AM fungi already at this stage, which is indicated by regular occurrence of slight wall thickening on the epidermal cell adjacent to the penetrating hyphae (Garriock *et al*., 1989). The thickenings do not

contain either celullose or lignin and do not prevent the penetration of fungal hyphae through the walls (Harrison and Dixon, 1994).

2.3.2 Two types of arbuscular mycorrhiza

Arbuscular mycorrhizal (AM) fungi are the most widespread mycorrhiza in nature and form two morphologies according to the structures of the intraradical mycelium, the *Arum*-type and the *Paris*-type (Dickson, 2004). In the *Arum*-type the fungal symbiont spread in the root cortex via intercellular hyphae. The determining factors defining the two different morphologies are not well understood (Ahulu *et al*., 2004). The *Arum*-type is commonly described in fast growing root systems of crop plants, while the *Paris*-type morphology has been more often seen in plants of natural ecosystems such as those occurring in herbaceous layers in temperate broadleaf forests (Brundrett and Kendrick, 1990b), various trees (Kubota *et al*., 2001), and plants of semi-arid systems (McGee, 1986). In the *Paris*-type, the hyphae develop intracellular coils and spread directly from cell to cell within the cortex. Arbuscules grow from these coils and are usually relatively short-lived. At least, in the *Arum*-type mycorrhiza, the hyphae are by comparison long-lived (Smith and Dickson, 1991).

Co-occurrence of *Arum*- and *Paris*-type morphologies of AM fungi is usually observed in cucumber and tomato (Kubota *et al*., 2005). AM fungal morphological types were recognized in 14 families and were confirmed as follows: *Arum*-type in Rosaceae, Oleaceae, Lauraceae, Vitaceae and Compositae, *Paris*-type in Aquifoliaceae, Ulmaceae, Araliaceae, Theaceae, Magnoliaceae, Rubiaceae and Dioscoraceae, and both and/or intermediate types in Caprifoliaceae and Gramineae (Kubota *et al*., 2005). Plant families whose AM fungal morphological status was previously unknown were clarified as follows: Polygonaceae and Commelinaceae showed *Arum*-type morphology whereas, Celastraceae, Menispermaceae and Elaeagnaceae demonstrated *Paris*-type morphology. The *Arum*-type to *Paris*-type species proportion has been found to decrease in the following order: annuals > perennials > deciduous species >

evergreen species and pioneer group > early successional group > late successional group. It had been reported that evergreen plants had a higher tendency to form *Paris*-type AM fungi than annuals, perennials and deciduous plants. The AM fungal morphology seems to be strongly influenced by the identity of the plant, though control by the fungal genome cannot be ruled out (Ahulu *et al*., 2004). Thus the most common morphological type has been generally regarded as the Arum-type due to the fact that most experimental studies use crop plants. However, as per the suggestion by Brundrett & Kendrick (1990b) the Paris-type might be just as common in natural communities as the Arum-type.

2.3.3 The use of AM fungi in phytoremediation

AM fungi provide an attractive system to advance plant-based environmental clean-up (Gohre and Paszkowski, 2006). AM fungi can contribute to plant growth, particularly in disturbed or heavy metal contaminated sites, by improving mineral nutrition or increasing resistance or tolerance to biotic and abiotic stresses (Bhalerao, 2014). They also provide an increased plant access to relatively immobile minerals such as P (Vivas *et al*., 2003; Yao *et al*., 2003), improving soil texture by binding soil particles into stable aggregates that resist wind and water erosion (Steinberg and Rillig, 2003), and by binding heavy metals into roots that restricts their translocation into shoot tissues (Kaldorf *et al*., 1999). They can alter plant productivity, because AMF can act as biofertilizers, bioprotectants, or biodegraders (Xavier and Boyetchko, 2002).

Plants which appear spontaneously in disturbed ecosystem are frequently devoid of mycorrhizal symbiosis and are mostly characterized by poorly developed root and shoot biomass when heavy metals are present (Pawlowska *et al*., 1996). The lack of mycorrhiza can hamper the revegetation of the metal-contaminated mine spoil or other degraded sites. The introduction of an AM fungal inoculum into these areas could be a strategy for enhancing the establishment of mycorrhizal herbaceous species (Meier *et al.*, 2011). AM fungal isolates differ in their effect on heavy metal uptake by plants (Leyval *et al*., 1997). Some reports indicate

higher concentrations of heavy metals in plants due to AM fungi (Joner and Leyval, 1997), whereas others have found a reduced plant concentration; for example, Zn and Cu in mycorrhizal plants (Heggo *et al*., 1990). Thus, selection of appropriate isolates could be of importance for a given phytoremediation strategy. AM fungal species can be isolated from areas which are either naturally enriched by heavy metals or old mine/industry waste sites in origin. Indigenous

AM Fungal species could be able to stimulate plant growth better than non-indigenous species. This is due to the fact that indigenous AM fungal ecotypes result from long-term adaptation to soils with extreme properties (Rahmanian *et al*., 2011). AM fungi are of importance as they play a vital role in metal tolerance (del Val *et al*., 1999) and accumulation (Jamal *et al*., 2002; Zhu *et al*., 2001). Their potential role in phytoremediation of heavy metal contaminated soils and water is also becoming evident (Jamal *et al*., 2002).

External mycelium of AM fungi provides a wider exploration of soil volumes by spreading beyond the root exploration zone (Khan *et al*., 2000; Malcova *et al*., 2003), thus providing access to greater volume of heavy metals present in the rhizosphere. A greater volume of metals is also stored in the mycorrhizal structures in the root and in spores. For example, concentrations of over 1200 mg kg^{-1} of Zn have been reported in fungal tissues of *Glomus mosseae* (currently known as *Funneliformis mosseae)* and over 600 mg kg^{-1} in *Glomus versiforme* (Chen *et al*., 2001). Another important feature of this symbiosis is that AM fungi can increase plant establishment and growth despite high levels of soil heavy metals (Enkhtuya *et al*., 2002), due to better nutrition (Feng *et al*., 2003), water availability (Auge, 2001) and soil aggregation properties (Rillig and Steinberg, 2002) associated with this symbiosis. The AM fungus is thus significant in the ecological improvement of the rhizosphere (Medina, *et al*., 2003; Azcón-Aguilar *et al*., 2003).

Hetrick *et al*. (1994) studied the influence of mycorrhizal fungi on revegetation of chat piles from mine spoils, where plants had failed to establish naturally. They showed that mycorrhizal colonisation by a mixed AM fungal inoculum improved the growth of the obligate mycotrophic plant *Andropogon gerardii*, but *Festuca arundinacea*, a facultative mycotroph which grows well without mycorrhiza in non-contaminated soil, also benefited from mycorrhiza in chat piles. The results showed that mycorrhizas in combination with fertilizers will improve plant establishment on chat piles, and also on other severely disturbed sites such as mine spoils or overburdens (Hetrick *et al*., 1994). The benefit from mycorrhizal fungi could be associated with increased tolerance to heavy metals, but also with better plant nutrition, since chat piles are poor in nutrients and have a very low water-holding capacity.

A number of biological and physical mechanisms have been proposed to explain metal tolerance of AM fungi and AM fungal contribution to metal tolerance of host plants. One of the mechanisms involves the immobilization of metals in the fungal biomass (Zhu *et al*., 2001). The research done by Lanfranco *et al*. (2002) implicates metallothionein-like polypeptides in Cd and Cu detoxification in AM fungal cells, since these polypeptides bind and sequester the toxic metals. An enhanced root/shoot Cd ratio in AM plants show a reduced transfer, which has been suggested as a barrier in metal transport (Joner *et al*., 2000b; Tullio *et al*., 2003). This may occur due to intracellular precipitation of metallic cations with PO_4^-. However, AM fungal metal tolerance consists of adsorption onto plant or fungal cell walls present in plant tissues, or onto or into extraradical mycelium in soil (Joner *et al*., 2000a). It also includes the chelation by such compounds as siderophores and metallothionens released by fungi or other rhizosphere microbes, and sequestration by plant-derived compounds like phytochelatins or phytates (Joner and Leyval, 1997). Olsson *et al*. (1998) reported a few indirect mechanisms which consist of the effect of AM fungi on rhizosphere characteristics such as changes in pH, microbial communities and root-exudation patterns.

Although AM fungi are reported to contribute to plant growth, mainly in disturbed or heavy metal contaminated sites, soil degradation produces changes in the diversity and abundance of AM fungal populations (Koomen *et al*., 1990). Such elimination of AM fungi populations can lead to problems with plant establishment and survival (Pfleger *et al*., 1994; Haselwandter and Bowen, 1996). This causes a disturbance not only of the plant communities, but also of the fungi living in the soil (Bever, 2002).

The number of spores and root colonisation of plants occurring at sites are often reduced by soil disturbance (Waaland and Allen, 1987). Thus, the host-specific differences in spore abundance reflect host-specific differences in relative rates of AM fungal population growth (Bever, 2002). However, AM fungal isolates adapted to local soil conditions can stimulate plant growth better than non-indigenous isolates (Sylvia and Williams, 1992). Therefore, isolation of indigenous stress-adapted AM fungi can be a potential biotechnological tool for inoculation of plants in disturbed ecosystems (Gaur and Adholeya, 2004). Like ectomycorrhizal fungi, AM species have a potential which can be employed in biomonitoring programmes. The decline of AM fungal occurrence (propagule density) and infectivity in metal-polluted soils can be used as bioindicators of soil contamination (Leyval *et al*., 1995). Mycorrhizal colonisation of plant roots after soil remediation can be a sign that the metal concentration or bioavailability has decreased. Since metal tolerance evolves in some fungi from metal-contaminated soils, a sensitive AM fungus could be used and tested for its ability to colonise roots in any metal polluted soils, providing useful information about their metal toxicity (Meier *et al.,* 2011).

2.3.4 AM fungal status of mine tailings in South Africa

Throughout the world, South Africa is a leader in mining industry due to the variety and quantity of minerals produced. The country has an abundance of mineral resources, accounting for a significant proportion of world production and

reserves, such as Au, Mn, V, chrome and Platinum Group Metals (PGM). The South African gold ore reserves, estimated at 40,000 tons, represent 40% of the global reserves. Over 80 % of the world's platinum reserves are found in South Africa (Mining Weekly, 2015); AngloGold Ashanti Company, 2004).

Despite the large economic benefits from the gold mining, there are environmental concerns as millions of tons of waste material are produced every year. Amongst the South African provinces, Gauteng region has major mining activities and as a result, the province produces a large number of slime dams, mine dumps and landfills in areas earmarked for low-cost housing projects. For every ton of gold produced about 200,000 tons of wastes are generated (AngloGold Ashanti Company, 2004). The production of such large-scale mining wastes poses serious socioeconomic and environment problems (Orłowska *et al*., 2011).

These mine dumps contain a large number of toxic elements such as U, As, Ra, Ni, Zn, and many other radioactive materials. Human exposure to these elements leads to various acute or chronic illnesses, such as cell mutation, cancer, respiratory diseases and many more (McGlasshan, 2004). Apart from health problems, they also cause injuries and pollution, such as destruction of buildings during floods or heavy rains, pollution of ground and surface water (Chen *et al*., 2005; Suruchi and Khanna, 2011).

The problem of environment metal pollution could be combated by establishment of AM vegetation on the surface of the mine tailings. Besides the toxicity of the substrate, such areas usually lack essential nutrients (mainly N, P, and K) and organic matter (Mendez and Maier, 2008b). AM fungi contribute to soil structure by forming micro- and macro- soil aggregates within the net of external hyphae (Miller and Jastrow, 2000). Their presence may reduce stress caused by lack of nutrients or organic matter and increase plant resistance to pathogens, drought, and heavy metals (Cardoso and Kuyper, 2006). Therefore, mycorrhizal fungi may

become the key factor in successful plant revegetation of industrially polluted areas by promoting the success of plant establishment and increasing soil fertility and quality.

AM status has not been fully investigated in South Africa, until recently. Grassing of slime dams has been considered the most effective means of reducing wind-caused erosion and protecting the surrounding environment. In the past, slime dams of the South African gold mining industry were grassed by using 'high-input' methods that involve intensive leaching, liming, fertilization and irrigation prior to planting with a suite of pasture grass species. Although this process incurred a great cost to the gold industry, these methods had proven ecologically and economically unsustainable (Weiersbye *et al*., 2006).

To investigate the AM status in South Africa, some surveys were conducted in Free State and North West regions. A survey of a chronosequence of slime dams conducted by Weiersbye *et al*. (2006) reported less than 5 percent of ruderal species that were introduced during grassing persisted once fertilization and irrigation ceased, although there was a high diversity of naturally-colonizing perennial plant species. A parallel survey of the arbuscular mycorrhiza status of plants on Au and U slime dams in the North West province was undertaken by Straker *et al*. (2007). In this survey root AM-colonisation parameters (total, hyphal, vesicular, arbuscular) and AM fungal spore status were assessed where samples of five indicator host plant species were taken from different sampling sites namely: Recently Vegetated (RV), Old Vegetated (OV) and Never Vegetated (NV) slime dams. The samples were also taken from different zones (the top, lower slopes, retaining wall and toe paddocks) as well as the surrounding natural soils ('veld'). The study concluded that the flat, polluted soils around slime dams and the flatter areas of OV and NV slime dams were sources of more acid-tolerant AM fungal inoculum. Because the survey undertaken by Straker *et al*. (2007) represented a single observation of plant and substratum AM fungal status in late summer and did not provide a reliable indication of the inoculum potential (i.e.

infectivity) of the substrata, another AM fungal status study was conducted to substantiate the findings.

The study performed infectivity assays on substrata from the same sites and along the same gradients, and in addition, to replicate the study in two different mining regions (Straker *et al*., 2008). Infectivity assays are a more accurate measure of the AM fungal inoculum potential of a substrate since they incorporate the infective ability of all propagules such as spores, soil mycelium, root fragments, auxiliary cells and sporocarps (Read *et al*., 1976). Substratum conductivity differed between zones in both regions, with minor interaction between region and zone was negatively correlated with pH, AM fungal infectivity and total spore numbers. The findings demonstrated that the ameliorant effects of liming and irrigation on substratum pH and conductivity are short-lived, but despite the physico-chemical constraints, a significant measurable AM fungal inoculum potential was found existing on all substrata. Amelioration of tailings with organic matter and use of acid and salt-tolerant AM fungal would be expected to contribute to more persistent AM fungal communities and vegetation on gold and uranium slime dams (Straker *et al*., 2008). In addition to enhancing nutrient acquisition, AM fungi may facilitate host growth in polluted soil substrata by contributing to pollutant immobilization, due to the presence of the vesicles and arbuscules of AM fungi in *Cynodon dactlyon* from South African Au and U tailings which have a higher affinity for radionuclides and heavy transition metals than the surrounding root tissues (Weiersbye *et al*., 1999). Orłowska *et al*., (2011) investigated the efficiency of mycorrhizal colonization in stimulation of plant growth and nutrient uptake in Non-sterilized seeds of *B. coddii* collected from Agnes Mine (Barberton area), Mpumalanga Province, South Africa. In their study, they found the highest shoot and root weight in plants inoculated with fungi originating from *B. coddii* rhizosphere, whilst the lowest weight was noted for plants inoculated with fungi originating from rhizosphere of another Ni hyperaccumulator, *S. coronatus* (Orłowska *et al*., 2011).

Thus successful rehabilitation of degraded and polluted substrata is dependent on an understanding of plant establishment and succession, factors which are strongly influenced by dynamic soil components such as organic matter and microbial communities. AM fungi are an essential component of the soil/plant community and many rehabilitation programs aim to accelerate the predominance of mycotrophic plant populations in order to create more stable communities (Smith and Read, 1997). Mycorrhizal inoculation of disturbed/degraded sites is important in promoting the dominance of mycotrophic species, which would lead to a more rapid rate of succession (Smith and Read, 2008). The inoculation of the plants with arbuscular mycorrhizal (AM) fungi enables the re-establishment of plant community in disturbed and polluted lands that are deficient in plant nutrients (Saito and Marumoto, 2002**).** Grass species are often introduced for rapid revegetation in devastated lands, due to their ability to quickly stabilize the fragile soil structure with their fibrous root systems; hence *Erograstic curvula* was used in this study. It was been reported that colonisation of *E. curvula* plants by AM fungi increases plant growth, and it may also increase the density of AM fungal propagules in the soils (Saito *et al*., 2011). This in turn, facilitates the development of subsequent vegetation (Greipsson and El-Mayas, 2000).

2.4 Traditional versus DNA-based techniques for classification of AM fungi

The identification of AM fungi is a very challenging process; however, it is a vital exercise since AM fungi form symbiotic relationships with a number of terrestrial plants. A great challenge with identification of AM fungi results from their hidden, biotrophic behaviour in the soil, few morphological characters, and the potential formation of dimorphic spores. This resulted in a large number of AM fungal species, phylogenetically belonging to different orders, being placed in one genus (*Glomus*) and, conversely, individual species forming different spore morphologies being described as members of different orders (Kruger *et al*., 2009).

The phylum Glomeromycota comprises about 200 described morphospecies that traditionally have been distinguished by features of the spores, which are formed around or within root systems, and particularly the spore wall (Opik *et al.*, 2010; Schüßler and Walker, 2010). The manner in which the spore is formed on the hyphae has been important to circumscribe genera and families, and the layered structure of the spore walls is used to distinguish species (Morton, 1988). Walker (1983) established the concept of ‘‘murographs’’ to describe and compare the layered structure of the spore walls more easily. Morton (1995) as well as Stürmer and Morton (1997, 1999a, b) and Stürmer (2012) included considerations of the spore development to group these wall components hierarchically into complexes linked by ontogeny (Redecker and Raab, 2006).

However, assessing AM fungi diversity from morphological spore identification has some limitations as spore production may be highly dependent on physiological parameters of the AM fungi and on environmental conditions. Under certain conditions or during certain seasons of the year, some AM fungi may produce numerous spores and therefore appear to be dominant root colonisers, whereas under different conditions, they may not sporulate at all. This phenomenon has been appropriately demonstrated by Stutz *et al*. (2000) who showed that the perceived low AM fungal diversity of arid ecosystems was due to low levels of sporulation in the field and the true AM fungal diversity of the systems could be assessed from successive trap cultures which induced all species present to sporulate. Bouamri *et al*. (2006) reported that all the AM fungal species isolated from palm grove soil, with the exception of two *Scutellospora* species, were detected at the first trapping cycle. *Scutellospora* species only sporulated during the second trapping cycle probably due to spore dormancy, and late root colonisation followed by a delay in sporulation.

Dalpé *et al.* (2005) also observed similar sporulation behaviour with *Scutellospora* species under pot-culture and under root-organ culture conditions. Moreover, the dynamics of spore production versus root colonisation may differ

among species (Bever *et al*., 1996, Spruyt *et al*., 2014). Another limitation of morphological identification is the fact that field-collected spores are often parasitized or degraded and therefore unidentifiable (Redecker *et al*., 2003). In nature, there can also be great variation in spore morphology even within an AM fungal species (Walker and Vestberg, 1998), and many AM fungi may reproduce only vegetatively without producing spores (Helgason *et al*., 2002). Non-sporulating species may not be detected at all whereas prolific spore-producers dominate the views of AM fungal ecology, as has been seen in the case of *Gigaspora* and *Archaeospora* (Young, 2012).

Molecular analysis provides a way around these limitations as it has the potential to identify actively growing fungi in field root samples and in spores isolated from soil samples independently of morphological criteria. The rRNA genes have been used in the majority of AM molecular ecology studies (Rosendahl and Stukenbrock, 2004), and these have generally agreed with classification based on spore morphology (Morton and Redecker, 2001; Schwarzott *et al*., 2001; Walker *et al*., 2004). Molecular markers have been successfully used to characterize the diversity of AM fungi in the field and have revealed an unexpectedly high diversity of phylotypes in some settings.

Studies by Husband *et al.* (2002a) and Vandenkoornhuyse *et al*. (2002) signify that the number of 200 described morphospecies might be a strong underestimation of the true diversity of the Glomeromycota. Characterization of the large subunit region (LSU) of ribosomal RNA genes, in combination with nested PCR, has proven suitable for analyzing phylogenetic relationships (Vandenkoornhuyse *et al.*, 2003) and developing molecular probes to detect AM fungal species colonizing plant roots and AM fungal spores in microcosm experiments (Kjøller and Rosendahl, 2000; Lee *et al.*, 2008), in the field (Gollotte *et al.*, 2004) or even in aquatic plants (Nielsen *et al.*, 2004). The use of nested AML primer pair targeting a portion of the SSU rRNA region (Lee *et al*., 2008) provides a reliable identification of AM fungi to the genus level while screening

out non-AM fungal organisms (Krüger *et al*., 2012). The recent revisions and consolidations in the phylotaxonomy of AM fungi have broadened the scope of AM fungal taxonomy and allow the basis of investigation into the diversity of AM fungi from environmental samples (Redecker *et al.*, 2013; Schüßler and Walker, 2010).

Molecular analysis has been critical in showing that the taxonomy of AM fungi was insufficient and needed a radical change which leads to assigning new names to the existing AM fungi (Young, 2012). There have been a number of discussions and studies revolving around the grouping of AM fungi. Schüßler *et al. (*2001) were the first to propose Glomeromycota as a monophyletic group raised to the taxonomic rank of a phylum based on SSU gene sequences. They also suggested that the Glomeromycota is a sister group of the Dikarya (Basidiomycota and Ascomycota) as did the six-gene phylogeny of James *et al*. (2006). However, the analysis of Liu *et al*. (2009), based on nucleus-encoded amino acid sequences, and that of Lee and Young (2009) on the mitochondrial genome of *Glomus intraradices* isolate 494 suggest a common ancestry of Glomeromycota with Mortierellales (Kruger *et al*., 2012). Hence Young (2012) recommended for more data from phylogenetically basal AM fungal to resolve immediate sister relationships to Glomeromycota, which are nonetheless clearly monophyletic and phylogenetically basal terrestrial fungi.

The work done by Kruger *et al.* (2012) shows that there are a number of clades within the Glomeromycota that form the basis for orders and families (Fig. 2.1). This led to most species previously known as *Glomus* to be placed into new genera. For example, *Glomus intraradices* has now been changed to *Rhizophagus irregularis* (Young, 2012). The most recent classification of Glomeromycota is based on a consensus of regions spanning ribosomal RNA genes: 18S (SSU), ITS1-5.8S-ITS2 (ITS), and/or 28S (LSU) (Kruger *et al*,. 2012), but Redecker *et al*. (2013) have proposed an evidence-based consensus for the classification of

Glomeromycota and redefined the phylogenetic framework which should be used to resolve contradictions in the literature (Fig. 2.1).

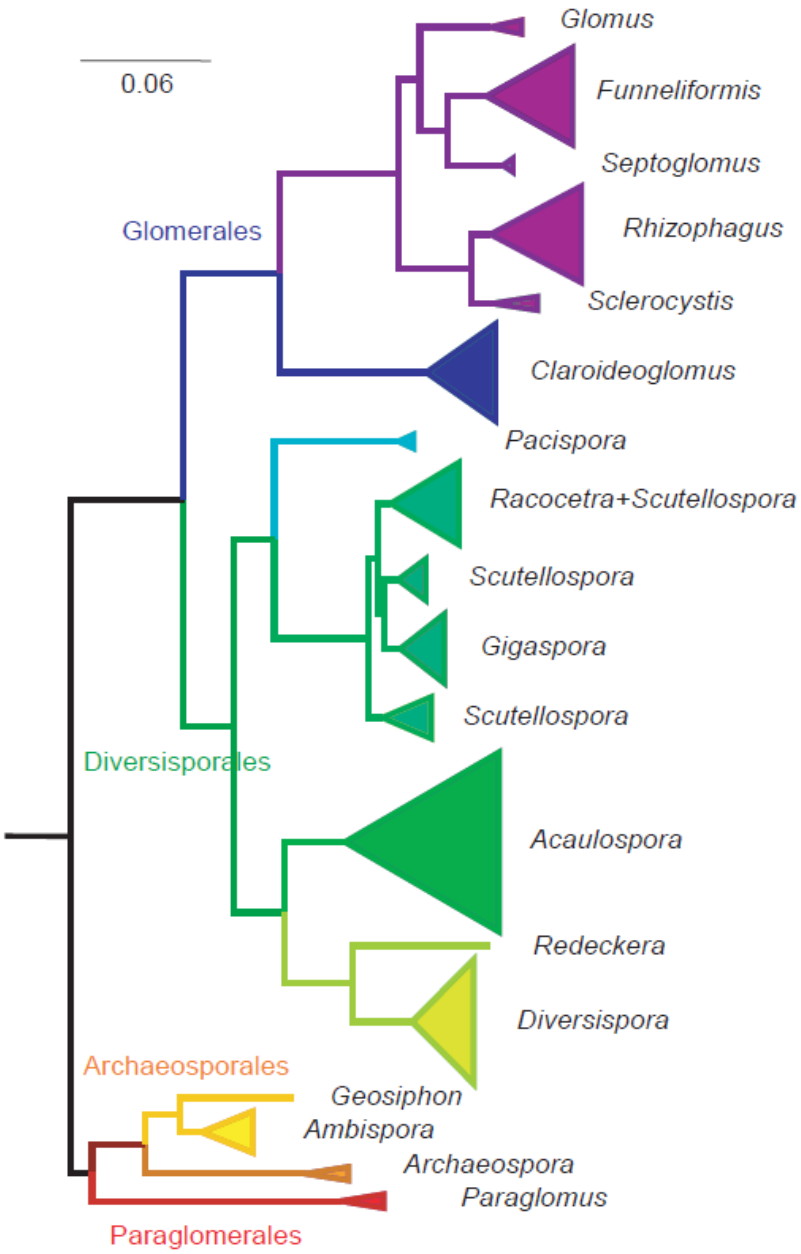

Fig. 2.1 Phylogeny of the Glomeromycota based on small sub-unit ribosomal RNA sequences, showing the relationships among the orders and genera. Families are indicated by distinct colours. Maximum Likelihood tree rooted with ascomycete outgroups, modified from a tree provided by A. Schüßler drawn with Fig Tree (Young 2012).

2.4.1 Molecular methods used in this study

Several investigators have reported that individual spores of AM fungi, which are multinucleate containing thousands of nuclei per spore for certain species, may contain substantial heterogeneity among ribosomal ribonucleic acid (rRNA) gene copies (Sanders, 2002) and show a high level of genetic diversity in the internal transcribed spacer (ITS) region of the nuclear rRNA genes. Ribosomal-based deoxyribose nucleic acid (DNA) sequence analysis has revealed genetic variation both within and between AM fungal species. Furthermore, the genes of this region are available in high copy number and possess highly conserved as well as variable sectors, which facilitate differentiation of taxa at different levels (Sharmah *et al.*, 2010). The nuclear SSU rDNA sequences (16S-like) evolve relatively slowly and are useful for studying distantly related organisms, whereas the mitochondrial rDNA genes evolve more rapidly and can be useful at the ordinal or family level. ITS are sequences located in eukaryotic rRNA genes between the 18S and 5.8S rRNA coding regions (ITS1) and between the 5.8S and 28S rRNA coding regions (ITS2) (Fig. 2.2). Studies on restriction site variation in the ribosomal DNA (rDNA) in populations have shown that while coding regions are conserved, spacer regions are variable. These spacer sequences have high evolution rate and are present in all known nuclear rRNA genes of eukaryotes (Renker *et al.,* 2006).

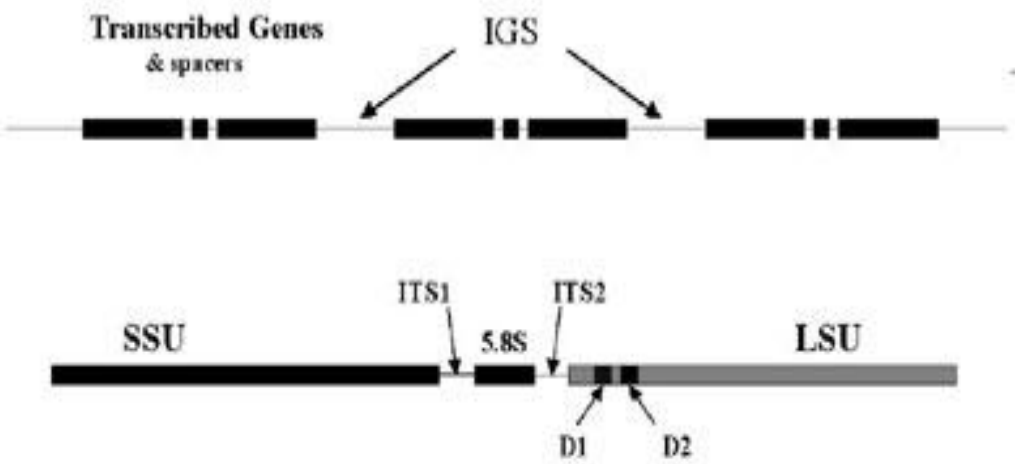

Fig. 2.2 Multicopy ribosomal genes carefully organised in the genome. Each ribosomal gene encodes for three subunits (18S [SSU], 5.8S and 28S [LSU]) separated from each other by an ITS. The genes themselves are separated from each other by an Inter Genic Spacer (IGS) (Dodd *et al.*, 2001).

A number of molecular taxonomy studies have been using ITS sequences (Redecker, 2000), although they are highly variable with AM fungal species and within the spores (Lloyd-Macgilp *et al.,* 1996). This poses a great challenge in finding features that are commonly shared among AM fungi but absent in other organisms (Lee *et al.* 2008). This study used the small subunit rRNA (SSU rRNA) gene due to its lower variability when compared to ITS gene, and at the same time allows enough resolution down to the species level. A set of specific PCR primers (AML1 and AML2) for all AM fungi designed by Lee *et al.* (2008) was employed. This set of PCR primers which has an ability to amplify all subgroups of arbuscular mycorrhizal fungi (Glomeromycota), but exclude sequences from other organisms, was designed to facilitate rapid detection and identification directly from field-grown plant roots. Because the 3' region of a primer is critical for specific amplification, the distinctiveness of this region is used to discriminate against non-AM fungi sequences. In addition, the most variable region of the AM fungal SSU rRNA gene was selected in order to achieve high sequence resolution within the AM fungi (Lee *et al.,* 2008). The primers (AML1 and AML2) target the small subunit rRNA gene because phylogenetic relationships among the Glomeromycota are well understood for this gene. Due to the sequence

comparisons done, these primers were reported to amplify all published AM fungal sequences except those from *Archaeospora trappei*. It was also reported that the AML1 and AML2 primers have much better specificity and coverage of all known AM fungal groups as compared to the established NS31 and AM1 primer combination (Lee *et al.,* 2008).

2.4.1.1. Nested polymerase chain reaction (PCR)

Nested PCR using taxon-specific primers for AM fungal species (morphotypes) is a highly sensitive method which allows detection of fungal hyphae present in roots as well as from soil (van Tuinen *et al*., 1998; Jacquot *et al*., 2000). The aim of the nested PCR reaction is to increase the specificity of the amplification reaction by performing two PCR amplifications one after the other. The first PCR reaction is performed as described below, but for the second reaction the amplification products obtained in the first amplification cycles are used as template using internal primers. In this way the specificity of the amplification is increased, since the target DNA to be amplified has acquired four primer binding sites. The efficiency of the amplification is increased as the number of cycles can be increased, without loss of specificity.

Two pairs of PCR primers are used for a single locus (Fig. 2.3). The first pair amplifies the locus as seen in any PCR experiment. The second pair of primers *(nested primers*) bind within the first PCR product and produce a second PCR product that is shorter than the first one. The logic behind this strategy is that if the wrong locus is amplified by mistake, the probability is very low that it would also be amplified a second time by a second pair of primers.

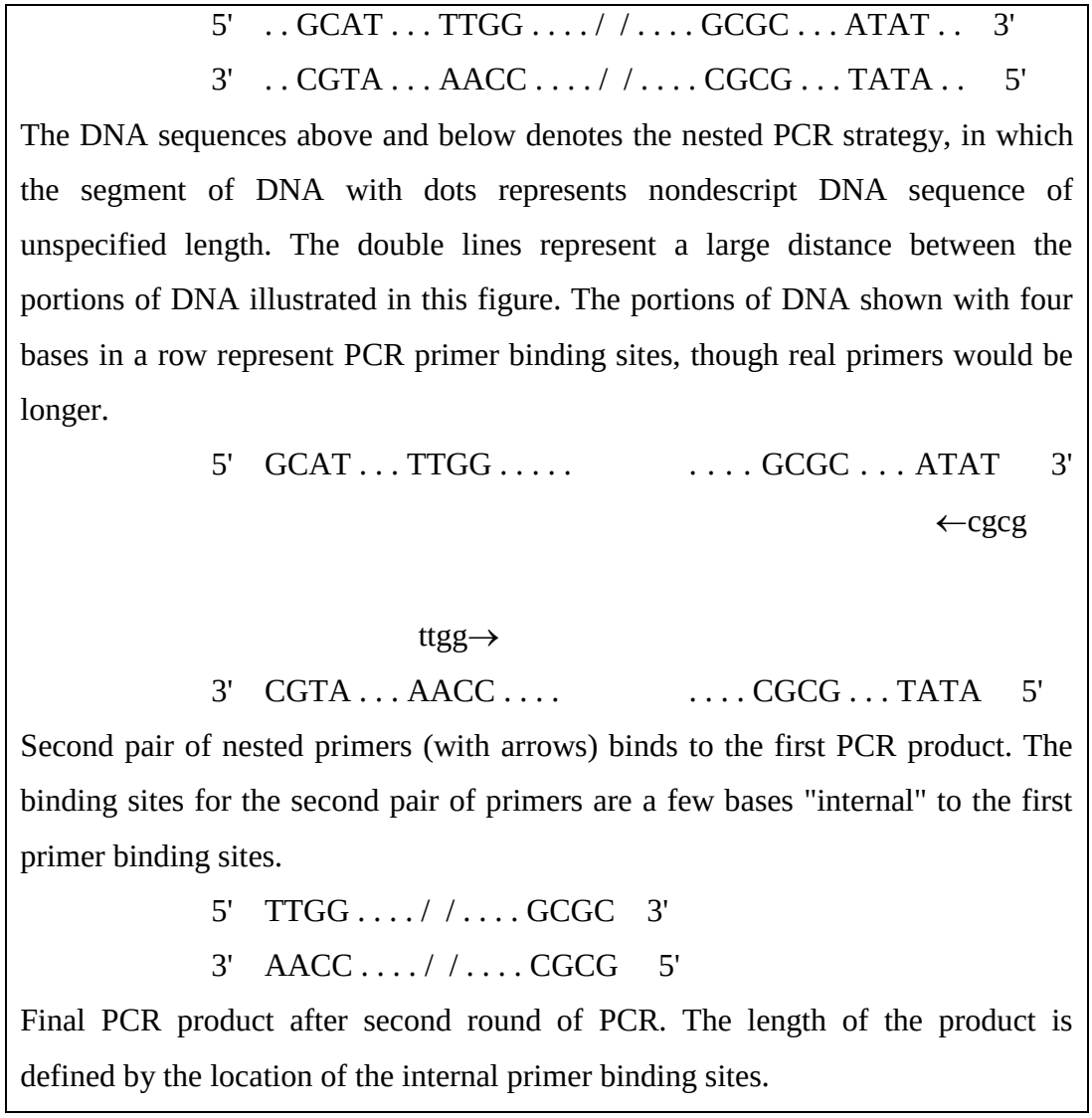

Fig. 2.3 Nested PCR using two pairs of taxon-specific primers for AM fungal species (morphotypes) (White *et al*., 1990).

2.5 The application of both bulk (ICP-MS) and micro-PIXE analytical methods in analysing the mechanisms of tolerance to metals and metalloids in arbuscular mycorrhizal fungi

There are a number of different analytical methods developed to study trace elements in environmental and biomedical samples. These techniques are divided into bulk and micro-analytical methods. The techniques for micro-analysis using X-ray emission spectrometry are of growing importance, as is the knowledge of the precision and accuracy of different techniques in order to make comparable measurements (Gomez-Morilla *et al.,* 2006). However, using highly sensitive techniques for bulk elemental analysis is usually the first, and often, the only step

in elemental analysis related to plant sciences. Some of these techniques such as Atomic Absorption Spectrometry (AAS), Atomic Emission Spectrometry (AES), Atomic Fluorescence Spectrometry (AFS), Inductively Coupled Plasma Atomic Emission Spectrometry (ICP-AES) and Inductively Coupled Plasma Mass Spectrometry (ICP-MS) have been successfully employed in various studies (Kaixuan *et al*., 2013).

ICP-MS determines concentration levels in parts per billion and below, while ICP-AES can only determine levels in parts per million and higher. In other words, ICP-MS works best in samples that require the lowest detection limits and the greatest level of productivity when it comes to sensitivity, accuracy and precision (Richaud *et al*., 2000) and it is considered one of the most sensitive techniques for measuring a wide-range of elements and isotopes in a variety of sample matrices (Boss and Fredeen, 1997; Salt *et al*., 2008).

The technique is relatively free from interferences and the interferences that do exist can often be reduced or removed through the use of a universal cell operating in either the collision mode or the reaction mode. In addition, ICP-MS technique measures most of the elements in the periodic table. In ICP-MS, the plasma is a means of generating individual atoms and ions which are then fed into the mass spectrometer and separated on the basis of their atomic weights. High-resolution ICP-MS is able to detect ultra-low concentrations of multiple metals rapidly, often achieving detection limits in the high pictogram per kilogram (pg kg^{-1}) range, so it is the technique of choice for initial screening.

The utility of the ICP-MS technique in the determination of both trace and major elemental concentrations has been observed in many studies ranging from tissues in neurodegenerative disorders (Yonghwang Ha, *et al.*, 2011) to plant (Salt *et al*., 2008) and soil components. Ram *et al.* (1997) have reported ICP–MS as the method of choice among the present-day technologies for determining Boron concentration and a convenient method for Boron isotope determination in plant

and soil samples. ICP-MS was successfully used in the study conducted by Larsen *et al.* (2006), in garlic to show a tenfold increase of selenium (Se) concentration due to the addition of mycorrhizas to the natural soil.

Methods for bulk elemental analysis are usually complemented by the use of micro analytical techniques such as Micro-Proton-Induced X-ray Emission (Micro-PIXE) (Mesjasz-Przybylowicz and Przybylowicz, 2002). Therefore, appropriate analytical methods for addressing particular questions of interest need to be carefully selected from among the broad array of analytical methods that are available. Micro-PIXE is one of the most modern, sensitive and reliable methods for the localisation and quantification of different elements in biological samples at the tissue and cellular levels (Vogel-Mikuš *et al.,* 2010).

2.5.1 Particle-Induced (Proton Induced) X-Ray Emission (PIXE)

PIXE is a technique used in determining the elemental composition of a material or sample. When a material is exposed to an ion beam, atomic interactions occur that give off EM radiation of wavelengths in the X-ray part of the electromagnetic spectrum specific to an element. The spectrum of characteristic X-rays emitted from the target, yields both qualitative and quantitative information concerning the concentration of the element in the sample (Mando and Przybylowicz, 2009). PIXE is a powerful yet non-destructive elemental analysis technique, now used routinely by geologists, archaeologists, art conservators as well as biologists and others to help answer questions of provenience, and authenticity.

The basic physical processes involved in this technique are at present well understood and can be modelled using readily available software codes that provide reliable results for a wide range of elements and the present refinement of data processing, using packages such as GeoPIXE-II opens up new frontiers in this type of application (Przybyłowicz *et al.,* 2005). Extension of PIXE using tightly focused beams (down to 1 μm) gives an additional capability for microscopic analysis. This technique, called micro PIXE, can be used to

determine the distribution of trace elements in a wide range of samples. Micro-PIXE has been used in plant science applications since its early days of its discovery (Bosch *et al.,* 1980; Legge *et al.,* 1979).

Although micro-PIXE is not an easy technique to operate due to many related technical problems, including the difficulty in preparation of plant specimen resulting from heterogeneity of plant tissues, it is an important tool for quantitative investigations of trace elements and their interactions with other elements (Mesjasz-Przybylowicz and Przybylowicz, 2002). Przybyłowicz *et al.* (2005) used the technique to observe the heavy metal distribution in mycorrhizal and non-mycorrhizal roots of *Plantago lanceolata* L. (Plantaginaceae), a common weed of cultivated land. Using Micro-PIXE, Orlowska *et al*. (2013) successfully demonstrated the significant influence of mycorrhizas on the concentration and distribution of elements in roots of *Berkheya coddii.*

They discovered a significantly higher concentration of P, Ca, Zn, and Cu in mycorrhizal roots compared to the non-mycorrhizal roots. Pallon *et al*. (2007) have found in their studies that the nuclear microprobe (NMP) using PIXE for elemental analysis and Scanning Transmission Ion Microscopy (STIM) was successful in investigating possible interactions between minerals and ectomycorrhizal (ECM) mycelia that form symbiotic associations with forest trees. These studies confirm the usefulness of micro-PIXE in studies on microscale activity of mycorrhizal fungi.

Witkowski and Weiersbye (1998) and Straker *et al.* (2007) reported a depletion of plant nutrients such as N and P in gold and uranium mine tailings of the Witwatersrand reef in South Africa. These tailings contain high concentrations of some metals and radionuclides such Fe, Ni, Cr, As, Y, Au, Pb, Th, Ra, and U**,** in which mostly, if not only, mycorrhizal plants species that colonise or survive in the tailings. Thus localisation and quantification of these toxic elements in plants and in mycorrhizal structures could assist in understanding the possible pathways of transport and mechanisms of detoxification and thereby suggest methods of

plant adaptations in adverse conditions. Weiersbye *et al.* (1999) used micro-PIXE to localise elements in mycorrhizal roots of *Cynodon dactylon* growing on mine tailings and the present study is intended to build on this preliminary work.

2.6 Study aim

The aim of this study was to identify AM fungi from a number of heavy metal sites in South Africa using both morphological and molecular techniques, followed by their evaluation of heavy metal localisation in mycorrhizal roots.

2.7 Specific objectives

1. To compare AM fungal diversity in selected heavy metal (HM) sites in the Republic of South Africa (RSA).
2. To use a molecular technique such as nested PCR to identify the AM fungal species associated with these sites.
3. To localise HM elements in plant roots and fungal structures using Particle Induced X-ray Emission (PIXE).
4. To conduct a statistical comparison between elemental concentrations in roots and AM fungal colonisation levels of roots

CHAPTER 3

3 MATERIALS AND METHODS

3.1 Site descriptions

Samples were collected from three different provinces namely Gauteng, Mpumalanga and North West provinces. The sites were selected based on their historical and current heavy metal contamination (Table 3.1). The overall topography of all three provinces is relatively flat with moderate undulating landscape. A diverse rainfall gradient is observed across the three provinces (Mucina and Rutherford, 2006). The estimated Mean Annual Precipitation (MAP) rainfall for North West (Vaal River, Lonmin) and Gauteng (West Wits, East Rand), ranges from 497 to 651 mm (South African Weather Service, 2006). Mpumalanga (Agnes Mine) is located in the high rainfall area of South Africa mainly occurring as thunderstorms and heavy showers with an overall MAP of 1194 mm (Mucina and Rutherford, 2006).

The three provinces are classified according to three dominant biomes namely grassland, savannah and azonal vegetation (Mucina and Rutherford, 2006). Vacant land is currently utilised for various uses including cattle ranching, game farming, agricultural crop farming such as maize and sunflower, but does not include commercial forestry plantations. Commercial forestry is unsuited to these areas, given the low annual rainfall and cold winter temperatures. However, some small stands, rows and isolated trees do exist along some water courses, farm boundaries and in areas adjacent to Tailings Storage Facilities (TSF)s through planting and natural establishment. Most of the Lonmin mine area is underlain by the mafic intrusive rocks of the Rustenburg layered suite of Bushveld Igneous Complex with rocks including gabbro, norite, pyroxenite and anorthosite. Predominant geological formations in Vaal River, East Rand, and West Wits study areas include dolomite and sand, chert-rich dolomite and shale, (AngloGold Ashanti, 2004) while Agnes serpentine mining site has its soil impacted by heavy metal contamination from a gold galvanising plant (Anhaeusser, 201 2).

3.2 Sites

3.2.1 Site 1: Lonmin Mining site, Marikana Thornveld, North West

3.2.1.1. Location

Lonmin Platinum Mine is the third largest producer in South Africa. It is located near Rustenburg, in the North West province. Although the general terrain of the area is rather flat, the Marikana Base Metal Refinery (BMR) at Lonmin Platinum is situated on the top of a gentle hill-slope at the base of the Jakkalskop kopjie. The BMR is situated directly within the historic run-off area from the kopjie and upslope of the seasonal wetland area and stream. As a result the BMR site is expected to be leaky, with storm-water entering the site, overflowing pollution control measures (e.g. culverts and ponds), and relatively large volumes of run-off exiting the BMR site (Fourie *et al.,* 2008). Its scope includes four major operations namely; Karee Mine, Western Platinum Mine, Eastern Platinum Mine in Marikana and Baobab shaft in Limpopo. The mine comprises fifteen tailings disposal facilities, approximately twenty rock dumps, twenty one open cast pits (some rehabilitated), four landfill sites, four large slag pile areas and several operational stockpile facilities. These mine wastes facilities cover more than 2500 ha. (Fourie *et al.,* 2008). The surface water run-off from the BMR site has been reported to be contaminated with sulphates and heavy metals. Present in the surface water run-off are: Sulphate (430 ppm), Ni (15 ppm), Cu (10 ppm), Co (1.3 ppm), Mn (1.9 ppm), Al (72 ppb), Zn (224 ppb), and Pb (22 ppb). Cr was present at 3 ppb (i.e. < the target water quality), (Weiersbye and Cukrowska, 2007), clastic sediments and minor carbonates.

A more accurate measure of elements immediately available to plants (i.e. not sorbed or bound) is the soil pore solution water. Elements reported to be present at elevated concentrations in the soil pore water are: sulphate (ranging from 500 – 5000 ppm on crusted areas), Mo (0.03 ppm), Al (0.6 ppm), Co (0.2 ppm), Cr (0.05 ppm), Cu (1 ppm), Mg (290 ppm), Mn (2 ppm), Na (115 ppm), Se (0.2 ppm), V (0.1 ppm), and Zn (0.4 ppm). These amounts could be taken up by plants but,

apart from Na, are well below plant toxicity levels. The soil pore water replenishes with ions on a seasonal basis, and under the influence of plant and micro-organism influences (Fourie *et al*., 2008). However, the results reported in this study, showed that some of these elements such as Cr, Cu, Mn, U, Ti to name but a few are above the acceptable limits for both plants and living organisms.

3.2.1.2. Geology and Soils

The mine is located on the basic rocks of the Merensky Reef and Chromitite layer of the Bushveld Igneous Complex. The soil is impacted by spillage from the base metal refinery (receives ore from the Merensky Reef and the UG2 Reef). The soils at the BMR site comprise Mispah formation around the BMR fence, with patches of deeper, sandier red soils around the granite outcrops. Most of the area is underlain by the mafic intrusive rocks of the Rustenburg layered suite of Bushveld Igneous Complex. Rocks include gabbro, norite, pyroxenite and anorthosite. Land types are mainly Ea, Ba and AE. Due to the type of soils below the BMR (black turf soils), significant amounts of the contaminants are sequestered in the topsoils. The resultant sink area is highly contaminated, although the high clay and organic content of the black turfs does limit leaching to groundwater. Unfortunately the seasonal swelling (wet season) and shrinking plus cracking (dry season) that occurs naturally in this self-mulching type of clay soil is steadily working the contaminants deeper into the soil profile and through the clay lens (Weiersbye and Cukrowska, 2007).

It has its basic rocks as chromitite, ultramafic at study site, pockets of sheet granite outcrops with heavy metal contaminants as Al, Mg, Na, S, Co, Cr, Cu, Fe, Mn, Ni, Se, Bi, V, As, Zn, Cd, La, Pt, Ir, Rh, Gd, Th, Te, Pb. The metals are included in the study because their concentration is above the acceptable levels in the plant.

3.2.2 Site 2: Mpumalanga, Agnes Serpentine Mining (AGM) Site

3.2.2.1. Location

Agnes Mine is located around the Barberton town, in the eastern portion of the Mpumalanga Province, South Africa. It has fragmented patches on the exposed ultramafic substrates in a triangular region extending from Malelane in the east, to Badplaas, Barberton and East Swaziland in the South to West of Nelspruit in the north (Antunes, 2010). It is generally situated at high altitudes in the Barberton region, ranging from 760 m in the North to 1 640 m in the Southwest. Agnes gold mining centres, together with some other centres such as Sheba-Fairview, New Consort, form separate complexes of epigenic mesothermal ore shoots that are part of the Barberton Greenstone Belt (BGB) (Fig. 3.1 below).

The samples were taken from an open field of *Berkheya coddii*, on serpentine soil, at the top of the hill above Agnes Mine. They were not taken on Agnes Mine itself, and not in receipt of any pollution from Agnes Mine. As a serpentine site, it is expected to be contaminated with Ni, Zn to name but a few. *Berkheya coddii* is Ni-hyperaccumulator and an endemic plant growing only on the soil containing high concentration of Ni.

The BGB is the largest Achaean greenstone belt and is one of the oldest goldfields in South Africa. It is located in the south eastern part of South Africa's Mpumalanga province, and is world renowned for its gold content (Antunes, 2010). It comprises an area of 770ha on the farm Portion 3 and R/E of Rhineland 330 JU (Mucina and Rutherford, 2006; Antunes, 2010).

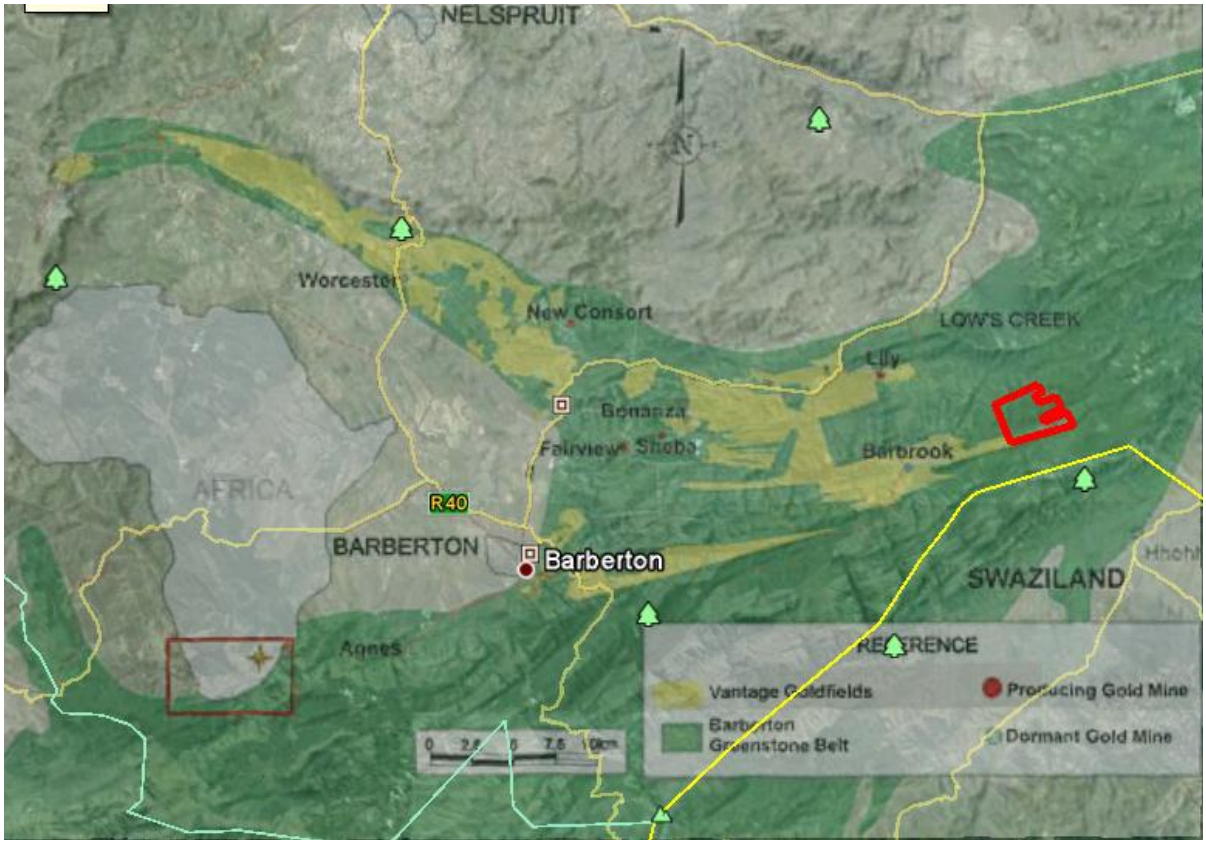

Fig. 3.1 The Barberton Greenstone Belt showing goldfields that include Agnes Mine, Sheba-Fairview, New Consort, Bonanza and several others (Anhaeusser, 2012).

3.2.2.2. Geology and Soil

The Agnes Mining site is positioned in a moderately flat to gently sloping terrain on lower slopes of the Barberton Mountains. It is a serpentine mine site with soil impacted by heavy metal contamination from a gold galvanising plant, Katspruit and Dolomitic. Despite numerous types of nickel such as nickeliferous magnetite (trevorite) (Trevor, 1920) several new and rare nickel minerals in the deposit (De Waal, 1986) showings in ultramafic rocks found throughout the Barberton greenstone belt, no nickel mine has yet been established (Ward, 1999; Anhaeusser, 2012).

Barberton Supergroup comprises of schists (metarmorphic rock which consists of layers of different minerals), gneiss, felspathic quartzites and various lavas of the

Figtree, Moodies and Onverwacht Formations (Mucina and Rutherford, 2006). New discoveries are still being made and old deposits are being re-investigated as techniques of mining and extraction improve. These developments and the recent discovery of a nickel-sulphide deposit associated with an old talc mine suggest that mining activities in the Barberton greenstone belt are set to continue well into the foreseeable future (Anhaeusser, 2012).

Barberton Goldfields mining area is characterised by steep to very steep topography with slopes that vary from 5° to 35°. The upper reaches of the mountainous terrain are characterised by steep and narrow drainage lines, while the lower reaches are characterised by open and wide gently flowing streams. The flood plains are generally wide, and subject to occasional flooding (seasonal) with moderate to large catchment areas. The BGB is a north-east trending, isoclinally folded, metamorphosed volcano-sedimentary succession entirely surrounded by intrusive granitoid rocks (Antunes, 2010). It consists predominantly of an assortment of ultramafic and mafic submarine volcanic rocks, including a number of sill-like, layered ultramafic complexes. This group is overlain by turbiditic greywacke sandstones and associated mudstones and banded ferruginous shales of the fig tree group (Antunes, 2010).

Host rocks to the gold mineralisation vary from greenstones to greywackes, shales, banded ferruginous shales, quartzites, and a variety of cherts. Wall-rock alteration associated with the mineralised fractures includes silicification, carbonatisation, sericitisation and sulphidation. The gold ores of this area are either free milling, moderately refractory or highly refractory depending on the extent to which the precious metal is occluded within the associated sulphides, commonly pyrite and arsenopyrite, or contained within arsenopyrite as submicroscopic gold. The lodes comprise mineralised gold (Antunes, 2010).

3.2.3 Site 3: Gauteng, East Rand (ER1) ERGO Brakpan slime dam footprint.

3.2.3.1. Location

Brakpan is situated on the East Rand of Gauteng, approximately 25km away from Oliver Tambo International Airport. The Brakpan tailings deposition site is part of DRDGold's Ergo gold recovery project called Ergo (ErgoGold). The quartzite rock is ground to fine sand and powder, deadly sodium cyanide is used to extract the gold, and the toxic waste sand is pumped to these great piles. The "lake" in the middle could pose a hazardous threat to both the environment and living organisms even for years after mining has stopped. Ergo's flagship metallurgical plant, some 50km east of Johannesburg in Brakpan, and the Knights plant in Germiston together comprise what is arguably the world's largest gold surface tailings retreatment facility. Together with the milling and pump station at Crown Mines and City Deep (both former plants), the new consolidated Ergo operation processes 2.0 - 2.1 million tonnes of gold-bearing material a month (GDACE, 2008).

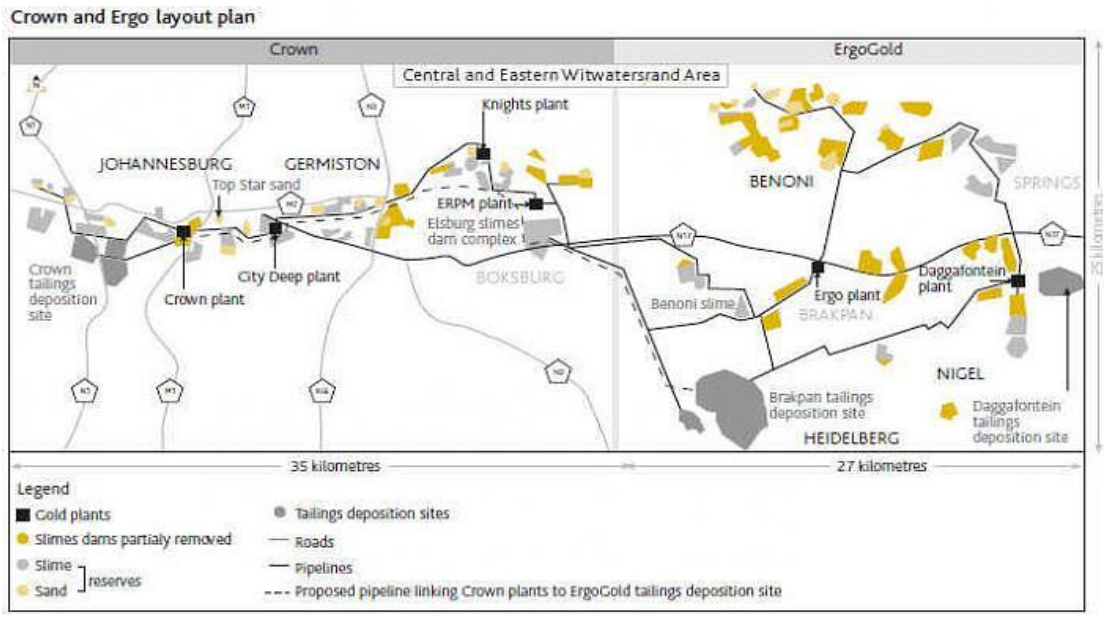

Fig. 3.2a Ergo's flagship metallurgical plant, together with the milling and pump station at Crown Mines and City Deep (GDACE, 2008).

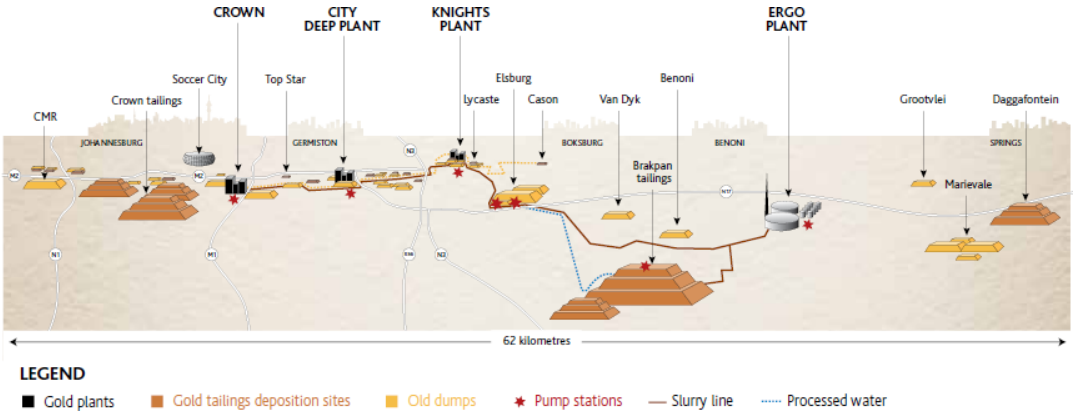

Fig. 3.2b Ergo's flagship metallurgical plant footprint, together with the milling and pump station at Crown Mines and City Deep (Integrated-report, 2013).

3.2.3.2. Geology and Soil

Gold in the Witwatersrand Supergroup and Black Reef Formation occurs in pyritic quartz pebble conglomerates, together with sub-economic to economic quantities of uranium as uraninite. The soil is impacted by Acid rock drainage (ARD) and slimes (i.e. footprint of the old Withok slime dam next to Brakpan slime dam), Katspruit and Dolomitic (chert poor). A number of other potentially hazardous metals occur together with the economic mineralisation (GDACE, 2008). Dolomitic bedrock is a high potential aquifer due to its chemical characteristics that result in formation of solution cavities (Weiersbye and Witkowski, 2003). Collapse of near-surface cavities forms sinkholes that can conduct contaminated surface water into the groundwater aquifer. The area has a high rate of wind and water erosion that distribute mining residues into the surrounding soil. Removal of mine residues for reprocessing leaves "footprints", where sand and tailings are mixed with soil. Leachates and other contaminated waters interact with natural soils, leaving hazardous precipitates, adsorbed metals and other contaminants (GDACE, 2008).

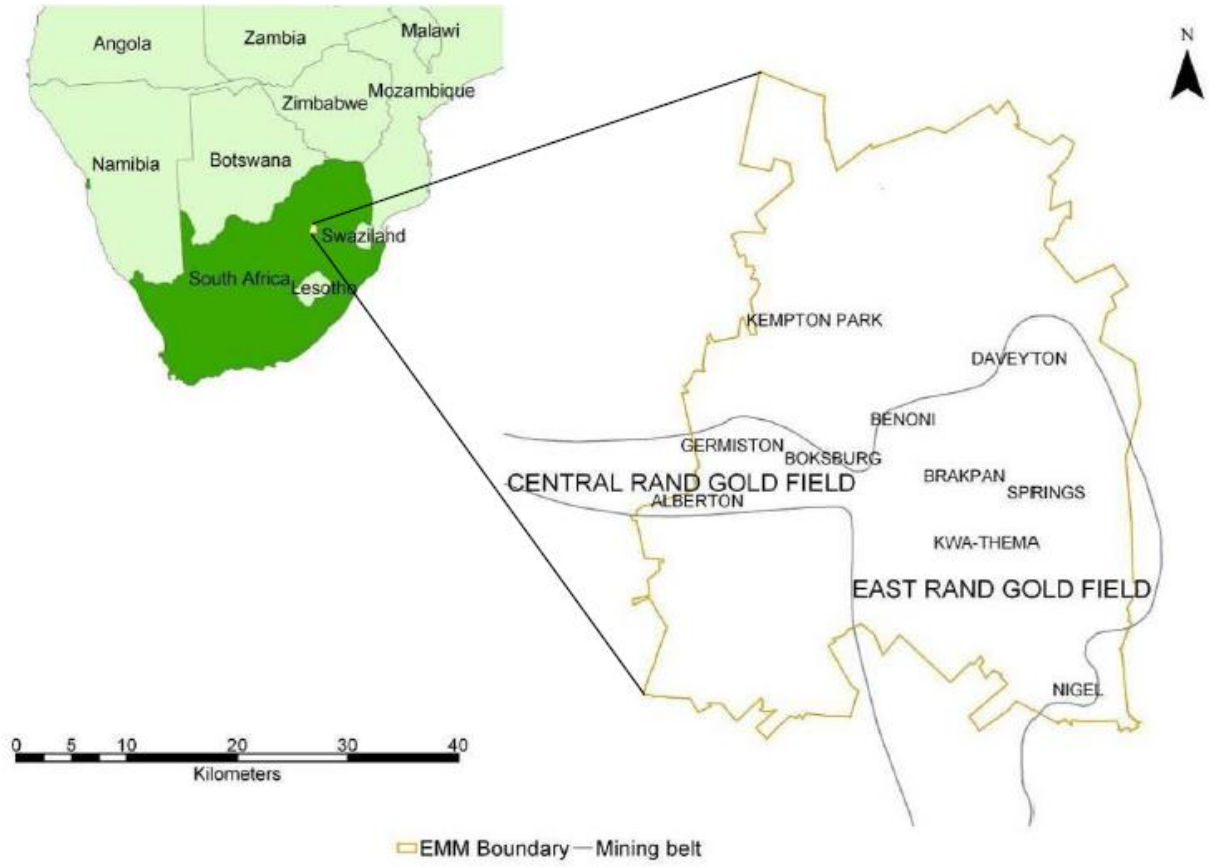

Fig. 3.3 Brakpan, Ergo mining site situated in Ekurhuleni Metropolitan Municipality containing parts of both Central and East Rand gold fields (Sutton, 2012, MSc Thesis, page 56).

3.2.4 Site 4: North West (Vaal Reefs- VRS) (S)

3.2.4.1. Location

The Vaal River Operations are located at the boundary between the North-West and Free State provinces. The mine is shared between the two provinces. The northern portion of the mine lease is situated within the City of Matlosana Local Municipality and under jurisdiction of Southern District Municipality (DC40) in the North West province, and the southern part within the Moqhaka Local Municipality, and under the Jurisdiction of District Municipality of Fezile Dabi (DC20) in the Free State Province. The total mining lease area of the Vaal River

operations is approximately 23 876 hectares (ha). The Local Map for Vaal River Operations within the Reference to AGA is shown in Fig. 3.4 below (AngloGold Ashanti, 2009).

The Vaal River Operations is surrounded by a number of following towns including Orkney which is surrounded by the Vaal River Operations; Klerksdorp that is located 18 km to the North-West; Potchefstroom which is located 50 km to the East; Bothaville which is located 45 km to the South; and Leeudoringstad that is located 56 km to the South–West (AngloGold Ashanti, 2009).

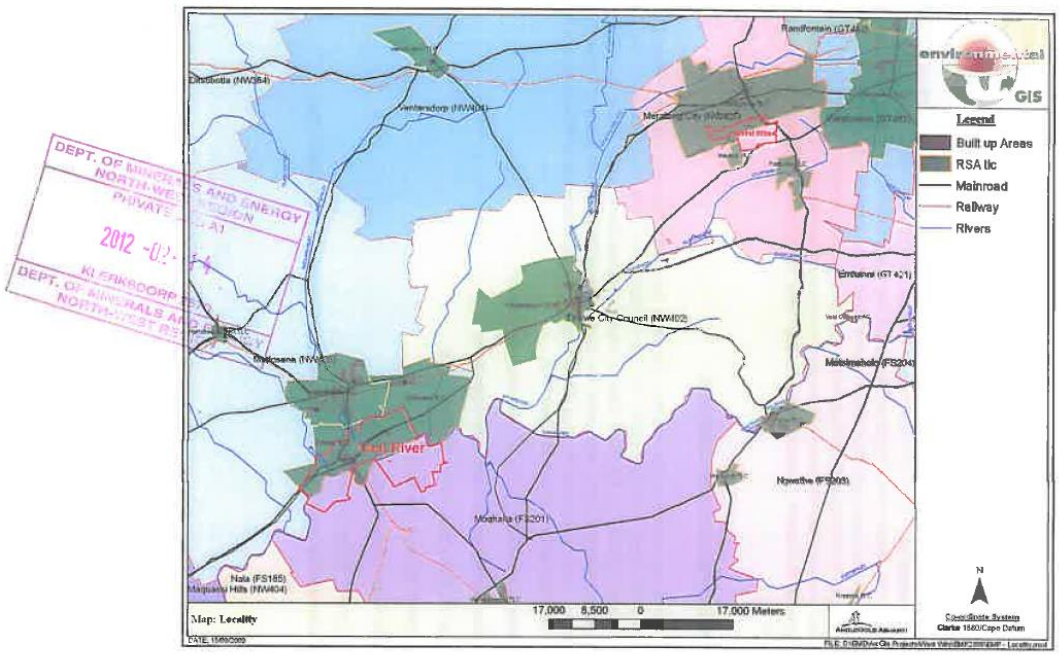

Fig. 3.4 The Local Map for Vaal River and West Wits mining Operations within the Reference to AGA (AngloGold Ashanti, 2009).

The Vaal River Operations comprises mainly of four (4) deep gold mines (Tau Lekoa Mine, Moab Khotsong Mine, Great Noligwa Mine and Kopanang Mine) and supporting infrastructure such as metallurgical plants (where gold, uranium and sulphuric acids are produced), a chemical laboratory, tailing storage facilities,

waste rock dumps and supporting services (land management, mine services, commercial services and sustainable development) (AngloGold Ashanti, 2009).

3.2.4.2. Geology and Soil

The Vaal Reef is usually 50 cm or less thick and well mineralized, with nodular and crystalline pyrite, gold, uraninite and carbonaceaous mater concentrated along the base of the conglomerate layer. The soil is impacted by acid rock drainage and slimes spillage (i.e. toepaddock soils next to slime dam). More than 50% of the main soil types are relatively shallow (50 -150 mm) and rocky, with dominant soil forms of Glenrosa & Mispah Dolomitic (chert-rich) (Mucina and Rutherford, 2006).

In general the conglomerate (reef) matrix consists micaceous minerals such as sericite, pyrophyllite, muscovite, chlorite and chloritoid (10-30%); pyrite (3-4%); other sulhides, e.g. pyrrhotite, chalcopyrite, pentlandite, galena, cobaltite, sphalerite, gersdorffite, linnacite and arsenopyrite (1-2%); grains of primary minerals such as chromite, rutile. garnet, zircon, xenotime, ilmenite and tourmaline, alteration products such as goethite and leaucoxene and secondary minerals such as anatase and skutterudite (1-2%). Gold and uranium (predominantly as uraninite (UO_2)) are mainly found in the matrix (Suruchi and Khanna, 2011, Liebenberg, 1957). A naturally rocky ridge (Black Reef rocks) constitutes the northern boundary of the mine lease area. Other man-made structures such as headgears, TSF and waste rock dumps altering the topography of the landscape, also occur (AngloGold Ashanti, 2009).

The main geological landscape in the Klerksdorp gold field includes the Witwatersrand, Transvaal, and Ventersdorp Supergroups as well as the Swazian Basement granites. Tailings from gold recovery still contain low concentrations of gold and may contain economically recoverable sulphur in the form of pyrites. Historically, low-grade (i.e. uneconomic) ore was sometimes disposed of on waste rock dumps (AngloGold Ashanti, 2009).

3.2.5 Site 5: West Witwatersrand Gauteng, (West Wits – WW) TSF.

3.2.5.1. Location

The West Wits Operations are situated approximately 75 kilometers (km) west of Johannesburg within the Gauteng Province. The site is approximately 7 km South of Carletonville, which is in North West Province. It is also surrounded by other neighbouring towns, namely Fochville and Potchefstroom, which are situated 12 km and 50 km respectively to the South and West of the mine. West Wits has occupied approximately 4176 hectares of land which straddle the boundary between Gauteng and North West Provinces (Rex *et al*., 2009). Fig. 3.5 below shows a regional map and Fig. 3.6 shows an operation area occupied by West Wits. Witwatersrand also denotes the greater Johannesburg metropolitan area, which spans the length of the gold-bearing reef. The metropolitan area is oblong in shape and runs from the area of Randfontein and Carletonville in the west to Springs in the east. It includes the vast urban areas of the East and West Rand, and Soweto.

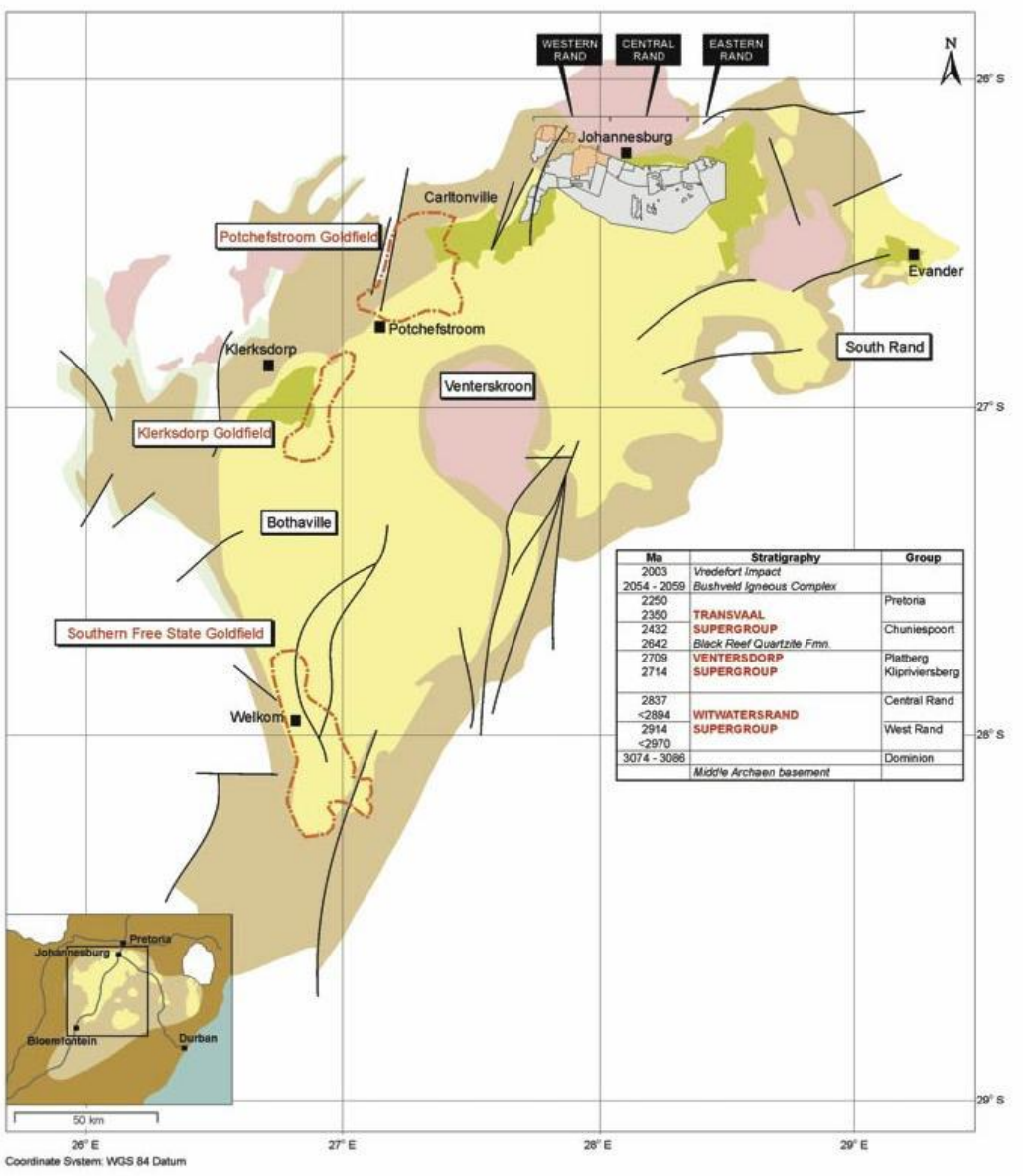

Fig. 3.5 Overview of the Witwatersrand Geological Formation (Source: West Wits Mining, 2008).

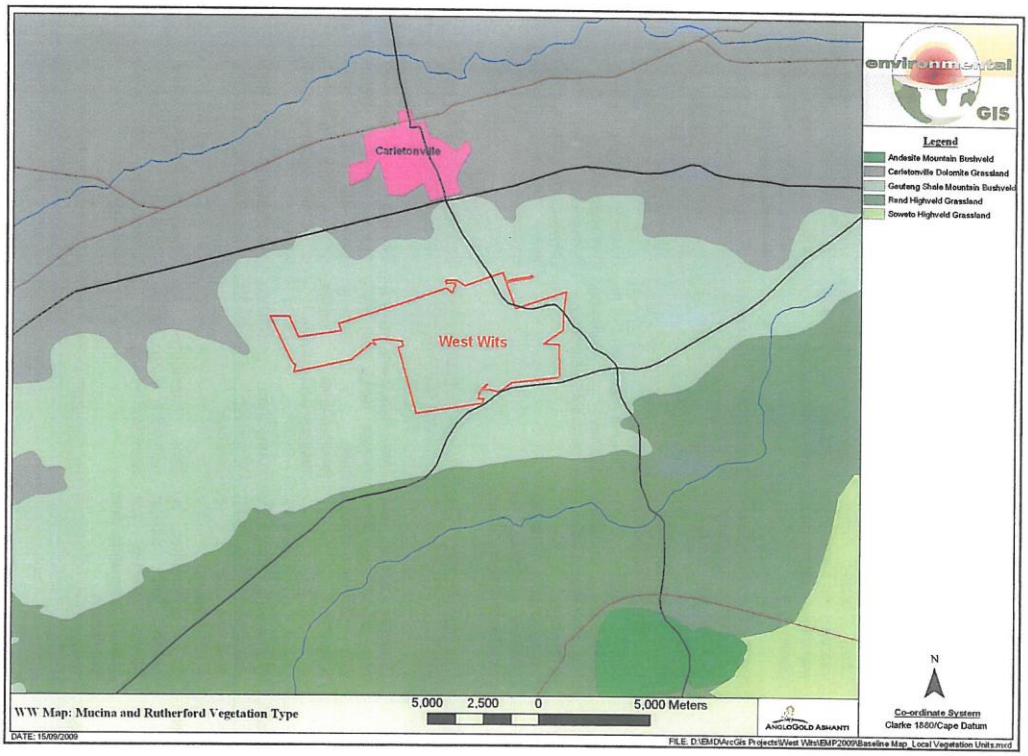

Fig. 3.6 An operation area occupied by West Wits (AngloGold Ashanti, 2009).

3.2.5.2. Geology and Soil

The Witwatersrand basin constitutes one of the great metalogenic provinces of the world when it comes to gold and uranium deposits. The Witwatersrand sedimentary basin has been deposited over an estimated time period of 360 million years (Ma) in the Proterosoic time period between 3 074 and 2 714 Ma (Robb and Robb, 1998) on a granite greenstone basement known as the Kaapvaal Craton (McCarthy and Rubidge, 2005). Soil is impacted by acid rock drainage and slimes spillage (i.e. toepaddock soils are next to slime dams). Clovelly, Avalon. Timeball Hill shales. Gold tailing dams from the Witwatersrand Basin usually contain elevated amounts of heavy metals and radionuclides. Uranium, in the form of uraninite (UO_2) and brannerite (UTi_2O_6) is normally associated with gold-bearing ores in the basin.

As a result of acid mining drainage (AMD), uranium is released into groundwater and fluvial systems. Its transport and immobilisation depend strongly on the uranium species and prevailing geochemical conditions. Mining of South Africa gold, platinum and base metal resources has given rise, in the Gauteng Province alone, to approximately 150 tailings dams, covering an approximate 12,000 ha of land. Uranium is generally associated with the gold ores of the Witwatersrand, at times at concentrations which may be economically viable for extraction as a by-product to the gold. Uranium and its radiogenic progeny are therefore found in many of the residues and waste produced in the mining and processing of Witwatersrand ores. Uranium has been an important by-product of gold mining.

It occurs with gold and a host of other minerals in the Witwatersrand Basin and can be at the elevated concentrations of between 100 and 300 ppm (Cole, 1998; Fourie *et al.,* 2008). West Wits Mines exploits the Carbon Leader Reef (CRF) and the Ventersdorp Contact Reef (VCR) gold bearing reefs, present in the Johannesburg and Turffontein subgroups, respectively. The Conglomerate (reef) Matrix generally consist of micaceous minerals such as sericite, pyrophyllite, muscovite, chlorite and chloritoid (10-30 percent): pyrite (3-4 percent): other sulphides (e.g. pyrrhotite, chalcopyrite, pentlandite, galena, cobaltite, sphalerite, gersdorffite, linnacite and arsenopyrite) (1-2 percent); grains of primary minerals such as chromite, rutile, garnet, zircon, xenotime, ilmenite and tourmaline, alteration products such as goethite and leucoxene and secondary minerals such as anatase and skutterudite (1-2 percent). Gold and uranium (predominantly as uraninite (UO2) are mainly found in the matrix (Suruchi and Khanna, 2011; Liebenberg, 1957).

3.2.6 Site 6: Gauteng, East Rand (ER2A) ERGO Metallurgical Plant (MP), (A2+A5).

3.2.6.1. Location

Soil impacted by emissions from the stack and spill. Hutton, Glenrosa. Dolomitic. Gauteng has an alternating climate between warm, moist summers and cool dry

winters. As mentioned in site 3 above, the mean daily temperatures vary between 21.2°C in the summer and 9.8°C in the winter (Schulze, 1997).

Fig. 3.7 The Gauteng grassland biomes (Schulze, 1997).

3.2.6.2. Geology and Soil

The host rock containing precious or industrial minerals is a critical aspect of any mining related development. The soil is contaminated with elements such as gold, and uranium. Apart from controlling the distribution and grade of mineral deposits, the rock structure, texture and mineralogy can impact the terrain morphology, drainage development and type of channels, groundwater flow and chemistry and the nature of solid, fluid or gaseous emanations that can affect the environment (GDACE, 2008).

3.2.7 Site 7: Gauteng, East Rand (ER2D) ERGO Metallurgical Plant (MP), (D1).

3.2.7.1. Location

Soil impacted by emissions from the stack and spill. Hutton, Glenrosa. Dolomitic. Gauteng has an alternating climate between warm, moist summers and cool dry

winters. As mentioned above Mean daily temperatures vary between 21.2°C in the summer and 9.8°C in the winter (Schulze, 1997). See site 3 and 6 above.

3.2.7.2. Geology and Soil

It resembles similar geological features as site 3 and site 6 above. Its soil is impacted by emissions from the stack and spill. Hutton, Glenrosa, Dolomitic. For more details see site 3 and site 6 above.

3.2.8 Site 8: North West - Vaal Reefs (M) (VRM).

3.2.8.1. Location

The Vaal River Operations are located at the boundary between the North-West and Free State provinces. The mine is shared between the two provinces. The total mining lease area of the Vaal River operations is approximately 23 876 hectares (ha). (AngloGold Ashanti, 2009). The Vaal River operation is surrounded by a number of towns including Orkney; Klerksdorp; Potchefstroom; Bothaville; and Leeudoringstad (AngloGold Ashanti, 2009). For more details see site 3 and 6 above.

3.2.8.2. Geology and Soil

Vaal River Operations is largely situated on dolomitic substrata which are subjected to the formation of sinkholes. Dolomite is a calcium-magnesium carbonate rock with a distinctive “elephant skin” texture. This kind of rock is susceptible to dissolution from the percolation of rainwater and the flow of sub-surface water, which results in the formation of underground cavities and caves. The process of weathering also results in the formation of a complex residual soil mantle known as “wad”, overlaying the dolomite bedrock. Wad is low density, weak material that is easily eroded and highly compressible, thus unsuitable for foundations. The host rock containing precious or industrial minerals is a critical aspect of any mining related development. Apart from controlling the distribution and grade of mineral deposits, the rock structure, texture and mineralogy can

impact the terrain morphology, drainage development and type of channels, groundwater flow and chemistry and the nature of solid, fluid or gaseous emanations that can affect the environment (GDACE, 2005). The soil is impacted by acid rock drainage and slimes spillage (i.e. toepaddock soils next to slime dams). Glenrosa & Mispah. Dolomitic (chert-rich). See site 4 above.

Table 3.1 Localities and the substratum characteristics of the sample sites

Sites	Mining Sites	Substratum Characteristics	Soil Class	Surface Geology	GPS Co-ordinates	Contaminants of concern:
Site 1	North West Rustenburg Lonmin (**L**) Platinum Base Metal Refinery spill.	Soil impacted by spillage from the base metal refinery (receives ore from the Merensky Reef and the UG2 Reef).	Mispah, & black turfs (vertisols), and Arcadia (deeper, red soils).	Basic rocks - chromitite, ultramafic at study site, pockets of sheet granite outcrops.	Not Recorded.	Al, Mg, Na, S, Co, Cr, Cu, Fe, Mn, Ni, Se, Bi, V, As, Zn, Cd, La, Pt, Ir, Rh, Gd, Th, Te, Pb,
Site 2	Agnes Serpentine Mine (**AGM**), Mpumalanga.	Soil impacted by HCl and metal contamination from a Zn galvanising plant. site is an open field of *Berkheya coddii*, on serpentine soil, at the top of the hill above Agnes Mine	Katspruit.	Dolomitic.	Not Recorded.	Al, Mg, Na, Cl, As, Se, Ni, Mn, Fe, V, Zn, Pb, Co, Cu, Cr, Cd, B, Mo.
Site 3	Gauteng, East Rand (**ER1**) ERGO Brakpan slime dam	Soil impacted by ARD and slimes (i.e. footprint of the	Katspruit.	Dolomitic (chert poor).	S - 26.2209	Al, Mg, Na, S, Ni, Mn, Fe, V,

	footprint.	old Withok slime dam next to Brakpan slime dam).			E 28.1846	Zn, As, Se, Co, Cu, Cr, Cd, Au, Bi, Pb, Hg, U.
Site 4	North West (Vaal Reefs-**VRS**)	Soil impacted by acid rock drainage and slimes spillage (i.e. toepaddock soils next to slime dam).	Glenrosa & Mispah.	Dolomitic (chert-rich).	S - 26.94672 E 26.6727	Al, Mg, Na, S, Ni, Mn, Fe, V, Zn, Co, Cu, Cr, Cd, Au, Bi, Pb, Hg, U.
Site 5	Gauteng, (West Wits – **WW**) TSF.	Soil impacted by acid rock drainage and slimes spillage (i.e. toepaddock soils next to slime dam).	Clovelly, Avalon.	Timeball Hill shales.	S - 26.26566 E 27.20901	Al, Mg, Na, S, Ni, Mn, Fe, V, Zn, Co, Cu, Cr, Cd, Au, Bi, Pb, Hg, U.
Site 6	Gauteng, East Rand (**ER2A**) ERGO Metallurgical Plant (MP), (A2+A5).	Soil impacted by emissions from the stack and spill.	Hutton, Glenrosa.	Dolomitic.	Not Recorded.	Al, S, Ni, Mn, Fe, V, Zn, As, Co, Cu, Cr, Cd, Pb, Hg, U

Site 7	Gauteng, East Rand (**ER2D**) ERGO Metallurgical Plant (MP), (**D1**).	Soil impacted by emissions from the stack and spill.	Hutton, Glenrosa.	Dolomitic.	Not Recorded.	Al, S, Ni, Mn, Fe, V, Zn, As, Co, Cu, Cr, Cd, Pb, Hg, U
Site 8	North West - Vaal Reefs (**VRM**).	Soil impacted by acid rock drainage and slimes spillage (i.e. toepaddock soils next to slime dam).	Glenrosa & Mispah.	Dolomitic (chert-rich)	S - 26.55443 E 26.46901	Al, Mg, Na, S, Ni, Mn, Fe, V, Zn, Co, Cu, Cr, Cd, Au, Bi, Pb, Hg, U
Control 1	Grown Nu + Zeolite	Plants were grown in nutrient solution and zeolite + Sand	N/A	N/A	N/A	N/A
Control 2	Control Nu + Zeo + Mycoroot.	Plants were grown in nutrient solution and zeolite + Sand and Mycoroot (a commercial mycorrhizal inoculum)	N/A	N/A	N/A	N/A

3.3 Propagation of AM fungi

3.3.1 Soil sampling and spore extraction

Soil and mine tailing samples were collected from rhizospheres of various plants including *Erograstic Curvula; Phragmites Australistrees*; *Eragrostis Lanchnantha; Berkheya Radula; Tamarix; Asporagus*; and *Exotic Acacia caffras* growing in heavy metal rich sites in South Africa (Gauteng, and North West provinces) (Section 3.1). A minimum of 5 samples were taken with a soil drill that was pushed down to 30 cm in the soil profiles. All soil samples were analysed for their AM fungal spore count, by modification of the methods for wet sieving (Gerdemann and Nicolson, 1963) and centrifugation (Walker *et al.,* 1982). The endo-mycorrhizal spores/sporocarps used were collected from both the field mine tailing soils and pot cultured soils.

Air-dry soil (100 g) was placed in an Erlenmeyer flask (2000 ml volume) and 1000 ml of tap water was added. The mixture was shaken vigorously using a stirring bar or spatula for 5 - 10 min. The flask was removed from the shaker and the soil suspension was allowed to sediment or settles for few minutes. The slurry was decanted or poured through a stack or series of sieves (1000 μm (top), 212 μm (middle), followed by 125 μm and 45 μm (bottom) placed on a wet sieve shaker and washed under continuous running water until water was clear. The content of the 1000 μm sieve was discarded since it contains mainly the organic debris. With a jet of water, the material collected on each sieve was rinsed so as to catch smaller particles on the sieve below. After the contents of the remaining sieves had been washed, they were transferred into three separate centrifuge tubes and centrifuged at 3000 rpm for 3 - 5 min. The supernatant was discarded since it contains substantial amounts of organic debris. After the supernatant had been discarded, 50% sucrose was added to each test tube and mixed thoroughly with a spatula (NB: the sucrose was used to balance the tubes for further centrifugation) before being centrifuged at 3000 rpm for 3 - 5 minutes. Sucrose was utilized here because it separates spores from denser soil components.

Immediately after the sucrose centrifugation, the supernatant was collected from each tube and transferred or poured back into each sieve according to its respective sieve width size. The supernatant was then rinsed and thoroughly washed with a jet of water to remove sucrose. Lines were drawn on the filter paper to create grids (parallel lines were approximately 1cm apart to separate microscope fields for spore counting). Spores were transferred into pre-wetted graded filter paper in a Buchner funnel before the suction filtrate was performed. Filter papers were dried and stored at 4/25°C in Petri dishes for further microscopic observation (Gerdemann and Nicolson, 1963).

3.3.2 Trap pots

To obtain sufficient AM fungi for the greenhouse experiment the AM fungal populations from selected samples were multiplied using *Eragrostis curvula* (*E. curvula*) as a trap plant, under greenhouse conditions. A total of 8 sites were sampled. In each site, 3 replicate pots were used for both experimental pots and controls. About 8 plants in each sample site were used for analysis including morphological and micro-PIXE analysis. Cores of field soil or soil samples were placed or sandwiched in between the 2 h autoclaved sand/silt mixture. Each pot represented a particular site. *Eragrostis curvula* seeds were washed/cleaned by water bubbled in compressed air for about three days to remove the fungicide until they germinated. Germinating seeds were transferred and spread over an autoclaved damped paper towel in a plastic tray. The seedlings were watered by autoclaved distilled water until they produced a cotyledon, which takes about five days depending on the temperature of the room. The seedlings with cotyledon were then planted in pots containing field soil samples sandwiched in autoclaved sand for about 3 to 4 months. The planted pot plants were irrigated three times a week. At maturity, after 4 months, the plants were harvested and new seeds were sown. The cultures were confirmed for root colonisation, and propagule numbers at regular intervals.

3.4 Visualisation of root colonisation

3.4.1 Root staining

For AM fungal colonisation observation, the roots were prepared by the method of Koske and Gemma (1989). Roots were preserved in 50% ethanol for several days, then cut after they had been thoroughly rinsed in tap water and in 50% ethanol. The rinsed roots were heated in 2.5% KOH for 10 to 15 min and rinsed three times in tap water. They were soaked in 20-50 vol of 1% HCl for 24 h and then stained in acidic glycerol/Trypan Blue for 15 min at 90°C. The roots were destained and stored in acid glycerol (50% v/v glycerol and 1% HCl). No bleaching step was performed as the roots were not highly pigmented.

3.4.2 Magnified intersections method for colonisation assessment

The method of McGonigle *et al*. (1990) was used for assessment of root colonisation. This technique involves the estimation of vesicular arbuscular mycorrhizal colonisation on an objective scale of measurement, involving inspection of intersections between the microscope eyepiece crosshair and roots at magnification x 200. This is referred to as the magnified intersections method. Whether the vertical eyepiece crosshair crosses one or more arbuscules is noted at each intersection. The estimate of colonisation is the proportion of root length containing arbuscules, called the arbuscular colonisation (AC). The magnified intersections method also determines the proportion of root length containing vesicles, the vesicular colonisation (VC), and the proportion of root length containing hyphae, the hyphal colonisation (HC). However, VC and HC are interpreted with caution as vesicles and hyphae, unlike arbuscules, can be produced in roots by non-mycorrhizal fungi.

3.5 Methods for morphological identification

Morphological identification was done, where spores were mounted in polyvinyl lactic acid glycerol (PVLG) (Appendix 8) for observation under compound microscope. AM fungal species were identified by spore colour, size, wall

structure, and other morphological characteristics using the manual by Schenck and Perez (1990). All the permanent slides were stored as digital images using a digital camera and subjected to image analysis, as follows. The phase contrast images of broken or whole mounts of a spore were taken with a point-and-shoot digital camera (Nikon CoolPix 990) on a microscope with the eyepiece left in place. The lens of the camera was put in direct contact with the eyepiece, both the camera and the computer were maneuvered until a good image was obtained and the picture was shot. Since the light paths in the camera and the microscope were aligned, there was enough light coming through the lens such that the shutter speed was less than $1/60^{th}$ of a second. The zoom feature on the computer was also used to get a more detailed view of the specimen's area of interest.

3.6 Methods for molecular analysis

3.6.1 Sample preparation

A known number of spores were stored frozen in small aliquots of sterile distilled water. Clean and shiny AM fungal spores (10-80) of the same morphotype according to spore size, shape and colour were collected with forceps from the Whatman filter paper in Petri dishes under a binocular microscope and transferred into 1.5 ml sterile microcentrifuge tubes containing 10 µl sterile deionised water. Prior to deoxyribose nucleic acid (DNA) extraction the spores were washed twice in sterile deionised water by vortexing and then centrifugation at 11 000 g for 1 min (Manian *et al.,* 2001).

3.6.2 Preparation of nucleic acids (DNA)

Nucleic Acids (DNA) were prepared in two ways, namely, manual extraction and direct PCR amplification from crushed spores.

3.6.3 Manual DNA extraction

The spores were frozen in liquid nitrogen in 0.5 ml tubes and liquid nitrogen was allowed to evaporate. This step was repeated three times before the spores were crushed thoroughly using a sterile disposable micropestle or a glass Pasteur pipette in 50 µl 2 % CTAB extraction buffer. The extraction buffer was then added to the test tube up to volume of 500 µl. An amount of 15 µl of Proteinase K (20 mg/ml) which was stored at - 20°C was also added to the sample tube which was incubated at 65°C for an hour to allow for cell protein digestion (Mello *et al*., 1996). To ensure mechanical disruption, about 5 sterile glass beads (1 mm in diameter) were placed into the micro centrifuge tubes and vortexed for 1 min before being centrifuged at 13 000 rpm for 2 min.

The supernatant was transferred to a new sterile micro centrifuge tube. Because the DNA is in the supernatant, care was taken so as to avoid getting any debris from the pellet into the separated supernatant. The debris was also frozen and kept as a backup of the sample. Proteins were denatured and removed from the sample by adding 500 µl cold phenol: chloroform: isoamyl alcohol (25:24:1 v/v/v). The samples were vortexed and centrifuged at 13 000 rpm for 2 min. The upper aqueous layer containing nucleic acids was removed and placed in a new sterile micro centrifuge tube. About 500 µl cold chloroform: isoamyl alcohol in a ratio of 24:1 was added to the micro centrifuge tube containing the nucleic acids to purify the DNA. The micro centrifuge was vortexed and centrifuged at 13 000 rpm for 2 min. The upper aqueous layer containing DNA was removed and placed in new sterile micro centrifuge tubes. An amount of 50 µl (3 M, pH 5.2) sodium acetate was added into the test tube and filled with 96% ethanol to precipitate out DNA.
The precipitated DNA was incubated at -20°C overnight. On the 2nd day, the sample tubes were removed and mixed gently before pelleting out the DNA by centrifugation at 13 000 rpm for 25 min at 4°C. The supernatant was gently removed and poured off. The pellets were air dried to remove all alcohol by placing the tubes upside down on Kleenex or left opened in rack. The pellet was

resuspended by pipetting up and down in the tube for few minutes in 50 µl sterile milli-Q water and stored at -20°C until required for PCR reactions *(*Manian *et al.*, 2001).

3.6.4 DNA amplification from crushed spores

DNA from single AM fungal spores was also amplified by crushing about 5 to 10 spores directly in a PCR tube using a needle. Spores were transferred into 1.5 ml sterile microcentrifuge tubes containing 10 µl sterile deionised water. Prior to amplification the spores were washed twice in sterile deionised water by vortexing and then centrifugation at 11 000 g for 1 min (Manian *et al.*, 2001). The crushed spores were used directly as template for PCR (White *et al*., 1990).

3.6.5 PCR amplification

PCR amplification was performed using two separate sets of primers; firstly the known universal primers, namely, ITS1 & ITS4 or NS31 & AM1; and secondly, the nested primers, NS1 & NS4 coupled with AML1 & AML2 in a MyCycler^{TM} Thermal Cycler (Bio-Rad, U.S.A).

3.6.5.1. The use of known universal primers

The first PCR amplification attempt was done using universal primers, ITS1 & ITS4 or NS31 & AM1. In both these sets of universal primers the same PCR parameters/conditions were used as follows. Polymerase Chain Reaction was carried out using 0.1mM dNTPs, 10 pmol of each primer, 5 U of *Taq* DNA polymerase and the supplied reaction buffer in total volume of 25 µl as follows: initial denaturation at 95°C for 5 min, followed by 45 cycles at 95°C for 30 sec, 50°C for 30 sec, 72°C for 2 min, followed by a final extension period at 72°C for 10 min. In some instances, the first PCR product from the ITS1 & ITS4 amplification was diluted 1/100 with 1 x Tris-EDTA (TE) buffer.

The dilutions were used as template DNA in a second PCR reaction performed using universal primers, NS31 and AM1 (Helgason *et al.,* 1998; Alguacil *et al*., 2009a) as follows: 3 min initial denaturation at 95 °C, followed by 10 cycles of 30 sec denaturation at 95 °C, 45 sec primer annealing at 48 °C and 2 min extension at 72°C, followed by 35 cycles of 30 sec denaturation at 95 °C, 30 sec primer annealing at 50 °C and 2 min extension at 72°C followed by a final extension period of 10 min at 72 °C and storage temperature of 4°C before the PCR products were removed. Many of these amplifications were unsuccessful, whereafter the nested primers, NS1 and NS4 coupled with AML1 and AML2 designed by Lee *et al*. (2008) were used.

3.6.5.2. The use of AML1 and AML 2 nested primers

Polymerase Chain Reaction was carried out using 0.1 mM dNTPs, 10 pmol of each primer (AML1 and AML 2), 5 U of *Taq* DNA polymerase and the supplied reaction buffer in total volume of 25 µl as follows: initial denaturation at 94°C for 3min, followed by 30 cycles at 94°C for 30s, 40°C for 1min, 72°C for 1min, followed by a final extension period at 72°C for 10 min. The first PCR product was diluted 1/100 with 1 x Tris-EDTA (TE) buffer. The dilutions were used as template DNA in a second PCR reaction performed using primers designed by Lee *et al.* (2008), AML1 (5'-ATC AAC TTT CGA TGG TAG GAT AGA-3´) and AML2 (5´-GAA CCC AAA CAC TTT GGT TTC C-3´) as follows: 3 min initial denaturation at 94 °C, followed by 30 cycles of 1 min denaturation at 94 °C, 1 min primer annealing at 50 °C and 1 min extension at 72°C, followed by a final extension period of 10 min at 72 °C. PCR products from AM fungal spores were not purified but instead were directly sent for sequencing, some to Inqaba Biotech, Pretoria, South Africa (SA) and some to the University of Stellenbosch, Central Analytical Facility, South Africa. The Inqaba Biotech used ABI 3130 XL Genetic Analyzer while Stellenbosch used 3730XL DNA Analyzer, Applied Biosystems.

3.6.6 DNA cloning

PCR, DNA cloning and sequencing of the results, reported in Fig. 5.2 were performed at Inqaba Biotech, Pretoria, South Africa. PCR was performed directly from spores extracted from 2 samples (WW_{05}) site 5 and ($ER_{7.3}$) site 3 using different set of primers (ITS1 & ITS4 or NS31 & AM1). About 1 µl of WW_{05} spore sample containing 10 crushed spores was used for PCR out of 10 µl spore dilution which contained about 104 crushed spores. Similarly about 1 µl of $ER_{7.3}$ spore sample which contained about 10 spores was also used for PCR out of 10 µl spore dilution which contained about 165 spores.

In cloning procedures, a specific DNA fragment is integrated into a rapidly replicating genetic element (plasmid or bacteriophage) so that it can be amplified in bacteria or yeast cells. A clone JET™ PCR Cloning Kit #K1231, #K1232 from Fermentas life science (www.fermentas.com/reviewer) was used. Out of the two types of DNA cloning procedures, namely, Blunt-End cloning and Sticky-End cloning, Blunt-end reaction was used and the blunting reaction was set up as follows:

Ten µl of 2x reaction buffer followed by 2 µl PCR product, 5 µl Nuclease –free water and 1 µl of DNA blunting enzyme were transferred into 1.5 ml sterile microcentrifuge tubes. The mixture was briefly vortexed and centrifuged for 3-5 sec before being incubated at 70 °C for 5 min. The mixture was briefly chilled on ice and the legation reaction was set up before the following blunting reaction mixture, 1 µl pJet 1.2/blunt cloning vector (50ng/5 µl) and 1 µl T4 DNA ligase (5u/ µl) were added to make up a total volume of 20 µl. It was again briefly vortex and centrifuged for 3 to 5 min before being incubated at room temperature (22°C) for 5 min. It should be noted that incubation time can be extended up to 30 min if the maximal number of transformants is required. The legation mixture was used directly for bacterial transformation as indicated in Appendix 7.

3.6.6.1. Transformation steps (PCR-Smart^{tm} Cloning Kit*)*

A 1.5 ml tube was placed on ice for few minutes. A 2 µl of the 20 µl samples ligation reaction mixture was added into the 1.5ml tube that was placed on ice. About 20 µl of the chemically competent cells were also added into 1.5 ml tube. The tube was placed on ice for 30 min after which it was removed and placed at 42°C for 45s and returned back to ice for 2 min. A total volume of 480 µl recovering medium was added to the test tube. This solution was incubated in the shaking incubator for an hour at a speed of 250 rpm. The contents were placed on LB^{AMP} in the following plates; 50 µl was placed in plate 1 while the rest of the solution was added to plate 2. The 2 plates were incubated overnight at 37 °C in a non-shaking incubator.

PCR was performed using P Jet 1, 2 reverse and forward primers. PCR products were sequenced, at Inqaba Biotech, Pretoria South Africa using ABI 3130 XL Genetic Analyzer.

3.6.7 Visualisation of fungal genomic extracts

Nucleic acids were visualized using agarose gel electrophoresis. A 1% agarose gel was prepared consisting of 1g molecular grade agarose (Hispanagar, H0901031) in 100ml 0.5 X TAE buffer diluted from 50 X TAE buffer stock (BioRad, 161-0773). The mixture was boiled until the agarose was completely dissolved and allowed to cool to approximately 40°C. On cooling, 3 to 5µl of 500mg/ml Ethidium Bromide was added to the agarose. The agarose was poured into a gel mould and a comb placed into the gel before it was allowed to set. Once set, the gel was placed in a gel tank filled with 0.5 X Tris-borate-EDTA (TBE) buffer.
When loading the gel, 2 µl of extracted genomic DNA was mixed with 10 µl DNA loading buffer (dye) before loaded into a well in the gel. Simultaneously, 10 µl of λ*Pst1* molecular marker was loaded into the gel to determine the molecular weights of the bands obtained on the gel. The gel tank was connected to a BioRad

Power Pac 300 and electrophoresed for 30 to 45 minutes at 100 volts (V). Gels were visualized using a UVP BioDoc-It Transilluminator System.

3.6.8 Phylogenetic analysis

The phylogenetic tree is made up of fungal sequences used in this experiment. The branch lengths are proportional to genetic distance, which is indicated by the bar. The sequence electropherograms were analysed using Chromas Lite and BioEdit; and manual adjustments were made where necessary for the consensus sequences. Following this, a BLAST was used on the sequence data using the megablast algorithm (Zhang *et al.*, 2000) and both the NCBI BLAST databases (http://blast.ncbi.nlm.nih.gov/Blast.cgi) and Maarj*AM* database (http://maarjam.botany.ut.ee) (Öpik *et al.*, 2010). The mycorrhizal sequences representing different gene regions of fungal isolates obtained from different mining sites were subjected to a multiple sequence alignment using MAFFT version 6 and phylogenetic analysis was performed using MEGA 5 to generate a bootstrapped neighbour-joining tree of the multiple sequence alignment which was visualised using TreeExplorer (Spruyt *et al.*, 2014).

3.7 Methods for ICP-MS and PIXE

3.7.1 Pot study design for synthesis of AM fungal roots

The design of the study included two treatments for each substratum type (see Chapter 3, Section 3.1 for descriptions of sites and Table 3.1) (background arbuscular mycorrhizal fungi only; background AM fungi plus additional mixture of indigenous AM fungal spore inoculum) and two controls (zeolite as growing medium with addition of commercial AM fungal inoculum; zeolite as growing medium without any AM fungi). The commercial inoculum was manufactured by Mycoroot (Pty.) Ltd. SA (http://www.mycoroot.com) and the zeolite was in the form of 1-3 mm granules (Pratley (Pty) Ltd., SA). Treatment pots (10 cm) were filled with slime/soil samples mixed with zeolite at a ratio of 3:1 (3 slime: 1 zeolite). Zeolite was used to increase the porosity of the soil. All treatment pots

were then treated with Previcur® N aqueous fungicide (AgrEvo South Africa) according to manufacturer's instructions and allowed to rest for a week to remove non-AM fungal contamination from the mixture. Previcur (active ingredient Propamocarb-HCl) is active against soil parasites such as *Pythium* but affects AM fungal minimally (http://www.pestmanagement.rutgers.edu/njinpas/postings/Previcurlabel.pdf).

After a week, treatment pots were planted with commercial uncoated *Eragrostis curvula* cv Ermelo seeds (AGRICOL Seed Company, Pretoria, South Africa) and ± 500 AM fungal spores extracted from the respective slime soil samples were added to the one set of treatments to increase the likelihood of root colonisation. The pots were placed in the greenhouse conditions between a temperature range of 20°C to 25°C and were allowed to grow for sixteen weeks, watered at a rate of 50% volumetric field capacity every third day and the controls fertilised once a week with 10 ml to 20 ml of a commercial multinutrient solution (Appendix 4) (Multifeed Classic, Plaaskem).

3.7.2 Soil analyses (pH, P, extractable cations & organic C)

It is important to determine the (a) total and (b) exchangeable, and (c) extractable concentrations (by various extractants with biological relevance to plants – such as the BCR sequential extraction methods), as well as (d) the natural levels of these elements in polluted metalliferous soils. This information assists in setting realistic and technically achievable end-points for site decontamination. The original slime soil samples were analysed by Bemlab (Appendix 6). Thus soil samples for chemical analyses were taken from the 0-30 cm layer with an auger. The soil was air dried, sieved through a 2 mm sieve for determination of stone fraction (weight/weight basis) and analysed for pH (1.0 M KCl), P (Bray II) and total extractable cations, namely K, Ca, Mg and Na (extracted at pH = 7 with 0.2 M ammonium acetate) and organic matter by means of the Walkley-Black method (The Non-affiliated Soil Analyses Work Committee, 1990). Micro-elements (Zn, Mn, Cu & Fe) were extracted with Di-ammonium EDTA (0.02 M) and boron (B) using a 1:2 hot water ratio (The Non-affiliated Soil Analyses Work Committee, 1990). The extracted solutions were analysed with a Varian ICP-OES optical emission spectrometer. Salinity was determined by measuring the resistance of saturated paste in an electrode cup according to the method described by The Non-affiliated Soil Analyses Work Committee (1990). Extractable acidity was extracted with 1M KCl and determined through titration with 0.05 M NaOH (The Non-affiliated Soil Analyses Work Committee, 1990).

3.7.2.1. Exchangeable acidity

Exchangeable acidity of the soil was expressed as the total OH^- that is neutralised by Al^{3+} and H^+ that occurs on the exchange sites. Both Al^{3+} and H^+ were extracted with 1N KCl and titrated to the end-point with NaOH (0.01M). The acidity is expressed as an equivalent of H^+ in cmol(+)/dm^3 soil (Soil Analyses Work Committee, 1990).

3.7.2.2. Total Phosphorus (P) in soil

Total P in soil was determined by a method adapted from that described by Sommers & Nelson (1972). The P was extracted from soil through acid digestion using a 1:1 mixture of 1 N nitric acid and hydrochloric acid at 80oC for 30 minutes. The P concentration in the extract was then determined with a Varian ICP-OES optical emission spectrometer.

3.7.2.3. Total Carbon (C) and Nitrogen (N) in soil

Both total C and N content of soil were determined through total combustion using a Leco Truspec® CN N analyser.

3.7.2.4. Total NH_4^+ and NO_3^- concentration in soil

Ammonia and nitrate are extracted from the soil with 1N KCl. Its concentration in the extract is then determined colorimetrically on a SEAL AutoAnalyzer 3.

3.7.2.5. Cation exchange capacity (CEC) of soil

The soil's CEC was determined using 0.2 M ammonium acetate (pH=7 as extractant of exchangeable cations) method as described by The Non-affiliated Soil Analyses Work Committee (1990), where after the soil is leached with 0.2 M K_2SO_4. The total NH_4^+ is then extracted with 1N KCl and determined colorimetrically as indication of CEC on a SEAL AutoAnalyzer 3 with a 15 mm flow cell and 520 nm filter.

3.7.2.6. Soil texture (% clay, silt & sand) and water holding capacity

Chemical dispersion was done using sodium hexametaphosphate (calgon) while three sand fractions were determined through sieving as described in the Non-affiliated Soil Analyses Work Committee (1990). Silt and clay were then determined using sedimentation rates at 20^{o}C, in a ASTM E100 (152H-TP) hydrometer. The soil water holding capacity is determined mathematically from

the soil texture using a calculation model adapted from that of Saxton *et al*. (2006).

3.7.2.7. Soil moisture

The gravimetric soil water content was determined on a mass/mass basis by drying the soil over night at 101^{o}C.

3.7.2.8. Bulk density

Bulk density of sieved soil was determined by weighing 60 cm^3 soil at 20^{o}C and expressing it as kg/m^3.

3.7.2.9. Total chloride in soil

Using the method described by Chapman & Pratt (1961), chloride concentration in soil was determined volumetrically through titration of a soil extract (0.1M KNO_3) with 0.043 M $AgNO_3$ using potassium dichromate (K_2CrO_4) as indicator. Titration is done up to the point when the extract changes colour from orange to brown-red.

3.7.3 ICP-MS analysis of roots

ICP-MS analysis was first performed on samples of the roots for the elements Cr, Fe, Ni, P, K, Pt, Ti, Mn, Cu, Zn, and U as baseline data for setting parameters during PIXE analysis (Appendix 9). The roots were processed as follows:
Five plants from each sample site were washed under running tap water until all the soil was removed, inserted into brown paper bag and oven dried at 70°C for 24 h. The dried plants were ground into powder using a pestle and mortar. A sample mass of 0.1 g was dissolved in 10 ml of a digestion solution (8 ml HNO_3 and 2 ml H_2O_2) before it was run into a Liners Teflon for 30 min at 600 Watts. The liquid was transferred into a 10 ml volumetric flask. Where the sample had lost 1 to 2 ml through evaporation, the volumetric flask was filled up with deionized water. The

ICP-MS was then run using a multiwave 3000 (Anton Paar GmbH) solvent also known as microwave digestion. The results are recorded in Appendix 9.

3.7.4 Preparation of plants for Micro-PIXE analysis.

Plants were washed under running tap water until all the soil ran out of the roots. The root length was measured and root samples from 2 to 3 plants were observed under phase contrast light microscopy to ascertain and document the extent of root colonisation so as to select the appropriate parts of the roots for cryopreparation **(**Fig. 4.1).

3.7.5 Cryofixation

Cryofixation is a low temperature method used to preserve the distribution and structure of all components in a biological system and aims at the ultra-rapid freezing of the specimen during which the intracellular movements are arrested in milliseconds (Hayat, 1989). A suitable cryogen is liquid propane, which has a much higher cooling rate than liquid nitrogen. Eight plants from each sample site were used for cryopreparation. Roots were thoroughly washed in deionized water and sections showing mycorrhizal colonisation were excised and transferred into gelatin capsules. The cryofixation process was performed in a clean environment using the Leica EM CPC cryo-workstation. The roots were quenched in liquid propane (-185°C) which was cooled by liquid nitrogen (-196°C).

3.7.6 Freeze drying

The frozen root samples were freeze-dried in a Leica EM SFD Cryosorption Freeze Dryer following a 48 h programmed cycle starting at - 80°C, and ending at ambient temperature. The chamber was cooled by a thermal junction connected with a Dewar filled with liquid nitrogen. After the termination of the freeze-drying process, the chamber was slowly heated up to room temperature to prevent water condensation on the samples. Both the root cross-section and the long root sections of the free-dried root samples were obtained by hand-sectioning under a

stereo-microscope using a stainless steel razor blade, and mounted between two layers of 1% (w/v) Formvar film with Araldite glue (Figs. 3.8 and 3.9). To prevent charge build-up during measurements, the Formvar membrane facing the proton beam was coated with a thin layer of carbon. Light micrographs of each specimen were taken before and after proton irradiation. In order to evaluate elemental distribution in various root tissues, only intact root cross-sections and long root sections were used in the micro-PIXE analysis.

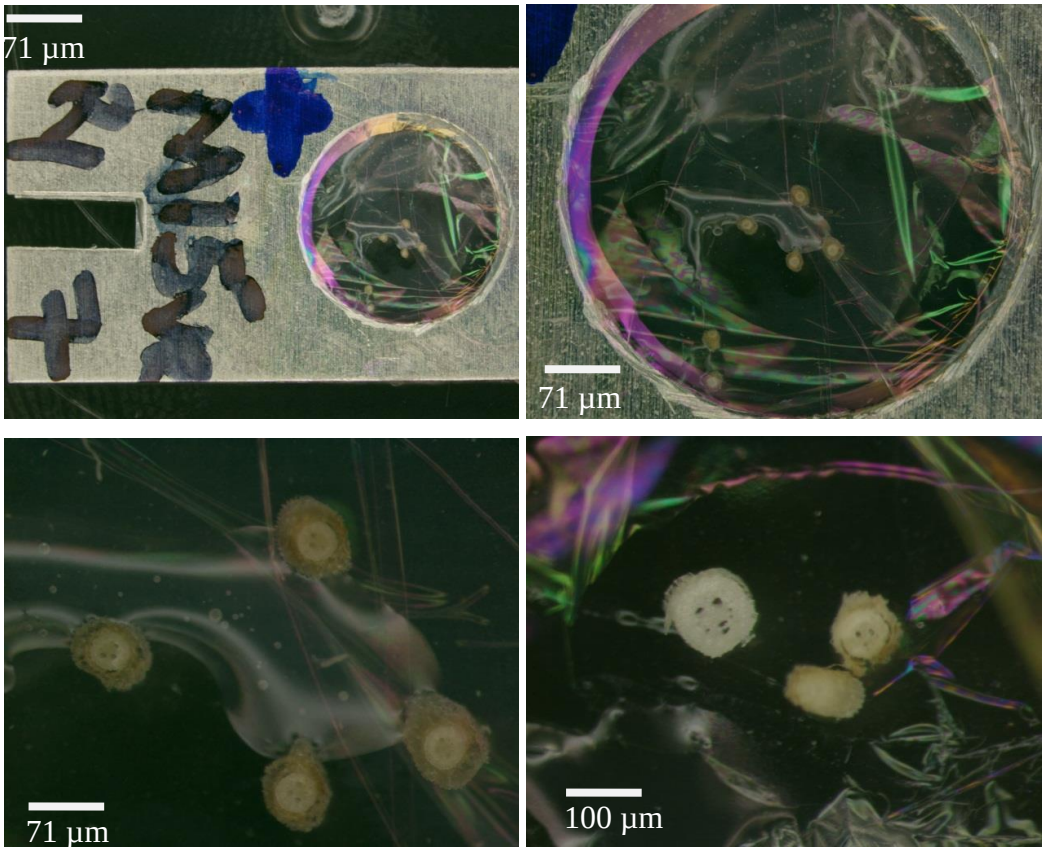

Fig. 3.8 Specimen holders with root cross-sections photographed under a SMZ 1500 Nikon light microscope.

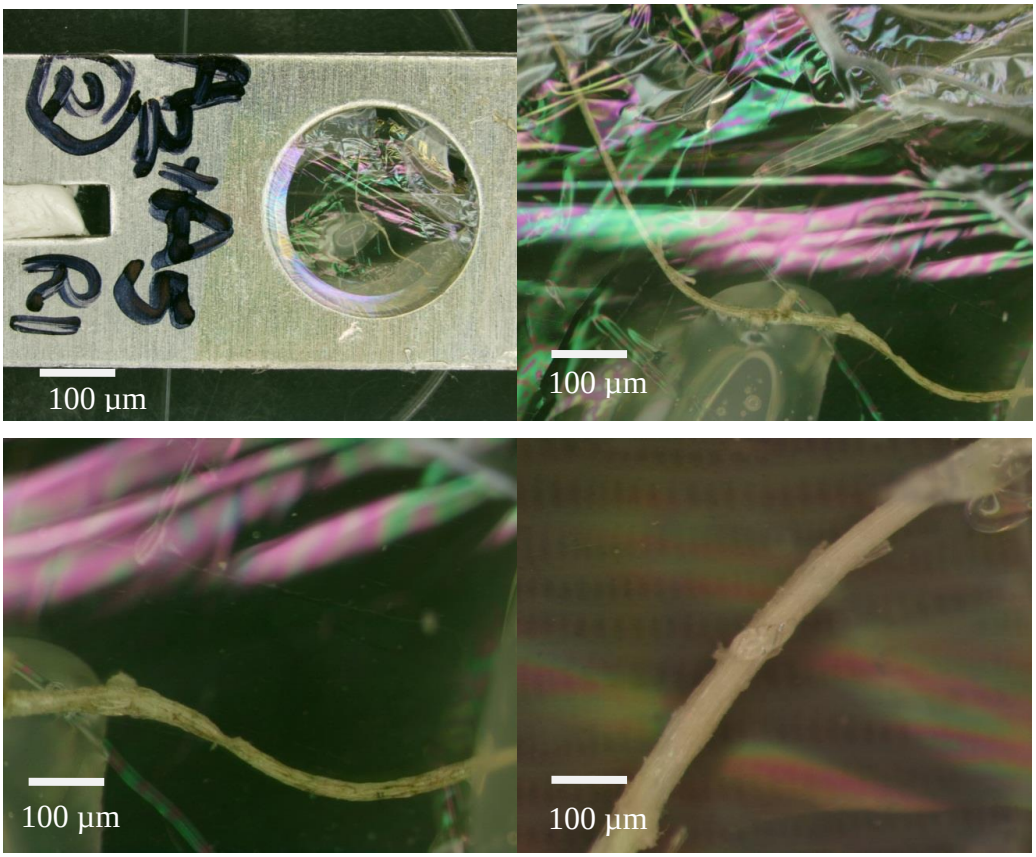

Fig. 3.9 Specimen holders with long roots photographed under a SMZ 1500 Nikon light microscope.

3.7.7 Instrumentation and analytical method

Microanalyses were performed using a nuclear microprobe (Fig. 3.10) at the Materials Research Department, iThemba LABS, South Africa as previously described (Prozesky *et al.,* 1995; Przybyłowicz *et al.,* 1999; Przybyłowicz *et al.,* 2005). A proton beam of 3 MeV energy, provided by the 6 MV single-ended Van de Graaff accelerator, was focused to a 3 x 3 μm^2 spot and raster scanned over the areas of interest (dwell time 10 ms), using square or rectangular scan patterns with a variable number of pixels (up to 128 x 128). Vacuum inside the chamber was of the order of $5.5x10^{-5}$ mbar during analysis and currents below 120 pA were used, to minimize beam damage of the specimens. Particle-induced x-ray emission (PIXE) and proton backscattering (BS) were used simultaneously. PIXE spectra were registered with a Si(Li) detector manufactured by PGT (30 mm^2 active area

and 8.5 μm Be window) with an additional 125 μm Be layer as an external absorber.

The effective energy resolution of the PIXE system (for the Mn Kα line) was 160 eV, measured for individual spectra. The detector was positioned at a take-off angle of 135^{o} and a working distance of 25 mm. The X-ray energy range was set between 1 and 36 keV. BS spectra were recorded with an annular Silicon (Si) surface barrier detector (100 μm thick) positioned at an average angle of 176°. Data were acquired in the event-by-event mode. The normalization of results was done using the integrated beam charge, collected simultaneously from a Faraday cup located behind the specimen and from the insulated specimen holder. The total accumulated charge per scan varied from 221 nC to 3546 nC.

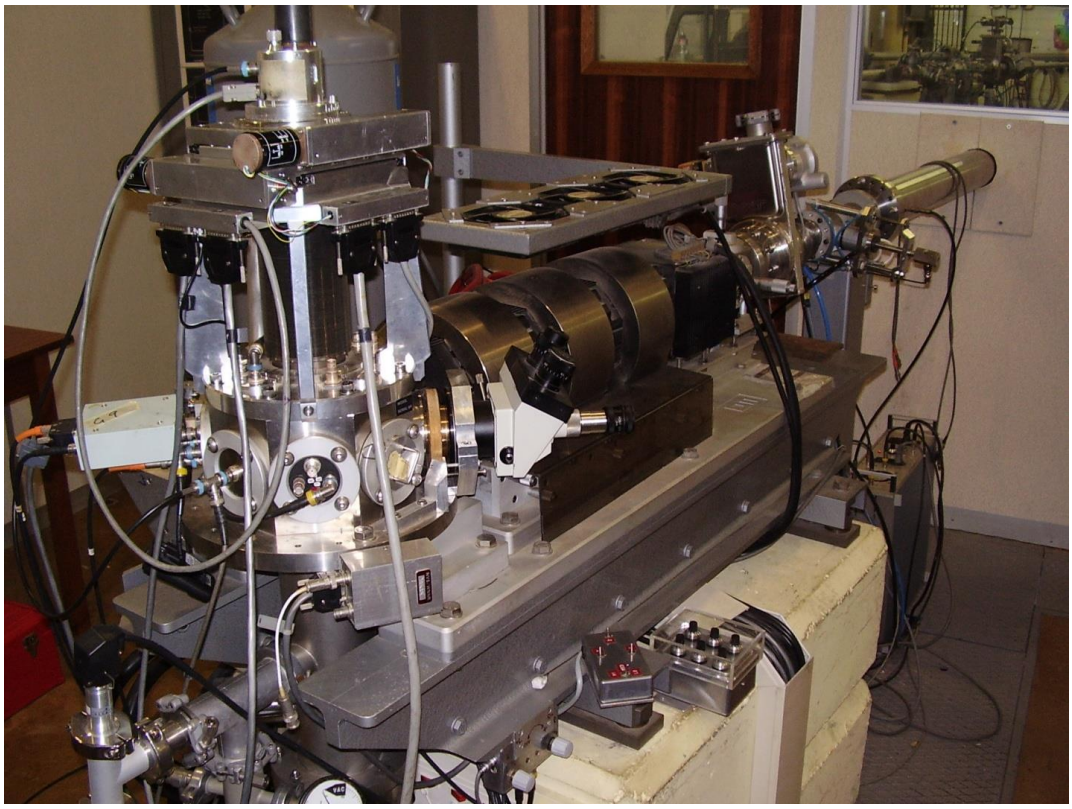

Fig. 3.10 Nuclear Microprobe (NMP)

Quantitative results were obtained by a standardless method using GeoPIXE II software package (Ryan *et al.,* 1990a; Ryan *et al.,* 1990b; Ryan, 2000). The error estimates were extracted from the error matrix generated in the fit, and the minimum detection limits (MDL) were calculated using the Currie equation (Currie, 1968). The detailed calibration of detector efficiency, the thickness of the selectable X-ray attenuating filters and studies on the accuracy and precision of the PIXE analyses using the nuclear microprobe (Fig. 3.10) at iThemba LABS have been reported by van Achterbergh *et al.* (1995).

The procedures reported were used for each new detector or added filter. Before each series of measurements, the calibration of the system was tested by a few measurements on pure elements, and synthetic glasses with known quantities of selected minor elements (internal standards), the X-ray peaks of which cover practically the whole measurable energy range. Such quality control helps in identifying potential problems related mostly to charge measurements and, occasionally, change of the specimen–detector distance (Przybyłowicz *et al.*, 2005). Quantitative elemental mapping was performed using the *Dynamic Analysis* method (Ryan and Jamieson, 1993; Ryan *et al.,* 1995; Ryan, 2000). This method generates elemental images which are (i) overlap-resolved, (ii) with subtracted background and (iii) quantitative, i.e. accumulated in mg kg^{-1} dry weight units. Maps were complemented by data extracted from arbitrarily selected microareas of roots.

These microareas were: (1) areas covering whole-root sections and (2) areas selected on the basis of root morphology, showing possible colonisation by mycorrhizal fungal structures (vesicles, hyphae and arbuscules), thus complementing the results from images. PIXE and BS spectra were employed to obtain average concentrations from these microareas using a full nonlinear deconvolution procedure to fit PIXE spectra (Ryan *et al.,* 1990a; Ryan *et al.,* 1990b), with matrix corrections based on thickness and matrix composition obtained from the corresponding BS spectra, fitted with a RUMP simulation package (Doolittle 1986) with non-Rutherford cross-sections for Carbon (C),

Oxygen (O), Nitrogen (N). Matrix corrections done on the basis of BS spectrometry results were essential due to the highly variable thickness of analyzed specimens (the area density range was between 0.21 mg/cm^2 and about 5 mg/cm^2). Above 5 mg/cm^2, the specimen was classified as "infinitely thick" for the purpose of PIXE analysis. Elemental concentrations from these areas are also reported in mg kg^{-1} dry weight.

3.8 Statistical Analysis

To determine the significance of concentration differences between the different sample sites and the controls, a Principal Component Analysis (PCA) was been used. PCA is a useful statistical technique that has found application in fields such as face recognition and image compression, and is a common technique for finding patterns in data of high dimension. It covers standard deviation, covariance, eigenvectors and eigenvalues. PCA is a mathematical procedure that uses a set of orthogonal transformations to convert a set of observations of possible correlated variables into a set of values of linearly uncorrelated variables called principal components.

Prior to running the analysis with Statistical Package for the Social Sciences (SPSS), the data was screened by examining descriptive statistics on each item, correlation matrix and possible univariate and multivariate assumption violation. SPSS is a computer program used for statistical analysis to create classification and decision trees for identifying groups and predicting behaviour**.**

3.8.1 Working with factor analysis

In factor analysis, the aim is to discover which variables in a data set form coherent subgroups that are relatively independent of one another. The more factors one permits, the better the fit and the greater the percent of variance in the data explained by the factor solution. The selection of the number of factors is probably critical. Eigenvalues represent variance; therefore any factor with an

eigenvalue less than 1 is not as important. The number of factors with eigenvalues greater than 1 is an estimate of the maximum number of factors.

3.8.1.1. Tests for factor analysis

Kaiser-Meyer-Olkin (KMO) and Bartlett's test of sphericity produce the KMO measure of the sampling adequacy of how the correlations are for factor analysis. Kaiser (1970 and 1974) indicated that a value of 0.70 or above is considered adequate while Bartlett's test provides a test of the following hypotheses:

H0: the variables are not correlated: versus:

H1: the variables are correlated.

Reject **H0** if p-value < 0.05 level of significance to proceed with the factor analysis.

The Scree plot provides the information to determine the number of factors or components.

CHAPTER 4

4 RESULTS AND DISCUSSION: Morphological Identification of AM fungal spores.

This chapter is divided into results and discussion of root colonisation, spore counts and identification of AM fungi from spore morphology. The results will only focus on the description of the findings while the discussion will focus on the explanation of the results.

4.1 Results

The data in this chapter represents observations and measurements from the pot studies reported in Chapter 3.

4.1.1 Observation and assessment of root colonisation

Some characteristic morphological features of glomeromycotan fungi namely, hyphae, arbuscules, vesicles and spores were observed in roots of *E. curvula* plant under the phase contrast and light microscope (Fig. 4.1). Root colonisation from a) to d) are live roots with no stain, which have extensive hyphae, vesicles and young spores and e) to j) were stained with Trypan Blue. They show proliferation of intracellular arbuscules (e & f), an extensive intraradical vesicles prolification (g) while (h) shows an intraradical storage vesicle and attached hyphae as well as i) & j) showing light micrograph of hyphal colonisation.

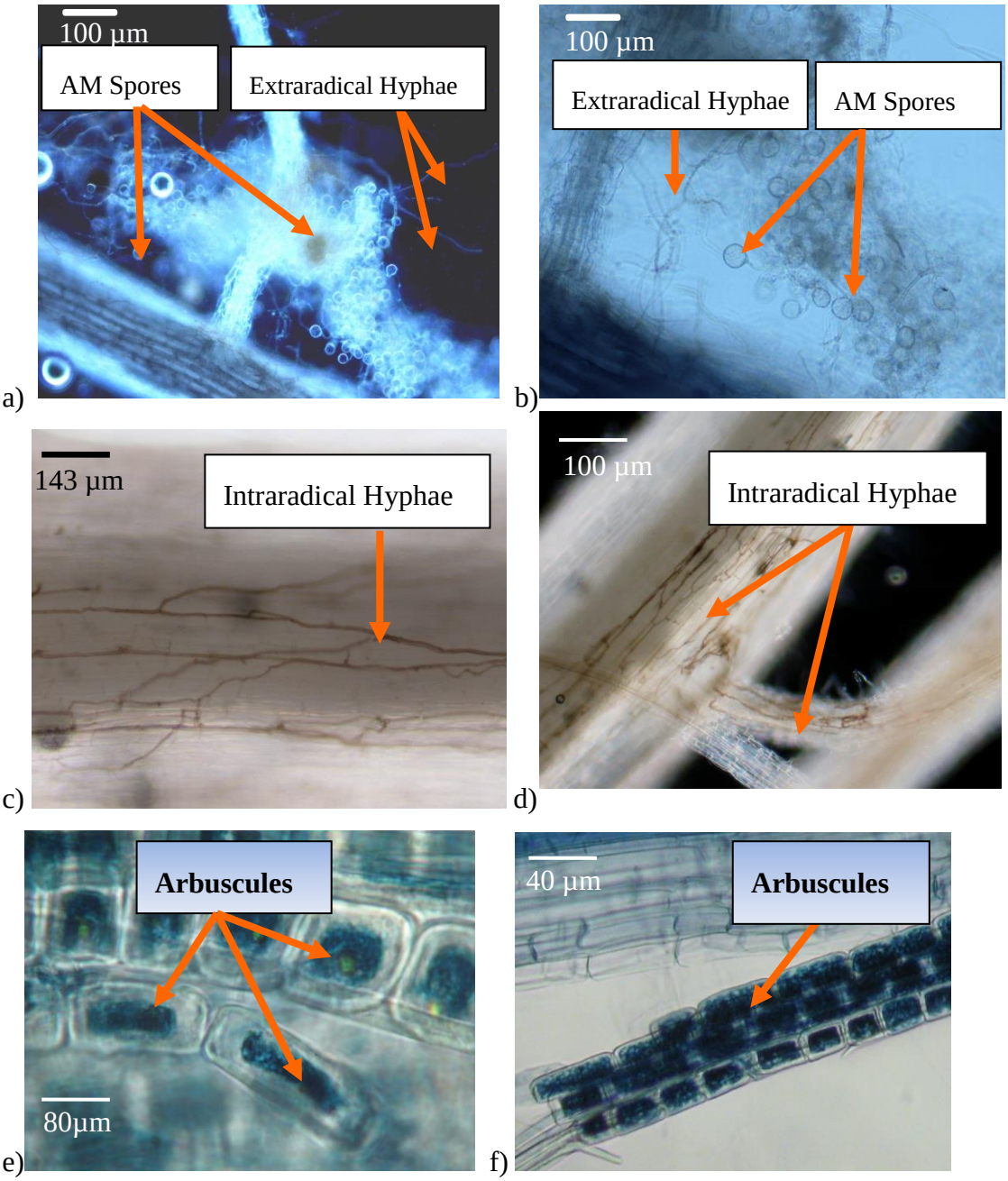

Fig. 4.1 Light micrograph of colonisation structures. a) and b) Extraradical hyphal networks and intercellular vesicles from live roots (site 3); c) and d): Intraradical hyphae from live roots (site 5). e) and f) Intracellular arbuscules (site 1, and 8).

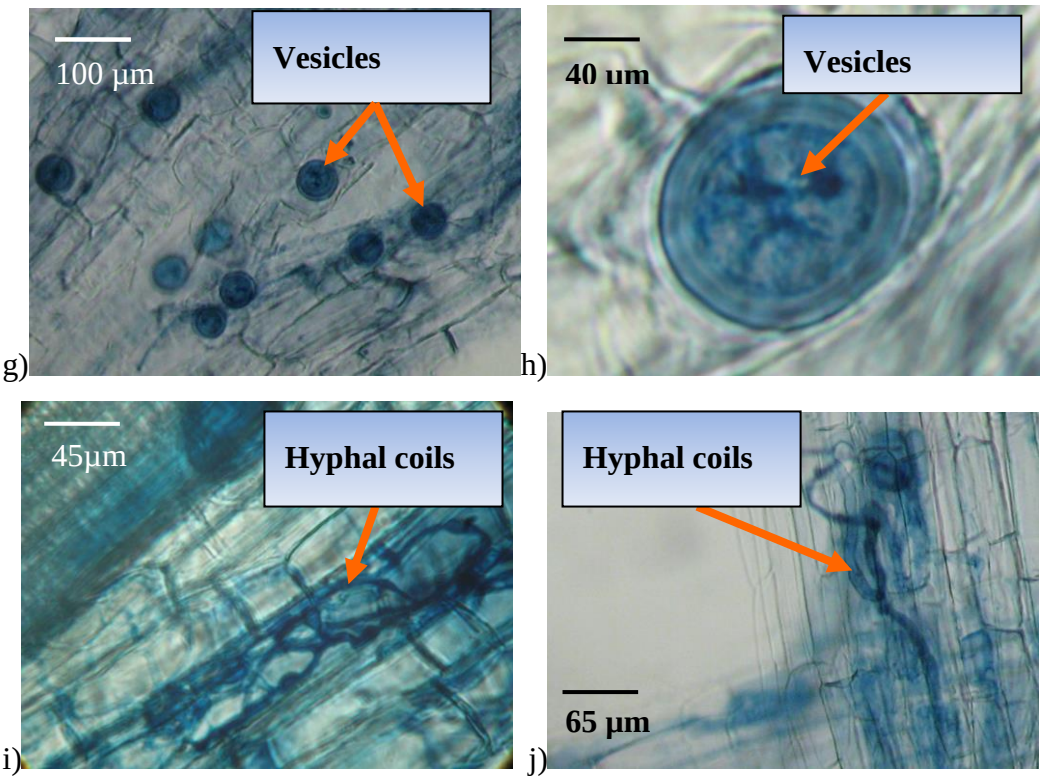

Fig. 4.1g) and h) Intercellular vesicles (site 1). i) and j) Intracellular hyphal coils (Site 8).

Stained roots from the pot plants samples were mounted in the microscope slides and observed under a binocular microscope. Arbuscules, vesicles and hyphae were observed in roots. Hyphae were found to be the most abundant in roots and were followed by vesicles then arbuscules (Fig. 4.2(a-b)). In all the mining sites shown in Fig. 4.2(a-b), the Eastern Reef site 6 showed higher total mycorrhizal root colonisation, followed by West Wits site 5, then site 7, 1, 3, 4, 2, 8 then control 2 and 1 respectively (Fig. 4.2(a-b)). Fig. 4.2b shows accumulative AM fungal colonisation results with the P-value of 0.8013, which is considered not significant as it is greater than 0.05.

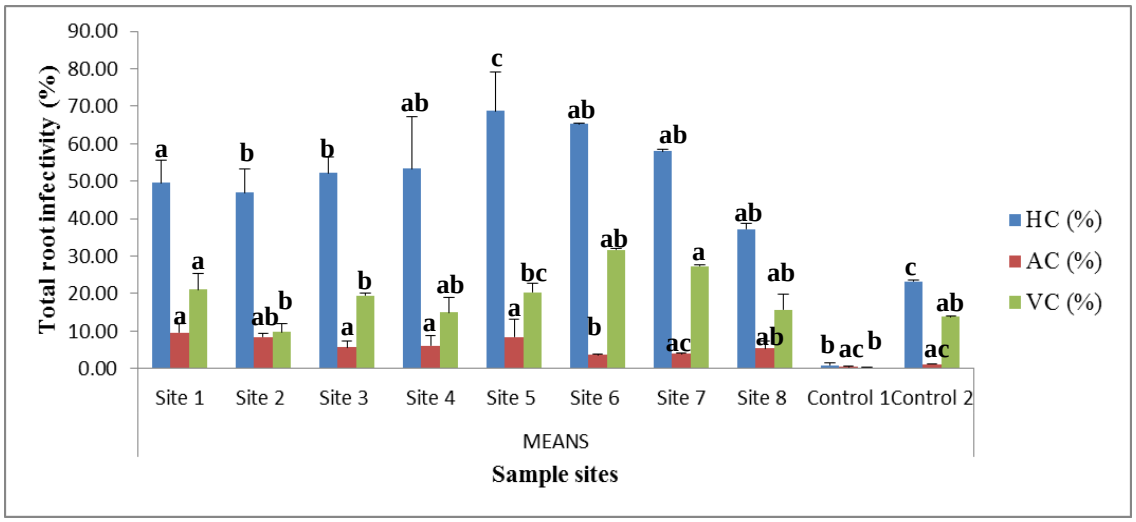

Fig. 4.2a Mycorrhizal colonisation levels in *Eragrostis curvula* (cv. Ermelo) inoculated with indigenous arbuscular mycorrhizal fungi and grown in substrata from various heavy metal sites (site 1 – 8, see Table 3.1). Values are means ± Standard Error of the Mean (SEM) from three replicate pots. VC is vesicular colonisation, AC is arbuscular colonisation and HC is hyphal colonisation**.**

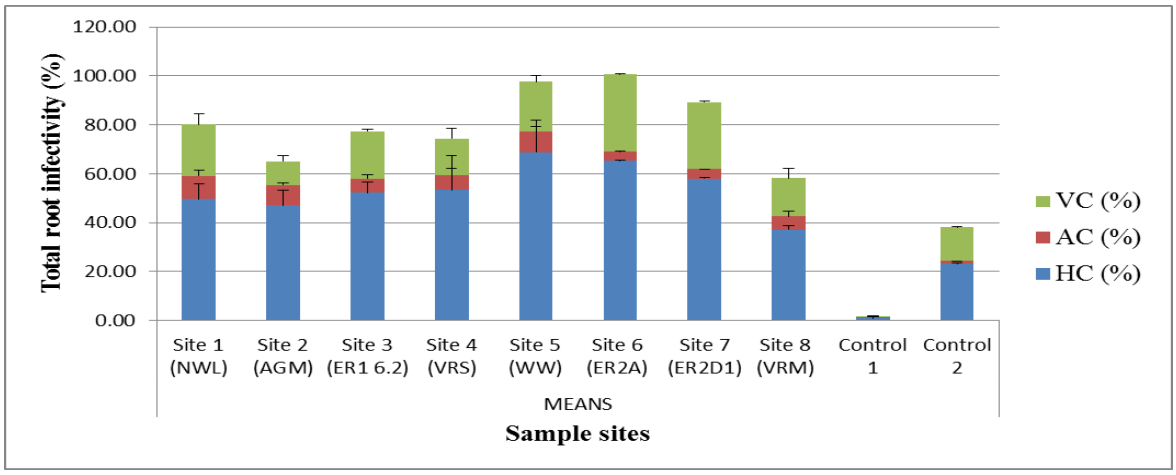

Fig. 4.2b Total mycorrhizal colonisation levels in *Eragrostis curvula* (cv. Ermelo) inoculated with indigenous arbuscular mycorrhizal fungi and grown in substrata from various high heavy metal sites (site 1 – 8, see table 3.1). Fig. 4.2b shows Accumulative AM fungal colonisation results.

4.1.2 Total spore counts

The graph in Fig. 4.3 is made up of the total number of spores isolated or extracted using three different sieve sizes namely, 212 µm, 125 µm and 45 µm. Most of the spores counted were observed in 45 µm sieve, these spores were tiny and had different sizes, colours and shapes. In almost all the samples, 125 µm sieve had more spore count as compared to 212 µm sieve. There was no significant difference on the overall spore count results as shown by a P value of 0.9356 which is greater than 0.05. However Anova showed a significant difference between sites 4 and most of the sites including sites 1, 3, 5, 6, 7, and 8 except site 2. A higher number of spores were extracted from mining site 4 followed by site 5 & 8, then site 3, followed by site 2; 7; 1 and lastly site 6 respectively (Fig. 4.3).

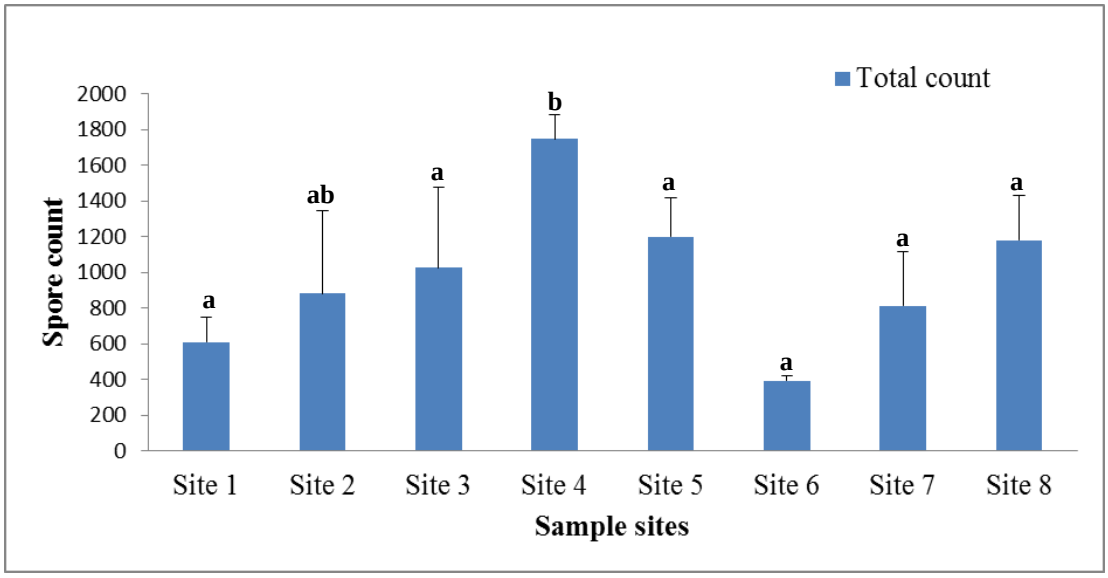

Fig. 4.3 Total spore counts from pots with substrata of various heavy metal sites (Site 1 – 8 as described in Table 3.1). Values are the means ± SEM of three replicate pots. There was a significant difference in some sites and it is shown by letters which are used for comparison between sites.

4.1.3 Morphological identification and AM fungal diversity

For spore identification, whole and crushed spores extracted from soil samples have been mounted on slides and identified according to their shape, colour, size and wall structure. The study identified a total of 14 AM fungal genera and 55 AM fungal species and these are *Glomus (15), Acaulospora (11), Scutellospora (6), Gigaspora (6), Rhizophagus (3), Funneliformis (3), Archaeospora (2), Claroideoglomus (2), Ambispora (2), Sclerocystis (1), Fuscutata (1), Entrophospora (1), Diversispora (1), Paraglomus (1)* (Table 4.1 to 4.4)**.** These are arranged according to the highest number of species obtained during identification or microscope observation, *Glomus* being the highest identified genus followed by *Acaulospora, Scutellospora, Gigaspora*. High Shannon Weaver (H) Index was reported with a value of more than 1 which indicates the high number of different species in the studied sites (Table 4.1 to 4.4). AM fungal diversity is very crucial to the maintenance and sustainability of the ecosystem. Table 4.1 to 4.4 below summarizes mycorrhizal community pattern expressed as percentage of occurrence with calculated Shannon-Weaver Index (H) and evenness (e) of 8 mining sites from three provinces namely, Gauteng, Mpumalanga and North West, South Africa.

Table 4.1 Summarized mycorrhizal community pattern expressed as percentage of occurrence with calculated Shannon-Weaver Index (H) and evenness (e) from Lonmin Mine (site 1), North West and Eastern Reef (site 3), Johannesburg, Gauteng South Africa.

Mycorrhizal species	North West Lonmin Mine		Eastern Reef Gold Slime Dam	
	Number of isolates (**Site 1**)	%	Number of isolates (**Site 3**)	%
1. *Acaulospora colombiana*	2	14.29	0	0.00
2. *Acaulospora delicata*	0	0.00	7	14.00
3. *Acaulospora dilatata*	0	0.00	1	2.00
4. *Acaulospora lacunosa*	0	0.00	1	2.00
5. *Acaulospora mellea*	1	7.14	0	0.00
6. *Archaeospora trappei*	2	14.29	4	8.00
7. *Claroideoglomus etunicatum*	0	0.00	2	4.00
8. *Entrophospora infrequens*	1	7.14	1	2.00
9. *Funneliformis mosseae*	1	7.14	0	0.00
10. *Gigaspora decipiens*	0	0.00	1	2.00
11. *Gigaspora rosea*	0	0.00	2	4.00
12. *Glomus albidum*	1	7.14	12	24.00
13. *Glomus claroides*	1	7.14	0	0.00
14. *Glomus fistulosum*	0	0.00	1	2.00

15. *Glomus globiferum*	0	0.00	1	2.00
16. *Glomus heterosporum*	0	0.00	1	2.00
17. *Glomus hoi*	0	0.00	5	10.00
18. *Glomus microcarpum*	0	0.00	1	2.00
19. *Glomus radiatum*	2	14.29	0	0.00
20. *Glomus tenebrosum*	0	0.00	1	2.00
21. *Glomus warcupii*	0	0.00	1	2.00
22. *Paraglomus occultum*	0	0.00	1	2.00
23. *Sclerocystis rubiformis*	2	14.29	3	2.86
24. *Scutellospora dipurpurescens*	1	7.14	1	2.00
25. *Scutellospora pellucida*	0	0.00	3	6.00
Total number of isolates (N or S)	14	100.00	50	100.00
Total number of species	10	71.43	20	40.00
Average (Nj/N)	0.56		2.00	
Shannon-Weaver Index (H) _	1.40		1.40	
Evenness (e)	1.22		0.82	

Table 4.2 Summarized mycorrhizal community pattern expressed as percentage of occurrence with calculated Shannon-Weaver Index (H) and evenness (e) from Agnes Serpentine Mine (AGM) (site 2), Mpumalanga and Vaal Reefs (site 4), North West, South Africa

Mycorrhizal species	Agnes Mine Mpumalanga		Vaal Reefs Slime Dam	
	Number of isolates (**Site 2**)	%	Number of isolates (**Site 4**)	%
1. *Acaulospora colombiana*	3	6.52	0	0.00
2. *Acaulospora delicata*	0	0.00	3	9.09
3. *Acaulospora mellea*	0	0.00	1	3.03
4. *Acaulospora taiwania*	1	2.17	0	0.00
5. *Acaulospora undulata*	1	2.17	0	0.00
6. *Ambispora jimgerdemannii*	1	2.17	0	0.00
7. *Ambispora leptoticha*	0	0.00	5	15.15
8. *Archaeospora trappei*	1	2.17	1	3.03
9. *Claroideoglomus etunicatum*	0	0.00	1	3.03
10. *Funneliformis fragilistratum*	1	2.17	0	0.00
11. *Fuscutata heterogama*	1	2.17	0	0.00
12. *Gigaspora albida*	0	0.00	2	6.06
13. *Gigaspora decipiens*	0	0.00	1	3.03

14. *Gigaspora margarita*	1	2.17	0	0.00
15. *Gigaspora margaspora*	1	2.17	0	0.00
16. *Gigaspora rosea*	1	2.17	1	3.03
17. *Glomus albidum*	2	4.35	0	0.00
18. *Glomus dimorphicum*	3	6.52	2	6.06
19. *Glomus globiferum*	1	2.17	0	0.00
20. *Glomus heterosporum*	1	2.17	0	0.00
21. *Glomus hoi*	3	6.52	1	3.03
22. *Glomus magnicaule*	2	4.35	0	0.00
23. *Glomus microcarpum*	2	4.35	0	0.00
24. *Glomus pansihalos*	0	0.00	6	18.18
25. *Glomus tenebrosum*	1	2.17	0	0.00
26. *Rhizophagus irregularis*	0	0.00	2	6.06
27. *Rhizophagus manihotis*	1	2.17	1	3.03
28. *Sclerocystis rubiformis*	8	17.39	5	15.15
29. *Scutellospora armeniaca*	1	2.17	0	0.00
30. *Scutellospora dipurpurescens*	1	2.17	0	0.00
31. *Scutellospora nigra*	2	4.35	0	0.00
32. *Scutellospora* spp.	6	13.04	1	3.03

Total number of isolates	46	100.00	33	100.00
Total number of species	24	52.17	15	45.45
Average (Nj/N)	1.44		1.03	
Shannon-Weaver Index (H) _	1.51		1.51	
Evenness (e)	0.91		0.99	

Table 4.3 Summarized mycorrhizal community pattern expressed as percentage of occurrence with calculated Shannon-Weaver Index (H) and evenness (e) from West Wits (site 5), and East Rand (site 6), Johannesburg, Gauteng South Africa

Mycorrhizal species	West Wits		East Rand Slime Dam	
	Number of isolates (**Site 5**)	%	Number of isolates (**Site 6**)	%
1. *Acaulospora colombiana*	5	16.13	3	15.00
2. *Acaulospora dialtata*	0	0.00	1	5.00
3. *Acaulospora gdanskensis*	0	0.00	1	5.00
4. *Acaulospora mellea*	4	12.90	0	0.00
5. *Acaulospora morrowiae*	0	0.00	2	10.00
6. *Acaulospora scrobiculata.*	0	0.00	1	5.00
7. *Archaeospora trappei*	1	3.23	1	5.00
8. *Archaeospora schenckii*	1	3.23	0	0.00
9. *Claroideoglomus claroideum*	1	3.23	0	0.00
10. *Entrophospora infrequens*	1	3.23	1	5.00
11. *Funneliformis caledonium*	0	0.00	1	5.00
12. *Fuscutata heterogama*	0	0.00	2	10.00
13. *Gigaspora rosea*	1	3.23	0	0.00

14. *Gigaspora* spp.	2	6.45	0	0.00
15. *Glomus albidum*	1	3.23	0	0.00
16. *Glomus claroides*	1	3.23	0	0.00
17. *Glomus dimorphicum*	1	3.23	0	0.00
18. *Glomus intraradix.*	0	0.00	1	5.00
19. *Glomus flavisporum*	0	0.00	1	5.00
20. *Glomus tenebrosum*	1	3.23	0	0.00
21. *Sclerocystis rubiformis*	1	3.23	1	5.00
22. *Scutellospora dipurpurescens*	1	3.23	4	20.00
23. *Scutellospora* spp.	9	29.03	0	0.00
Total number of isolates	31	100.00	20	100.00
Total number of species	15	48.39	13	65.00
Average (Nj/N)	1.35		0.87	
Shannon-Weaver Index (H) _	1.36		1.35	
Evenness (e)	0.91		1.05	

Table 4.4 Summarized mycorrhizal community pattern expressed as percentage of occurrence with calculated Shannon-Weaver Index (H) and evenness (e) from East Rand (ER D2) (site 7), Gauteng and Vaal Reefs (VRM) (site 8), North West, South Africa

Mycorrhizal species	East Rand Slime Dam		Vaal Reefs Slime Dam	
	Number of isolates (**Site 7**)	%	Number of isolates (**Site 8**)	%
24. *Acaulospora colombiana*	2	10.53	5	7.94
25. *Acaulospora gdanskensis*	2	10.53	0	0.00
26. *Acaulospora mellea*	0	0.00	2	3.17
27. *Acaulospora rugosa*	1	5.26	0	0.00
28. *Archaeospora trappei*	0	0.00	2	3.17
29. *Diversispora spurca*	1	5.26	0	0.00
30. *Entrophospora infrequens*	0	0.00	2	3.17
31. *Funneliformis caledonium*	0	0.00	1	1.59
32. *Funneliformis mosseae*	0	0.00	1	1.59
33. *Fuscutata heterogama*	4	21.05	0	0.00
34. *Gigaspora decipiens*	0	0.00	1	1.59
35. *Glomus albidum*	0	0.00	2	3.17
36. *Glomus claroides*	0	0.00	2	3.17
37. *Glomus hoi*	0	0.00	3	4.76

38. *Glomus microcarpum*	0	0.00	2	3.17
39. *Glomus pansihalos*	0	0.00	2	3.17
40. *Glomus radiatum*	0	0.00	2	3.17
41. *Glomus tenebrosum*	1	5.26	2	3.17
42. *Rhizophagus fasciculatus*	1	5.26	2	3.17
43. *Sclerocystis rubiformis*	6	31.58	23	36.51
44. *Scutellospora calospora*	0	0.00	1	1.59
45. *Scutellospora dipurpurescens*	0	0.00	2	3.17
46. *Scutellospora pellucida*	0	0.00	1	1.59
47. *Scutellospora scutata*	0	0.00	2	3.17
48. *Scutellospora spinosissima*	1	5.26	1	1.59
49. *Scutellospora* spp.	0	0.00	2	3.17
Total number of isolates	19	100.00	63	100.00
Total number of species	10	52.63	22	34.92
Average (Nj/N)	0.70		2.33	
Shannon-Weaver Index (H) _	1.43		1.43	
Evenness (e)	1.12		0.80	

4.1.4 Representative light micrographs showing a morphological identifications of AM fungi from whole and crushed spore mounts extracted from pots with *E. curvula* growing in substrata from different HM sites

A *Acaulospora dilatata*: Spores are formed singly in the soil, borne laterally on hyphae, each ending in a globose to subglobose hyphal terminus with 105 – 142 µm spore diameter. It has three layers (L1, L2, and L3), the outer continuous layer with the wall of the neck of the parent sporiferous saccule and the latter being synthesized with development of the spore. It has a thin, hyaline outer layer of spore wall (swL1); with laminated inner layers of spore wall (swL2 and swL3). It also consists of two flexible hyaline germinal inner walls (gw1 and gw2) which are readily separated from each other and from the spore wall. First bilayered hyaline germinal inner wall (gw1); outer layer of inner wall one (gw1L1); inner layer of inner wall one (gw1L2); second hyaline inner wall (gw2); outer layer of second inner wall (gw2L1) with beads; inner layer of second inner wall (gw2L2) staining red-purple in Melzer's reagent and measurable in PVLG, (Fig. 4.4A; INVAM; Schenck and Péres, 1990).

B *Glomus magnicaule*: Spores form singly and brown in soil with varying amounts of adhering debris, globose to subglobose, 125–175 µm diameter. Spore wall consists of two layers, outer brown and finely laminated layer of spore wall (swL1); laminated inner layers of spore wall (swL2), with colourless to light brown. Subtending hyphae (h) often slightly pinched in at the point of attachment, Plug (p) of the wall-like material gradually built up on inner wall of subtending hypha till pore occluded completely at maturity with germination shield (gs) in the centre of the spore (Fig. 4.4B; Schenck and Péres, 1990).

C *Scutellospora pellucida*: Spores formed singly in the soil or in roots; borne terminally on a bulbous subtending hypha; glistering with oil droplets, hyaline to pale grey, globose, ellipsoid, or irregular; 58-183(-250) x 58-241(-410) µm diam. Permanent, smooth, hyaline outer layer of spore wall (swL1); laminated, hyaline inner layers of spore wall (swL2). Subtending hyphae (h) often slightly pinched in

at the point of attachment. First bilayered hyaline germinal inner wall (gw1); outer layer of flexible, hyaline inner wall one (gw1L1); inner layer of flexible, hyaline inner wall one (gw1L2); second hyaline inner wall (gw2); outer layer of flexible, coriaceous, hyaline, second inner wall with beads (gw2L1); inner layer of second plastic, hyaline, inner wall (gw2L2) staining beetroot-purple in Melzer's reagent and measurable in PVLG, (Fig. 4.4C; INVAM; Schenck and Péres, 1990).

D *Paraglomus occultum*: Chlamydospores borne singly or in loose clusters in the soil, or in compact clusters in the cortex of roots, often broader than long, avoid to abovoid to irregular, frequently globose to subglobose, with 15 – 100 x 20-120 µm diam, hyaline to white in colour (INVAM). The spore consists of three layers (L1, L2, and L3). Outer layer of spore wall (swL1) is generally a sloughing layer, often separating and degrading to form a granular layer. Spores then appear to have a thin coating of organic debris on their surface and can look "dirty". No reaction in Melzer's reagent. Permanent inner layers of spore wall (swL2 and swL3) continuing into the wall of the subtending hypha (h); produces a light yellow (0-0-10-0) reaction in Melzer's reagent (Fig. 4.4D; Schenck and Péres, 1990; Redecker *et al*., 2013).

E *Scutellospora dipurpurescens*: Spores formed singly in the soil; borne terminally on a bulbous suspensor-like cell; usually globose to subglobose, with (152)-197(-250) µm diam., but occasionally ellipsoid 144 – 216 x 176-224 µm diam., shiny smooth, yellow to greenish-yellow, turning yellow-brown after storage for more than 2 months in formalin or lactophenol. It has two layers (L1 and L2) that are adherent that in juvenile spores are of equal thickness, with the laminate layer thickening as the spore wall is differentiated (Schenck and Péres, 1990). Outer permanent rigid layer (swL1), smooth, pale yellow and so tightly adherent to L2 and (swL2) A laminate layer consisting of very fine adherent sublayers (= laminations). The innermost sublayers separate slightly and produce undulations that can be mistaken for an inner flexible wall with germination shield (gs). Iw1, one hyaline layer, often adherent to L2 (laminae) of the spore wall, It stains a light pink (0-20-20-0) in Melzer's reagent. iw2, two hyaline layers (L1

and L2) that almost always are adherent. Iw2L1 often produces a weak pink reaction (0-10-20-0) in Melzer's reagent that is detected only when it breaks away from the spore wall. Iw2L2 is hyaline and exhibits enough plasticity in acidic mountants to have been described as amorphous (INVAM). Thickness varies in PVLG-based mountants, depending on the degree of pressure applied to it while breaking the spore (Fig. 4.4E; Redecker *et al*., 2013).

F *Archaeospora (Acaulospora) trappei*: Spores formed singly in the soil or occasionally within the roots, sessile, borne laterally on shiny smooth, unbranched hyphal cell that terminates nearby in a subglobose to ellipsoid or to obovoid vesicle 50 – 82 x 42-72 µm diam, colourless, containing rounded to polyhedral oil globules, (Fig. 4.4F; Schenck and Péres, 1990). It consists of three hyaline layers (L1, L2 and L3), all of which exhibit some flexibility when broken with applied pressure in a slide mountant. Thin, hyaline outer layer of spore wall (swL1); thin, hyaline inner layer layers of spore wall (swL2); and a thicker hyaline layer (swL3) than either L1 or L2, ranging from 1.3-4 µm thick near attachment (Fig. 4.4F; Morton and Redecker, 2001).

G and H *Glomus heterosporum*: Sporacarps light to dark brown, globose to subglobose, 242-726 x 242 -641 µm diam., consisting of a single, ordered layer of chlamydospores originating from central core of thick interwoven hyphae. It has three walls of sporocarp hyaline spore (L1, L2 and L3). Chlamydospore with multiple hyphal (h) attachment. Smooth, thin, hyaline outer layer of spore wall (swL1); laminated brown membranous inner layers of spore wall (swL2 and (swL3). The inner content of the third inner wall staining red-purple in Melzer's reagent and measurable in PVLG with inner flexible germination shield (gs). Colour: light to dark brown, globose to subglobose, (Fig. 4.4G, H; Schenck and Péres, 1990).

I *Glomus globiferum*: Spores formed singly, or in pairs or triplets adhering to each other by common peridial hyphae; orange brown to rich red-brown, to (rarely) fuscous black, globose to subglobose 150 – 260 x150-270 µm diam,

colourless, containing rounded to polyhedral oil globule. Spore with vesiculate swellings (V) of peridial hyphae. It has three to four walls of hyaline spore (L1, L2 and L3). Hyaline to pale yellow-brown outer layer (swL1) of spore wall; laminated orange-brown to red-brown second layer (swL2) of spore wall. Hyaline, membranous inner layer (swL3) of spore wall, with approximately 1 µm thick attached to each other by a thin, amorphous cement-like layer, (Fig. 4.4I; Schenck and Péres, 1990).

J *Glomus microcarpum*: Chlamydospores borne free in soil in loose aggregations in small compact clusters unenclosed in a peridium or in sporocarps with a peridium. Spores are globose or subglobose, (30 -45) x (30-40) µm diam. Spore wall is smooth and composed of a single layer, 4-6 µm thick, hyaline, light yellow or yellow-brown, that may have numerous laminations. Subtending hypha (h) with a width of 4-8.5 µm thick at the point of the attachment to the spore (p). The pore of the subtending hypha either remains open, or is partially or completely occluded by thickening of the spore wall (Fig. 4.4J; Schenck and Péres, 1990).

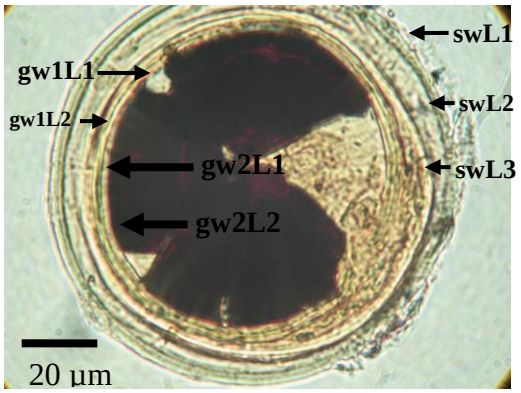

A *Acaulospora dilatata*

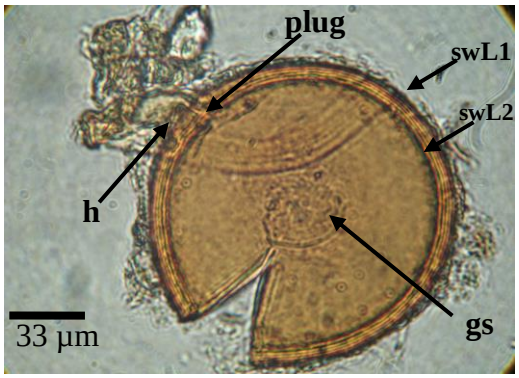

B *Glomus magnicaule*

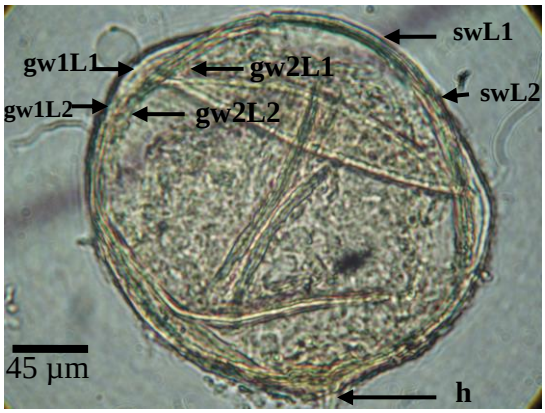

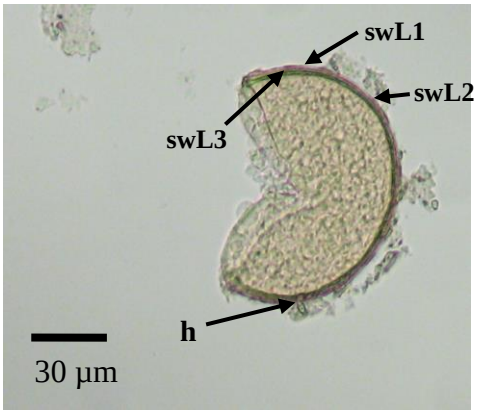

C *Scutellospora pellucida*

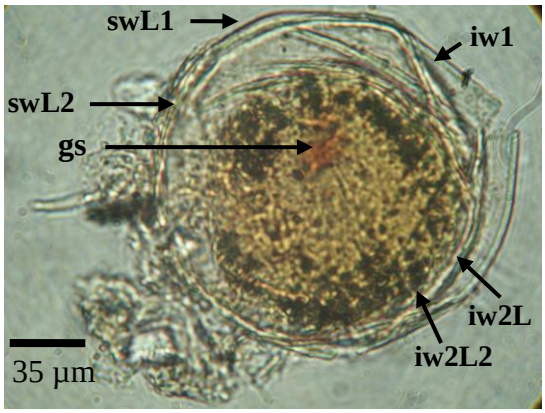

D *Paraglomus occultum*

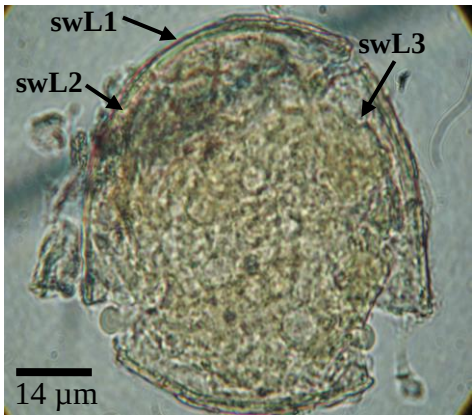

E *Scutellospora dipurpurescens*

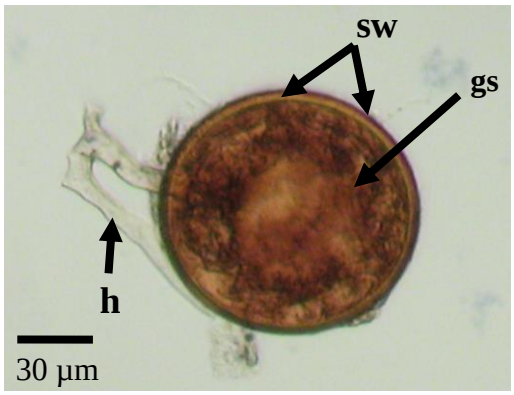

F *Archaeospora trappei*

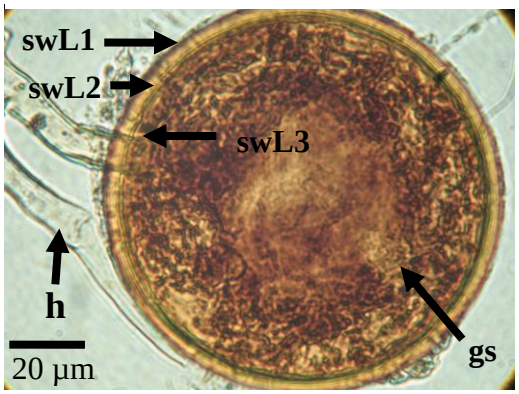

G *Glomus heterosporum*

H *Glomus heterosporum,*

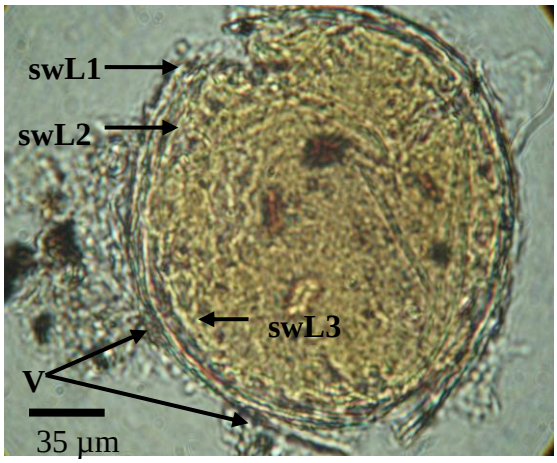

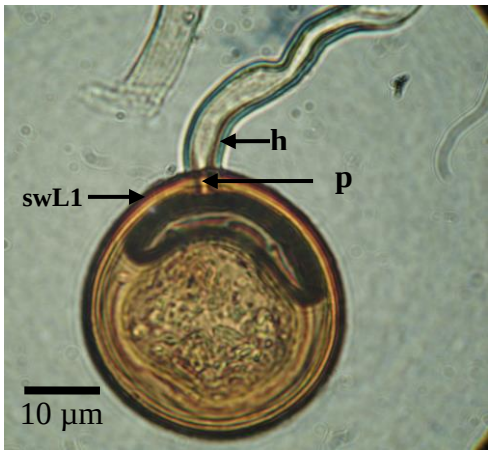

I *Glomus globiferum*

J *Glomus microcarpum*

Fig. 4.4 Spores of mycorrhizal species isolated from Eastern Reef slime dams (Site 3). (A-J) subtending hypha (h); spore wall (sw); outer layer (swL1) one of spore wall; inner layer two (swL2)of spore wall; inner layer three (swL3) of spore wall; spore with vesiculate swellings (V) of peridial hyphae; first germinal inner wall (gw1); outer layer of inner wall one (gw1L1); inner layer of inner wall one (gw1L2); second hyaline inner wall

(gw2); outer layer of second inner wall (gw2L1) with beads; inner layer of second inner wall (gw2L2) usually staining red-purple in Melzer's reagent and measurable in PVLG. One hyaline layer (iw1), Two hyaline layers (1w2) (L1 and L2) that almost always are adherent. Thickness varies in PVLG-based mountants, depending on the degree of pressure applied to it while breaking the spore.

A *Glomus tenebrosum*: The spores are globose or subglobose, (200 – 270) x (205 -270) µm diam. Spore wall (sw) composed of a single layer, 13-26 µm thick, yellow to a very dark brown. The outer surface of the spore (swL1) is smooth or may be flattened tubercules. Open-pored subtending hypha (h) with a hyaline and inner wall with germination shield (gs). The outer surface of the spore is smooth or may bear flattened tubercules (Fig. 4.5A; Berch and Fortin, 1983; Schenck and Péres, 1990; Schüßler and Walker, 2010).

B *Scutellospora armeniaca*: Spores formed singly in the soil or in roots; borne terminally or laterally on a bulbous sporogenous cell; apricot yellow (5B6) to yellowish brown (5E8); globose to subglobose; (140-) 196 (-240) µm diam; sometimes ovoid; 140-200 x 220-250 µm. Spore wall composed of three layers (swL1-3). Spore wall Layer 1 (swL1) is permanent, greyish orange (5B5), usually tightly adherent to layer 2. Spore wall Layer 2 (swL2), laminate, apricot yellow to yellowish brown, usually staining garnet red in Melzer's reagent. Spore wall Layer 3 (swL3) flexible, hyaline, easily separating from layer 2. A germinal wall (gw1) contains two layers (gw1L1 and 2). Flexible, hyaline germinal wall 1 (gw1L1); flexible, hyaline, germinal wall 2 (gw1L2) staining pinkish white in Melzer's reagent, measurable in PVLG (Fig. 4.5B, INVAM; Blaszkowski, 1992).

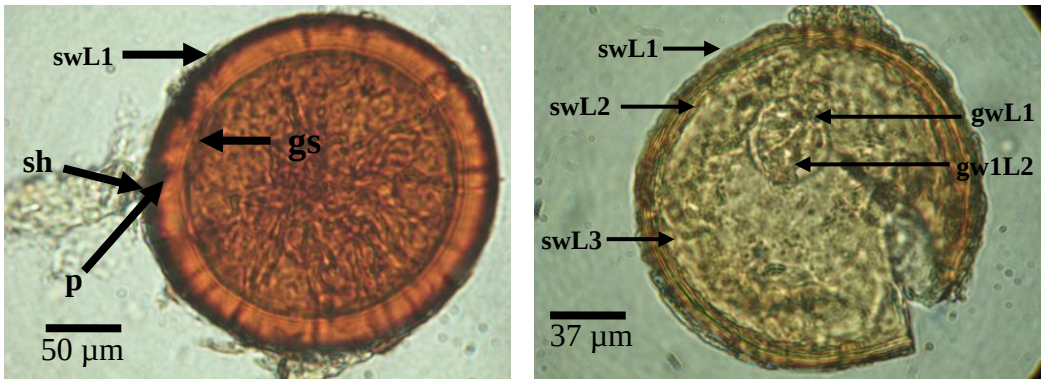

A *Glomus tenebrosum* **B** *Scutellospora armeniaca*

Fig. 4.5 Spores of mycorrhizal species isolated from Agnes Mine (AGM) Serpentine slime dams (site 2). (A-B), Spores wall (sw); The outer surface of the spore (swL1); Open-pored Subtending hypha (h) with a hyaline; outer spore wall Layer one (swL1). Inner spore wall Layer two (swL2); spore wall Layer three (swL3). Germinal wall 1 contains two layers (gw1L1 and 2). Flexible, hyaline germinal wall 1 (gw1L1) while flexible, hyaline, germinal wall 2 (gw1L2) staining pinkish white in Melzer's reagent.

A-B *Acaulospora delicata*: Spores borne singly in the soil laterally on the neck of a sporifererous saccule; hyaline to pale yellowish-cream, sparkling from the nature of the spore contents; globose to subglobose (rarely ovoid to obvoid), 80-125(-150) x 80-110 (-140) µm. Occasionally spores occurring in the cortical cells of senescent roots. *A.delicata* has two spore wall layers (L1 and L2), the outer spore wall layer (swL1): Hyaline, degrading to form a granular coating or sloughing completely. (swL2): A layer consisting of very fine and adherent sublayers (or laminae) that often are difficult to discern; very pale yellow (0-0-10-0) in colour, at maturity, the spore detaches from the sporiferous saccule (sac) and is sessile. The germinal wall has two hyaline flexible inner walls layers (gw1L1 and gw1L2) which are formed sequentially in spores after the spore wall has completed differentiation and the spore has ceased expansion. First bilayered hyaline germinal inner wall (gw1); outer layer of inner wall one (gw1L1); inner layer of inner wall one (gw1L2). The inner layer of the inner wall staining red-purple in Melzer's reagent (Fig. 4.6A, B, Walker *et al*., 1986; Schenck and Péres, 1990).

C *Rhizophagus (Glomus) irregularis*: Chlamydospore formed singly or in clusters in the root, rarely formed outside the root. Spores are predominately globose and sometimes subglobose, irregular with many spores elliptical (especially those extracted within mycorrhizal roots). It has three layers (L1, L2 and L3), with only the first layer present in juvenile spores and subtending hyphal wall (so they are colourless); subtending hypha (h); spore wall (sw); outermost layer one of spore wall (swL1), hyaline, mucilaginous, staining pinkish red to pale purple in Melzer's reagent when intact in juvenile spores. With age, this layer almost always degrades and decomposes naturally and from the action of microorganisms, after which it appears granular and may accumulate some debris; layer two of spore wall (swL2); hyaline. With age, this layer degrades concomitant with L1 and also acquires a granular appearance or sloughs in patches. Mature spores often lack both L1 and L2 or they are present together as rough patches. Layer three of spore wall (swL3); consists of pale yellow-brown sublayers (or laminae) that either remains adherent or separate with applied pressure. This layer forms simultaneously in the wall of the subtending hypha (h) (Fig. 4.6C, INVAM).

D *Claroideoglomus (Glomus) etunicatum*: Chlamydospore formed singly in soil and dead roots, globose to subglobose 68-144 (162) µm diameter smooth or roughened from decomposition of outer wall and adherent debris. Spore wall (sw) consists of two layers, L1 and L2 (Fig. 4.6D). Outer spore wall Layer one (swL1) is the outer mucilaginous layer (showing some plasticity and an uneven outer surface); 2.5 µm thick which may degrade as the spore ages to develop a granular appearance. SwL2 consists of thin adherent sub-layers (laminae), light orange-brown to red-brown in colour but thickening in the region of the subtending hypha. An occlusion between the innermost sub-layer of the laminate layer of the spore wall is present which resembles a septum(s) (Fig. 4.6D; Straker *et al.*, 2010; Schenck and Péres, 1990).

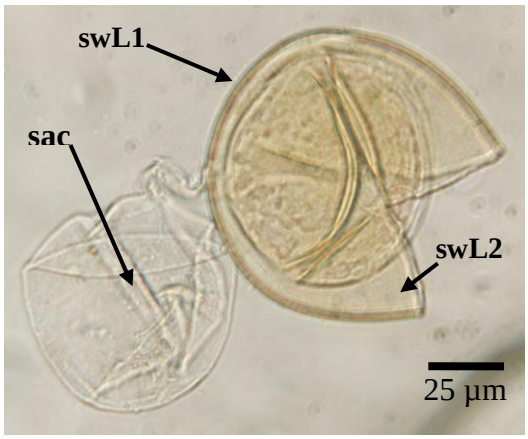

A *Acaulospora delicata*

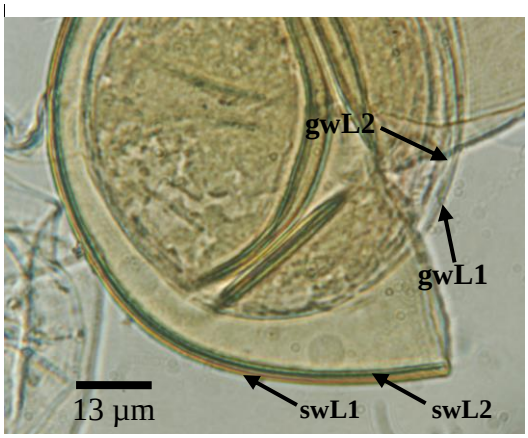

B *Acaulospora delicata*

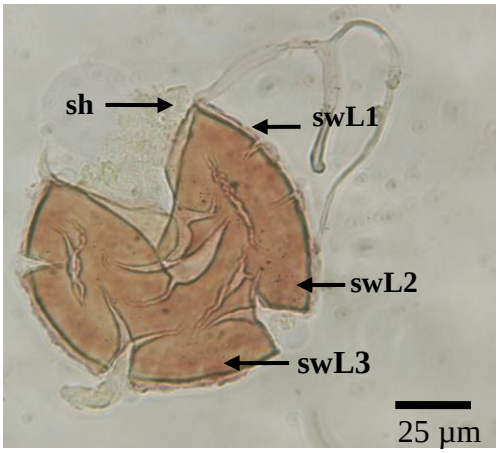

C *Rhizophagus irregularis*

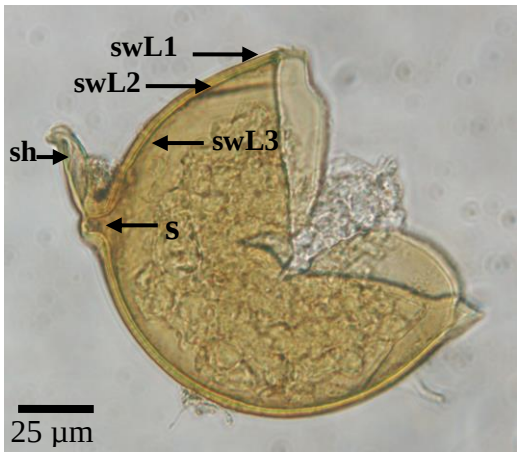

D *Claroideoglomus etunicatum:*

Fig. 4.6 Spores of mycorrhizal species isolated from Vaal Reefs slime dams (site 4). (A-D), Spores wall (sw); The outer surface of the spore wall (swL1); Open-pored subtending hypha (h) with a hyaline; outer spore wall Layer one (swL1). Inner spore wall Layer two (swL2); inner spore wall Layer three (swL3); sporiferous saccule (sac); hypha (h); septum (s). Outer layer of germinal inner wall one (gwL1); inner layer of germinal inner wall two (gwL2);

***A Acaulospora colombiana* (previously called *Kuklospora and Entrophospora colombiana*):** Azyspores produced singly in soil and occasionally in roots. Spores developing within a slightly tapering hypha. Azyspores at first are subhyaline to white becoming pale yellow to light golden brown at maturity and globose to subglobose with 75 – 135 µm in diameter. It has three layers (L1, L2, and L3). thin, hyaline outer layer of spore wall (swL1) of the saccule neck; laminated second inner layer of spore wall (swL2); and a third single inner layer of spore

wall (swL3), with 0.5-0.6 µm thick, probably concolorous (difficult to determine due to thinness); The three germinal inner walls, gw1, gw2 and gw3 tend to separate much more in PVLG with Melzer's reagent than in PVLG**.** first flexible hyaline germinal inner wall (gw1); second and third flexible hyaline inner wall (gw2 and gw3) which most of the time appears as one wall due to their thinness to resolve adherence (Fig. 4.7A; INVAM; Schenck and Péres, 1990).

B Archaeospora schenckii*, previously called *Entrophospora schenckii:
Archaeospora schenckii differs from *Acaulospora* species due to their unique spore subcellular structure. It has no flexible inner walls; hence germination occurs through the spore wall. Interestingly, this same subcellular structure is the phenotype of *Ar. trappei* spores (Schüßler and Walker (2010). The whole spore is mostly globose, subglobose, but also ellipsoid to ovoid in shape, with size ranging from 50-80 µm, mean = 64. The spore wall consists of three hyaline layers (L1, L2 and L3), all of which exhibit some flexibility in broken section. As a result, the spore wall contains numerous folds from any or all of the layers. SwL1 has a thin hyaline layer of 1 µm thick, which is continuous with the wall of the neck of the sporiferous saccule. SwL2 also consists of a thin hyaline layer, with 1 µm thick, which usually is adherent to the innermost layer (swL3). While swL3 has a thicker hyaline layer than either swL1 or swL2, ranging from 1.3-4 µm thick, which together with swL2 form an endospore which encloses the spore contents (Fig. 4.7B; INVAM; Schüßler and Walker, 2010).

C–D *Acaulospora mellea:* Spores formed singly in soil; borne laterally on haphae appearing sparkling from the nature of the spore contents; globose to subglobose (rarely ovoid to obvoid), 80-125 (-150) x 80-110 (-140) µm. Spore wall (sw) consists of three layers, swL1, swL2 and swL3. SwL1 is thin and hyaline and sloughs on many spores; swL2 consists of laminae with a smooth surface if outer layer has sloughed; swL3 is yellow-brown and also consists of laminae which can separate from each other but generally merge to be part of the spore wall. There are two flexible hyaline germinal inner walls that that separate from each other and the spore wall. Germinal inner wall 1 (gw1) is a bilayered hyaline wall which

separates clearly from the spore wall but the two layers do not often separate from each other. Outer layer of germinal inner wall one (gw1L1); inner layer of germinal inner wall one (gw1L2); Germinal inner wall 2 (gw2) consists of two adherent hyaline layers with gw2L1 showing granular excrescences or "beads" and gw2L2 staining red-purple in Melzer's reagent (Fig. 4.7D). A cicatrix (scar showing region of contact between spore and saccule neck during spore synthesis is circular to oval-shaped, (Fig. 4.7C, D; Straker *et al*., 2010; Schenck and Péres, 1990).

(E-F) ***Acaulospora tuberculate***: Spores formed singly in soil; sessile, borne laterally on a light yellow thick-walled, with, globose to subglobose, 255–327x 255- 340 μm. Spore wall consists of three layers (L1, L2, L3) (Fig. 4.7E, F). L1 is hyaline, 1.2 μm thick that remains after tubercles on L2 have formed. L2 thickens by formation of yellow-brown sub-layers (laminae) (Fig. 4.7E, D) and forms polygonal spines or tubercles. L3 is yellow-brown to red-brown in colour and mostly appears to be an inner sub-layer of L2 (Fig. 4.7E, F). Two flexible, hyaline inner walls (iw1 and iw2) are present. Two layers of near equal thickness comprise iw1 (L1 and L2) (Fig. 4.7F). Similarly, iw2 comprises two adherent hyaline layers (L1 and L2) and L2 stains pinkish red to red-brown in Melzer's reagent (Fig. 4.7E, F; Straker *et al.*, 2010).

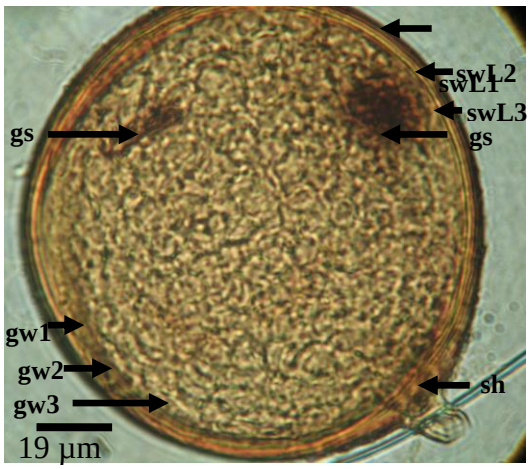

A *Acaulospora colombiana*

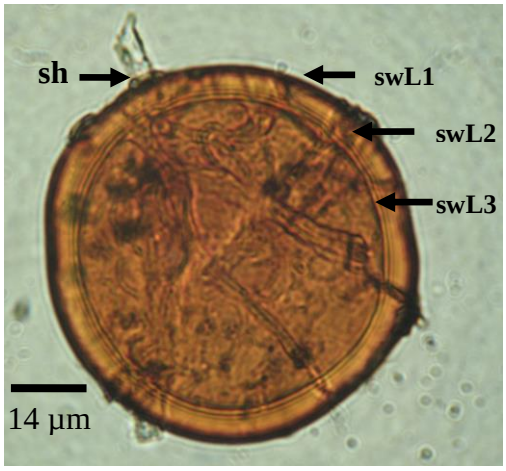

B *Archaeospora (Entrophospora) schenckii*

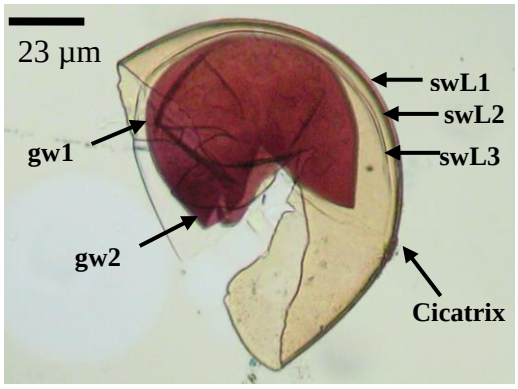

C *Acaulospora mellea*

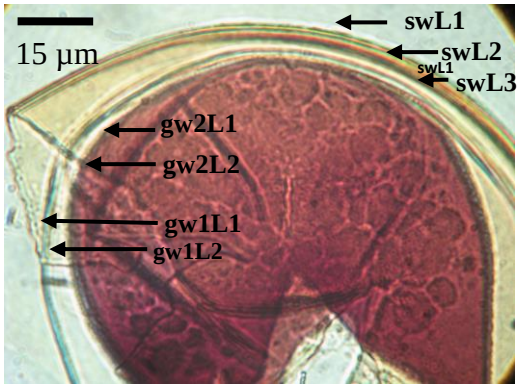

D *Acaulospora mellea*

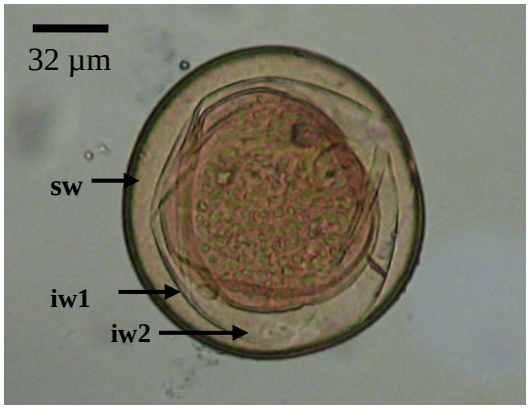

E *Acaulospora tuberculata*

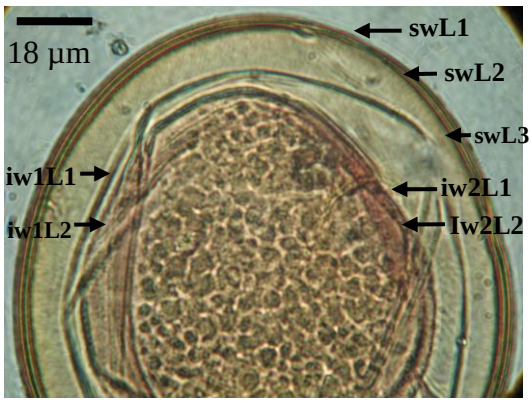

F *Acaulospora tuberculata*

Fig. 4.7 Spores of mycorrhizal species isolated from West Wits, slime dams (site 5), (A-F) (sw) spore wall; hyaline outer layer of spore wall (swL1); middle layer of spore wall (swL2) with tubercles (t); inner sublayer (swL3) of swL2; outer layer of first hyaline inner wall (iw1L1); inner layer of inner wall one (iw1L2); outer layer of innermost inner wall two (iw2L1); inner layer of inner wall two (iw2L2); first bilayered hyaline germinal

inner wall (gw1); outer layer of germinal inner wall one (gw1L1); inner layer of germinal inner wall two (gw1L2); second hyaline inner wall (gw2); outer layer of second inner wall layer one (gw2L1); germinal inner layer two of second inner wall (gw2L2) staining red-purple in Melzer's reagent *(*Straker *et al.,* 2010*),* (Schenck and Péres, 1990).

A *Rhizophagus (Glomus) irregularis*: Chlamydospore formed singly or in clusters in the root, rarely formed outside the root. Spores are predominately globose and sometimes subglobose, irregular with many spores elliptical (especially those extracted within mycorrhizal roots). It has three layers (L1, L2 and L3), with only the first layer present in juvenile spores and subtending hyphal wall (so they are colourless); subtending hypha (h); spore wall (sw); spore wall (sw); hyaline and mucilaginous outer layer of spore wall (swL1); middle layer of spore wall (swL2) with tubercles (t). Mature spores often lack both L1 and L2 or they are present together as rough patches; pale yellow-brown inner sublayer (swL3) or laminae; subtending hypha (h). The spore shape is globose, subglobose, irregular, with many spores elliptical (especially those extracted from within mycorrhizal roots) (Fig. 4.8A; INVAM).

B *Funneliformis geosporum* previously known as *Glomus geosporum*: Chlamydospores formed singly in soil, clusters in the root, globose or broadly ellipsoid, 110 – 290 µm, smooth and shiny, roughened from adherent debris; with light yellow brown and transparent to translucent when young, becoming dark yellow to dark red brown at maturity. It forms spore content (sc) of uniform oil droplets when young becoming increasingly granular in appearance at maturity. Whole spore with subtending hypha (h); spore wall (sw); hyaline outer spore wall (swL1); yellow-brown to orange-brown laminated middle wall (swL2); yellow to orange light-brown inner spore wall (swL3) (Fig. 4.8B; INVAM; Schenck and Péres, 1990).

C *Scutellospora dipurpurescens*: Spores formed singly in the soil; borne terminally on a bulbous suspensor-like cell; usually globose to subglobose, with (152)-197(-250) µm diam but occasionally ellipsoid 144 – 216 x 176-224 µm

diam, shiny smooth, yellow to greenish-yellow, turning yellow-brown after storage for more than 2 months in formalin or lactophenol. Germination shield (gs); plug (p); spore wall (sw) constituting an outer wall (swL1) forming an outer permanent rigid layer, smooth, pale yellow with a green tint and laminated inner layers of spore wall (swL2). The spore also has two flexible hyaline inner walls (iw1 and iw2) that are formed, first hyaline germinal inner wall (iw1); outer hyaline layer of second inner wall (iw2L1); inner hyaline wall 2 (iw2L2), amorphous layer of second inner wall staining red-purple dark red-purple in Melzer's reagent (Fig. 4.8C; INVAM; Schenck and Péres, 1990).

D Acaulospora colombiana, Azyspores produced singly in soil and occasionally in roots. Spores developing within a slightly tapering hypha. Azyspores at first are subhyaline to white becoming pale yellow to light golden brown at maturity and globose to subglobose with 75 – 135 µm in diameter. It has three layers (L1, L2, and L3). Thin, hyaline outer layer of spore wall (swL1) of the saccule neck; (swL2) laminated second inner layer of spore wall; and a third single inner layer of spore wall (swL3), with 0.5-0.6 µm thick, probably concolorous (difficult to determine due to thinness); the three germinal inner walls, gw1, gw2 and gw3 tend to separate much more in PVLG with Melzer's reagent than in PVLG. First flexible hyaline germinal inner wall (gw1); second and third flexible hyaline inner wall (gw2 and gw3) which most of the time appears as one wall due to their thinness to resolve adherence (Fig. 4.8D; INVAM; Schenck and Péres, 1990).

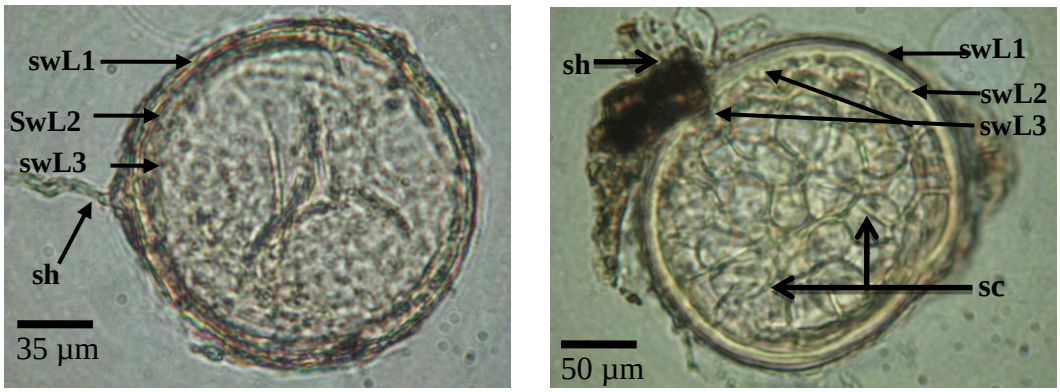

A *Rhizophagus irregularis* **B** *Funneliformis geosporum*

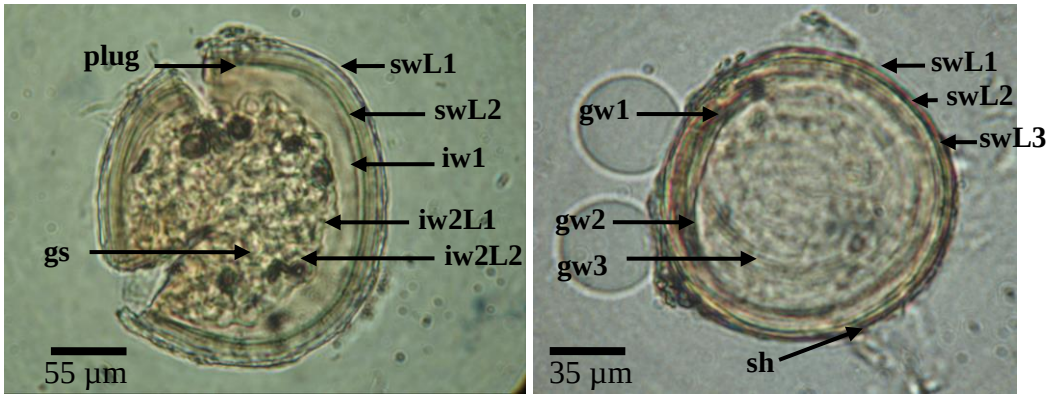

C *Scutellospora dipurpurescens* ***D*** *Acaulospora colombiana,*

Fig. 4.8 Spores of mycorrhizal species isolated from West Wits, slime dam (site 6). (A-D) Thin, hyaline outer layer of spore wall (swL1); laminated inner layers of spore wall (swL2 and swL3); subtending hypha (h); germination shield (gs); plug (p); spore content (sc); outer layer of first hyaline inner wall (iw1L1); inner layer of inner wall one (iw1L2); outer layer of innermost inner wall two (iw2L1); inner layer of inner wall two (iw2L2) (INVAM).

A-B *Fuscutata heterogama* formerly called *Scutellispora heterogama*: Spores formed singly in the soil; borne terminally, or subterminally, or laterally on a bulbous suspensor-like cell; usually globose to subglobose or irregular, with 150 - 120 µm diam; pale yellow-brown to red - brown to yellow-brown. It has three layers (L1, L2, and L3) with the middle layer (L2) undergoing a dramatic transformation from the juvenile to the mature state. This transformation is expressed in the transition in spore colour. SwL1 has an outer permanent rigid layer of spore wall (sw) with pale brown in colour. SwL2 and swL3 have very thin hyaline flexible inner layers of spore wall (Fig. 4.9A); first bilayered hyaline

germinal inner wall (gw1); outer layer of inner wall one (gw1L1); inner layer of inner wall one (gw1L2) with the germination shield (gs); second hyaline inner wall (gw2); (outer layer of second inner wall gw2L1) with beads; inner layer of second inner wall (gw2L2) staining pinkish-purple to slightly darker purple in Melzer's reagent (Fig. 4.9B; INVAM; Schenck and Péres, 1990).

C *Acaulospora gdanskensis*: Azygospores formed singly in the soil; pale yellow to yellow brown, globose to subglobose, with 55 - 75 µm in diam; sessile on a hypha tapering to a globose to subglobose swollen hyphal terminus contents hyaline. It has three layers (L1, L2 and L3), thin, hyaline, sloughing, outer layer of spore wall (swL1) of the saccule neck; laminated inner layer of spore wall (swL2); and a single inner layer of spore wall (swL3), with yellow to pale brown; subtending hypha (h) (Fig. 4.9C; Schenck and Péres, 1990).

D *Acaulospora colombiana* previously called *Kuklospora and Entrophospora colombiana*: Azyspores produced singly in soil and occasionally in roots. Spores developing within a slightly tapering hypha. Azyspores at first are subhyaline to white becoming pale yellow to light golden brown at maturity and globose to subglobose with 75 – 135 µm in diameter. It has three layers (L1, L2, and L3). Thin, hyaline outer layer of spore wall (swL1) of the saccule neck; laminated second inner layer (swL2) of spore wall; and a third single inner layer (swL3) of spore wall, with 0.5-0.6 µm thick, probably concolorous (difficult to determine due to thinness); the three germinal inner walls, gw1, gw2 and gw3 tend to separate much more in PVLG with Melzer's reagent than in PVLG**.** First flexible hyaline germinal inner wall (gw1); second and third flexible hyaline inner wall (gw2 and gw3) which most of the time appears as one wall due to their thinness to resolve adherence (Fig. 4.9D; INVAM; Schenck and Péres, 1990).

E-F *Scutellospora spinosissima*: Spores formed singly in the soil. Pale pinkish cream when immature; ochraceous to fulvous or rust when mature, appearing matt from surface ornamentation, globose to subglobose to broadly ellipsoid (rarely ovoid or irregular), (121 - 230) µm, with a terminal or laterally-attached bulbous

base produced from a septate subtending hypha. Bulbous spore base ochraceous to sienna (8±11), 19±32 µm, wide, with or without one or more peg-like projections. It has three layers (L1, L2, and L3) with the middle layer (L2) undergoing a dramatic transformation from the juvenile to the mature state. This transformation is expressed in the transition in spore colour. SwL1 has an outer permanent rigid layer of spore wall (sw) with pale to brown in colour. SwL2 and swL3 have a hyaline flexible inner layers of spore wall; with the multiple germination shield (gs); first bilayered hyaline germinal inner wall (gw1); outer layer of inner wall one (gw1L1); inner layer of inner wall one (gw1L2); second hyaline inner wall (gw2); outer layer of second inner wall (gw2L1) with beads; inner layer of second inner wall (gw2L2) staining dark brown in Melzer's reagent, (Fig. 4.9F; INVAM; Walker *et al*., 1998).

G-H *Rhizophagus fasciculatus* Formerly: *Glomus fasciculatum*: Consisting of three layers (L1, L2, and L3) which form sequentially, based on the pattern of spore wall differentiation observed in all other *Glomus* species. SwL1 has an outer hyaline layer of spore wall (sw) producing a pinkish-red reaction in Melzer's reagent; adherent to L2. SwL2 is composed of a layer consisting of thin adherent sublayers (or laminae), light yellow-brown. All sublayers form a dark red to slightly purplish red colour in Melzer's reagent. SwL3 has a thin flexible inner spore layer; it forms a component part of the spore wall and appears to form a fragile septum. Multiple germination shield (gs) showing the complex infolding and subtending hyphae (h). (Fig. 4.9G, H; INVAM; Schenck and Péres, 1990; Walker and Koske, 1987).

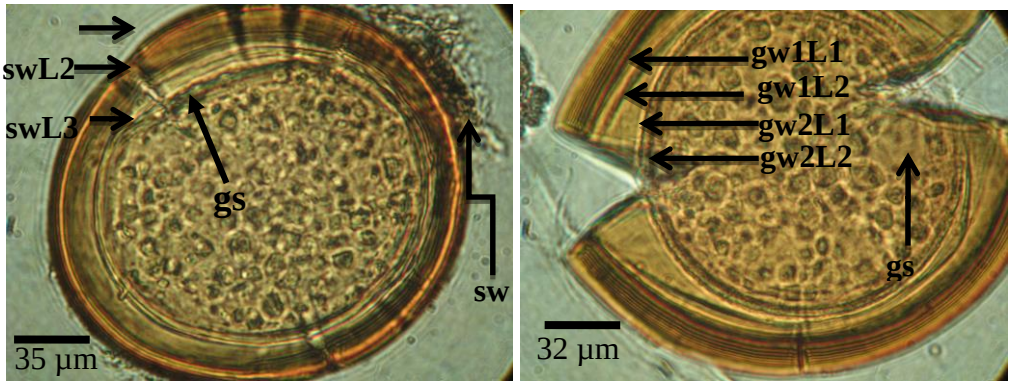

A *Fuscutata heterogama*

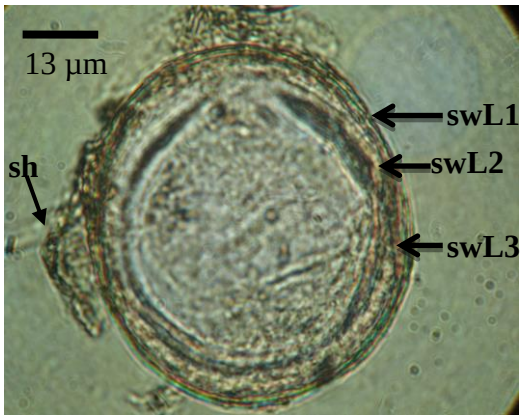

B *Fuscutata heterogama*

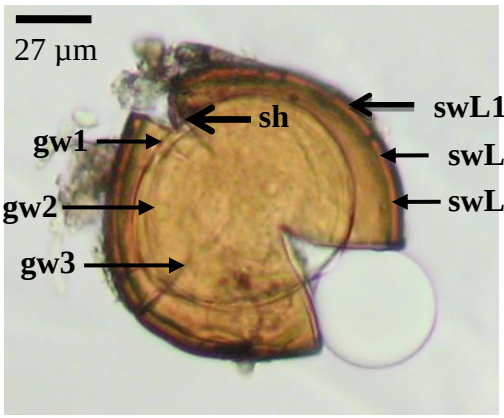

C *Acaulospora gdanskensis*

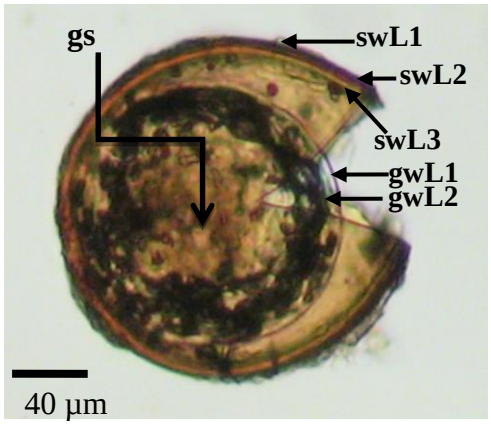

D *Acaulospora colombiana*

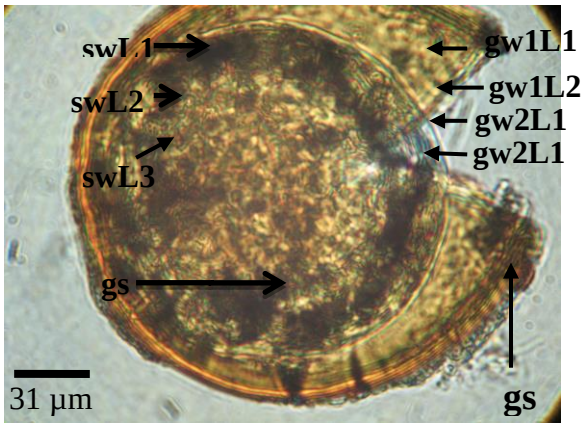

E *Scutellospora spinosissima*

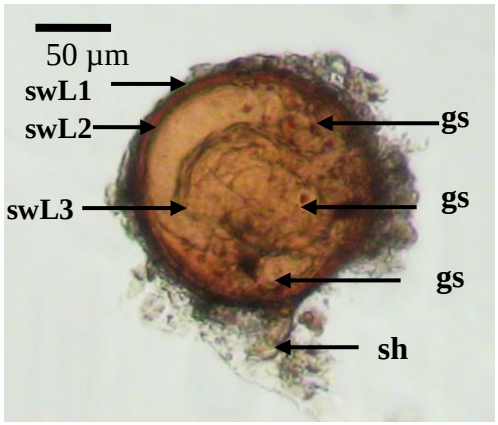

F *Scutellospora spinosissima*

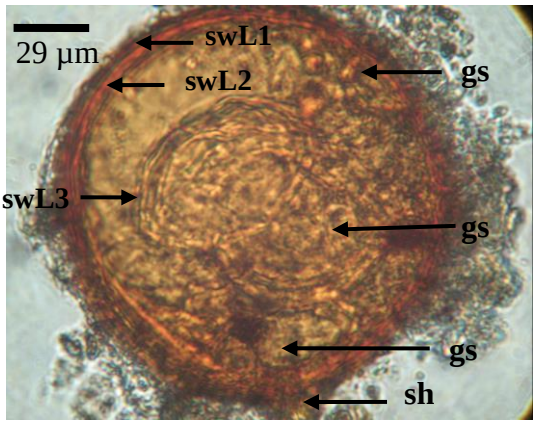

G *Rhizophagus fasciculatus*

H *Rhizophagus fasciculatus*

Fig. 4.9 Spores of mycorrhizal species isolated from East Rand slime dam (site 7). spore wall (sw); hyaline outer layer (swL1) of spore wall; middle layer of spore wall (swL2); inner sublayer (swL3) of swL2; sporiferous saccule (sac); subtending hypha (h); septum (s); germination shield (gs); first bilayered hyaline germinal inner wall (gw1); outer layer of germinal inner wall one (gw1L1); inner layer of germinal inner wall one

(gw1L2); second hyaline inner wall (gw2); outer layer of second inner wall layer one (gw2L1); germination inner layer two of second inner wall (gw2L2) staining red-purple in Melzer's reagent (INVAM; Schenck and Péres, 1990; Straker *et al*., 2010),

A *Entrophospora infrequens*: Azygospores produced singly in soil by expansion within a smooth, unbranched hyphal cell that terminates in a globose or subglobose to ellipsoid or obovoid vesicle, 126-214 x 157 µm, diam.; vesicle contents dense white, emptying as the spore develops, Spore white at first, becoming dull orange to brown, 69 -183 (-225) x 69-164 µm, diam.; subglobose or ellipsoid. There are four layers (L1, L2, L3 and iw1), with L1-L3 continuous with the wall of the neck of the parent sporiferous saccule and inner wall (iw1) forming de novo. thin, hyaline outer layer of spore wall (swL1) continuous with outer layer of the saccule, degrading and sloughing as the spore ages; A hyaline spore wall layer (swL2), that is initially solid with shallow indentations on the inner surface and which later has imbedded in it the projections (or spines) of L3 and then eventually degrades and sloughs; it is very thin (< 0.5 µm) in the saccule wall and thus is difficult or impossible to see. SwL3 is made up of the formation of spines with five sides (pentagonal) and central depression layers of the spore wall. Inner wall (iw) thins, hyaline, semi-flexible inner wall; sporiferous saccule (sac) (Fig. 4.10A; INVAM; Schenck and Péres, 1990).

B *Sclerocystis rubiformis:* Sporocarps are yellow brown to dark brown, subglobose or obovoid to ellipsoid, (180 x 180-375x675) µm, diam., consisting of a single layer of chlamydospores *with laminate* spore wall (sw) and a small pore (p) opening into a thick-walled central plexus subtending hypha (h) and with perforated projections (pp) on inner surface (Fig. 4.10B). The outer wall is hyaline, but frequently absent in mature spores (Fig. 4.10B; INVAM; Schenck and Péres, 1990).

***C Scutellospora calospora*:** Spores formed singly in the soil; borne terminally on a bulbous suspensor-like cell; transluscent, hyaline to pale greenish-yellow; globose, ellipsoidal or cylindrical, occasionally broader than long; 114-285(-511)

x 110 -412 (-511) µm, diam.; whole spore (s); sporogenous cell (sc); spore wall distinctly bi-layered with outer spore wall (osw); laminate inner spore wall (isw) of equal thickness; One flexible inner wall with darker-coloured germination shield (gs) is present, inner wall (iw) (Fig. 4.10C; Straker *et al*., 2010; Schenck and Péres, 1990).

D *Gigaspora decipiens*: Spores are orange-brown to dark-brown in colour, globose to sub-globose and even ellipsoid, 310 µm–500 µm. Spores are borne terminally on a bulbous suspensor-like sporogenous cell, 60 µm at widest point. It consists of three layers (L1, L2, and L3), The first two layers are adherent and of equal thickness in juvenile spores, with L2 thickening as the spore wall is differentiated; L3 differentiates as a prelude to germ tube formation, an outer permanent rigid layer (swL1), smooth, adherent to sublayers of L2, 2.5-3.2 µm thick, often hard to see in relation to L2. A second layer (swL2) consisting of hyaline sublayers (or laminae) that increase in number with thickness, are rigid, exhibit some plasticity when broken, pale yellow turning to darker brownish yellow with age and storage. Sublayers stain dark red-purple (almost black) in Melzer's reagent. A "germinal" layer (swL3) that is concolorous and adherent with the laminate layer. sporogenous cell (sc), germination shield (gs). Spores dark red-brown in colour, globose to subglobose, (Fig. 4.10D). Spores turn orange brown in Melzer's reagent with no distinctive difference in colouration of spore wall (Fig. 4.10D; INVAM; Straker *et al*., 2010, Schenck and Péres, 1990).

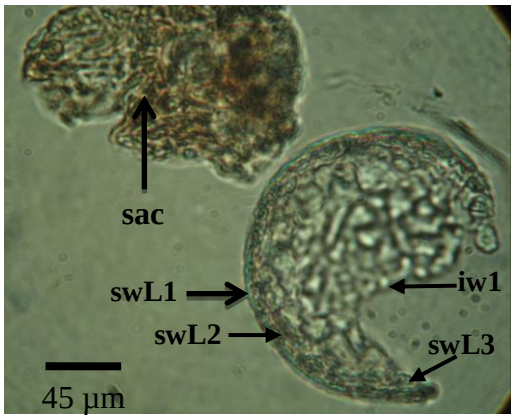

A *Entrophospora infrequens*

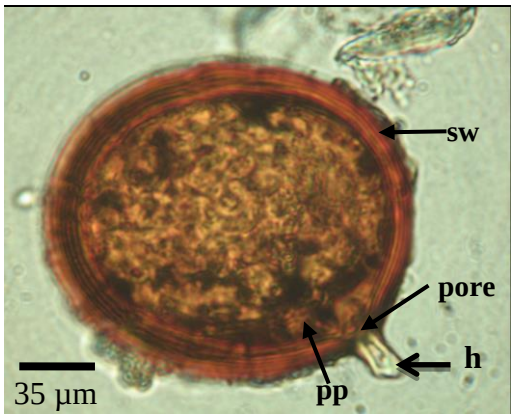

B *Sclerocystis rubiformis*

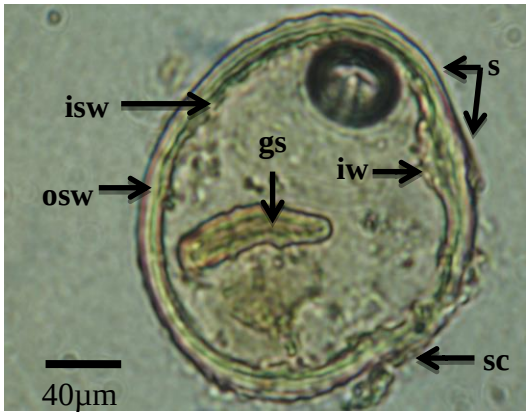

C *Scutellospora calospora*

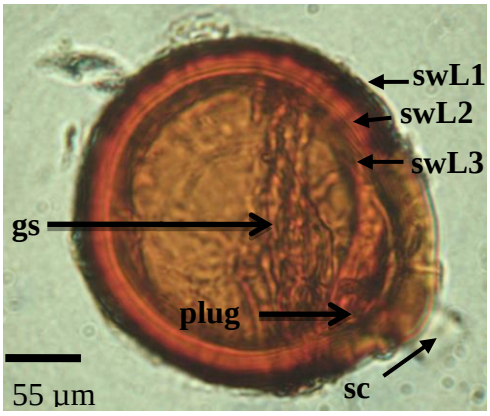

D *Gigaspora decipiens*

Fig. 4.10 Spores of mycorrhizal species isolated from West Wits, slime dam (site 8). (A-D) Thin, hyaline outer layer (swL1) of spore wall; laminated inner layers of spore wall (swL2 and swL3); subtending hypha (h). germination shield (gs); plug (p); sporogenous cell (sc); pore (p); perforated projection (pp); sporiferous saccule (sac); whole spore (s); outer spore wall (osw); inner spore wall (isw); inner wall (iw), outer layer of first hyaline inner wall (iw1L1); inner layer of inner wall one (iw1L2); outer layer of innermost inner wall two (iw2L1); inner layer of inner wall two (iw2L2). One hyaline layer (iw1), Two hyaline layers (L1 and L2) of inner wall (iw2) that almost always are adherent. Thickness varies in PVLG-based mountants, depending on the degree of pressure applied to it while breaking the spore.

4.2 Discussion

Spores have been successfully used in the past for the identification and classification of AM fungi. Spores are resistant to damage and are able to survive adverse conditions for an extended period of time while remaining dormant. They

have the capacity to be dispersed by different modes of transport such as animals, wind, and water (Smith and Read, 2008). The degree to which the AM fungi sporulate varies between species (Pearson and Schweiger, 1993) and it is influenced by a number of factors such as environmental conditions (Vestbery, 1995), soil nutrient levels, host colonisation level, to name but a few (Stutz and Morton, 1996). Some AM fungi have been reported to produce large quantities of spores in certain seasons of the year and under specific conditions thus appearing as dominant root colonisers, but under alternative conditions, AM fungi may produce little or no spores at all (Redecker *et al*., 2003). Some AM fungi sporulate in late spring while others sporulate at the end of summer, which indicates that AM fungi have their preference seasons (Schultz *et al*., 1999). This might explain the fact that most of the spores counted in this study were observed in 45 µm sieve, compared to 125 µm sieve, and 212 µm sieve. These spores were tiny and had different sizes, colour and shapes. The spores were identified according to the broad guidelines found in the Manual for the identification of VA Mycorrhizal Fungi, (Schenck and Péres, 1990) and INVAM as well as using the recently published articles (Schüßler & Walker, 2010; Straker *et al*., 2010; Kruger *et al*., 2012).

This study identified *Glomus* and *Acaulospora* as the most common genera followed by *Scutellospora*, then *Gigaspora*. This tallies with the findings by Daniell *et al*. (2001) who found that *Glomus* species were predominant in roots at various arable sites, and suggested one reason for this may be the ability of the Glomaceae (unlike the Gigasporaceae) to recolonise roots from mycelial fragments, coupled with the ability of *Glomus* species, unlike *Gigaspora* or *Scutellospora*, which are able to establish anastomoses between separate mycelia. Gunwal *et al.* (2014) also reported *Glomus* as the most abundant species amongst the AM fungal species isolated in their study. In addition, *Glomus* species have been reported for various ecosystems such as tropical forests (Husband *et al*. 2002b), agricultural sites (Alguacil *et al*., 2008; Hijri *et al.*, 2006), wetland soils (Wirsel, 2004), gypsum soil (Alguacil *et al*., 2009b), or polluted soils (Vallino, *et al.*, 2006). The possible reasons for the predominance of *Glomus* spp. are that

spores of *Glomus* species have different temperature and pH preferences for germination (Wang *et al*., 1997) and *Acaulospora* species are often associated with acidic soils (Abbott and Robson 1991; Morton 1986). These two species may, therefore, be particularly well adapted to recolonise roots following disruption of the soil mycelium. The North West, Mpumalanga and Gauteng sites are regularly affected by flooding, presumably causing major soil disturbance, and this could be another factor contributing to the predominance of both *Glomus* and *Acaulospora* species at these sites.

Straker *et al*. (2010) reported a very low AM fungal species diversity of the original field soil samples with only two species from each locality being isolated in South Africa as compared with some other studies from Africa which have shown higher levels, especially in tropical ecosystems. This low diversity is not unusual as spores isolated directly from a field soil sample may represent only those AM fungi with sufficient root colonizing activity and biomass to trigger sporulation, and in arid sites it is found that little or no sporulation occurs but roots are clearly colonised (Morton *et al*., 1993). This accords with Daniell *et al*. (2001) who also reported a very low AM fungal species diversity at the arable sites, with just two *Glomus* species dominating colonisation in a range of crops. To combat this low AM fungal species diversity, trap pots were used which were able to stimulate spore germination of additional species from the studied soil samples (Straker *et al*., 2010).

The present study was able to isolate a high number of AM fungal species using trap plants grown in pot soil samples from slime dams (Tables 4.2 to 4.5). Thus the use of trapping in both Straker *et al*. (2010) and in this study to establish a conducive environment for effective root colonisation and sporulation of all indigenous species present was very successful. The study isolated 14 AM fungal genera and 55 AM fungal species from mine tailings (Tables 4.2 to 4.5), compared to Musoko *et al.* (1994) who isolated only 11 species or species aggregates from undisturbed moist forest in Cameroon and Mason *et al.* (1992) who identified 17 species from *Cameroonian Terminalia* plantations with a strong

overlap between those identifications and the ones from the present study. Wilson *et al.* (1992) identified 41 species in Côte d'Ivoire; Jefwa *et al.* (2006) isolated 12 species in Malawi; but Dalpé *et al.* (2000) found only five species associated with the legume, *Faidherbia albida*, in Senegal. Although 55 AM fungal species were identified, only 31 species which were identified in large quantities were described.

Furthermore, the high Shannon-Weaver index (H) reported in this study is the indication of high diversity and presence of the mycorrhizal species in slime dams (Tables 4.2 to 4.5). A Shannon-Weaver index (H) of zero indicates no species diversity, i.e. there is only one species type in the dataset, a Shannon-Weaver index (H) close to zero indicates a very low species diversity and Shannon-Weaver index (H) closer to and above one indicates high species diversity (Magurran 2004). The higher species diversity in the studied samples may be indirectly related to lower fertilizer-derived nutrient levels in these soils. Low external availability of P for N sufficient plants, for example, can lead to an increased root colonisation by AM fungi (Smith and Read, 1997) and P uptake characteristics by external hyphae can vary greatly between fungi (Smith *et al*., 2000) such that these soils may be selecting only for high P-tolerant strains (Table 6.1)**.** Hence, AM fungal diversity is very crucial to the maintenance and sustainability of the ecosystem. Effects of AM fungi on plant species diversity (mostly evenness) range from positive to negative. The direction and magnitude of the effect is hypothesized to be related to the relative mycorrhizal dependency of the dominant and subordinate plant species of a community (Urcelay & Diaz 2003).

Amongst the number of species identified in this study, *Claroideoglomus etunicatum* formerly known as *Glomus etunicatum* has been reported to be an extremely widespread species with many ecotypes, and has been found associated with cassava in Brazil (De Souza *et al*., 1999). This species has been reported in a number of countries in the African continent. It was identified in undisturbed secondary semi-deciduous moist forest in Cameroon (Mason *et al*. 1992; Musoko

et al., 1994). Wilson *et al.,* 1992 identified it in *Terminalia* plantations in Côte d'Ivoire, while in Malawi it was found in farming systems (Jefwa *et al*., 2006). In South Africa, the species has been found associated with a number of plants, such as the wild fruit tree, *Vangueria infausta* (Gaur *et al*., 1999), rhizosphere of plants (Stutz *et al*., 2000), cassava and soil samples (Straker *et al*., 2010). Spruyt *et al*. (2014) found that *Claroideoglomus* species were typically associated with the *T. usneoides* plant host at different mining sites such as ABB Zinc, Impala Platinum, and Northern Cape sites. *Claroideoglomus etunicatum* also appears to be a cosmopolitan species found in many soil types (Khade, 2008), which may explain its commonality to some of our studied sites such as site 2, 3 and 6.

Acaulospora mellea has been reported in 4 sample sites in the present study, namely site 1, 4, 5 and 8. Its spores have been vastly reported in the literature in different sample types in a number of countries. They were reported in sandy soils (Schenck and Perez 1990). In Poland, they were found in wild and cultivated plants growing in forest nurseries, uncultivated and cultivated soils (Blaszkowski, 1993a), as well as in maritime (Blaszkowski, 1993b, 1994) and inland (Blaszkowski *et al*., 2002) sand dunes of Poland. While in Florida, Massachusetts, North Carolina, and Rhode Island, USA, the species was found in cultivated and uncultivated soils (Douds and Schenck, 1990; Koske and Gemma, 1997), Brazil (Schenck *et al*., 1984; Grandi and Trufem, 1991), Mexico (Estrada-Torres *et al*., 1992), Colombia (Dodd *et al*., 1990), China (Mei-ging and You-shan, 1992). The species has also been reported in a number of African countries such as Cameroon in Terminalia and undisturbed semi-deciduous moist forests (Musoko *et al*., 1994), Western Kenya in low input farm, forest and grassland soils (Shepherd *et al*., 1996). *Acaulospora* species are considered facultative symbionts and reported to adapt to a wide range of soils and host species, appearing in soils of widely differing pH and nutrient availability (Sieverding, 1991; Shepherd *et al*., 1996; Gunwal *et al.,* 2014) which may account for the presence of *A. mellea* in 4 out of 8 of the present sample sites.

In addition to *Glomus* and *Acaulospora* which have been identified as the highest species in the study, it is pleasing to indicate that it is the first time *Acaulospora colombiana* has been identified in the studied or sampled sites in South Africa and it was identified in almost all the sites. This species was also confirmed by molecular identification (chapter 5).

The *Acaulospora colombiana* was formerly known as *Entrophospora colombiana* which was organised into *Kuklospora colombiana.* The *Acaulospora colombiana* is currently placed into the family of the Acaulosporaceae (Sieverding and Oehl, 2006; Krüger *et al.,* 2012; Redecker *et al*., 2013). It was first isolated as *Kuklospora colombiana* from various locations in Colombia (Schenck *et al*., 1984). It was also reported from several States in Brazil (Caproni *et al*., 2003; Dos Anjos *et al*., 2010); India (Mehrotra, 1998; Selvam and Mahadevan, 2002) and the Philippines (Oba *et al*., 2004) and in trap cultures inoculated with tropical soils from Benin showed the presence of *Acaulospora colombiana* (Sieverding and Oehl, 2006). Sieverding and Oehl, (2006) have been infrequently finding it in grasslands of lowlands and at mountainous elevations in Southern Germany and Switzerland. Previous studies reported *Acaulospora* species to be associated with acidic soils (Abbott and Robson 1991; Morton 1986). In Germany, *A. colombiana* was also isolated from an acidic sandy soil near Berlin (Baltruschat, pers. com) (Sieverding and Oehl, 2006). Thus this explains the reason why for the first time in South Africa, we have identified it in the heavy metal contaminated sites with predominantly acidic soil. Similarly to *Glomus* species, *Acaulospora colombiana* has the ability to better adapt in various ecosystems including the disturbed environments such as heavy metal mining sites (Gunwal *et al.,* 2014).

In conclusion, this study provides a valuable contribution to the database of the Glomeromycota in general, especially to that which is found in both South African and African soils. This shows the potential of using mycorrhizas to remediate the soil contaminated with toxic heavy metals. To our knowledge, this is the first time these genera have been discovered in heavy metal contaminated sites in South Africa and especially the species *Acaulospora colombiana.* The

morphological studies perfomed by Straker *et al.* (2010) and the molecular identification studies performed by Spruyt *et al*. (2014) found *Glomus etunicatum* (now *Claroideoglomus etunicatum*), the genera *Gigaspora, Scutellospora* and *Acaulospora mellea* species typically associated with the *T. usneoides* plant host at different mining sites such as ABB Zinc, Impala Platinum, and Northern Cape sites. In addition, this study identified about 6 more AM fungal species such as *Rhizophagus*, *Funneliformis*, *Archaeospora*, *Ambispora*, *Fuscutata*, *and Paraglomus* (Tables 4.2 to 4.5). This suggests that both *Glomus* species and *Acaulospora colombiana*, are the AM fungal isolates responsible for the survival of plants growing in heavy metal sites and thus it could be useful to solve the heavy metal contamination of the mine dumps. Most of the fungal strains identified by morphological analysis were also confirmed by molecular analysis (Chapter 5). The study also highlights that AM fungal diversity is crucial to the maintenance and sustainability of the ecosystem.

CHAPTER 5

5 RESULTS AND DISCUSSION FOR MOLECULAR IDENTIFICATION OF AM FUNGAL DIVERSITY IN MINES OF SOUTH AFRICA

5.1 Results

Different primer sets were employed in this study for PCR amplification. DNA samples were amplified using universal primers, ITS1 & ITS4 or NS31 & AM1. Fig. 5.1 shows that only amplification of extracted spore DNA with ITS1/ITS4 primers produced positive results (lanes 4 and 10 - Site 2 - Agnes Mine, lane 11 - Site 4 - Vaal Reefs (S)). Amplification of extracted spore DNA with NS31/ AM1 primers from the following sites was unsuccessful:

Lane 7 & 9: Site 1 – Lonmin mine.

Lane 12: Site 3 - ERGO Brakpan.

Lane 6: Site 5 –West Wits TSF.

Lane 2: Site 7 – ERGO Metallurgical Plant.

Lane 3: Site 8 - Vaal Reefs (M).

However, using cloned DNA, NS31 and AM1 produced a very good band from a site 5 sample (West Wits) in lane 3 while ITS1 and ITS4 primers also produced a good band from a site 3 sample (ERGO Brakpan) in lane 7 (Fig. 5.2). The faint bands observed at the bottom of each lane are primer dimers or fragments.

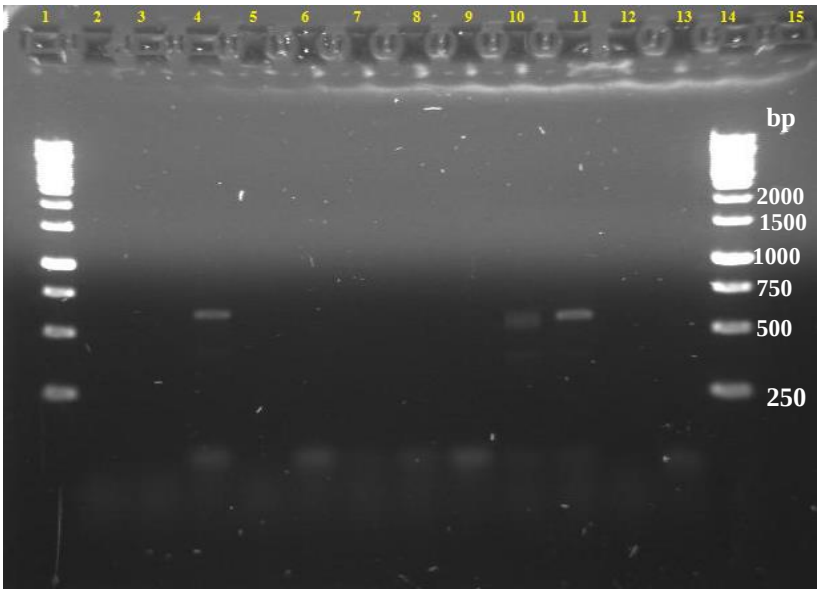

Fig. 5.1 Amplicons from spore DNA amplification using ITS1 & ITS4 or NS31 & AM1 primers. Lanes 1 & 14: molecular size markers, 1kb ladder; Lane 2: site 7; Lane 3: site 8; Lane 4: site 2; Lane 5: site 4; Lane 6: site 5; Lane 7: site 1; Lane 8: site 1; Lane 9: site 1; Lane 10: site 2; Lane 11: site 4; Lane 12: site 3; Lane 13: H_2O control with no DNA template.

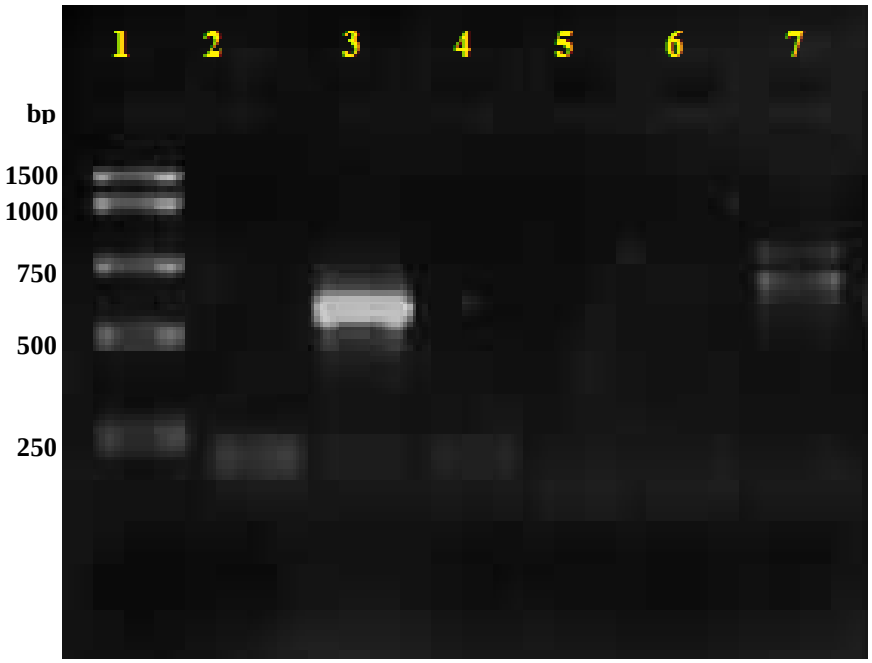

Fig. 5.2 Amplicons from PCR amplification of cloned DNA using ITS1 & ITS4 or NS31 & AM1 primer pairs. Lane 1: molecular size marker, 1kb ladder, Lane 2: H_2O control with no DNA template, Lane 3: site 5; Lane 4: site 3; Lane 5: H_2O control with no DNA template; Lane 6: site 5; Lane 7: site 3. Lanes 3 and 4 are products from NS31/AM1

amplification and lanes 6 and 7 are products from ITS1/ITS4 amplification. Initial PCR was performed directly from spores.

The majority of the samples were amplified using primers designed by Lee *et al. (*2008) namely NS1 and NS4 coupled with AML1 and AML2. Figs. 5.3 and 5.4 demonstrate representative gels showing examples of successful amplifications from primers, NS1 and NS4 coupled with AML1 and AML2.

Fig. 5.3 shows that amplification directly from spores only occurred successfully for samples from site 2 (Agnes Mine) in lanes 9 and 10, whereas no amplification occurred for samples from site 4 (Vaal Reefs (S)). However, amplification from spore DNA extracts occurred successfully for samples from site 2 (Agnes mine), site 3 (ERGO Metallurgical), site 4 (Vaal Reefs (S)) and site 8 (Vaal Reefs (M)) (Fig. 5.4). Altogether, the nested PCR approach yielded at least one amplicon from each site and these were sequenced for subsequent BLAST analysis.

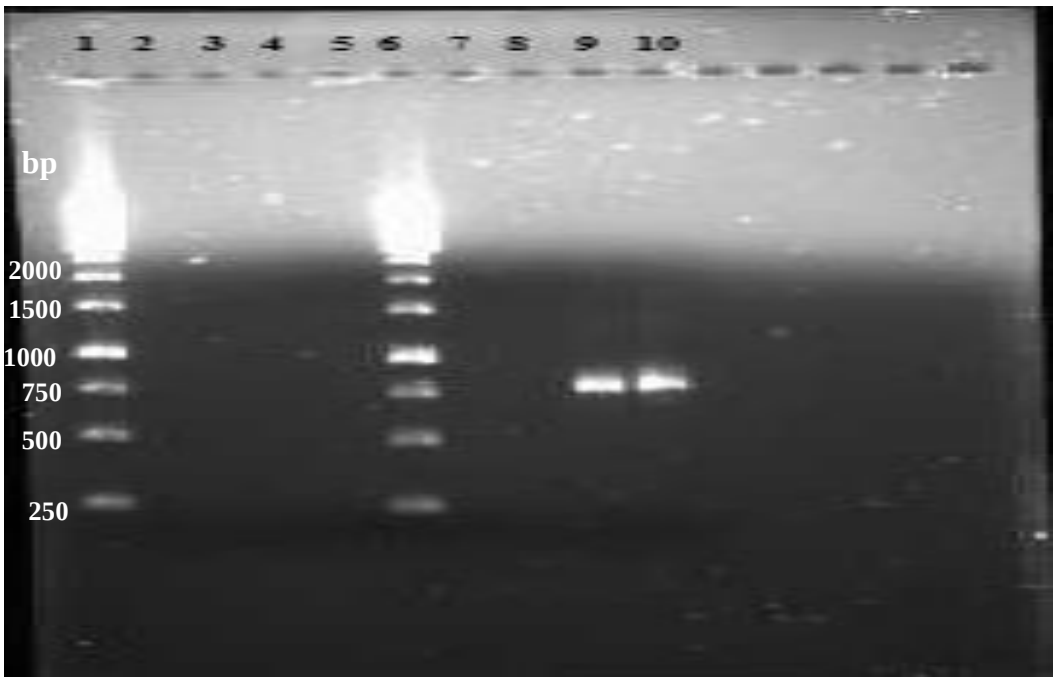

Fig. 5.3 Amplicons from direct PCR amplification of spores using the nested primers, NS1 & NS4 coupled with AML1 & AML2. Lane 1 & 6: molecular size marker, 1kb ladder; Lane 2: site 4; Lane 3: site 4; Lane 4: site 4; Lane 5: site 4; Lane 7: H_2O control with no DNA template; Lane 8: H_2O control with no DNA template; Lane 9: site 2; Lane 10: site 2.

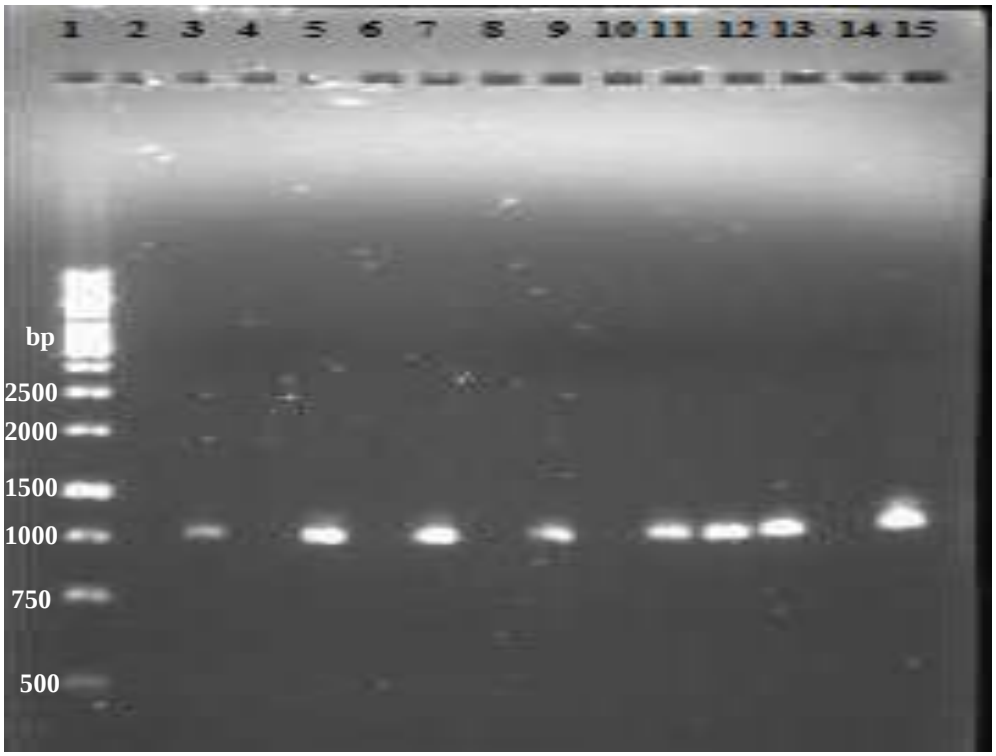

Fig. 5.4 Amplicons from spore DNA amplification using the nested PCR primers, NS1 & NS4 coupled with AML1 & AML2. Lane 1: molecular size marker, 1kb ladder; Lane 2: site 8; Lane 3: site 8; Lane 4: site 2; Lane 5: site 2; Lane 6: site 4; Lane 7: site 4; Lane 8: site 3; Lane 9: site 3; Lane 10: site 3; Lane 11: site 3; Lane 12: site 8; Lane 13: site 4; Lane 14: site 4; Lane 15: site 4.

This study, targeting the SSU rRNA gene sequences and using a combination of NCBI and Maarj*AM* databases has identified species from seven AM fungal genera, namely, *Acaulospora*, *Ambispora*, *Claroideoglomus*, *Diversispora*, *Glomus*, *Rhizophagus* and *Scutellospora*, using a nested PCR from spores isolated from metal contaminated mining sites. Three genera were identified by blasting in the NCBI website (Table 5.1, Fig. 5.6), and four additional genera were identified when blasting in the Maarj*AM* website (http://maarjam.botany.ut.ee). (Table 5.1, Fig. 5.5). Furthermore new taxa names were identified from Maarj*AM* website replacing the old names. For example, both *Entrophospora* and *Kuklospora* were replaced by *Acaulospora*.

Acaulospora colombiana would appear to be the most common species on these sites, being identified from Agnes Mine, Vaal Reefs (S & M), West Wits and East Rand (ER2A) (Table 5.1). The Lonmin site also yielded a *Glomus* and a *Scutellospora* sp. and the same *Scutellospora* sp. identification appeared in Vaal Reefs (S) together with *Acaulospora* sp. 2. The Agnes Mine site was the only site to yield *Diversispora torrecillas*, whereas East Rand (ER1) yielded *Rhizophagus irregularis*, *Ambispora appendicular*, *Glomus clarum* and *Acaulospora* sp. 1 (Table 5.1). *Acaulospora* sp. 3 was identified from East Rand (ER2A) whereas *Acaulospora* sp. 4, *Glomus kohout*, *Scutellospora* sp. 2 and *Claroideoglomus claroideum* were identified from East Rand (ER2D) (Table 5.1). Together, therefore, the East Rand sites showed the richest diversity.

Table 5.1 Spore morphotypes and origins used for PCR amplification and showing the new AM fungal species identified using Maarj*AM* Genbank Blast (http://maarjam.botany.ut.ee) and NCBI Genbank Blast. (http://blast.ncbi.nlm.nih.gov/Blast.cgi).

Site		Morphotype	Number of Spores	E-Value	% Identity	Accession No.	Fungal species
Site 1	Lonmin Mine(NWL)	Oval Black	20	0	91	HQ258983	Scutellospora sp.
Site 2	Agnes Mine(AGM)	Oval Light Brown	9	1.9	100	AY236236	Glomus sp.
	Maarj*AM*	Oval Light Brown	9	0.29	90	HE615058	*Diversispora torrecillas*
		Oval Light Brown	9	0.0	98	AB220170.1	*Acaulospora colombiana*[1]
	NCBI	**Oval Light Brown**	**9**	**0.0**	**99**	**AB220170.1**	***Acaulospora colombiana***[2]
Site 3	East Rand (ER1) –	Oval Light Brown	11	0.28	100	FM865581.1	*Rhizophagus irregularis*
	(Brakpan)	Oval Light Brown	11	0.0	99	GQ140615	*Acaulospora* sp.
	Maarj*AM*	Oval Brown	11	0.0	100	FN547526	*Ambispora appendicular*
		Oval Light Brown	11	1.9	99	FR773148	*Glomus clarum*
	NCBI	**Oval Light Brown**	**11**	**0.0**	**99**	**AJ852597.1**	***Glomus clarum***
		Oval Light Brown	**11**	**0.0**	**99**	**GQ140615.1**	***Acaulospora clone* sp.**
Site 4	Vaal Reefs (VRS)	Oval Brown	9	0.0	91	HQ258983	*Scutellospora* sp.
	Maarj*AM*	Oval Brown	9	0.0	98	AB220170.1	*Acaulospora colombiana*[3]
		Oval Brown	10	0.0	100	AY394664	*Acaulospora* sp.
	NCBI	**Oval Brown**	**9**	**0.0**	**91**	**HQ258983**	***Scutellospora* sp.**
		Oval Brown	**9**	**0.0**	**99**	**AB220170.1**	***Acaulospora colombiana***
		Oval Brown	**10**	**0.0**	**93**	**AY394664**	***Acaulospora* sp.**
Site 5	West Wits (WW)	Oval Light Brown	104	0.0	99	AB220170.1	*Acaulospora colombiana*
	NCBI	**Oval Light Brown**	**104**	**0.0**	**99**	**AB220170.1**	***Acaulospora colombiana***
Site 6	East Rand (ER2A) MP	Oval Light Brown	9	0.07	100	AM420373.1	*Acaulospora* sp.
	Maarj*AM*	Oval Light Brown	29	0.0	99	AB220170.1	*Acaulospora colombiana*

[1] *Acaulospora sp* (AB220170.1) from Maarj*AM* is the same as *Entrophospora* colombiana (AB220170.1) from NCBI.

[2] *Entrophospora colombiana* (AB220170.1) from NCBI is the same as *Acaulospora* sp (AB220170.1) *from* Maarj*AM.*

[3] *Kuklospora* sp from Maarj*AM* is the same as *Acaulospora colombiana.*

	NCBI	**Oval Light Brown**	**29**	**0.0**	**99**	**AB220170.1**	***Acaulospora colombiana***
Site 7	East Rand (ER2D)	Oval White	29	0.0	93	AJ276079.2	*Claroideoglomus claroideum.*
	Maarj*AM*	Oval White	29	1.2	100	JN581962	*Glomus kohout*
		Oval White	29	0.0	100	AJ276079.2	*Acaulospora* sp.
		Oval White	29	0.0	100	EU332722	*Scutellospora* sp.
	NCBI	**Oval Brown**	**29**	**0.0**	**96**	**EU332722**	***Scutellospora* sp.**
Site 8	Vaal Reefs (VRM)	Oval Light Brown	81	0.0	99	AB220170.1	*Acaulospora colombiana*[4]
	NCBI[5]	**Oval Light Brown**	**81**	**0.0**	**99**	**AB220170.1**	***Acaulospora colombiana***[6]

[4] *Acaulospora sp* (AB220170.1) from Maarj*AM* is the same as *Entrophospora colombiana* from NCBI.
[5] Bold font represents NCBI Blast while normal font represents Maarj*AM* Blast.
[6] *Entrophospora colombiana* (AB220170.1) from NCBI is the same as *Acaulospora* sp from Maarj*AM.*

There were inconsistencies with the grouping in the phylogram, for instance, the *Acaulospora (Kuklospara)* sp (AB220170.1) data sequences did not all group together nor did the *Glomus clarum* (FR773148) with the *Glomus kohout* 12 OTU37 (JN581962), equivalent match, group together separately from the other *Glomus* sequences, instead *Glomus* grouped with the *Scutellospora* and *Ambispora appendicular* (Fig. 5.5). Similarly, in Fig. 5.6 the grouping in the phylogram had inconsistencies, but not as bad as in Fig. 5.5. Most of *Acaulospora colombiana* data sequences grouped together, with the exception of *Glomus clarum* (AJ852597.1) which grouped with some *Acaulospora colombiana* (AB220170).

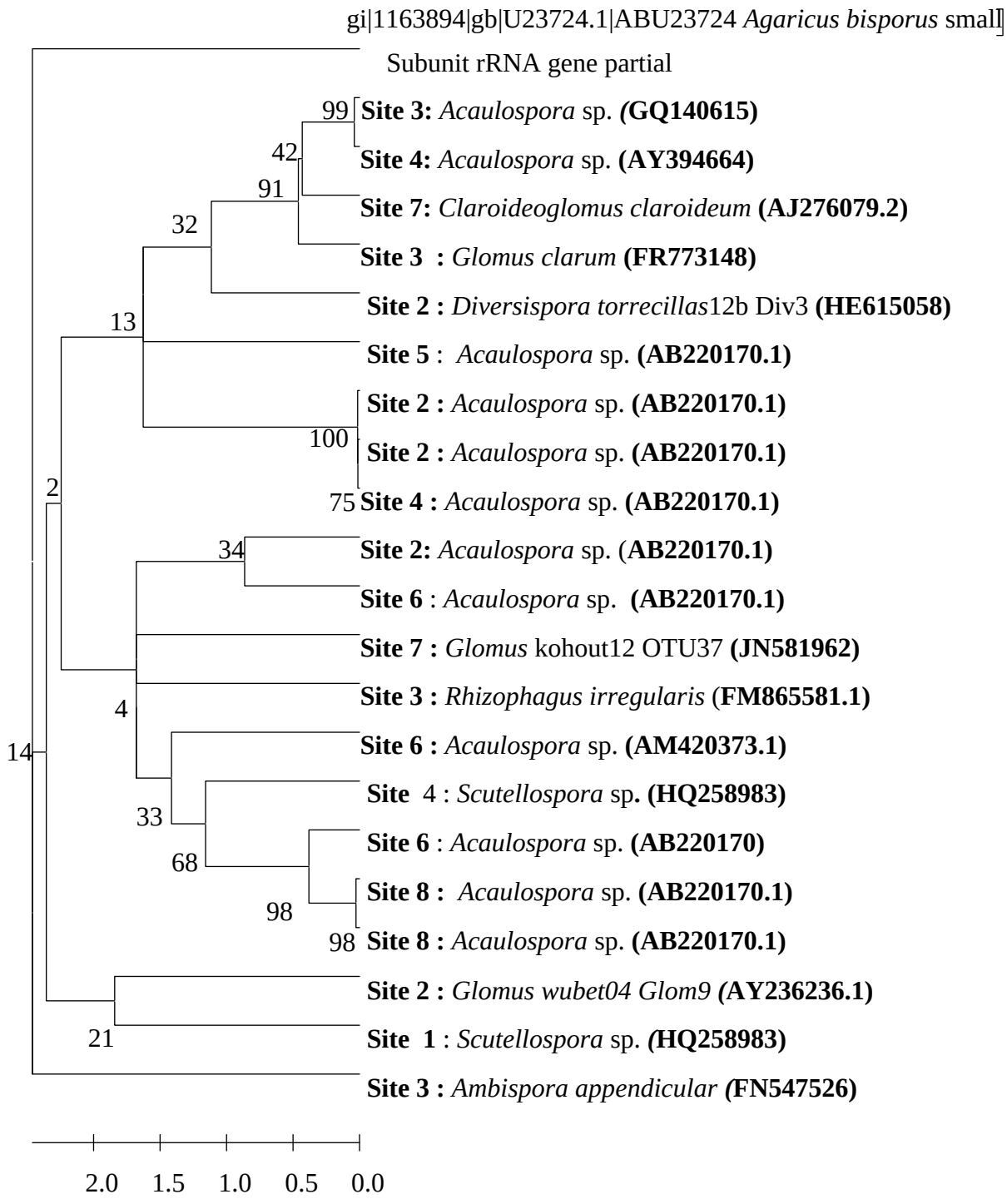

Fig. 5.5 Rooted neighbour-joining tree based on SSU rDNA from AM fungal spores using Maarj*AM* Genbank database (http://maarjam.botany.ut.ee). Bootstrap values (based on 1000 replicates) are shown at the nodes and *Agaricus bisporus* served as the outgroup. *Acaulospora* sp. in the fig represents *Acaulospora colombiana* (http://maarjam.botany.ut.ee).

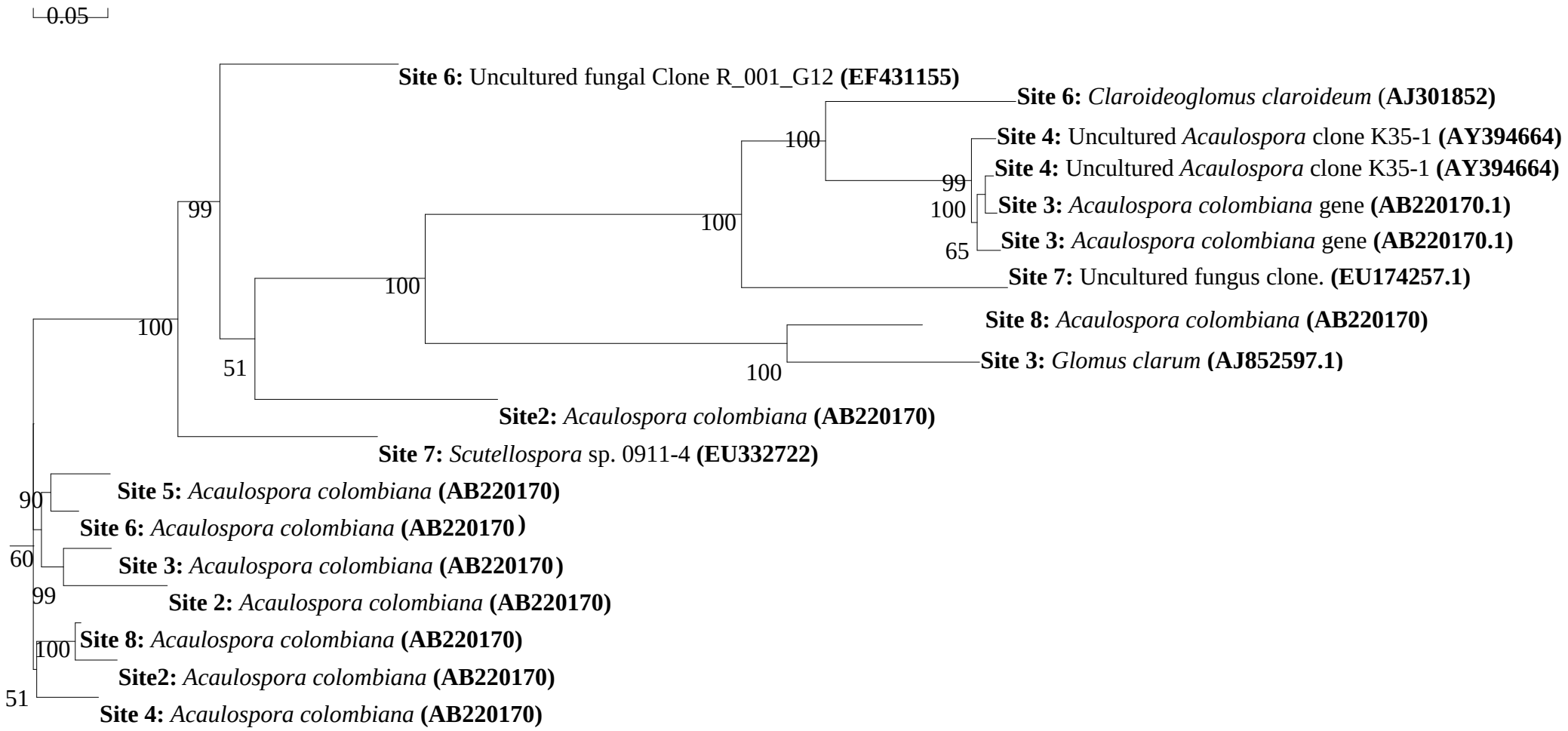

Fig. 5.6 Rooted neighbour-joining tree based on SSU rDNA from AM fungal spores using NCBI Genbank database (http://blast.ncbi.nlm.nih.gov/Blast.cgi).

The sequence identity percentages of NCBI Genbank Blast differed from that of Maarj*AM* Genbank Blast. NCBI had lowest sequence identity percentages ranging from 84% to 99% for each sequence, while Maarj*AM* Genbank Blast had sequence identity percentages ranging from 90%, to 100% for each sequence (Table 5.1).

5.2 Discussion

Molecular analysis is crucial for accurate AM fungal identification as some species exhibit more than one morphology and several cryptic taxa exist which can only be revealed or disclosed by molecular biological analyses (Schüßler *et al*., 2011). AM fungal identification, only by the 'classical' characterization based on spore appearance may be inconsistent because of limited morphological differentiation. Thus, it is very important to always complement the morphological identification with molecular analysis (Krüger *et al.*, 2012).

The two sets of nested PCR primers namely NS1 & NS4 coupled with AML1 & AML2 employed in this study have been reported to amplify all subgroups of arbuscular mycorrhizal fungi, but exclude sequences from other organisms. They were designed to facilitate rapid detection and identification directly from field-grown plant roots and mycorrhizal spores (Lee *et al.*, 2008). These primers (AML1 and AML2) were constructed to target the small subunit rRNA gene because phylogenetic relationships among the Glomeromycota are well understood for this gene. Sequence comparisons had shown that the two primers mentioned above could amplify all published AM fungal sequences except those from *Archaeospora trappei* as it has been seen in our study. Molecular identification was able to confirm most of the genera identified by morphological identification which revealed AM fungal species diversity of thirteen genera namely, *Glomus, Acaulospora, Gigaspora, Archaeospora, Scutellospora, Rhizophagus, Claroideoglomus, Ambispora, Sclerocystis, Fuscutata, (Dentiscutata Scutellospora, heterogama), Entrophospora, Paraglomus* and *Diversispora,* (Table 4.1 to 4.4) as mentioned above, except *Gigaspora* and *Archaeospora*.

The molecular identification results do not only assist in revealing the AM fungal diversity of HM polluted mine tailing environments but also contribute to our knowledge of their diversity in South Africa. This is vital since in Africa for instance, there is a lack of understanding of the distribution of AM fungi geographically due to low levels of molecular data from some areas (Öpik *et al.*, 2010).

The most abundant AM fungal species identified by molecular analysis using NCBI Genbank Blast in Fig. 5.6, starting with the highest species were *Acaulospora colombiana* (13) followed by *Glomus* (2), and *Scutellospora* (1) species. The most abundant AM fungal species identified by molecular analysis using Maarj*AM* Genbank Blast (Fig. 5.5), starting with the highest species were *Acaulospora* (12) followed by *Glomus* (3), *Scutellospora* sp. (2), *Claroideoglomus claroideum* (1) *Diversispora* (1) and *Ambispora appendicular* (1) species. This suggests that *Acaulospora colombiana* is an AM fungal ubiquitous species able to withstand a range of heavy metal sites.

About 18 *Acaulospora* spp. with smooth spore surfaces and 15 Acaulospora spp. with ornamentation of the outer wall are known (Sieverding and Oehl, 2006). As indicated in Chapter 4, *Acaulospora colombiana* has been reported in a number of countries including Colombia, Brazil (Dos Anjos *et al*., 2010), Philippines (Oba *et al*., 2004), Germany and Switzerland (Sieverding and Oehl, 2006). However none of the above studies reported it on heavy metal contaminated tailings. Germany for example reported it on an acidic sandy soil near Berlin (Baltruschat, pers. com) (Sieverding and Oehl, 2006).

Consequently, identified AM fungi can be compared to previous AM fungal community investigations that used either morphological or molecular identification methods. In addition to the AM fungal species namely, *Glomus etunicatum* (now *Claroideoglomus etunicatum*), *Glomus rubiforme* (now *Sclerocystis rubiformis*), three species from the *Acaulospora* genus and the genera *Gigaspora* and *Scutellospora* identified in the study performed by both Straker *et*

al. (2010) and Spruyt *et al.*, (2014), this study identified about 9 more AM fungal species such as *Rhizophagus*, *Funneliformis*, *Archaeospora*, *Claroideoglomus*, *Ambispora*, *Sclerocystis*, *Fuscutata*, *Diversispora*, *Paraglomus* (Tables 4.2 to 4.5). Due to the higher number of species identified in this study, the overlap of AM fungal species identified in these various investigations appears to be moderate, which suggests that the previous analyses may underestimate AM fungal diversity. As previous analyses were performed on spores, the AM fungal community in South Africa may be even more diverse than has been revealed in this study. Future research in this field would be to analyse the AM fungal diversity using both spores and colonised roots of plant species at different environmental conditions such as mine tailings, HM metal polluted sites and undisturbed environments.

The recent revisions and consolidations in the phylotaxonomy of AM fungi have provided the necessary basis for comprehensive investigation into the diversity of AM fungi from environmental samples (Krüger *et al*., 2012; Redecker *et al.*, 2013; Schüßler and Walker, 2010). The lack of consensus in the system of nomenclature to be applied to AM fungi identified by molecular data in the past, has greatly affected the investigation of AM fungal communities (Krüger *et al*., 2012; Öpik *et al*., 2010; Redecker *et al.,* 2013). Since the classification of AM fungi as an independent phylum within the fungal kingdom in 2001 (Schüßler *et al*., 2001), several taxonomic restructurings have been proposed by different groups (Stürmer, 2012). This has brought some confusion when identifying these fungi, where the same phylogroups of AM fungi are identified with different names in different studies (Öpik *et al.,* 2010). Similar to the study by Spruyt *et al.* (2014), this study used the phylogenetic reference data describing interspecific genetic variability of described Glomeromycota species which has recently been made possible by Krüger *et al.*, (2012). This allows the relationship or comparison for new analyses of the molecular diversity of AM fungal communities. The low levels of molecular data from certain regions, especially in Africa and particularly in South Africa, is a great challenge when it comes to the current understanding of the geographical distribution of AM fungi (Öpik *et al*., 2010, Spruyt *et al.,* 2014).

Although this study has provided an increased knowledge of AM fungal species diversity in South Africa, there is still more to be discovered about the diversity and distribution of AM fungi in South Africa (Spruyt *et al*., 2014).

To our knowledge, this is the first time *Acaulospora colombiana* species has been discovered in heavy metal contaminated sites in South Africa. The molecular identification studies performed by Spruyt *et al*. (2014) found *Claroideoglomus etunicatum* species and *Acaulospora mellea* species typically associated with the *T. usneoides* plant host at different mining sites such as ABB Zinc, Impala Platinum, and Northern Cape sites. This suggest that both *Acaulospora colombiana* and, *Glomus* species identified in this study are the AM fungal isolates responsible for the survival of plants growing in heavy metal sites and thus it could be useful to solve the heavy metal contamination of the mine tailings.

CHAPTER 6

6 RESULTS AND DISCUSSION: MICROANALYSIS

6.1 ICP-MS and Micro-PIXE analysis of total values

ICP-MS analysis was performed in roots of *E. curvula* plant to determine concentration levels as baseline data for setting parameters for the Micro-PIXE analysis. Al, Br, Ca, Cl, Pt, S, Si, and V could not be detected at all by the ICP-MS technique while they were all detected by Micro-PIXE except Pt which was not localised by PIXE. All the elements were also present in controls but in lower concentration than experimental samples except for few elements such as K, Cu, Zn and Mn which were detected at high concentration in control 2 with Mycoroot. The presence of elements in the controls was due to the elements from the nutrient solution (Appendix 4) while the high concentration of elements in control 2 was due to the presence of Mycoroot (Appendix 9 and Table 6.1). The pattern in Table 6.1 shows that in all sites but site 7 (ER2D, MP) Si has a highest concentration. The average concentrations of elements in root both longitudinal and root cross-sections as well as limit of detection were recorded and presented in Appendix 3 and Table 6.1. Values are the means of PIXE measurements of 3 to 7 replicates SEM which indicates that in some samples there were three replicates while others were 5 or 7 replicates.

There was a significant difference between some elemental concentrations amongst sites (Table 6.1). The concentration of Al was found to be highest site 3 and lowest in site 5 with significant difference as shown by alphabetic letters “a” and “b”, while Si was highest in site 6 and lowest in site 7 and control 2, however their differences were not significant as shown by alphabetic letters “ab” (Table 6.1). There were no significant differences in P except in control 2. S concentration was highest in site 7 and lowest in site 3 with no significant difference amongst the sites. There was no significant difference in Cl concentration amongst the sites although its highest concentration was observed in site 3 except control 1 which showed a significant difference. Both Ca and K had highest concentrations in site 3 and lowest concentration in control 1. There was a

significant difference in K between site 3 and other sites except for control 1; while Ca concentration was recorded highest in site 3 followed by Site 6 then site 7 with no significant difference amongst the sites (Table 6.1).

Similarly both Mn and Ti had highest concentration in site 3 and 4 while the lowest for Mn was observed in site 5 and Ti in site 8. Statistics could not be done for Ti due to insufficient replication. Highest concentration for Fe has been observed in site 3, 2 and 4 and lowest in site 8 with no significant difference between the sites. Ni had a highest concentration in site 2 (AGM Serpentine) as compared to other sites, while both Cu and Zn had highest concentrations in site 4 and 6 (Table 6.1). The high concentration of Ni in site 2 is due to the fact that this site is a serpentine site with a pronounced concentration of Zn, Fe to name but a few. The concentration of Ti, V, Cr, Mn, Ni, Cu, Zn, and Br were lower and the concentrations of As, Se, Sr, Ba, Pb and U were generally very low, often below the respective limits of detection (Appendix 3, and Table 6.1[7]). Although U was detected at a very low concentration by both techniques (ICP-MS and Micro-PIXE), a pronounced concentration of U was observed in site 4 (VRS) and site 5 (WW) which are high in gold and uranium (Fig. 6.21k). Although high Pt concentration was observed in the soil (Fig. 6.21b), surprisingly it could not be detected at all in plants by both ICP-MS and Micro-PIXE, from all the sampling sites including the Lonmin Platinum Mine site. Roots from plants growing from the East Rand Brakpan site 3 showed up to 5 fold increase in aluminum compared to other sites. Phosphorus is observed to be in the same range in almost all the sites except control 2 which is higher than other sites (Table 6.1). Both techniques

---

- [7] Replicates represent PIXE measurements with values representing the means of a number of random (or selected) point measurements made over the area being probed by the beam in a single root sample.
- Au, U Pt and Cd were measured but they were less than the detection limit thus they could not be included in table 6.1.

detected P, K, and Cu at higher concentration in control 2 and lowest concentration in control 1 (Appendix 9 and Table 6.1).

Generally phosphorus was detected at higher concentration in all the sites especially when ICP-MS was used (Appendix 9). In general both techniques showed agreement in the detection of the elements.

Other elements such as Ti, Mn, Fe, Zn, were detected at high concentration at different sites. Thus there were some inconsistencies between the two techniques. For instance, Micro-PIXE detected Fe at high concentration in site 3 (ER1 BP) while ICP-MS showed high concentration of Fe in site 2 (AGM). Similarly to Mn, which was detected by ICP-MS at high concentration in control 2 while PIXE showed high concentration of Mn in site 3 (ER1 BP). In overall, both the ICP-MS and PIXE had similar or common elemental concentrations.

Table 6.1 Elemental totals in roots of *E. curvula* growing in substrata from different metal sites inoculated with mixture of spores extracted from the substrata. Values are the means of PIXE measurements of 3 to 7 replicates SEM. Concentrations are reported in ppm (mg/kg^{-1}). Common alphabetic letters indicate no significant difference between sites for each element ($p \leq 0.05$). The statistics could not be done for elements V, Cr, Ni, and Br, due to insufficient replication. Acronym "nd" indicates not detected.

Sites	Code	Al	Si	P	S	Cl	K	Ca	Ti	V	Cr	Mn	Fe	Ni	Cu	Zn	Br
Site 1	NW (L)	1542 ± 358^{ab}	6950 ± 1525^{a}	219 ± 49^{a}	4925 ±1535^{a}	1051 ±303^{ab}	747 ±522^{b}	641 ±336^{a}	10 ±5	2	13	22 ±10^{a}	272 ±143^{a}	38	50±25^{ab}	23 ±10^{ab}	18
Site 2	ABB	2452 ± 1312^{ab}	12754 ± 2956^{a}	294 ± 53^{a}	4861 ±1134^{a}	1279 ±187^{ab}	1519 ±318^{b}	726 ±140^{a}	45 ±33	nd	14	17 ±4^{a}	1589 ±1140^{a}	74	40 ±19^{ab}	19 ±6^{ab}	2
Site 3	ER1 (BP)	4388 ± 179^{a}	8030 ± 1093^{a}	367 ± 11^{a}	996 ±65^{a}	1427 ±70^{ab}	2348± 253^{a}	1333± 429^{a}	75 ±15	8	5	150 ±58^{b}	2092 ±405^{a}	7	35±11^{ab}	64 ±10^{ab}	10
Site 4	VRS	3609 ± 1251^{ab}	12138 ± 714^{a}	269 ± 23^{a}	2077 ±262^{a}	753 ±103^{b}	1579 ±465^{b}	816 ±174^{a}	65 ±46	7	6	111 ±47^{bc}	1584 ±979^{a}	5	81 ±39^{ab}	121 ±46^{ab}	11
Site 5	WW	917 ± 166^{b}	6817 ± 1498^{a}	163 ± 17^{a}	3310 ±1067^{a}	1356 ±192^{ab}	322 ±71^{b}	542 ±83^{a}	16 ±3	2	4	7 ±1^{a}	185±34^{a}	3	16 ±2^{a}	32 ±3^{ab}	8
Site 6	ER2A (MP)	1248 ± 220^{ab}	13951 ± 2076^{a}	352 ± 67^{a}	4990 ±2701^{a}	1216 ±348^{ab}	239 ±74^{b}	909 ±425^{a}	28 ±10	2	5	15 ±6^{a}	366 ±195^{a}	2	86 ±29^{b}	178 ±80^{b}	7
Site 7	ER2D (MP)	1316 ± 520^{ab}	6451 ± 950^{a}	248 ± 36^{a}	8736 ±1718^{a}	825 ±170^{b}	539 ±116^{b}	862 ±445^{a}	23±11	8	6	37 ±19^{ac}	331 ±148^{a}		24±9^{a}	77 ±43^{ab}	9
Site 8	VRM	835 ± 133^{b}	6860 ±1723^{a}	303 ±199^{a}	3718 ±1391^{a}	1219 ±478^{ab}	269 ±71^{b}	538 ±138^{a}	7 ±2	1	nd	15 ±4^{a}	55 ±7^{a}	Nd	14 ±4^{ab}	19 ±4^{ab}	3
Control 1	CTR1	926 ± 137^{b}	6540 ± 1229^{a}	120 ± 16^{a}	2434 ±819^{a}	1243 ±213^{ab}	217 ±63^{b}	100 ±23^{a}	11±4	4	10	23 ±8^{a}	81 ±29^{a}	4	23 ±7^{ab}	12 ±3^{a}	0
Control 2	CTR2	1636 ± 444^{ab}	5408 ± 2068^{a}	785 ± 167^{b}	5016 ±1558^{a}	2329 ±390^{a}	4077 ±934^{a}	888 ±145^{a}	23±7	nd	nd	50 ±8^{a}	320 ±79^{a}	16	99±12^{b}	44 ±7^{ab}	7

6.2 Microscopic observations of colonisation

The highest percentage of mycorrhizal root colonisation observed in almost all the sites was caused by hyphae followed by vesicles and then arbuscules. An exception was site 5, 6, 8 and control 1 where the arbuscule % colonisation was higher than that of vesicles (Table 6.2). Control 1 showed the lowest percentage of root colonisation as expected. However it is a surprise to observe some root colonisation; this might be due to the cross contamination. Control 2 was inoculated with a Mycoroot, a commercial mycorrhiza; hence the percentage of root colonisation is higher than that of control 1 (Table 6.2)**.** However it has been noted that root colonization of control 2 by Mycoroot, was lower that the colonization by indigenous mycorrhiza fungi. This might be due to the high concentration of some elements in the commercial multi – nutrient solution that was used in the control pots. Since the commercial Mycoroot was preserved for long time, it might take time to be restored. Lastly, the fungicide used to coat the *Eragrastis curvula* seeds might play a part in the delayed colonization in Control 2.

.

Table 6.2 Mean (%) of mycorrhizal root colonisation, Hyphal Colonisation (HC); Arbuscular Colonisation (AC) and Vesicular Colonisation (VC).

Sites	Code	Sites	HC (%)	AC (%)	VC (%)
Lonmin Mine (L)	NW (L)	Site 1	55.88	15.80	32.66
Agnes Serpentine Mine (AGM), Mpumalanga	AGM	Site 2	79.65	31.20	45.06
Eastern Reef (Brakpan) (1.2; 4.1)	ER1(BP)	Site 3	81.03	29.06	50.03
North West (Vaal Reefs - S)	VRS	Site 4	64.53	20.39	42.90
West Wits (WW)	WW	Site 5	35.04	16.72	13.31
East Rand (Metallurgical Plant - MP) (A2+5)	ER2A (MP)	Site 6	59.96	41.61	14.73
East Rand (Metallurgical Plant - MP) (D1,)	ER2D (MP)	Site 7	58.00	4.00	27.00
North West (Vaal Reefs -M)	VRM	Site 8	93.08	40.71	21.95
Control 1 (Nu + Zeolite)	CTR1	Control 1	0.91	0.50	0.20
Control 2 (Nu + Zeo + Mycoroot)	CTR2	Control 2	23.21	1.12	13.84

6.3 Elemental maps of colonised roots

6.3.1 Elemental concentration and distribution

Elemental maps of both the whole root and root cross-sections are presented on Fig. 6.1 to Fig. 6.19 below. Due to a large data of elemental maps produced, only maps that showed some colonisation are reported. The rest of the maps are reported in Appendix 1 (in a CD). Elemental distribution maps showed that Al, Si, P, S, Cl, K, Ca and Fe were localised and detected at maximum concentration in both the longitudinal and root cross sections in all the sampling sites.

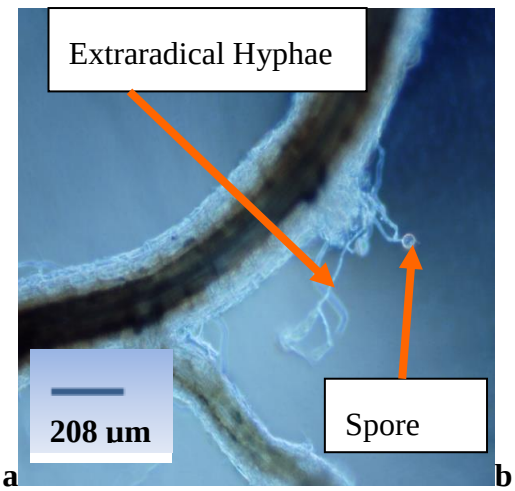

a

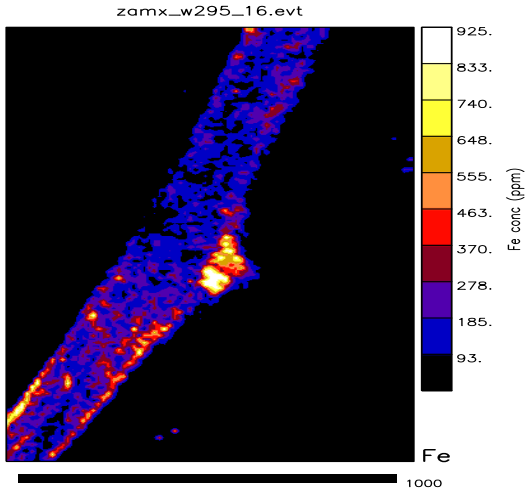

b

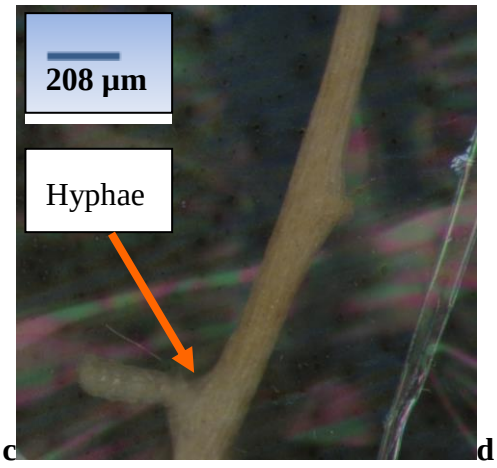

c

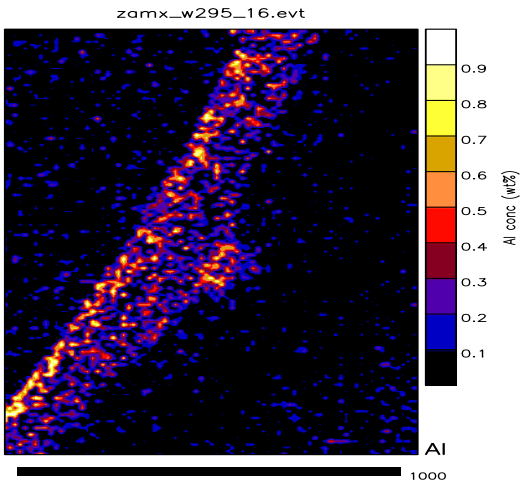

d

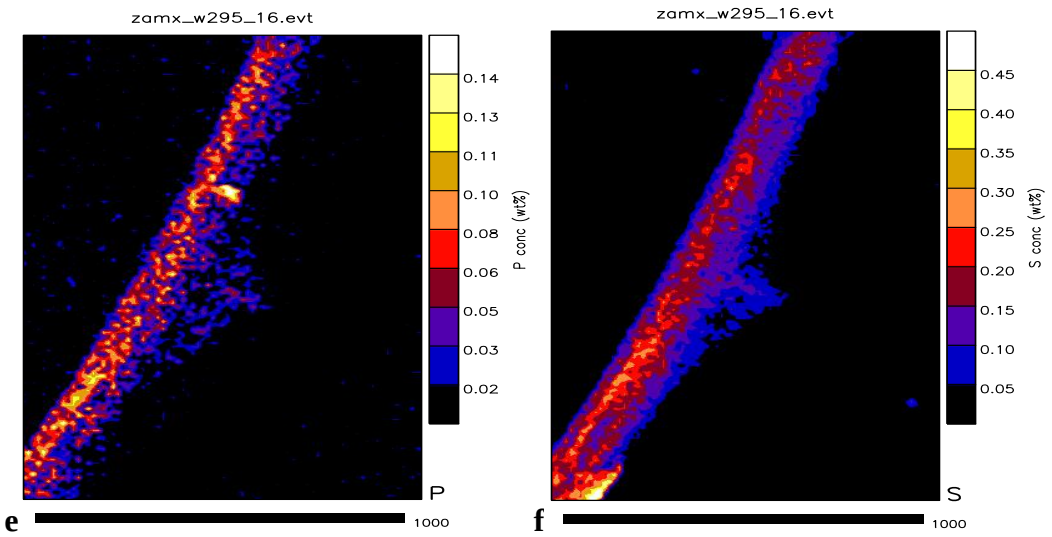

Fig. 6.1 Whole colonised root segment of *E. curvula* plants growing in substratum from North West (Rustenburg) Lonmin Platinum Mine, site 1. a) and c): Light micrograph of fresh colonised root segment. b), d), e), f): Elemental PIXE maps of colonised root segments.

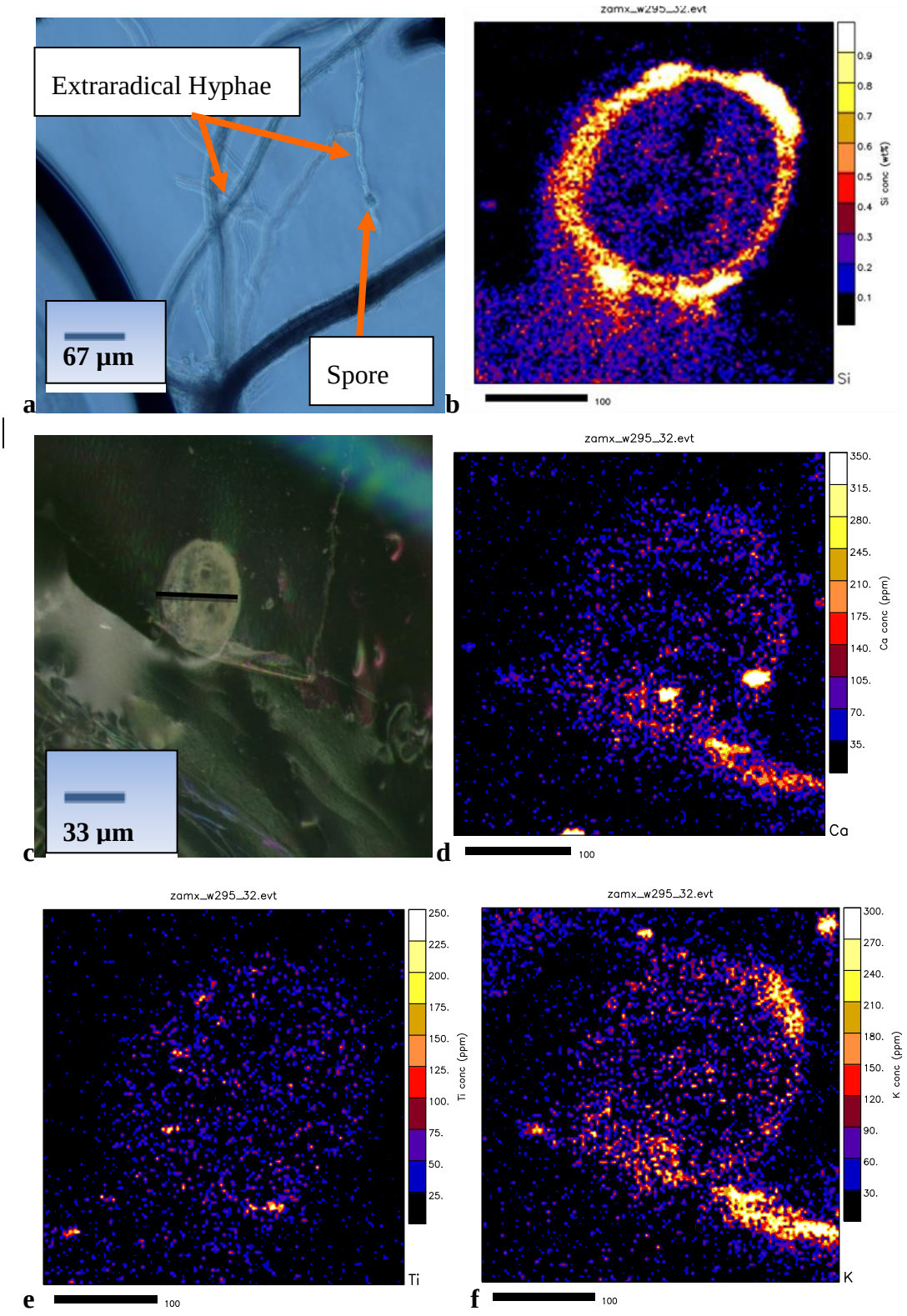

Fig. 6.2 Colonised cross-sections of *E. curvula* roots growing in substratum from North West (Rustenburg) Lonmin Platinum Mine, site 1. a) and c): Light micrograph of colonised root segment; b), d), e) and f): Elemental PIXE maps of colonised root segments.

Low magnification maps of colonised roots from plants grown in soils from Lonmin platinum mine showing both external and intraradical hyphae prior to fixation (Fig. 6.1a, c), were observed to accumulate relatively high concentrations of Fe, Al, P and S mainly in the cortical areas of the roots. The maps are also showing high localised concentrations in an area which may be that of secondary root initiation or dense external hyphal activity (Fig. 6.1b, d, e, f). Cross section maps showed Si to accumulate in a continuous band in the cortical area (Fig. 6.2b). Ca and K show a similar distribution, although not as continuous, with some localised pockets of high concentration (Fig. 6.2d, f) and small scattered deposits of low concentration in other parts of the root, whereas Ti appeared as less numerous discrete deposits in the cortex (Fig. 6.2e).

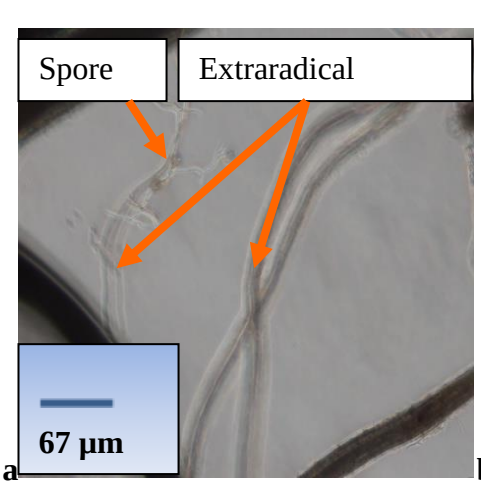
Spore
Extraradical
67 µm

a

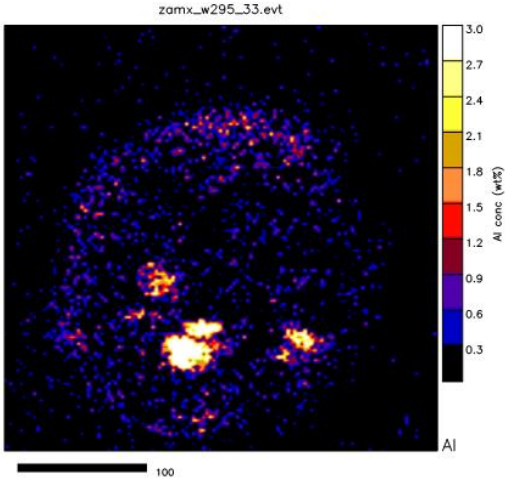
zamx_w295_33.evt
3.0
2.7
2.4
2.1
1.8
1.5
1.2
0.9
0.6
0.3
Al conc (wt%)
Al
100

b

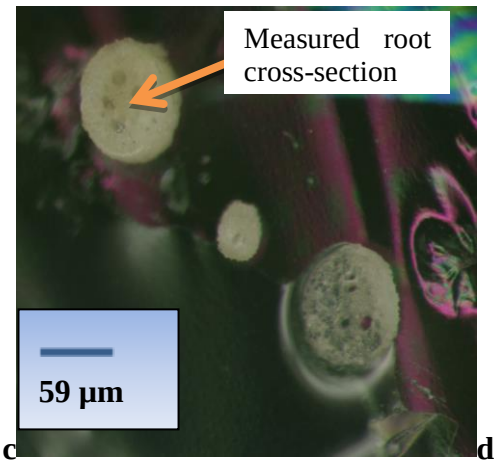
Measured root cross-section
59 µm

c

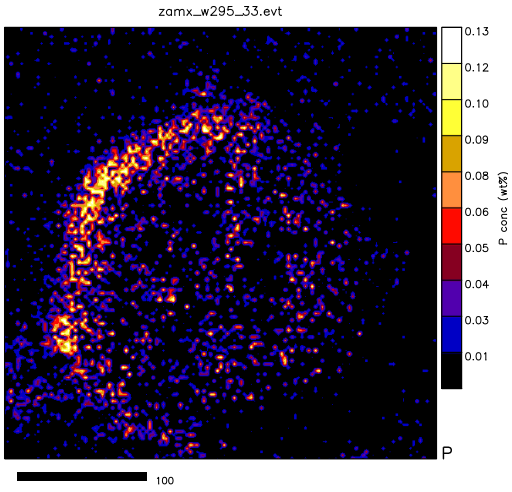
zamx_w295_33.evt
0.13
0.12
0.10
0.09
0.08
0.06
0.05
0.04
0.03
0.01
P conc (wt%)
P
100

d

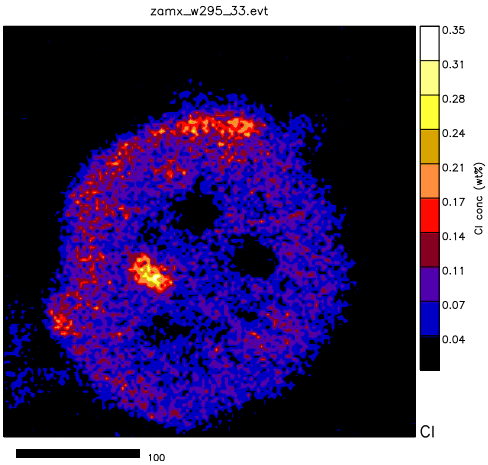
zamx_w295_33.evt
0.35
0.31
0.28
0.24
0.21
0.17
0.14
0.11
0.07
0.04
Cl conc (wt%)
Cl
100

e

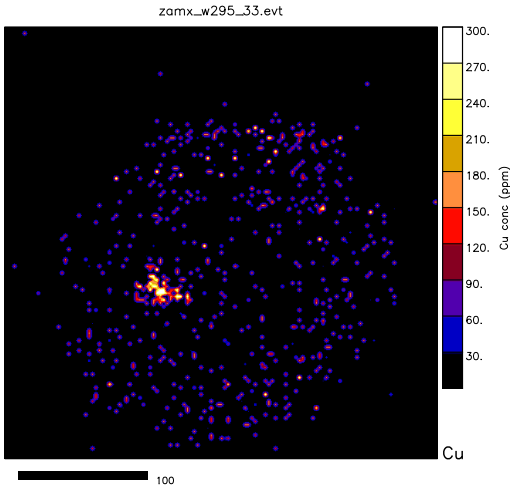
zamx_w295_33.evt
300.
270.
240.
210.
180.
150.
120.
90.
60.
30.
Cu conc (ppm)
Cu
100

f

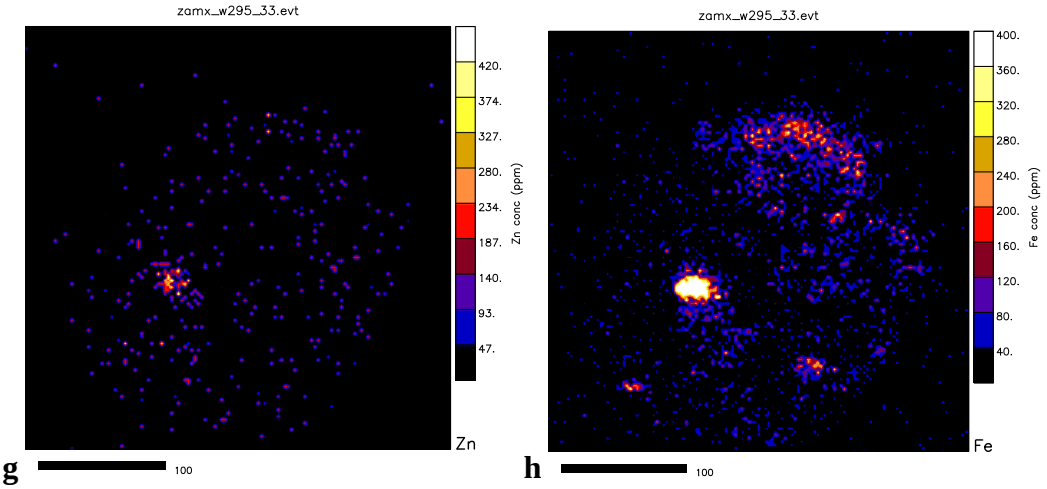

Fig. 6.3 Colonised root cross-sections of *E. curvula* plants growing in substratum from North West (Rustenburg) Lonmin Platinum Mine, site 1. a) and c): Light micrograph of colonised root segment; b), d), e) f), g), and h): Elemental PIXE maps of root segments.

Cross-sections of another root from the same site, with extraradical hyphae (Fig. 6.3a, c), revealed a similar wide distribution of P and Cl in the cortex (Fig. 6.3d, e), and high concentrations of Al and Fe in localised discrete cortical sites and considerable commonality in the localisation of Al, Cl, Cu, Zn and Fe in these sites (Fig. 6.3b, e, f, g, h).

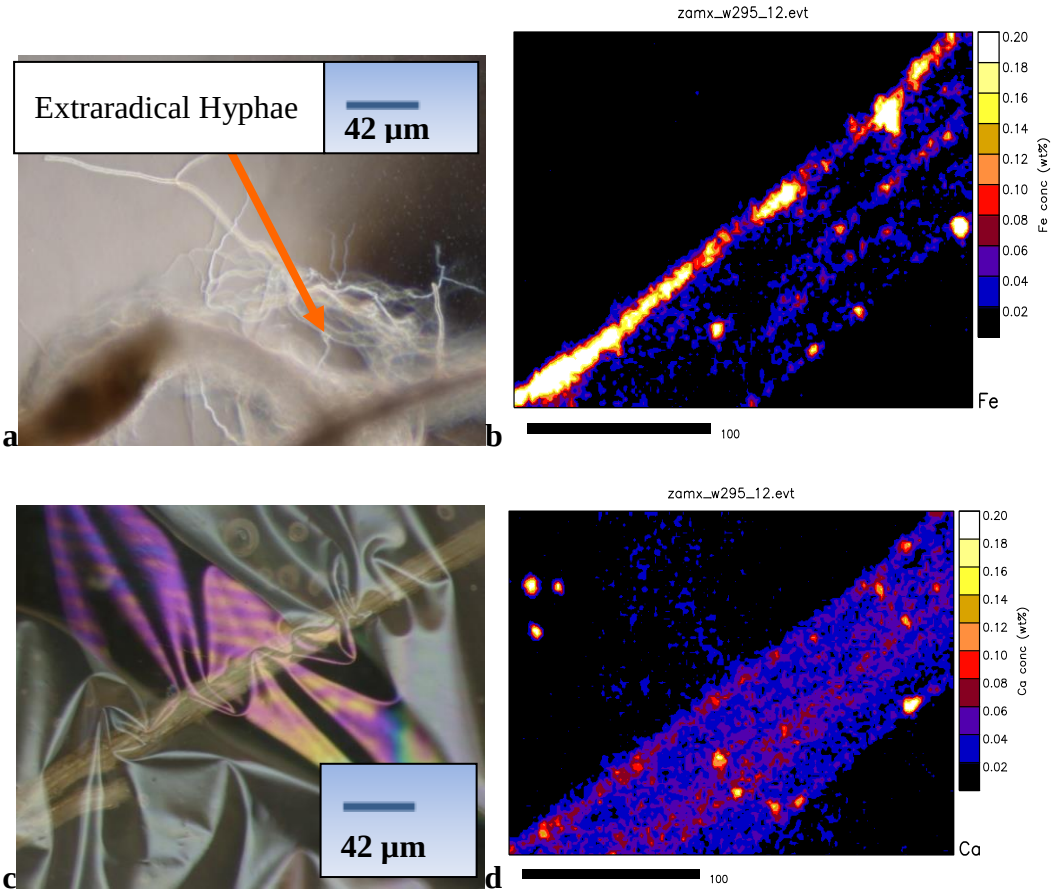

Fig. 6.4 Whole colonised root segment of *E. curvula* plants growing in substratum from site 2. a) and c): Light micrograph of colonised root segment; b), d): Elemental PIXE maps of root segments.

Roots of plants grown in high zinc soils from site 2 (AGM) serpentine mine (Fig. 6.4a, c) revealed a continuous band of accumulation of Fe in the distal cortex/epidermis with other discrete deposits scattered in the root (Fig. 6.4b), whereas Ca was observed to be concentrated in discrete bodies in the cortical areas, but also more generally dispersed in low concentrations in the vascular cylinder (Fig. 6.4d). Cross sections of the root (Fig. 6.5c) confirmed the localisation of Fe in the outer zones in bodies of high concentration (Fig. 6.5b) and Ti accumulated in localised areas in the cortex/epidermis but also scattered in low concentrations in the root interior (Fig. 6.5d).

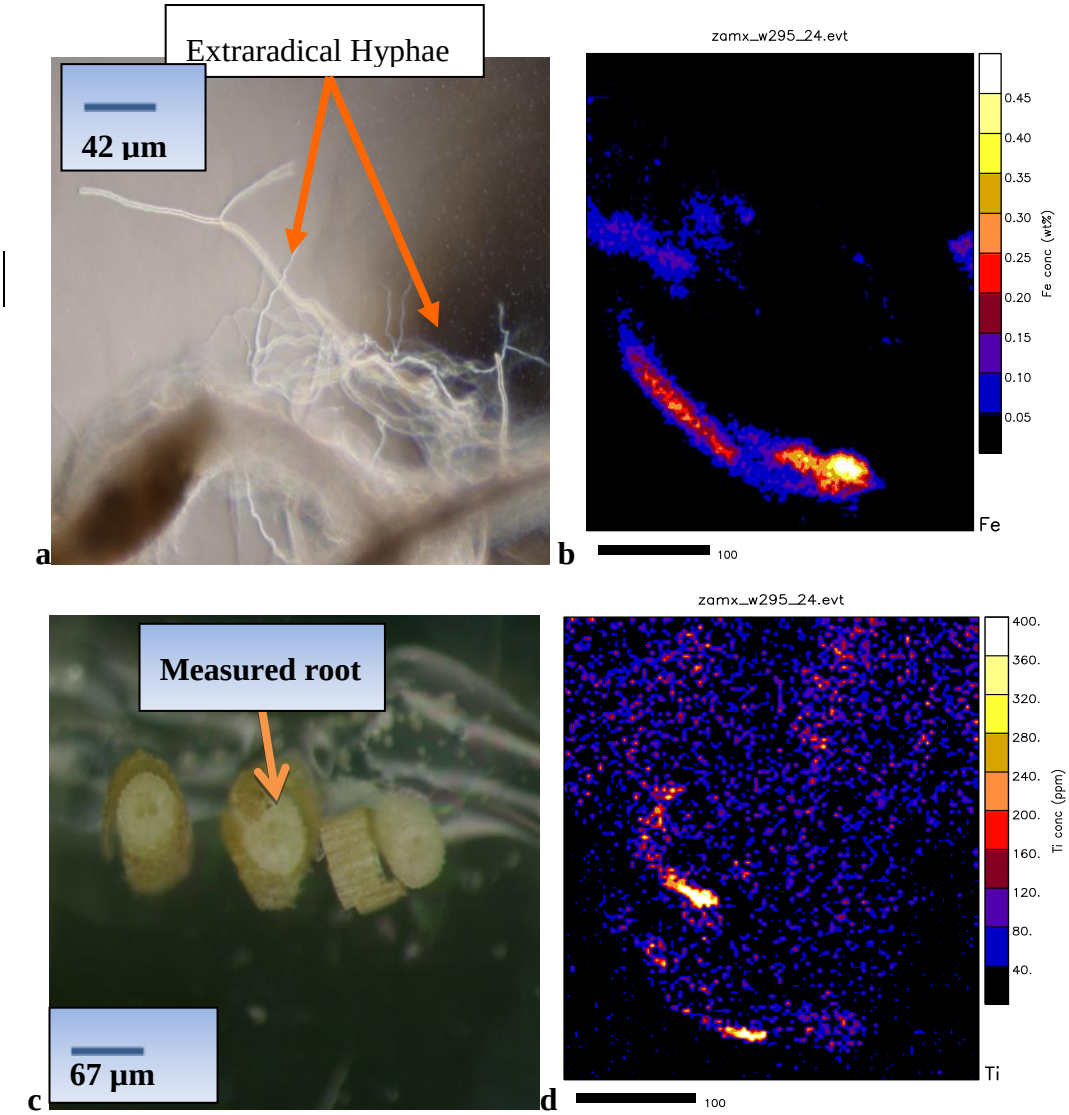

Fig. 6.5 Colonised root cross-sections of *E. curvula* plants growing in substratum from Agnes Mine, site 2. a) and c): Light micrograph of colonised root segment; b) and d): Elemental PIXE maps of root segments.

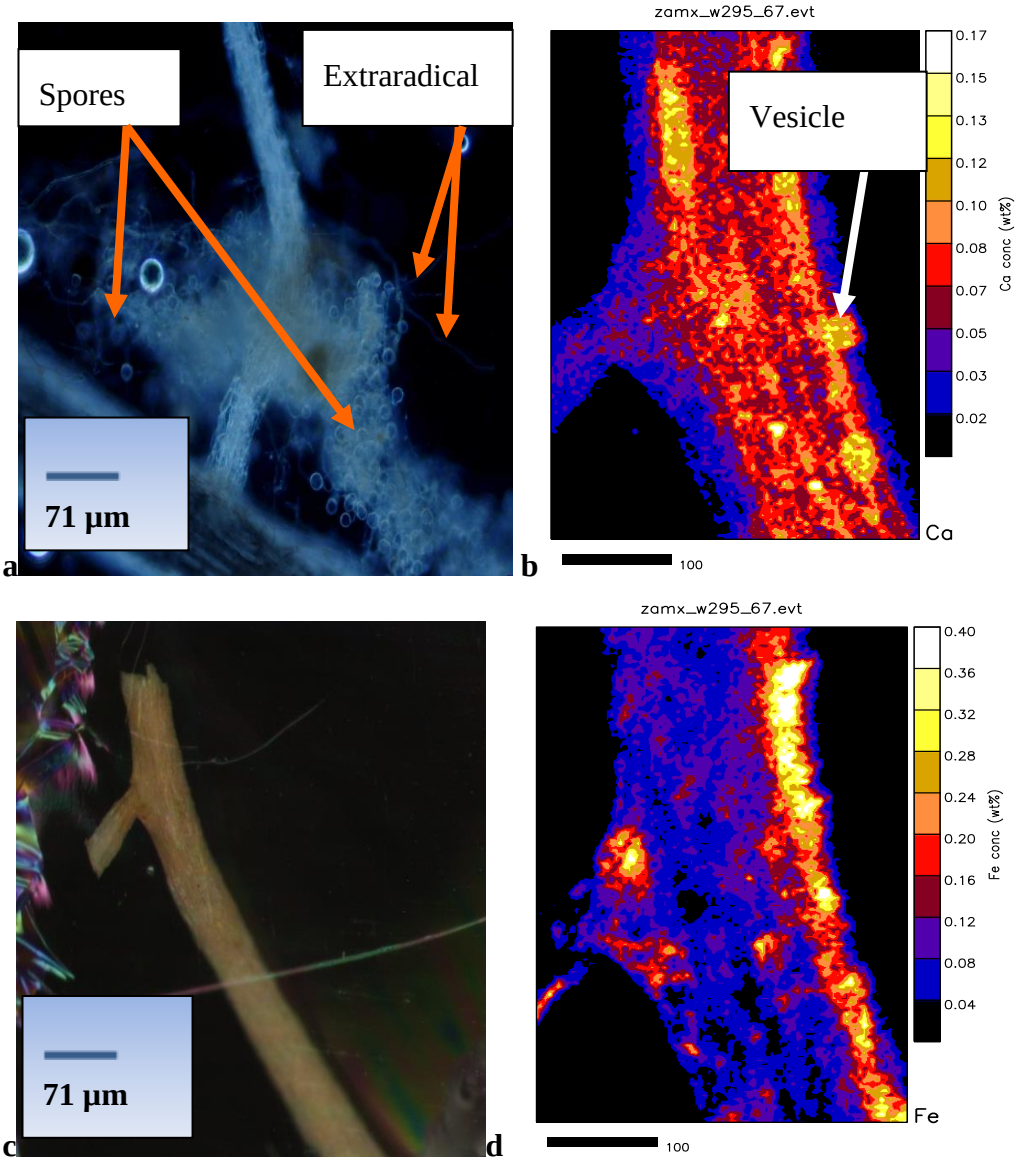
Spores
Extraradical
71 µm
a
zamx_w295_67.evt
Vesicle
0.17
0.15
0.13
0.12
0.10
0.08
0.07
0.05
0.03
0.02
Ca conc (wt%)
Ca
100
b
71 µm
c
zamx_w295_67.evt
0.40
0.36
0.32
0.28
0.24
0.20
0.16
0.12
0.08
0.04
Fe conc (wt%)
Fe
100
d

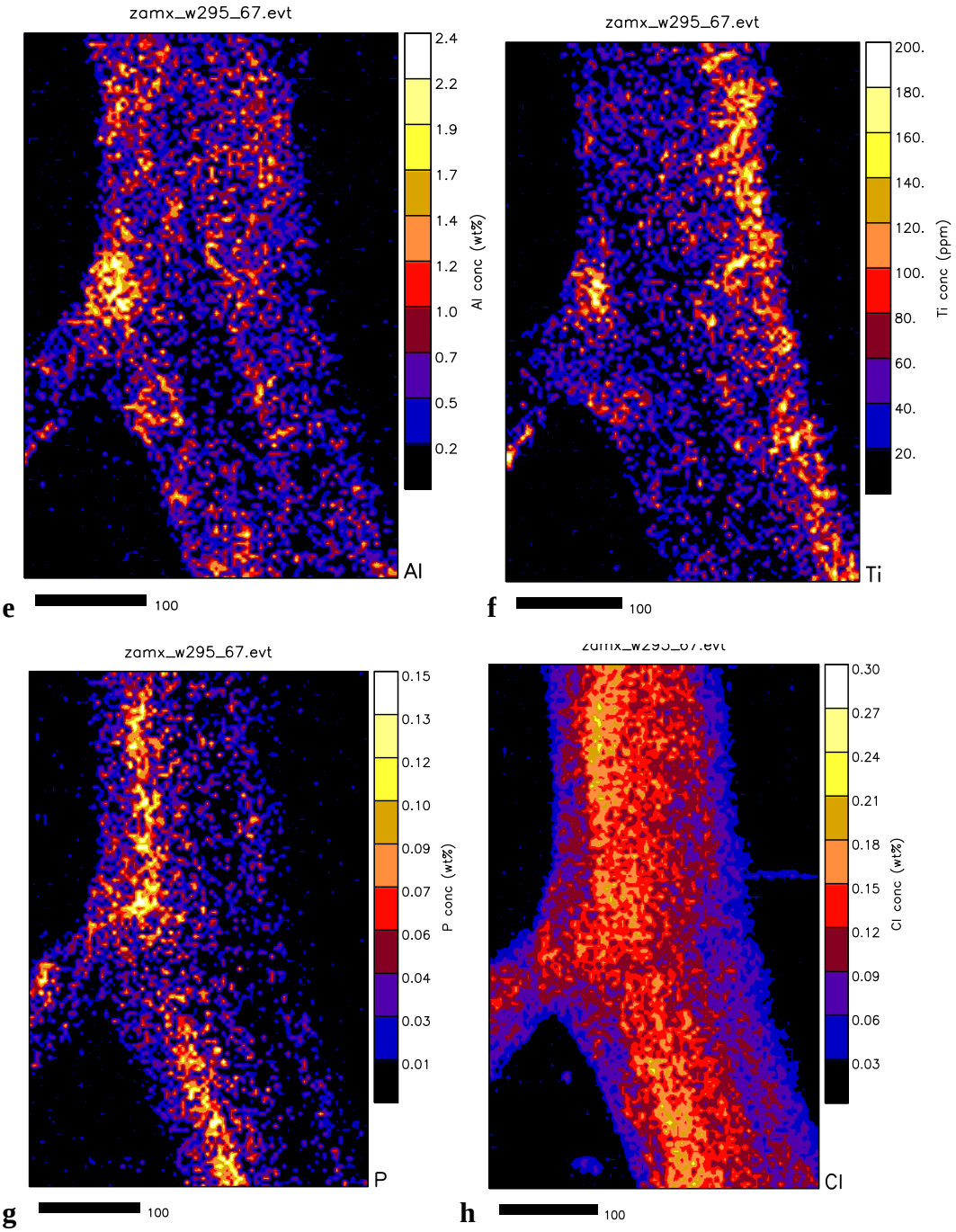

Fig. 6.6 Whole colonised root segment of *E. curvula* plants growing in substratum from East Rand, site 3. a) and c): Light micrograph of colonised root segment; b), d) e), f), g) and h): Elemental PIXE maps of root segments.

An intensely colonised root with a dense presence of extraradical hyphae and spores, from another East Rand site (Fig. 6.6a, c) was probed to reveal an apparently widespread distribution of Ca throughout the root, excepting the

epidermis (Fig. 6.6b) with Fe and Ti following a similar distribution patterns but largely in the cortical regions (Fig. 6.6d, f). P and Cl showed a similar distribution pattern concentrated in the inner cortex but on the opposite side of the root (Fig. 6. 6g, h), whereas a discrete pocket of Al was observed at the junction with a side root (Fig. 6.6e).

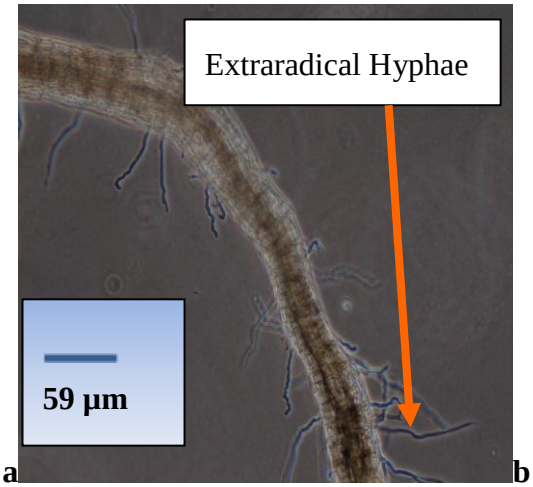

a

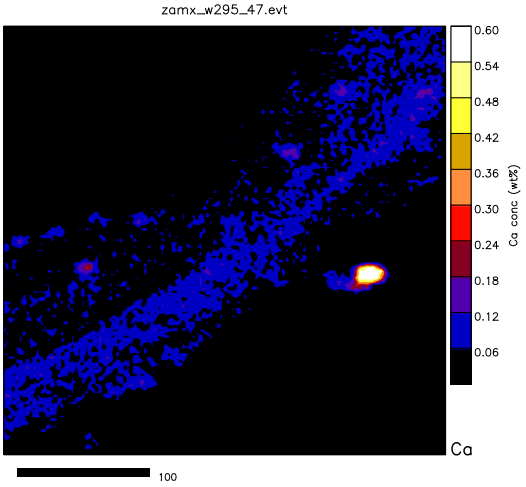

b

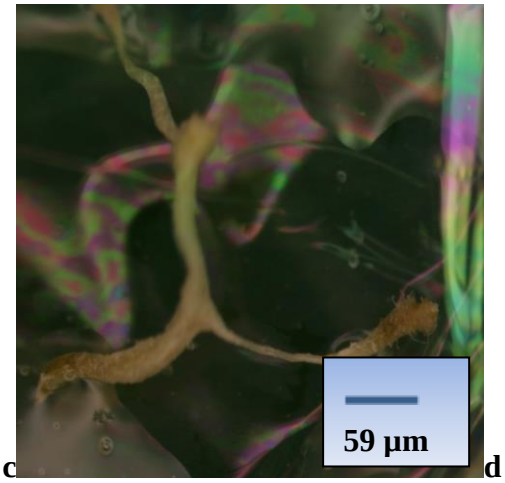

c

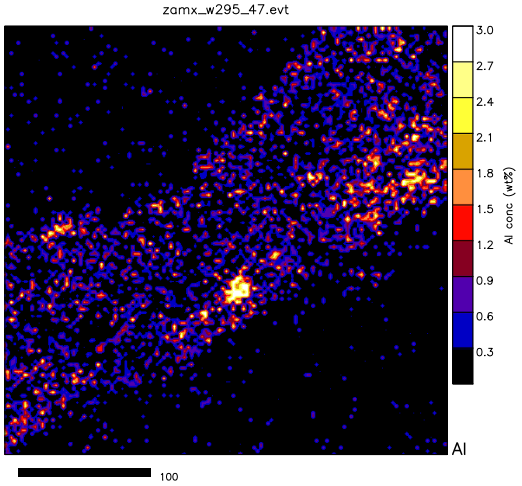

d

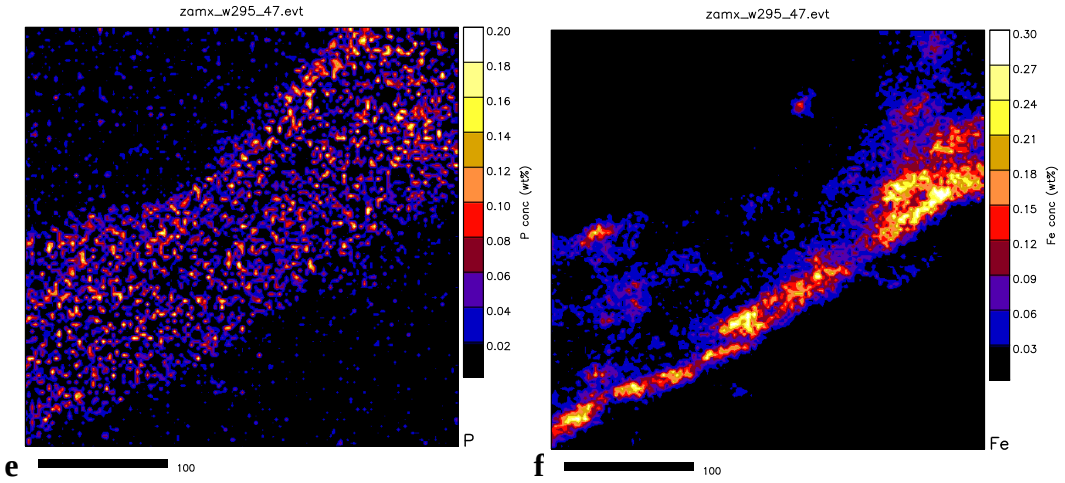

Fig. 6.7 Whole colonised root segments of *E. curvula* plants growing in substratum from North West, Vaal Reefs site 4. a) and c): Light micrograph of colonised root segment; b), d), e) and f): Elemental PIXE maps of root segments.

Light micrographs of colonised roots from plants growing in acidic toepaddock substrata of Vaal Reefs gold and uranium mining site (Fig. 6.7a, c), showed low concentrations of Al and Ca, apparently accumulated in fungal structures such as vesicles/spores and hyphae with Fe widely dispersed in the cortex of the root (Fig. 6.7b, d, f). A wide scattering of P in low concentration is observed across the root (Fig. 6.7e).

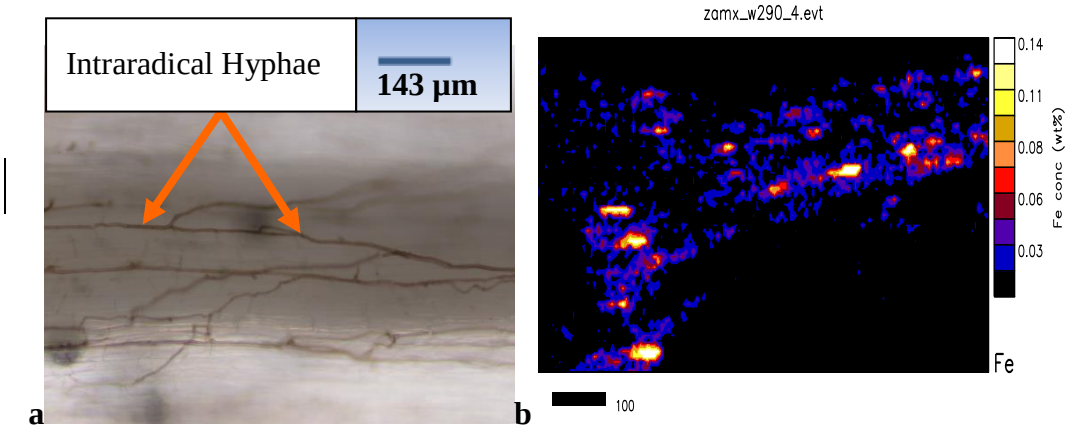
Intraradical Hyphae
143 µm
a
zamx_w290_4.evt
0.14
0.11
0.08
0.06
0.03
Fe conc (wt%)
Fe
100
b

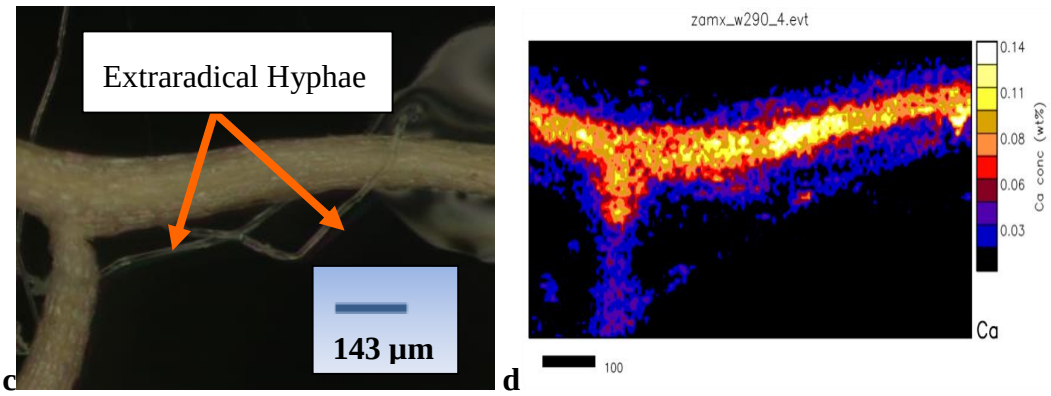
Extraradical Hyphae
143 µm
c
zamx_w290_4.evt
0.14
0.11
0.08
0.06
0.03
Ca conc (wt%)
Ca
100
d

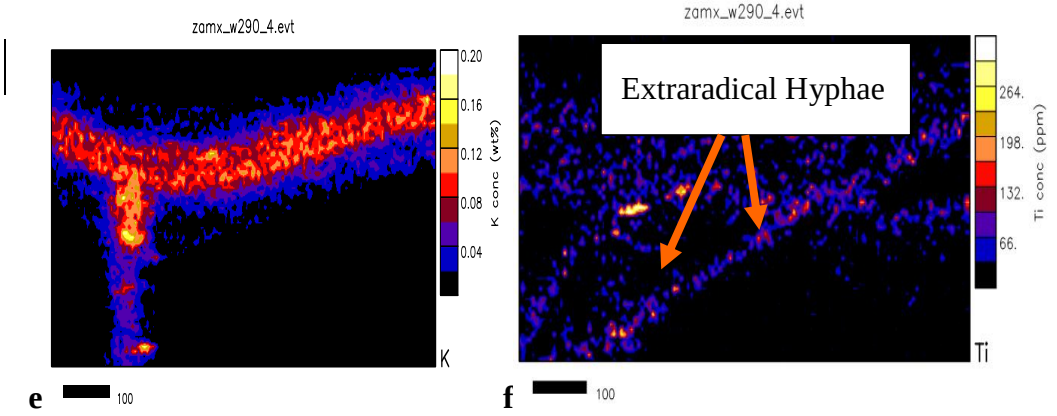
zamx_w290_4.evt
0.20
0.16
0.12
0.08
0.04
K conc (wt%)
K
100
e
zamx_w290_4.evt
Extraradical Hyphae
264.
198.
132.
66.
Ti conc (ppm)
Ti
100
f

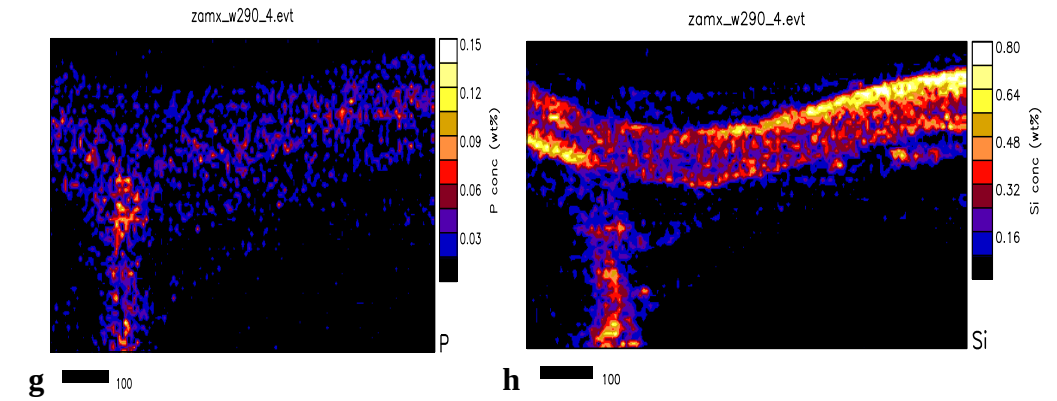
zamx_w290_4.evt
0.15
0.12
0.09
0.06
0.03
P conc (wt%)
P
100
g
zamx_w290_4.evt
0.80
0.64
0.48
0.32
0.16
Si conc (wt%)
Si
100
h

Fig. 6.8 Whole colonised root of *E. curvula* plants growing in substratum from West Wits, site 5. a) and c): Light micrograph of colonised root segment; b), d), e), f), g) and h): Elemental PIXE maps of root segments.

Light micrographs of roots from the toepaddocks of the West Wits gold and uranium TSF showed intracellular hyphal colonisation and external hyphae (Fig. 6.8a, c) and elemental maps indicated the heavy concentration of Ca and K throughout the vascular cylinder (Fig. 6.8d, e) with Fe and Ti in localised pockets in the cortical areas and Ti also present in external hyphae (Fig. 6.8b, f). The distribution of P is not well resolved, but Si shows heavy accumulation in the outer cortex/epidermis (Fig. 6.8g, h). Higher magnification maps of Fe and Ti sites (Fig. 6.9b, d) illustrate discrete deposits in shapes reminiscent of AM fungal vesicles which are resolved at different planes of focus and Fe is more enriched than Ti. Cross-sections (Fig. 6.10c) derived from a whole colonised fresh root showing intraradical hyphae (Fig. 6.10a) confirm the localisation of Fe deposits in the outer cortex overlapping with those of Cr (Fig. 6.10b, d) indicating identical sites of accumulation for both metals although Fe is more concentrated than Cr.

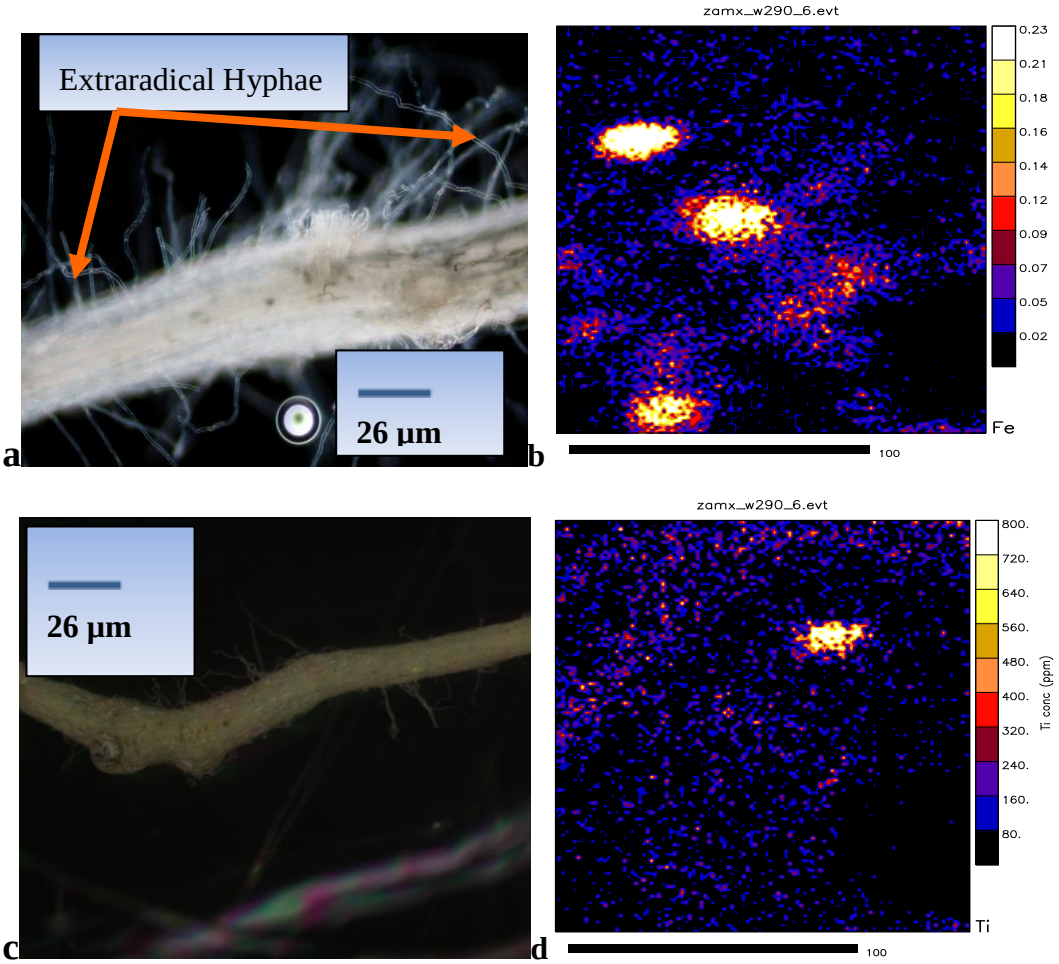

Fig. 6.9 Whole colonised root of *E. curvula* plants growing in substratum from West Wits site 5. a) and c): Light micrograph of colonised root segment; a) and d): Elemental PIXE maps of root segments.

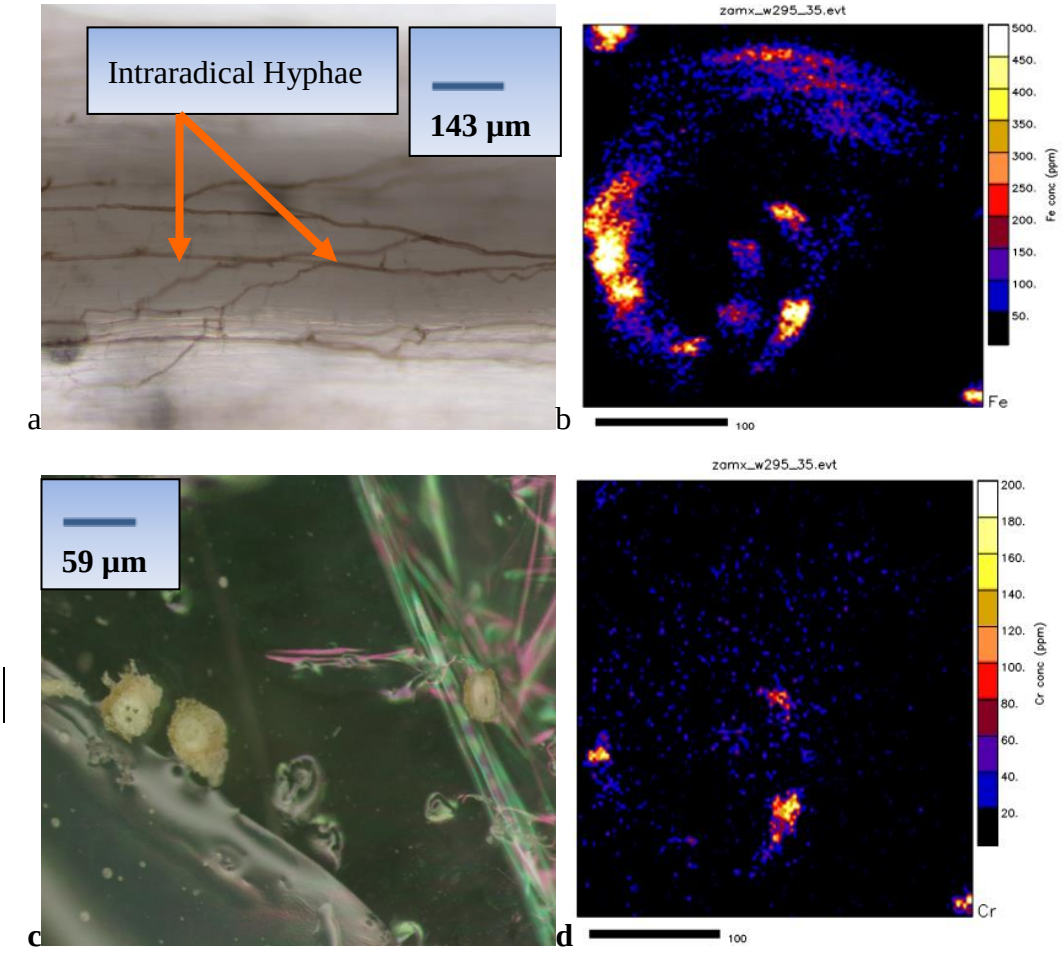

Fig. 6.10 Cross-section of colonised root segment of *E. curvula* plants growing in substratum from West Wits site 5. a) and c): Light micrograph of colonised root segment; a) and d): Elemental PIXE maps of root segments.

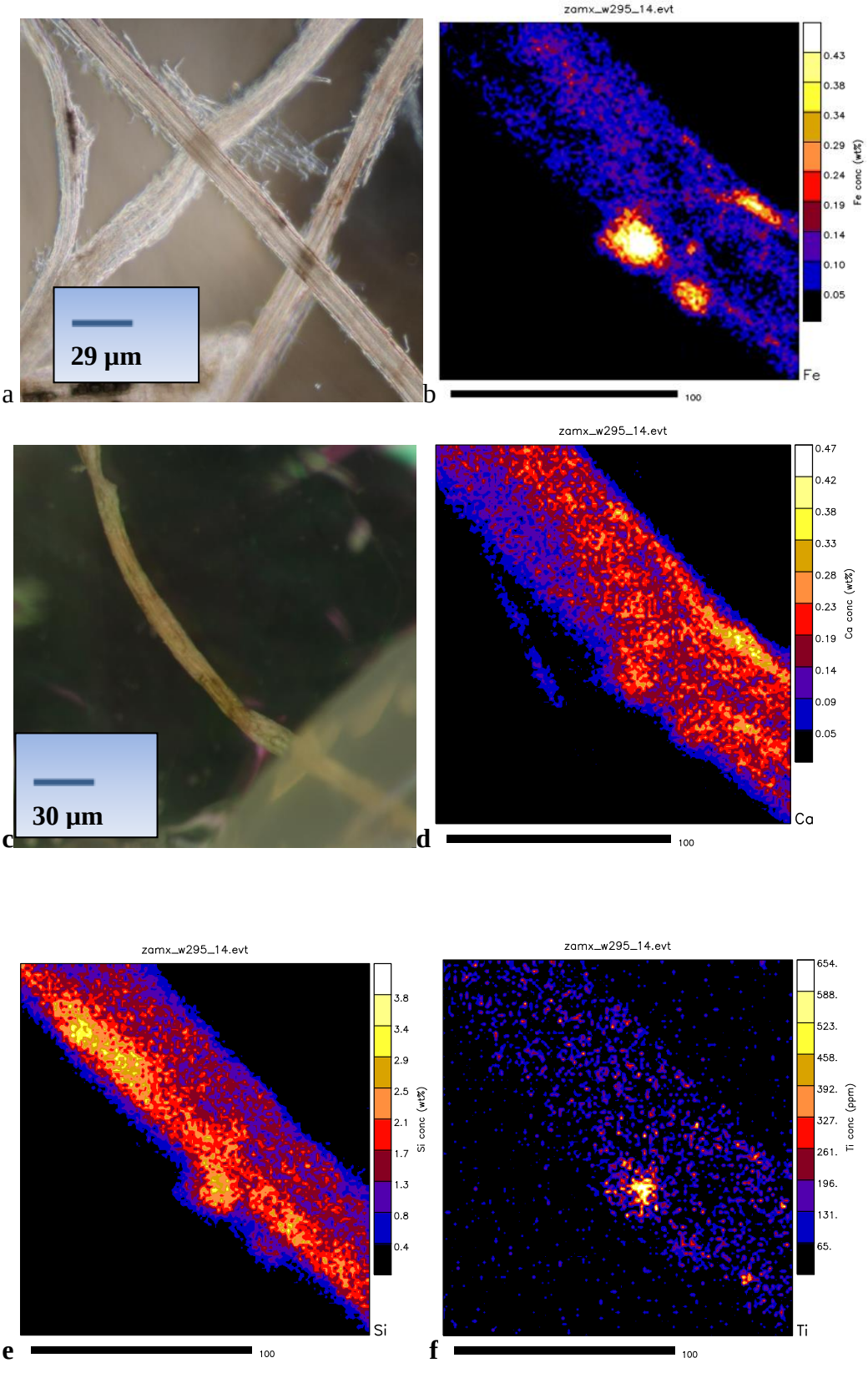
29 µm
a
zamx_w295_14.evt
0.43
0.38
0.34
0.29
0.24
0.19
0.14
0.10
0.05
Fe conc (wt%)
Fe
100
b
30 µm
c
zamx_w295_14.evt
0.47
0.42
0.38
0.33
0.28
0.23
0.19
0.14
0.09
0.05
Ca conc (wt%)
Ca
100
d
zamx_w295_14.evt
3.8
3.4
2.9
2.5
2.1
1.7
1.3
0.8
0.4
Si conc (wt%)
Si
100
e
zamx_w295_14.evt
654.
588.
523.
458.
392.
327.
261.
196.
131.
65.
Ti conc (ppm)
Ti
100
f

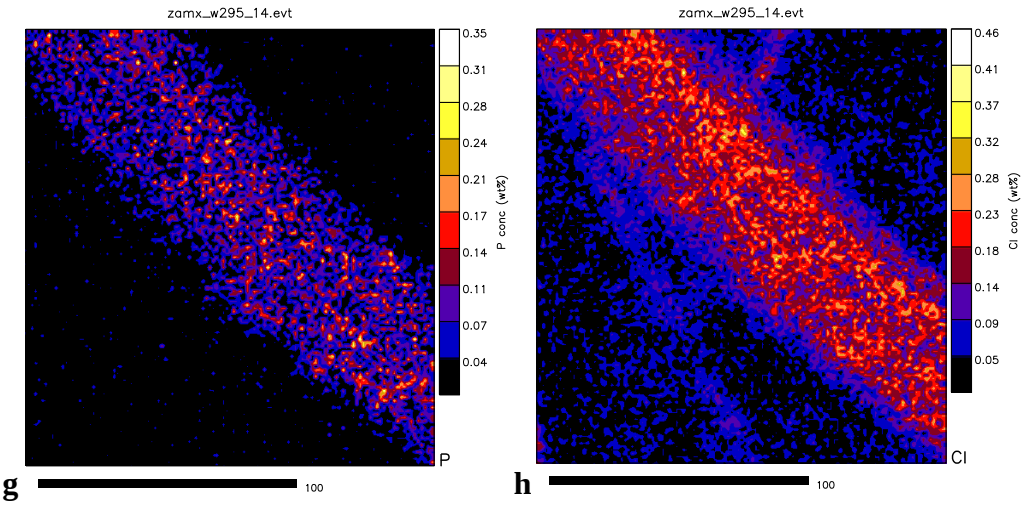

Fig. 6.11 Whole colonised root segment of *E. curvula* plants growing in substratum from East Rand metallurgical plant, site 6. a) and c): Light micrograph of colonised root segment; b), d), e), f), g) and h): Elemental PIXE maps of root segments.

Heavily colonised roots from the substratum from another East Rand site contaminated with gold and uranium mine tailings (Fig. 6.11a, c), showed a widespread distribution of Ca, Cl and Si with highest concentrations in the cortical regions (Fig. 6.11d, e, h). High concentrations of Fe were localised in discrete bodies in the cortex with one of the deposits corresponding with a high localised concentration of Ti (Fig. 6.11b, f). Fe, Ti and P were also sparsely distributed in other parts of the roots in low concentrations. Cross sections of these roots (Fig. 6.12a, c) showed discrete deposits of high concentrations of Fe in the cortical regions (Fig. 6.12b) with overlap between some of these deposits and those of Cr and Ni (Fig. 6.12e, f). K was concentrated in high concentrations in a discrete deposit in the cortical area on the distal side of the root and more generally distributed in lower concentrations in other parts of the root (Fig. 6.12d).

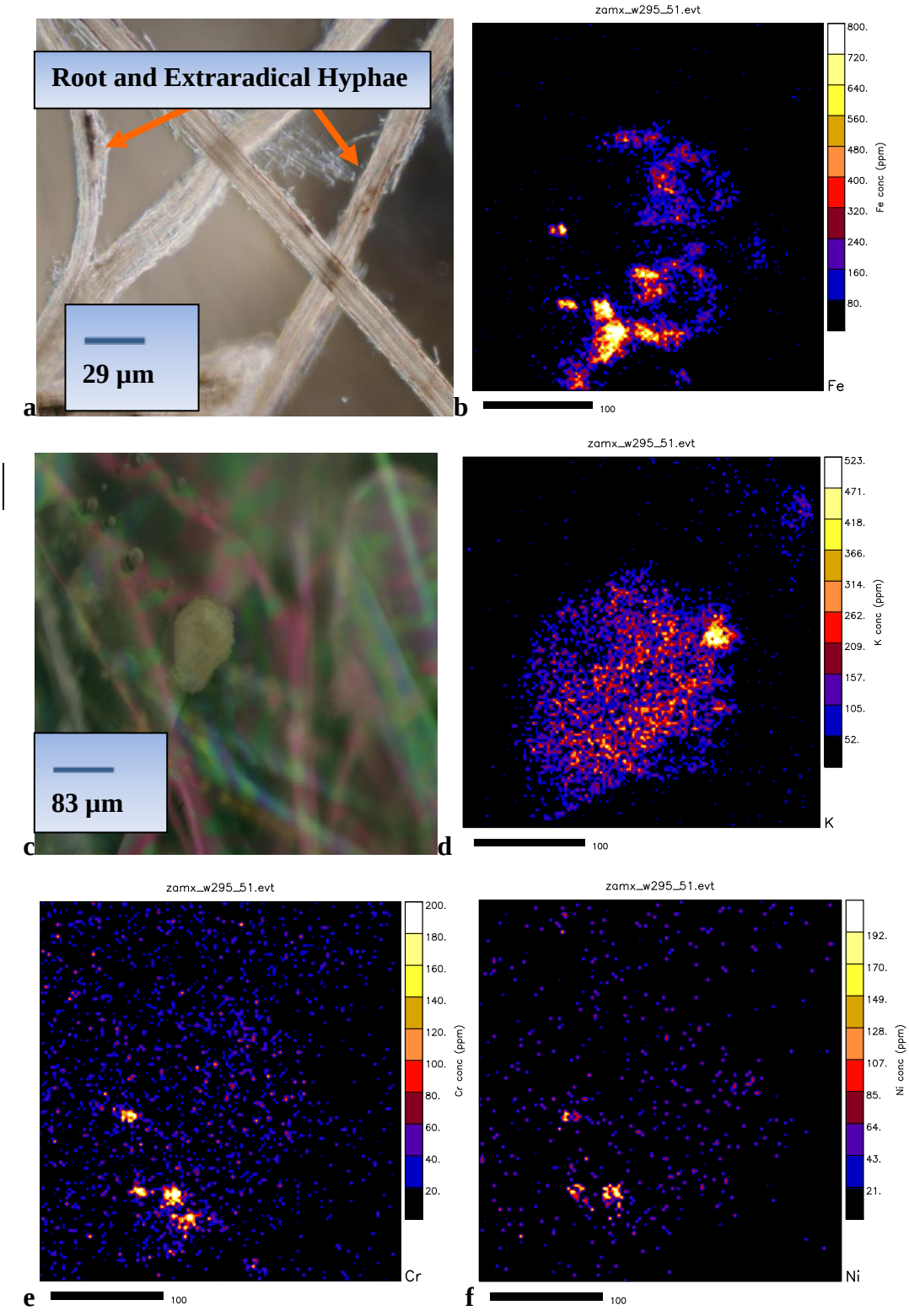

Fig. 6.12 Colonised root cross sections of *E. curvula* plants growing in substratum from East Rand metallurgical plant, site 7. a) and c): Light micrograph of colonised root segment; b), d), e), f): Elemental PIXE maps of root segments.

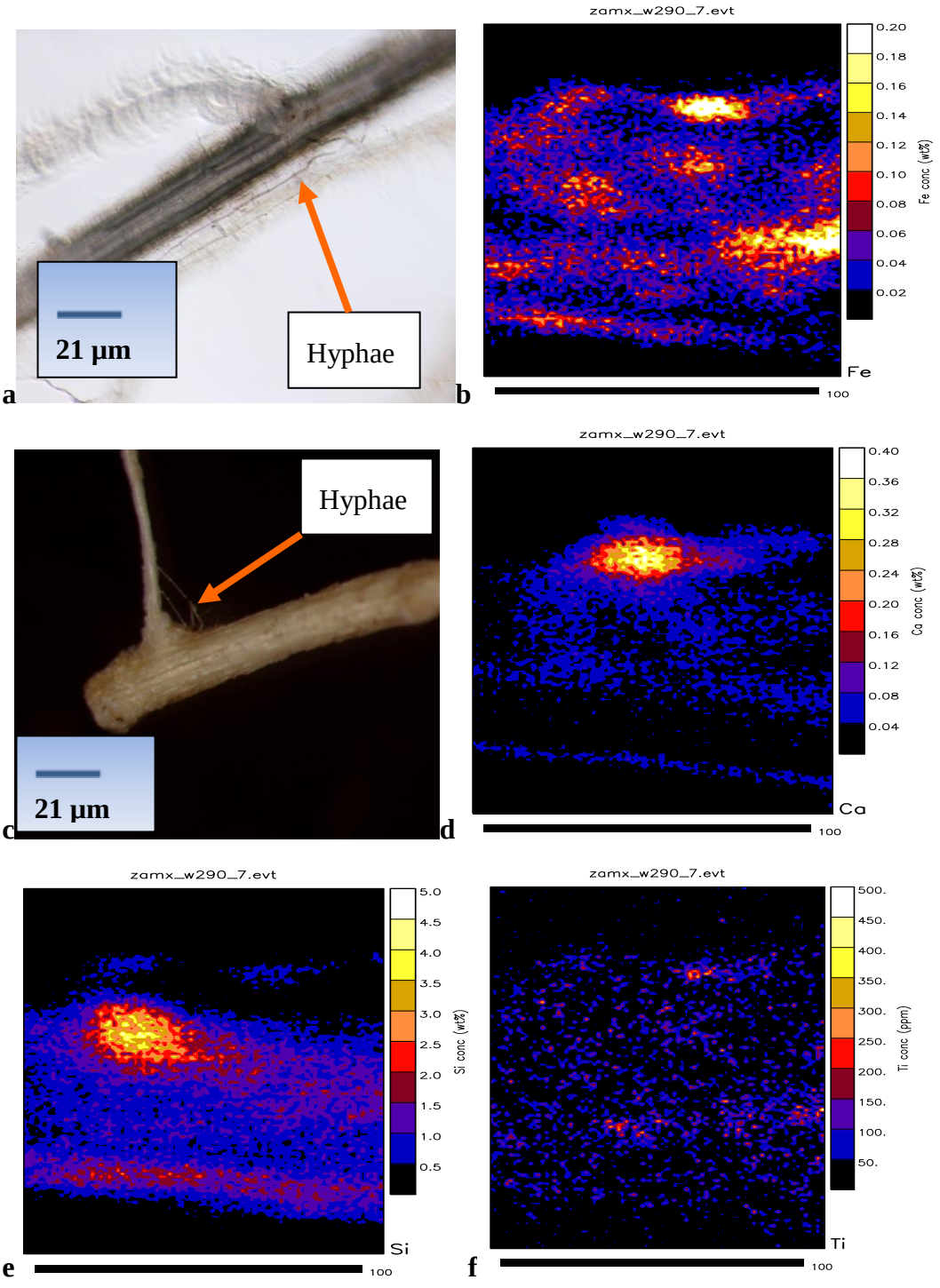

Fig. 6.13 Whole colonised root segment of *E. curvula* plants growing in substratum from East Rand) metallurgical plant site 7. a) and c): Light micrographs of colonised root segment; b), d), e) and f): Elemental PIXE maps of root segments.

High magnification elemental maps derived from colonised roots of plant growing in the East Rand metallurgical plant soil, contaminated with gold and uranium TSF slimes (Fig. 6.13a, c), show discrete sites of accumulation of Ca and Si, once again in vesicular shapes, with Ti more sparsely distributed in lower concentrations (Fig. 6.13d, e, f). Cross sections of these roots (Fig. 6.14a, c) were mapped to show Ca distributed in both central and cortical areas of the root, with discrete vesicular-shaped sites of accumulation in the cortex (Fig. 6.14b). Discrete sites of Fe accumulation were also localised in the cortical and central regions (Fig. 6.14d), whereas localised sites of Cr and Ti accumulation were less numerous and in lower concentrations (Fig. 6.14e, f).

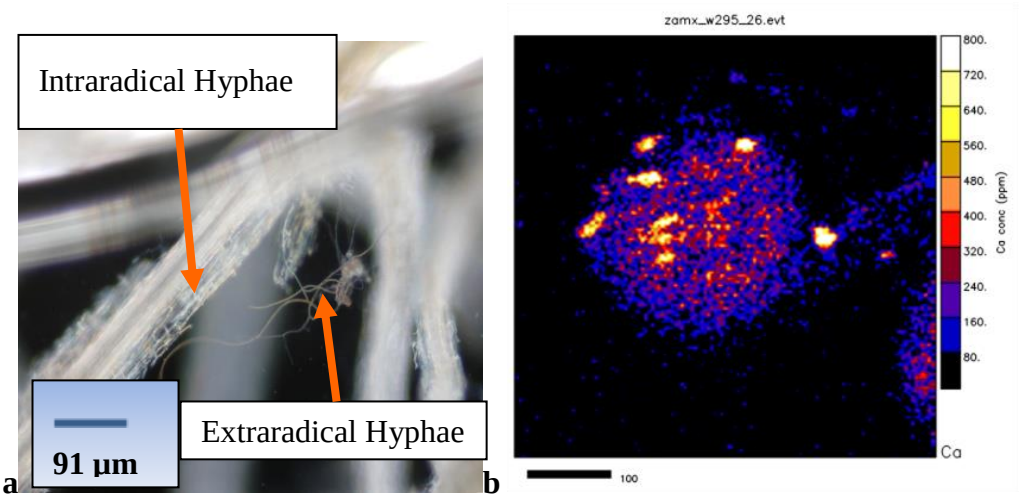

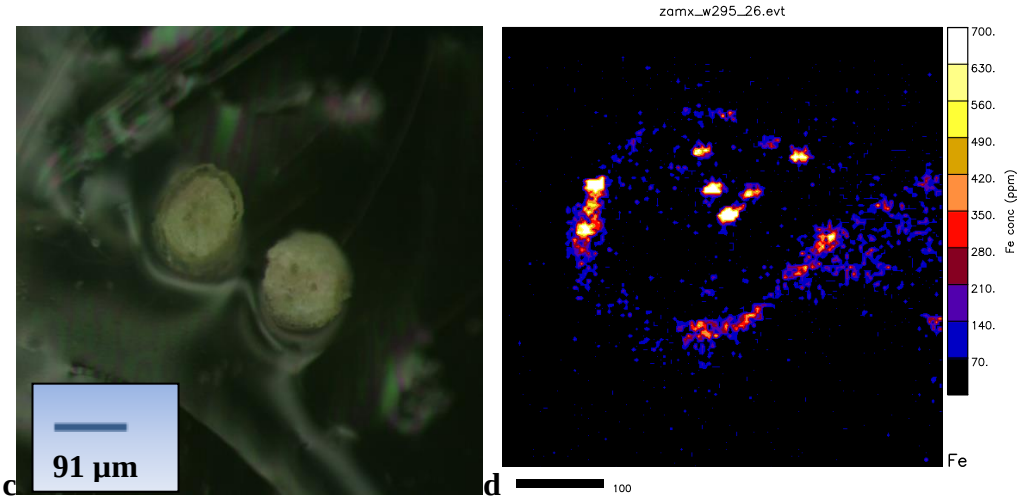

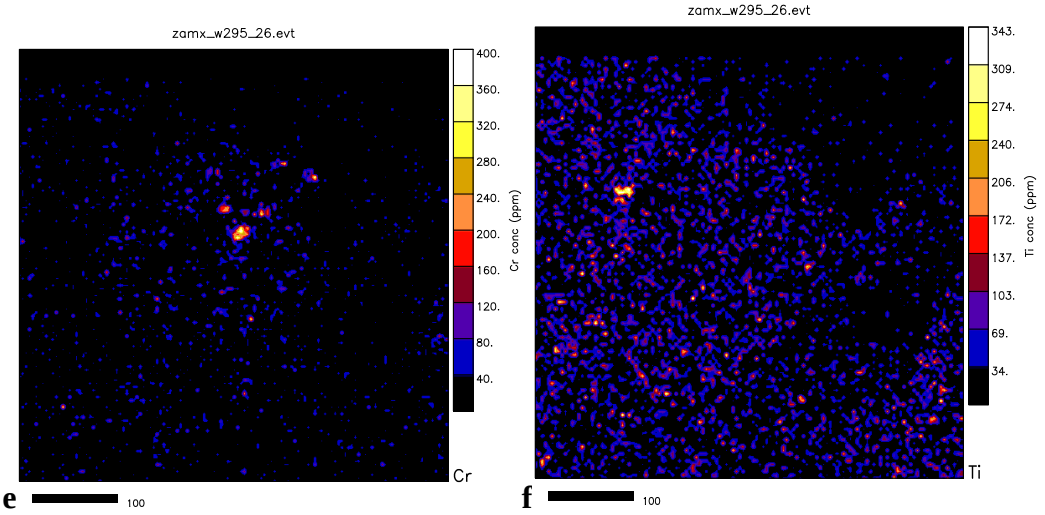

Fig. 6.14 Cross-section of colonised root segment of *E. curvula* plants growing in substratum from East Rand metallurgical plant site 7; a) and c): Light micrograph of colonised root segment. b), d), e) and f): Elemental PIXE maps of root segments.

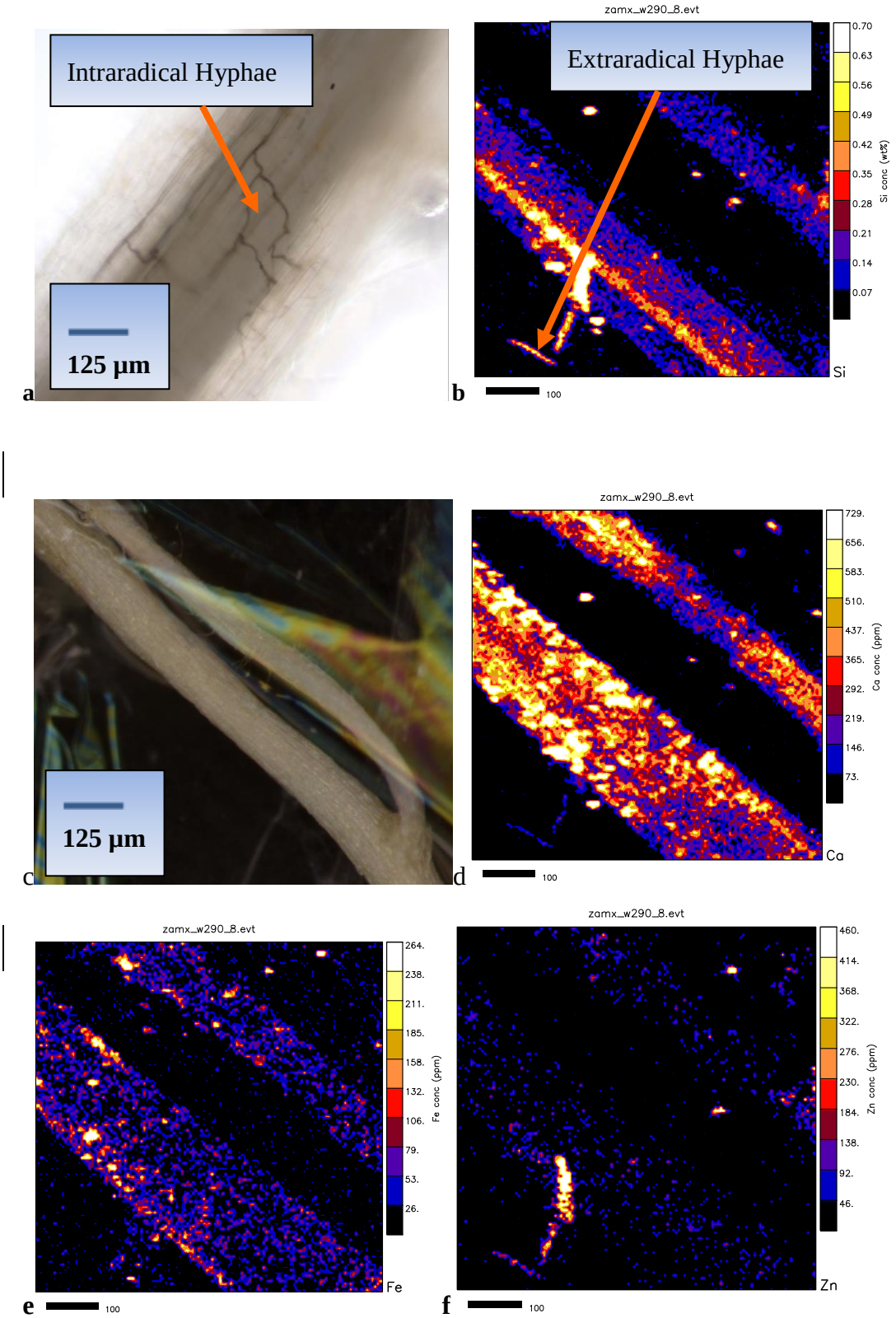

Fig. 6.15 Whole colonised root segment of *E. curvula* plants growing in substratum from Vaal Reefs site 8. a) and c): Light micrograph of colonised root segment site 8 M1 VR - f x 120; b), d), e) and f): Elemental PIXE maps of root segments.

Elemental maps of colonised roots from plants growing in acidic toepaddock substrata of Vaal Reefs gold and uranium TSFs (Fig. 6.15a, c), showed high concentrations of Ca, apparently widely dispersed in all regions of the root (Fig. 6.15d) with Si and Fe enriched in what appear to be intraradical AM fungal hyphae and structures (Fig. 6.15b, e). Si and Zn are also concentrated in extraradical hyphae (Fig. 6.15b, f). Cross sections of these roots (Fig. 6.16a, c) reveal a constant band of high levels of Si in the cortical area (Fig. 6.16b), with Fe and Ca in more localised cortical deposits (Fig. 6.16d, e) overlapping with more sparse accumulations of Ti (Fig. 6.16f). The cross section maps confirm the accumulation of elements in the cortical region rather than throughout the root.

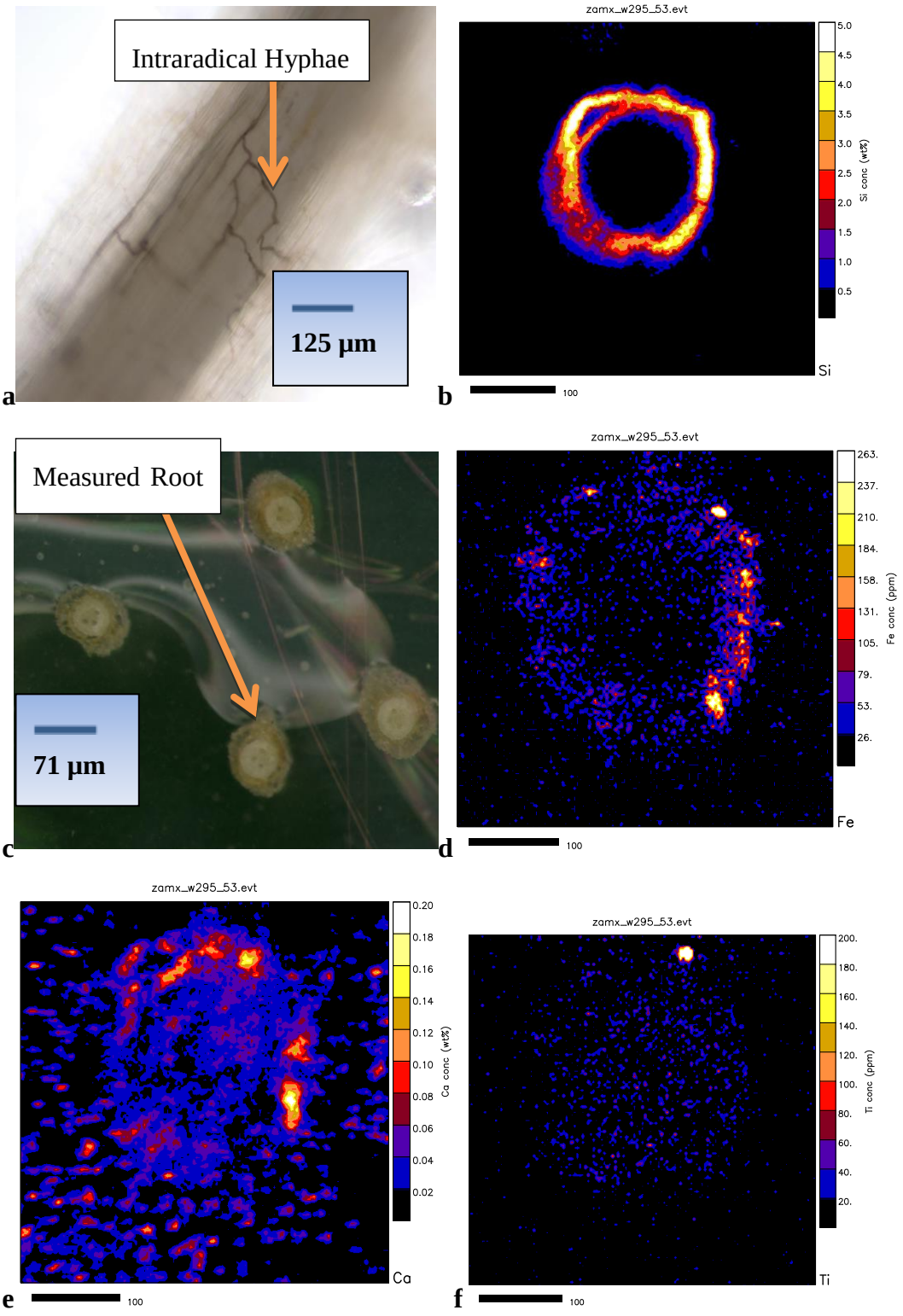

Fig. 6.16 Cross-section of colonised root segment of *E. curvula* plants growing in substratum from Vaal Reefs site 8; a) and c): Light micrograph of colonised root. a), d), e) and f): Elemental PIXE maps of root segments.

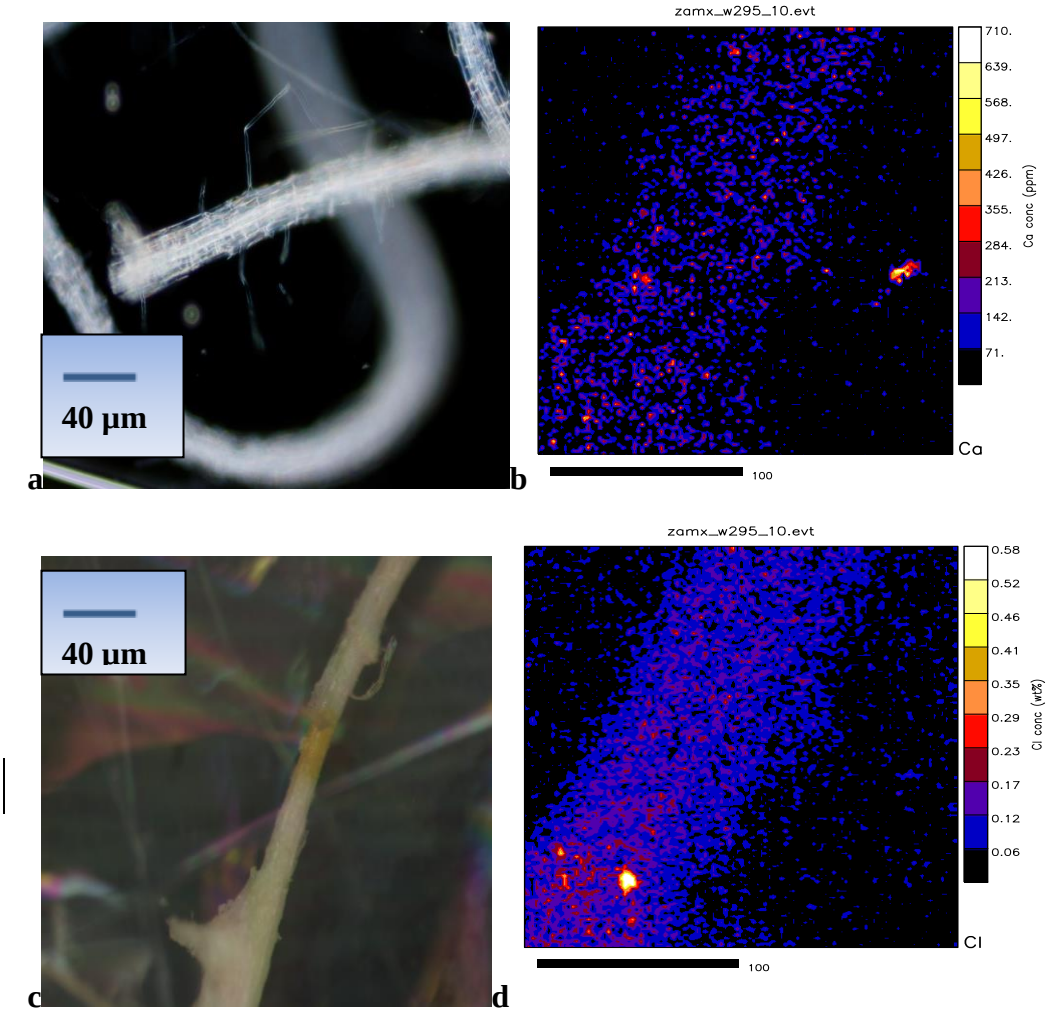

Fig. 6.17 Control 1, uninoculated control root segment of *E. curvula* plants growing in zeolite. a) and c): Light micrograph of colonised root segment; b) and d): Elemental PIXE maps of root segment.

Although the control consisted of uninoculated plants fertilised with a defined nutrient medium evidence of colonisation was observed (Fig. 6.17a), probably due to cross contamination from mycorrhizal pots. However, elemental maps of Ca and Cl revealed only small localised areas of accumulation in low concentrations Fig. 6.17b, d).

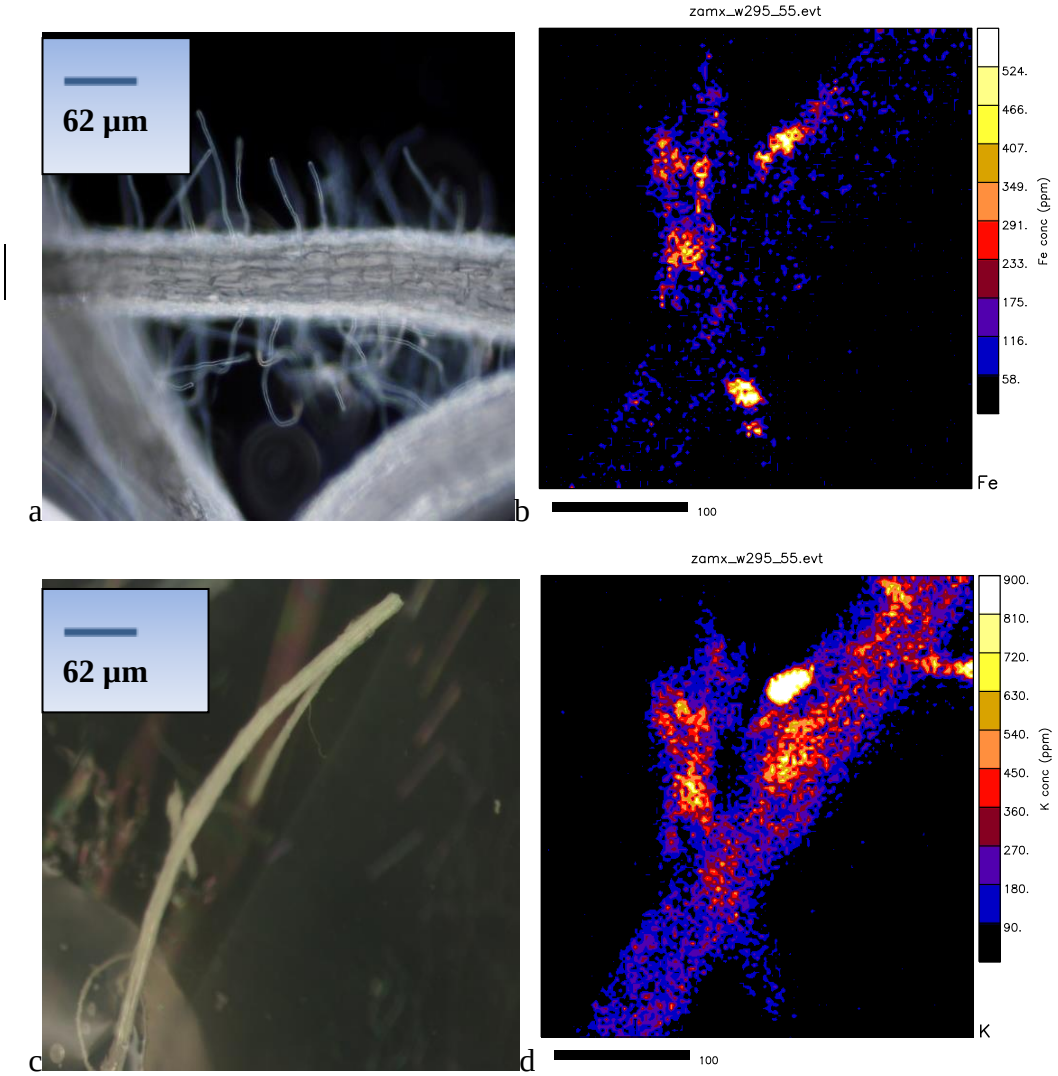
62 µm
zamx_w295_55.evt
524.
466.
407.
349.
291.
233.
175.
116.
58.
Fe conc (ppm)
Fe
100
a
b
62 µm
zamx_w295_55.evt
900.
810.
720.
630.
540.
450.
360.
270.
180.
90.
K conc (ppm)
K
100
c
d

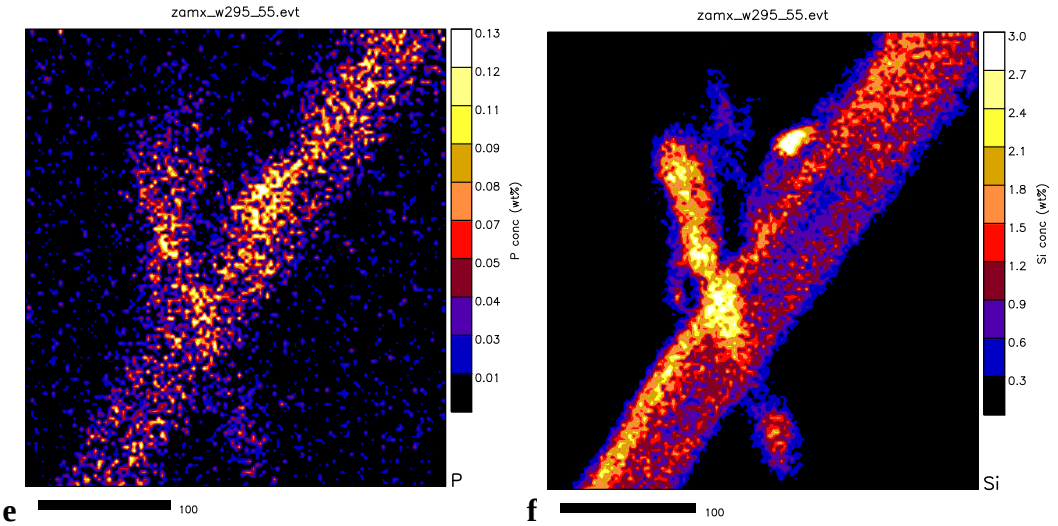

Fig. 6.18 Control 2, whole colonised root segments of *E. curvula* plants inoculated with commercial inoculum and grown in zeolite; a) and c): Light micrograph of colonised root segment; b), d), e) and f): Elemental PIXE maps of root segments.

Whole roots inoculated with a commercial inoculum (Fig. 6.18a-f) showed the accumulation of Fe in localised sites (Fig. 6.18b) and an apparently wider distribution of K in the central portion of the root, although the map may just be reflecting the depth of beam penetration into the cortex overlying the vascular cylinder (Fig. 6.18d). Once again, there are common sites of accumulation of P and Si (Fig. 6.18e, f), suggesting deposits in fungal structures. Cross-sections of the root confirmed the presence of high concentrations of Fe in discrete deposits (Fig. 6.19b) but a more widespread distribution of Ti (Fig. 6.19d).

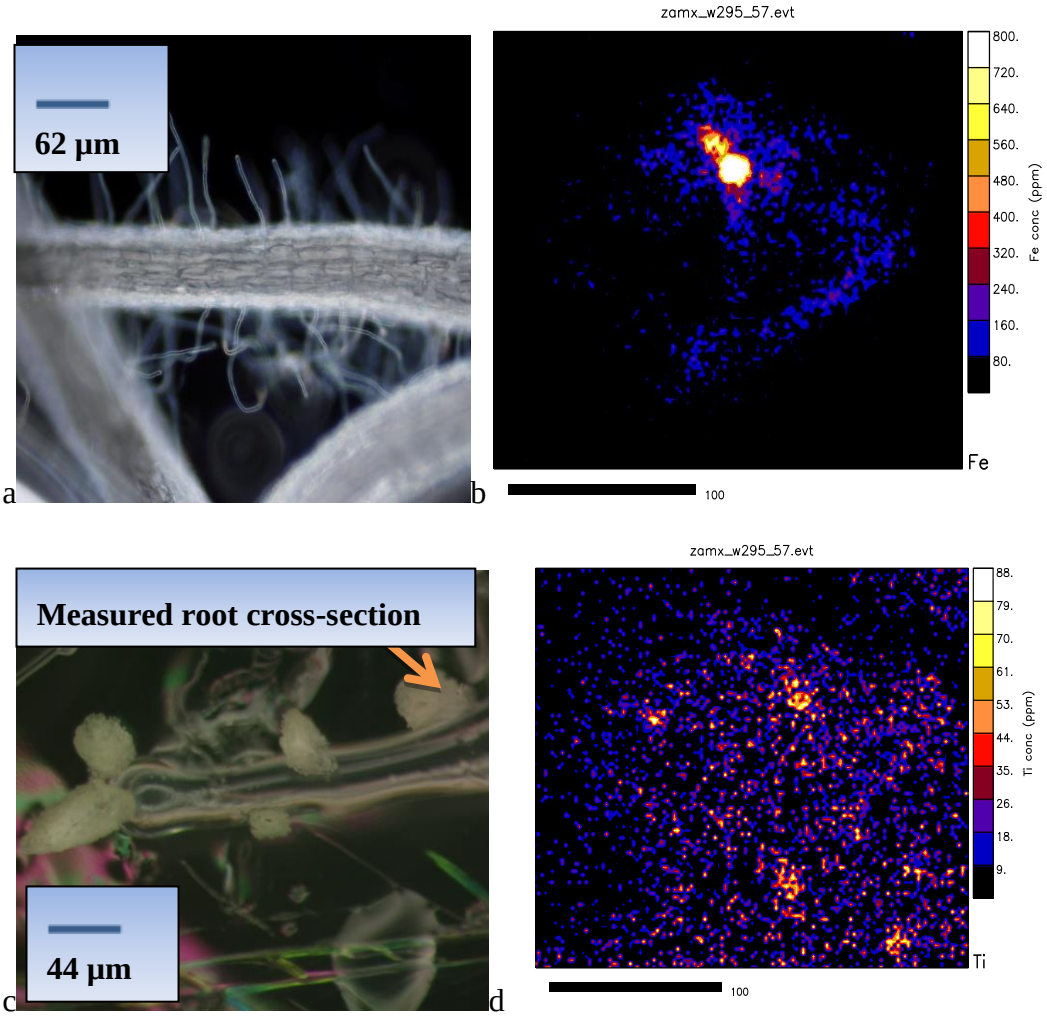

Fig. 6.19 Control 2, cross-sections of root of *E. curvula* plant colonised with a commercial inoculum and grown in zeolite; a) and c): Light micrograph of colonised root segment; b), and d): Elemental PIXE maps of root segments.

In summary, the conclusions which can be drawn from the elemental maps generated from micro-PIXE analysis are the following:

The highest concentration of elements was either localised in the plant root or in fungal structures. In site 1, Ti, Al, Fe including Cl and Zn were localised in the plant root (Fig. 6.1 - 6.3). While in site 5, Cr, Fe and Ti concentrations were pronounced in AM fungal structures (Fig. 6.8 – 6.10). In both site 1 and 8, Si, Fe was more pronounced in AM fungal structures including hyphae and in the same sites Fe, Cu and Ti were observed to be highest in the cortex (Fig. 6.15 – 6.16). In site 4, pronounced concentration of Al, and Ca was observed in AM fungal

structures (Fig. 6.7). In site 3, a widespread distribution of Ca, P and Cl throughout the root, with Fe and Ti following a similar distribution patterns but largely in the cortical regions whereas a discrete pocket of Al was observed at the junction with a side root (Fig. 6.6). In site 7, Ca, Si, Fe, Cr, and Ti were localised in the AM fungal structures more specifically in the vesicles (Fig. 6.12 – 6.14). Similarly, in site 6, Fe, Ti, and Si were localised in the AM fungal structures (Fig. 6.11). In site 2 Fe was mostly localised in the cortex, surprisingly a very low concentration of Zn was observed, such that the map could not be included (Fig. 6.4 – 6.5). In control 1, elemental maps of Ca and Cl revealed only small localised areas of accumulation of the plant root, while control 2 showed the pronounced accumulation of Fe, P and Si localised in both plant root and AM fungal structures (Fig. 6.1 – 6.19).

AM fungal structures are mostly located in the outer cortex or outer epidermal layer of the root, as shown by the more significantly enriched Si in the vesicles and arbuscules (Fig. 6.2). The maps also demonstrate that most elements are accumulated in vesicles (Fig. 6.1 – 6.19). Control 1 showed no or very little mycorrhizal colonisation as expected, with low elemental concentration which resulted from the nutrient solution. It is always advantageous to analyse both longitudinal and root cross-section as they give details of both the AM fungal colonisation and elemental concentration in different dimensions. Although live root showed AM fungal colonisation such as hyphae, arbuscules, the PIXE analysed root only showed roots colonised by vesicles with very few roots that showed hyphae.

6.4 Results of Statistical Analysis

6.4.1 Statistical comparison between elemental concentrations in roots and colonisation levels of roots.

An exploratory factor analysis, using a principal component extraction method and a Varimax rotation of sixteen items was conducted. Prior to running the analysis with SPSS, the data was screened by examining descriptive statistics on

each item, correlation matrix and possible univariate and multivariate assumption violation. The Bartlett's test of sphericity was significant (P-value < 0.05), indicating sufficient correlation between the variables to proceed with analysis.
Using the Kaiser-Guttman criterion of Eigenvalues greater than 1.0, from the two distributions used: the first had two -factor solution accounted about 92% of the total variance in the final average in sample sites and the second had five - factor solution accounted about 95% of the total variance in the concentration of elements in roots from different metal sites (Appendix 2). The present two- factor and five –factor models were deemed the best solution because of its conceptual clarity and case of interpretability.

6.4.2 Part 1. Elemental analysis between sites and elements:

Part1 is made up of two parts, namely, Part 1A and Part1B. Part 1A comprises the correlation tables of both the final average of elements in sample sites and the total concentration of elements in roots from different metal sites (Appendix 11).

6.4.3 Part 1 A: Final average in sample sites

6.4.3.1. Descriptive statistics tables

Table 6.3 Extraction Method: Principal Component Analysis. Rotation Method: Varimax with Kaiser Normalization.

Component Transformation Matrix

Component		1	2
Dimension	1	.908	.420
	2	-.420	.908

Extraction Method: Principal Component Analysis. Rotation Method: Varimax with Kaiser Normalization.

There are only two components that could be considered in the study as indicated in Table 6.3 above. Because - 0.420 is less than 0.5 in both component 1 and 2 is not considered, thus only 0.908 is considered in each component.

6.4.4 Part 2: Factor analysis

In factor analysis as indicated above, the aim is to discover which variables in a data set form coherent subgroups that are relatively independent of one another.
The more factors one permits, the better the fit and the greater the percent of variance in the data explained by the factor solution. The selection of the number of factors is probably critical. Eigenvalues represent variance; therefore any factor with an **eigenvalue less than 1** is not as important. The number of factors with **eigenvalues greater than 1** is an estimate of the maximum number of factors.

6.4.5 Working with factor analysis

6.4.5.1. Principal component analysis (PCA) solution

The assessment of the KMO and Bartlett's test of sphericity in Table 6.4 below shows positive results. This means that the KMO value is near than the heuristic of 0.70; indicating that the correlations matrix is adequate for factor analysis and principal component analysis. Likewise, a significant Bartlett's test enables us to reject the null hypothesis Ho of the lack of sufficient correlation between the variables. This Bartlett's test outcome gives us confidence to proceed with the analysis.

Table 6.4 The assessment of the results of the KMO and Bartlett's test of sphericity

KMO and **Bartlett's Test**

Kaiser-Meyer-Olkin Measure of Sampling Adequacy.		0.622
Bartlett's Test of Sphericity	Approx. Chi-Square	494.232
	Df	45
	Sig.	0.000

The communalities below currently indicate the degree to which each variable is participating or contributing to the component solution. The results in the tables in Appendix 10 show that there is no variable that appears to be particularly low for removal except Br, from both analyses (the final average of elements in sample sites and the total concentration of elements in roots from different metal sites) and the analysis is therefore continued.

6.4.6 Part 3: Mycorrhizal fungal colonisation

Part 3: comprises the correlation between elemental concentrations versus arbuscular mycorrhizal fungal colonisation in plants. **Part 3** also comprises the tables of both the final averages of AM fungal accumulation and their graphical bar charts.

6.4.7 Data analysis

Tables and figures below display the correlation of the sample sites averages of elements. The findings are all significant as P-value is less than 0.05 levels (Table 6.6 and 6.7). This indicates that there is a relationship between the two variables examined. For example, in site 1, Al and Si were mostly concentrated in hyphae with concentrations of 9 and 42 respectively. Si has the highest normalised concentration percentage of 42% followed by Sulphur with 30%. Only site 1 that is reported here as an example, results of other sites are reported in Appendix 5. Almost all the figures below (Fig. 6.20) indicate that most elements are accumulated in vesicles followed by hyphae then arbuscules. This applies to all the sites examined. Some elements like Si appear in all the fungal structures (Hyphae, Arbuscule and Vesicle) while some only appear in one or two of the AM fungal structures (Table 6.5 and Appendix 5). For example Ca, appears only in VC not in HC and AC because its concentration after normalisation was too low to be included in both the table and figures.

Table 6.5 The correlation of the sample sites averages of elements versus mycorrhizal colonisation. Elemental concentration was converted to a total of 100.

Count

		Site 1 elements								Total
		Al	Si	P	S	Cl	K	Ca	Fe	
Site 1 Mycorrhizal	HC	9	42	1	1	0	0	0	0	53
	AC	0	0	0	15	0	0	0	0	15
	VC	0	0	0	14	7	5	4	2	32
Total		9	42	1	30	7	5	4	2	100

Chi-Square tests on table 6.6 below indicate the results for P -value. Similarly, the Test of Coefficient of Correlation (Table 6.7) which shows similar results as Chi-Square Test also depicts the results for P Value which is less than 0.05 (see last column of Table 6.6 and 6.7).

Table 6.6 Chi-Square Tests which indicate the results for P value of 0 (see the last column) depicts a significant difference as P value is less than 0.05

Chi-Square Tests

	Value	df	Asymp. Sig. (2-sided)
Pearson Chi-Square	124.843[a]	14	.000
Likelihood Ratio	148.198	14	.000
Linear-by-Linear Association	63.356	1	.000
N of Valid Cases	100		

a. 19 cells (79.2%) have expected count less than 5. The minimum expected count is.15.

Test of Coefficient of Correlation

Table 6.7 Test of Coefficient of Correlation which shows similar results as **Chi-Square** Test that indicate the results for P value of 0 (see last column) also depicts a significant difference as P value is less than 0.05.

Symmetric Measures

		Value	Asymp. Std. Error[a]	Approx. T[b]	Approx. Sig.
Interval by Interval	Pearson's R	.800	.040	13.198	.000[c]
Ordinal by Ordinal	Spearman Correlation	.909	.013	21.590	.000[c]
N of Valid Cases		100			

a. Not assuming the null hypothesis.

b. Using the asymptotic standard error assuming the null hypothesis.

c. Based on normal approximation.

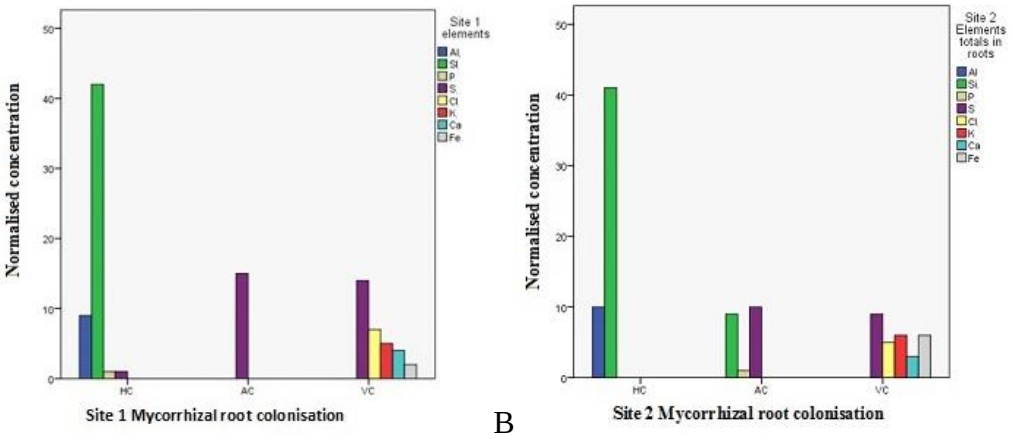

A B

Fig. 6.20 The percentage of elemental concentration in A) North West, Platinum Mine (L) (Site 1). B) Mpumalanga, Agnes Serpentine Mine (AGM), site (Site 2).

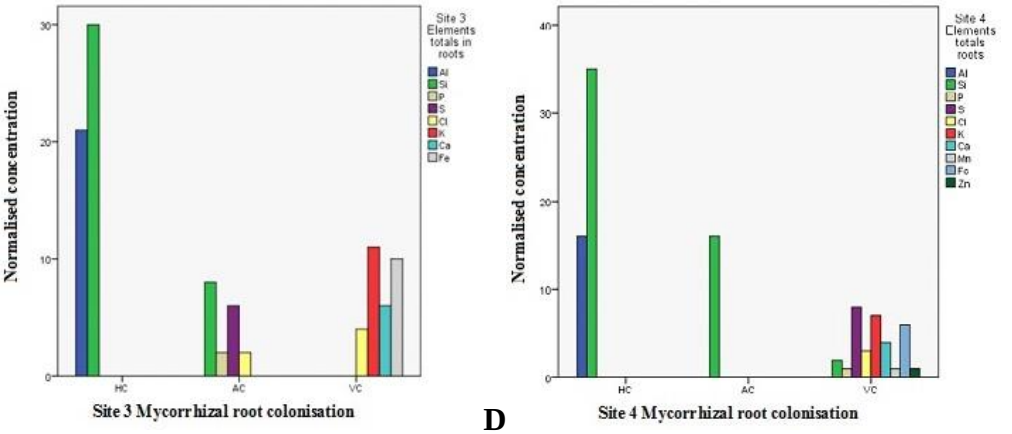

C D

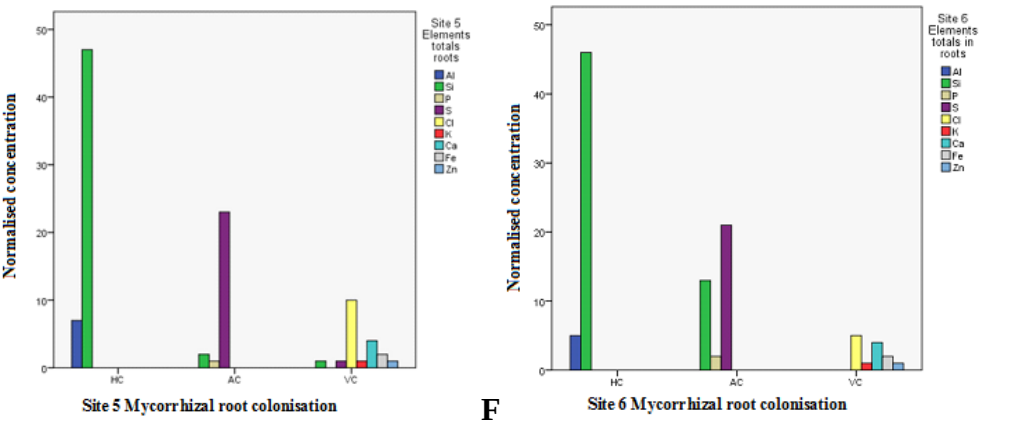

E F

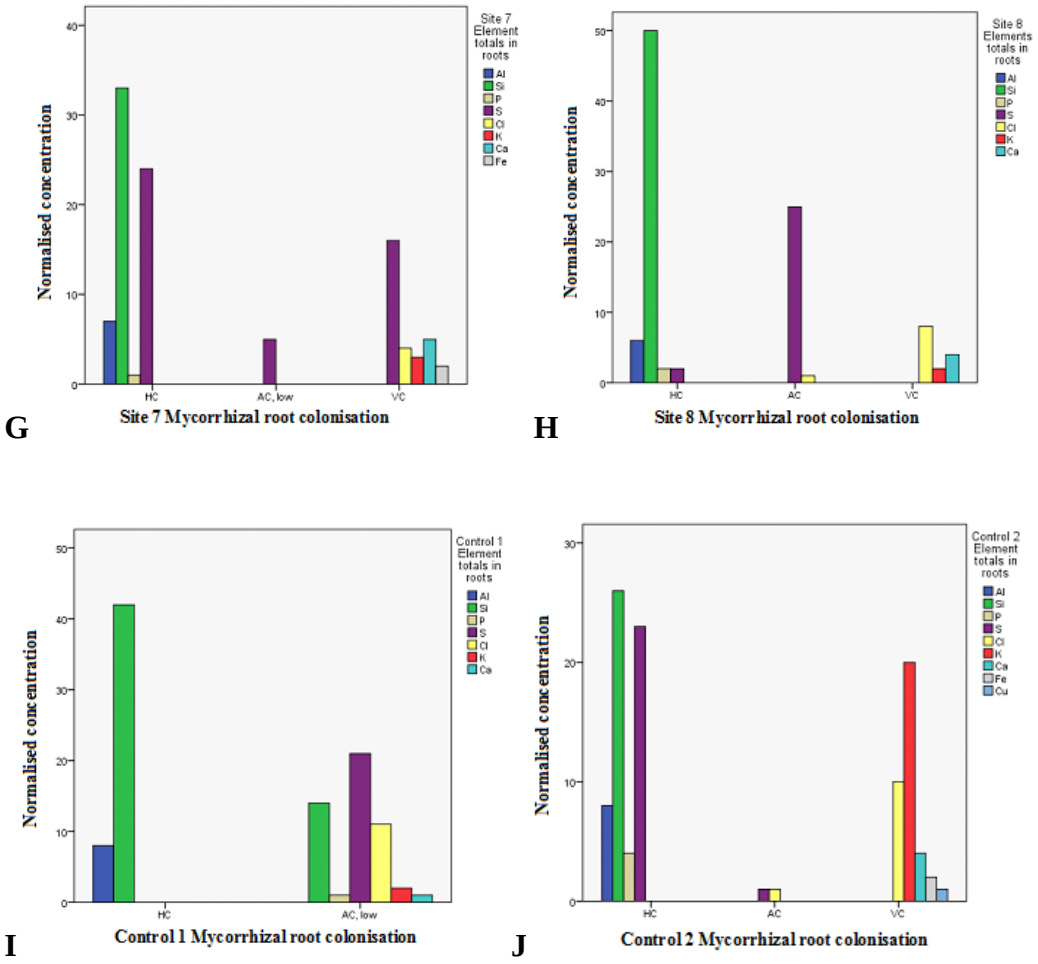

Fig. 6.20 The percentage of elemental concentration in C) Gauteng East Rand, ERGO Brakpan (ER1- BP) mine site (Site 3). D) North West, Vaal Reefs (VRS mine site (Site 4). E) Gauteng, TSF, (West Wits Au and U) (Site 5). F) Gauteng, East Rand (ER2A) ERGO - Metallurgical Plant (MP) mine site (Site 6). G) Gauteng, East Rand (ER2D) ERGO Metallurgical Plant (MP),) mine site, (site 7). H) North West (Vaal Reefs VRM) mining site (site 8). I) Control 1 that was without the Mycoroot. J) Control 2 that was with Mycoroot grown in nutrient solution and zeolite (Ctr Nu + Mycoroot).

The figure also displays the correlation of the sample sites averages of elements versus mycorrhizal colonisation. Elemental concentration was converted to a total of 100 while a mycorrhizal colonisation was calculated as a percentage (%) of mycorrhizal root colonisation of *E. curvula* plant species growing in substrata from sites (site 1 - 8) inoculated with a mixture of spores extracted from the substrata. Values are means of 3 to 10 replicates Standard Error of the Mean (+/-

SEM) (Fig. 6.20). The graphs in the figure indicate that most elements are accumulated in vesicles followed by hyphae then arbuscules. This applies to all the sites and agrees with the elemental maps.

All the elements in all the mining sites (site 1 to 8) have their concentration above the normal level required for plants (Table 6.8), except Al in site 1 which has a normal concentration (Kabata, 2011). In site 1 (Fig. 6.20a) for instance, Al and Si have highest concentration in Hyphal Colonisation (HC), followed by S in Arbuscular Colonisation (AC) and Vesicular Colonisation (VC); Fe and P are observed in VC while Al is observed in HC (Table 6.5). In Site 2, Si has a high accumulation in HC and AC with S pronounced in both AC and VC while Fe and AL are pronounced in VC and HC respectively. In site 3 a high concentration of Si was observed in both HC and VC while Al and S were high in HC and AC respectively.

Similarly Fe and P were high on VC and AC respectively. In site 4, high colonisation of Si was observed in HC and AC same in VC as well. Al was more pronounced in HC while P, Fe, Mn, Zn and S were highest in VC. Site 5 had highest concentration of Si in HC same in AC and VC with low concentration of Al in HC. Highest concentration of Si, and P were observed in AC while Fe and Zn were highest in VC. In site 6, S and P are highest in AC and Fe and Zn are highest in VC. In site 7, S was highest in HC, AC, VC while P and Fe ware highest in HC and VC respectively. In site 8, S is more pronounced in HC and AC, with Cl appearing in both AC and VC. Si and Al were observed only in HC. Control 1 showed a high concentration of Al and Si in the HC while all other elements such as P, S, Cl, K, and Ca localised in AC. Similarly control 2, reveal high concentration of elements such as Al, Si, S and P in HC with low concentration of Al and P in AC. A number of elements including K, Ca, Cl, Fe and Cu were localised in VC.

6.4.8 Soil chemistry results

6.4.8.1. Statistical comparison between elemental concentrations of roots and soil substrata

High heavy metal concentration derived from both the soil total and extractable heavy metal content and plant elemental accumulation (PIXE) from eight different mining sites and control (Fig. 6.21(a-k), show a high concentration of heavy metal total content as compared to both extractable and PIXE analysis. However, a higher concentration of elements has been observed in some elements where PIXE heavy metal concentration was more than the total soil content (Fig. 6.21h). It should be noted that during PIXE elemental analysis, some of the elements such as Pt, Ag, Cd, Hg, Pb, Au, and U were measured but they were detected at a very low concentration, often below the respective limits of detection as reported in this figure hence some figures do not have PIXE graphs. Al (Fig. 6.21g) followed by Pt (Fig. 6.21d) shows a high heavy metal concentration in almost all the sites.

Common alphabetic letters indicate no significant difference between sites for each element; similarly different letters depicts a significant difference between sites for each element ($p \leq 0.05$). High Pt concentration in site 2 has been observed compared to other sites reported in this study, whereas such high concentration of Pt was expected on site 1 as a Pt mining site. Ti showed a highest Total Heavy Metal (HM) concentration in sites, 2, 3, 5 and 7 with much lower extractable concentration in these sites. Letters are not included in Ti for PIXE because the P value was greater than 0.05 thus anova did not calculate the post tests. Similarly letters for Ni were not included in the figure because there were not enough values in the columns. PIXE showed a higher elemental concentration in sites 3, 4 and 6 than extractable. There was a significant difference between, site Cr and Ni showed higher concentration only in site 2 while Pt concentration was also high in site 2 but not detected by PIXE. Both Cd and Hg showed high concentration in site 6 for both total HM and extractable with no PIXE results as these elements were not detected by PIXE. Tables of the graphs in Fig. 6.21 are presented in Appendix 6.

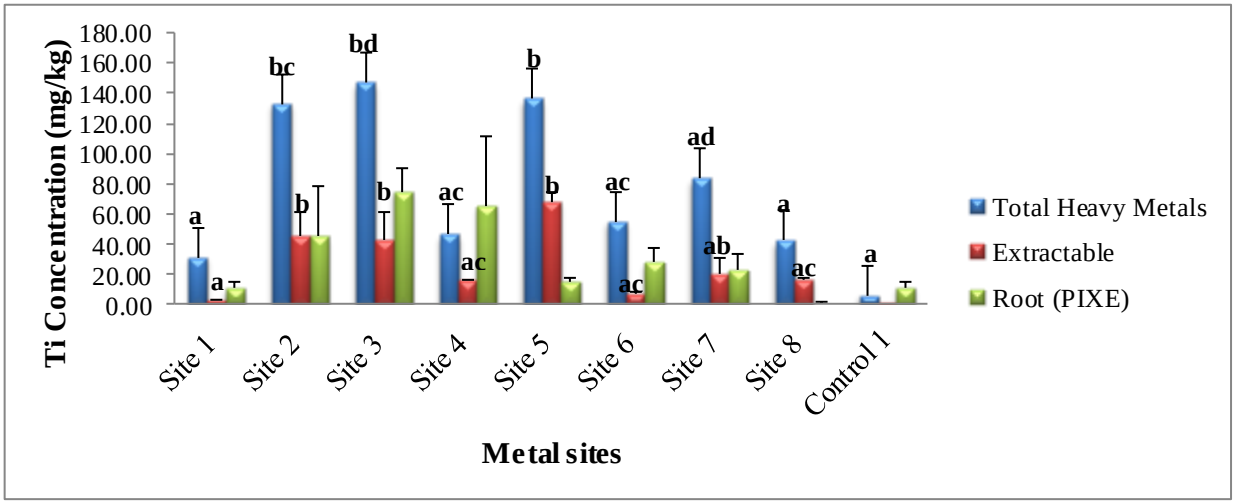
Ti Concentration (mg/kg)
180.00
160.00
140.00
120.00
100.00
80.00
60.00
40.00
20.00
0.00
Site 1
Site 2
Site 3
Site 4
Site 5
Site 6
Site 7
Site 8
Control 1
Metal sites
Total Heavy Metals
Extractable
Root (PIXE)

a)

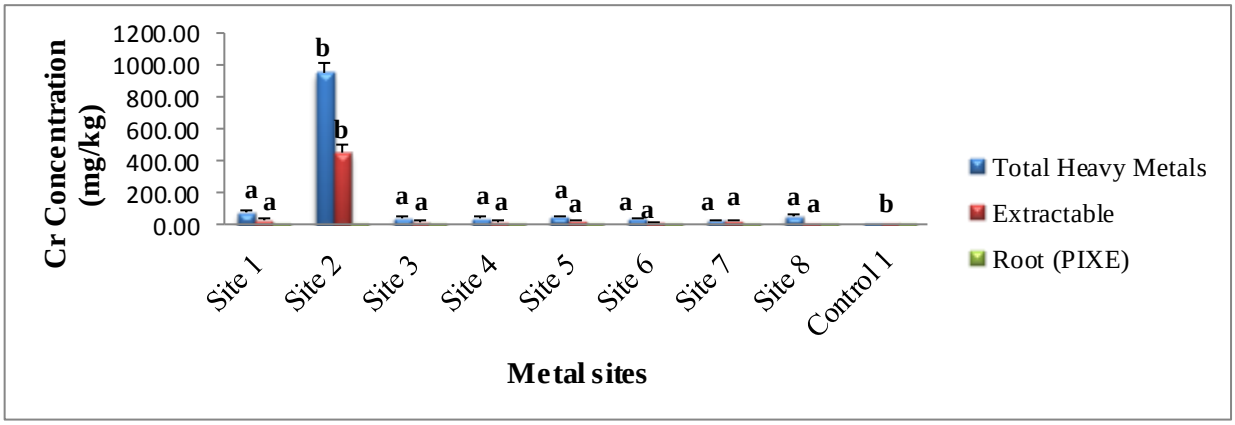
Cr Concentration (mg/kg)
1200.00
1000.00
800.00
600.00
400.00
200.00
0.00
Site 1
Site 2
Site 3
Site 4
Site 5
Site 6
Site 7
Site 8
Control 1
Metal sites
Total Heavy Metals
Extractable
Root (PIXE)

b)

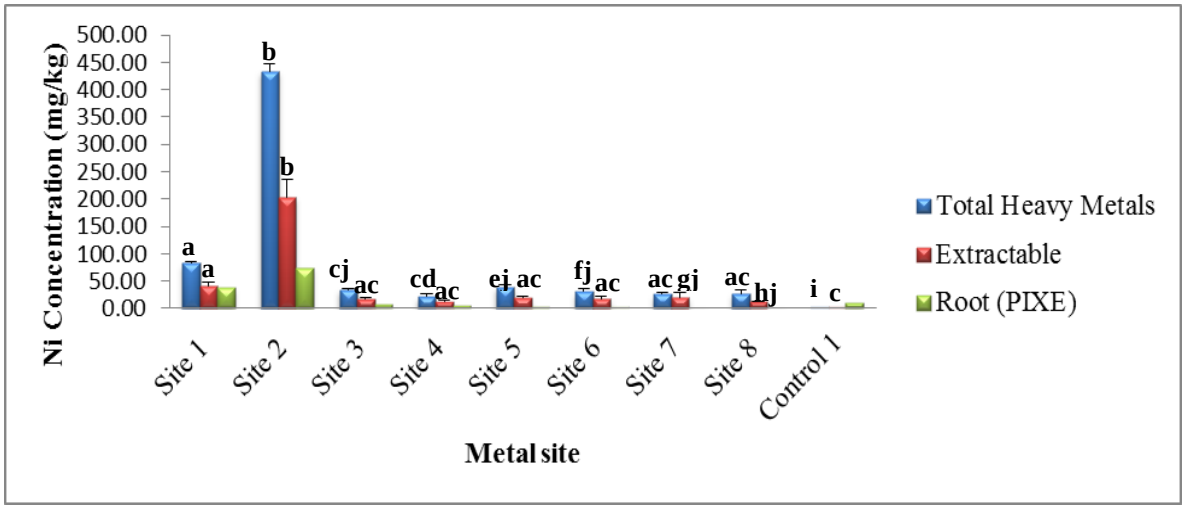
Ni Concentration (mg/kg)
500.00
450.00
400.00
350.00
300.00
250.00
200.00
150.00
100.00
50.00
0.00
Site 1
Site 2
Site 3
Site 4
Site 5
Site 6
Site 7
Site 8
Control 1
Metal site
Total Heavy Metals
Extractable
Root (PIXE)

c)

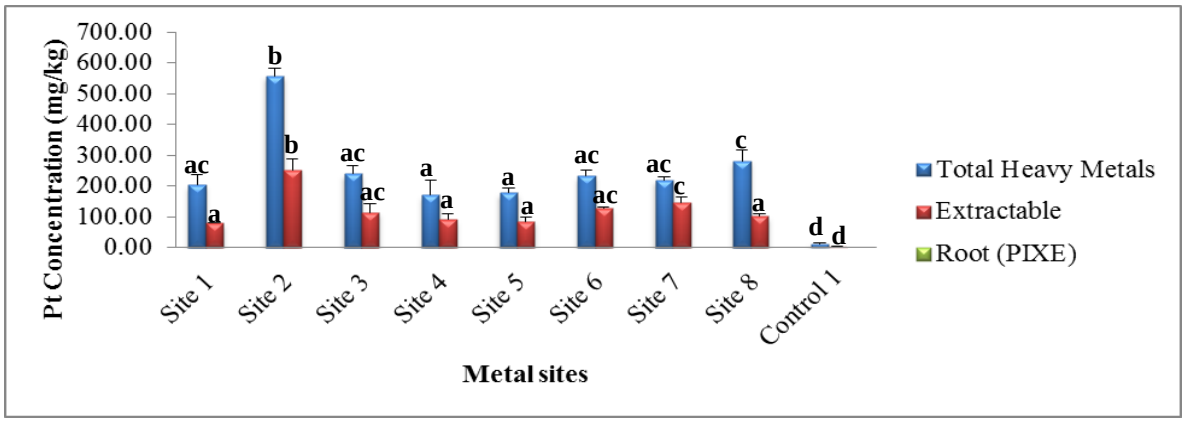
Pt Concentration (mg/kg)
700.00
600.00
500.00
400.00
300.00
200.00
100.00
0.00
Site 1
Site 2
Site 3
Site 4
Site 5
Site 6
Site 7
Site 8
Control 1
Metal sites
Total Heavy Metals
Extractable
Root (PIXE)

d)

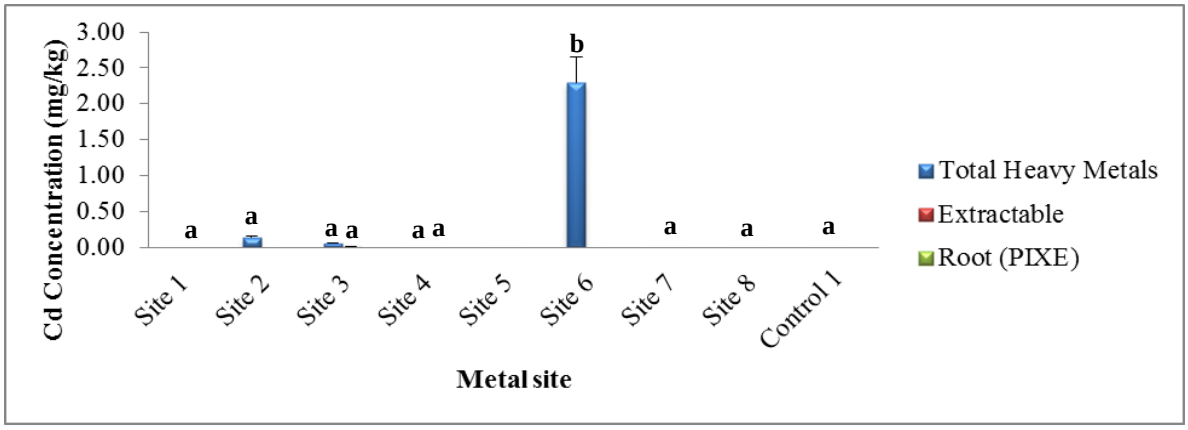
Cd Concentration (mg/kg)
3.00
2.50
2.00
1.50
1.00
0.50
0.00
Site 1
Site 2
Site 3
Site 4
Site 5
Site 6
Site 7
Site 8
Control 1
Metal site
Total Heavy Metals
Extractable
Root (PIXE)

e)

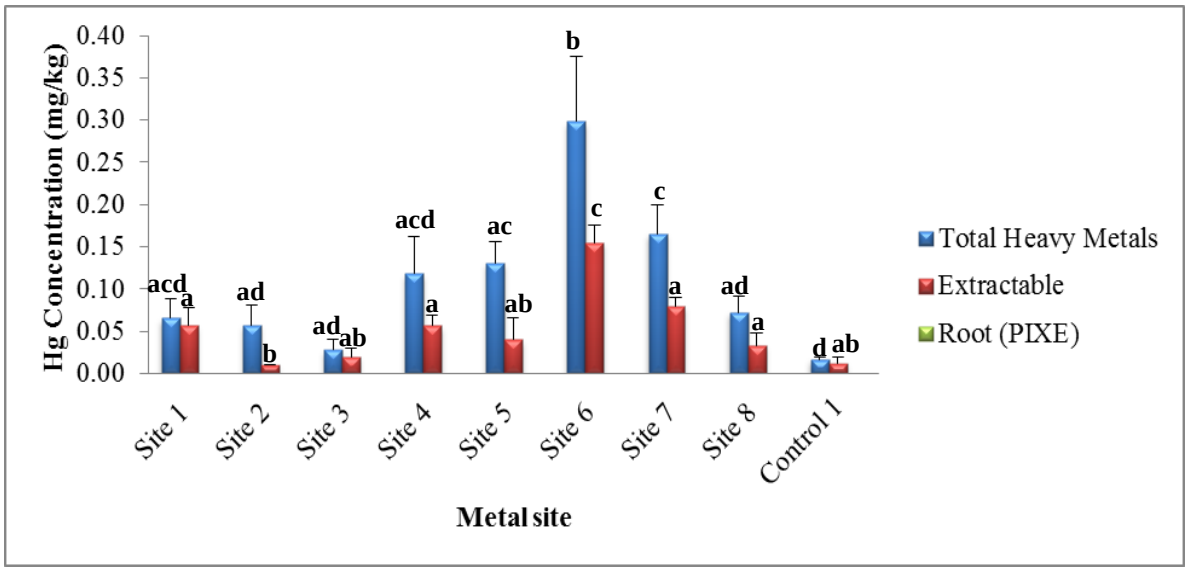
Hg Concentration (mg/kg)
0.40
0.35
0.30
0.25
0.20
0.15
0.10
0.05
0.00
Site 1
Site 2
Site 3
Site 4
Site 5
Site 6
Site 7
Site 8
Control 1
Metal site
Total Heavy Metals
Extractable
Root (PIXE)

f)

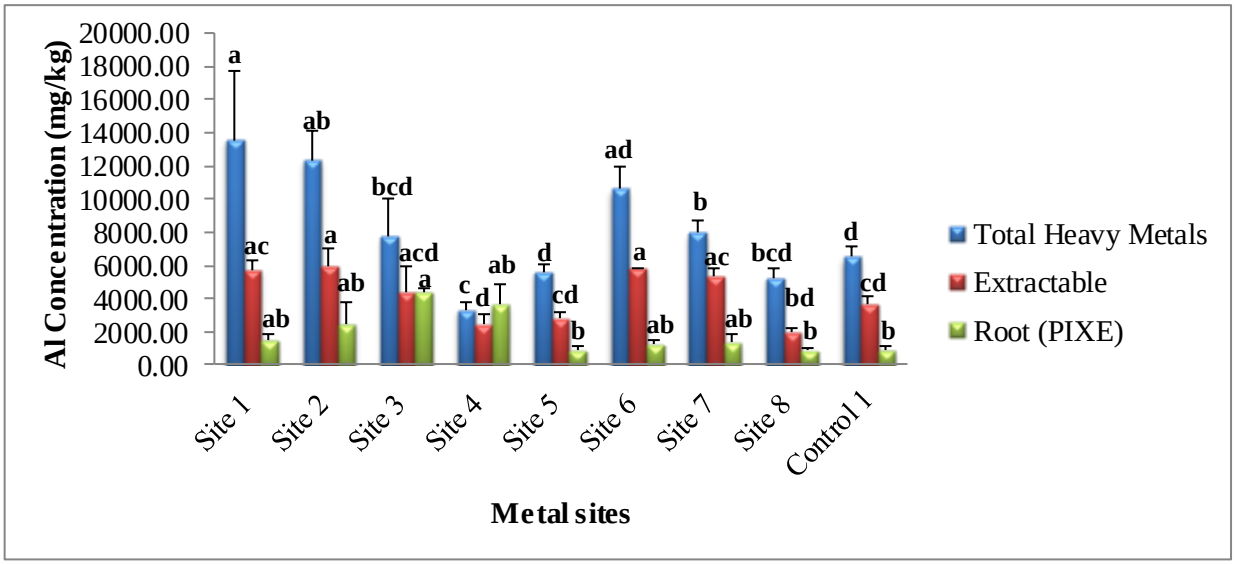
Al Concentration (mg/kg)
20000.00
18000.00
16000.00
14000.00
12000.00
10000.00
8000.00
6000.00
4000.00
2000.00
0.00
a
ac
ab
ab
a
ab
bcd
acd
a
c
d
ab
d
cd
b
ad
a
ab
b
ac
ab
bcd
bd
b
d
cd
b
Site 1
Site 2
Site 3
Site 4
Site 5
Site 6
Site 7
Site 8
Control 1
Metal sites
Total Heavy Metals
Extractable
Root (PIXE)

g)

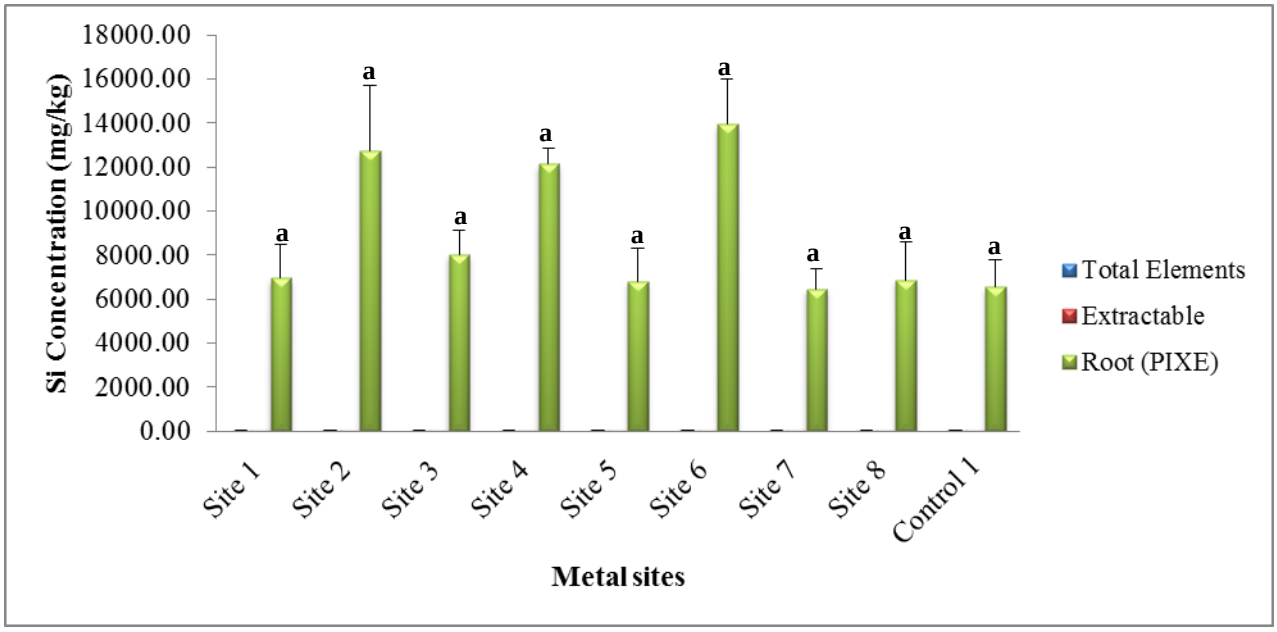
Si Concentration (mg/kg)
18000.00
16000.00
14000.00
12000.00
10000.00
8000.00
6000.00
4000.00
2000.00
0.00
a
a
a
a
a
a
a
a
a
Site 1
Site 2
Site 3
Site 4
Site 5
Site 6
Site 7
Site 8
Control 1
Metal sites
Total Elements
Extractable
Root (PIXE)

h)

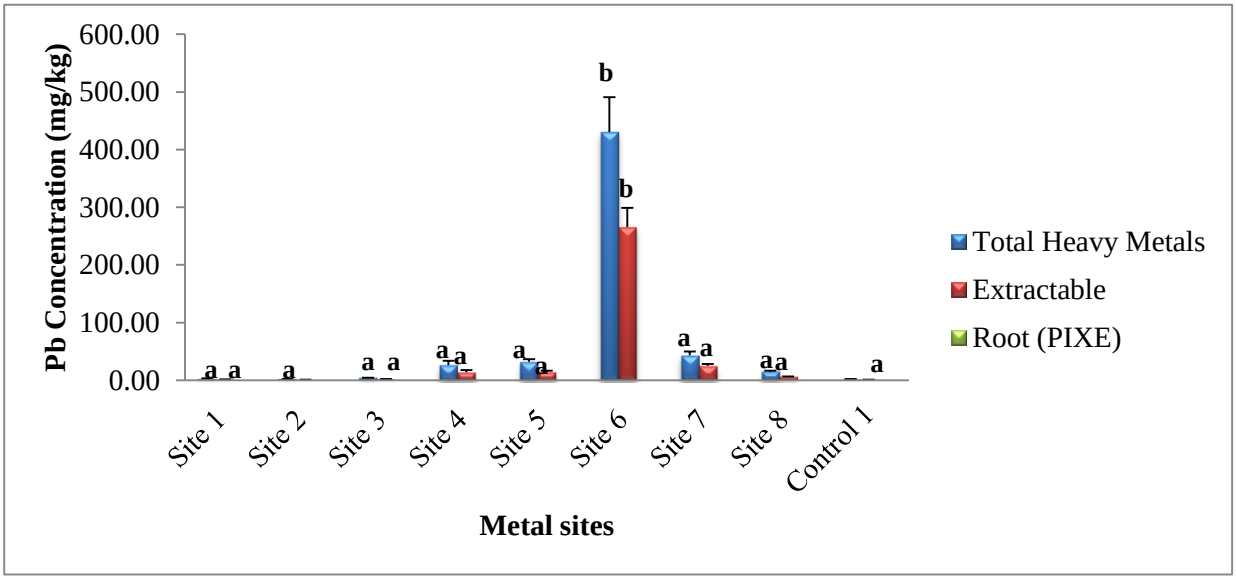
Pb Concentration (mg/kg)
600.00
500.00
400.00
300.00
200.00
100.00
0.00
Site 1
Site 2
Site 3
Site 4
Site 5
Site 6
Site 7
Site 8
Control 1
Metal sites
Total Heavy Metals
Extractable
Root (PIXE)

i)

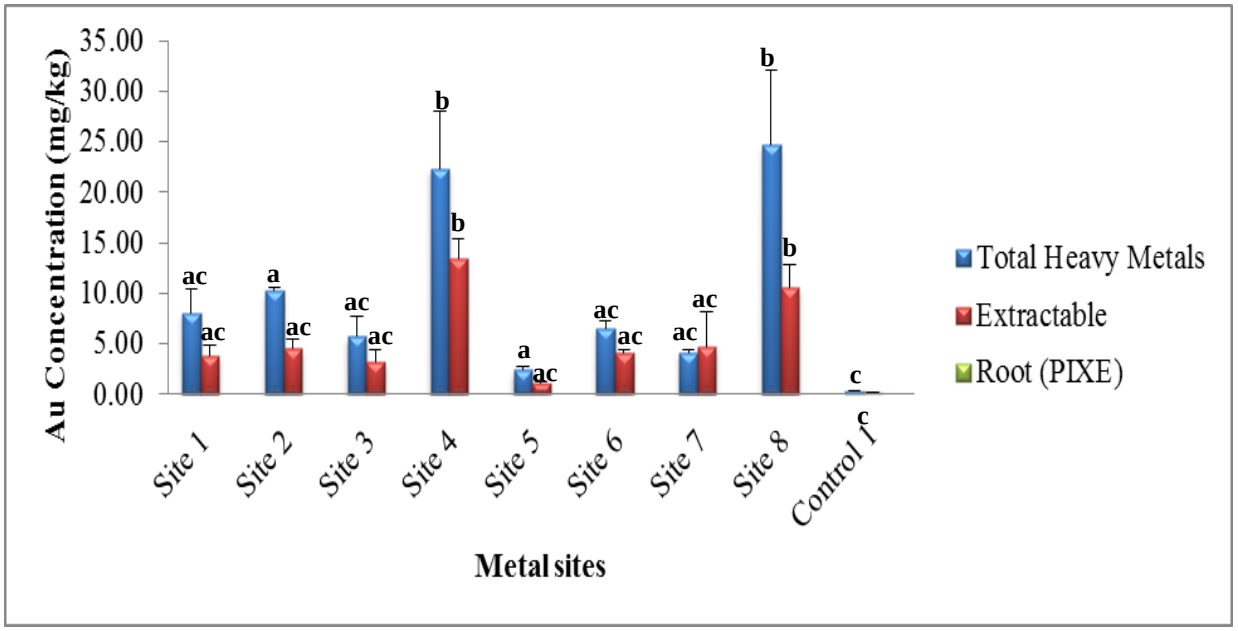
Au Concentration (mg/kg)
35.00
30.00
25.00
20.00
15.00
10.00
5.00
0.00
Site 1
Site 2
Site 3
Site 4
Site 5
Site 6
Site 7
Site 8
Control 1
Metal sites
Total Heavy Metals
Extractable
Root (PIXE)

j)

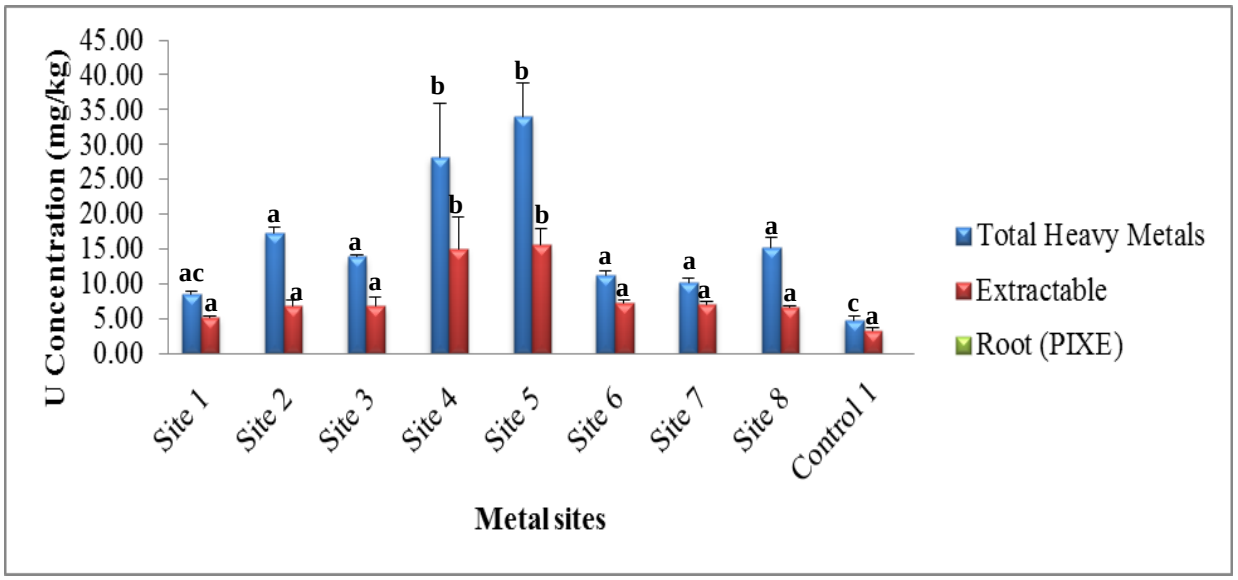
U Concentration (mg/kg)
45.00
40.00
35.00
30.00
25.00
20.00
15.00
10.00
5.00
0.00
Site 1
Site 2
Site 3
Site 4
Site 5
Site 6
Site 7
Site 8
Control 1
Metal sites
Total Heavy Metals
Extractable
Root (PIXE)

k)

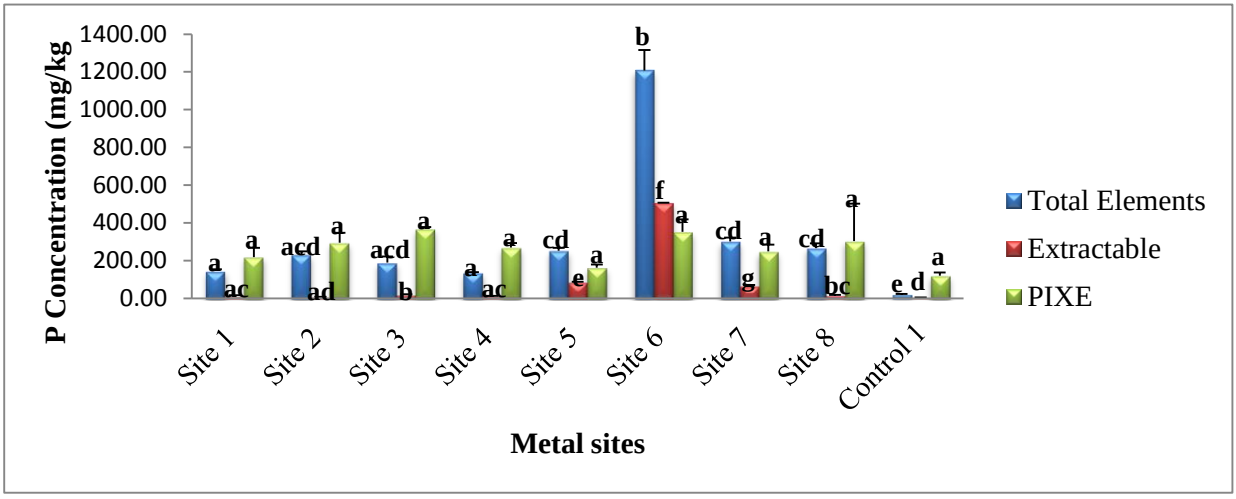
P Concentration (mg/kg
1400.00
1200.00
1000.00
800.00
600.00
400.00
200.00
0.00
Site 1
Site 2
Site 3
Site 4
Site 5
Site 6
Site 7
Site 8
Control 1
Metal sites
Total Elements
Extractable
PIXE

l)

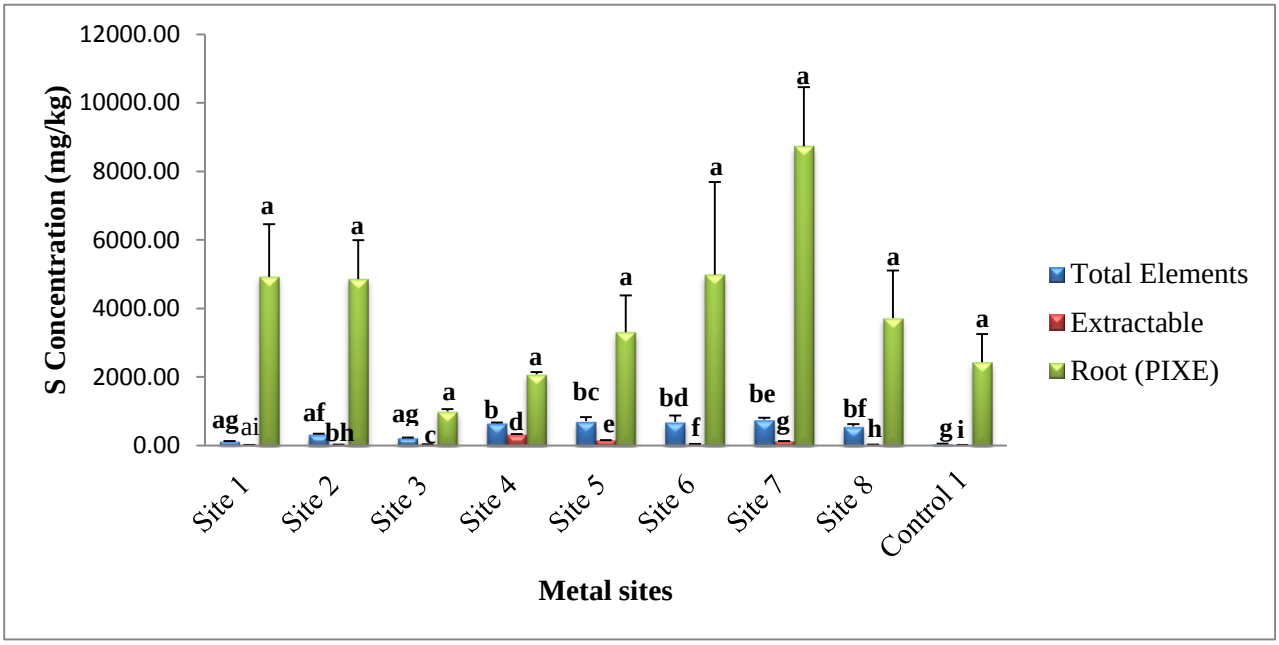
S Concentration (mg/kg)
12000.00
10000.00
8000.00
6000.00
4000.00
2000.00
0.00
Site 1
Site 2
Site 3
Site 4
Site 5
Site 6
Site 7
Site 8
Control 1
Metal sites
Total Elements
Extractable
Root (PIXE)

m)

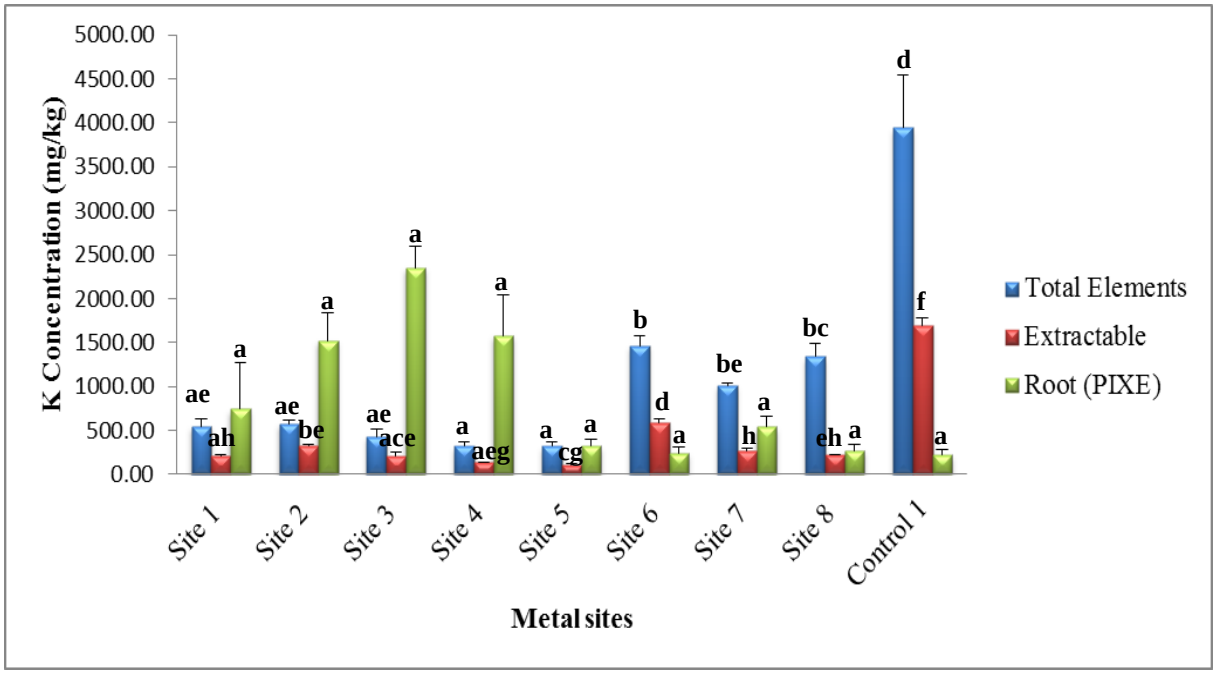
K Concentration (mg/kg)
5000.00
4500.00
4000.00
3500.00
3000.00
2500.00
2000.00
1500.00
1000.00
500.00
0.00
Site 1
Site 2
Site 3
Site 4
Site 5
Site 6
Site 7
Site 8
Control 1
Metal sites
Total Elements
Extractable
Root (PIXE)

n)

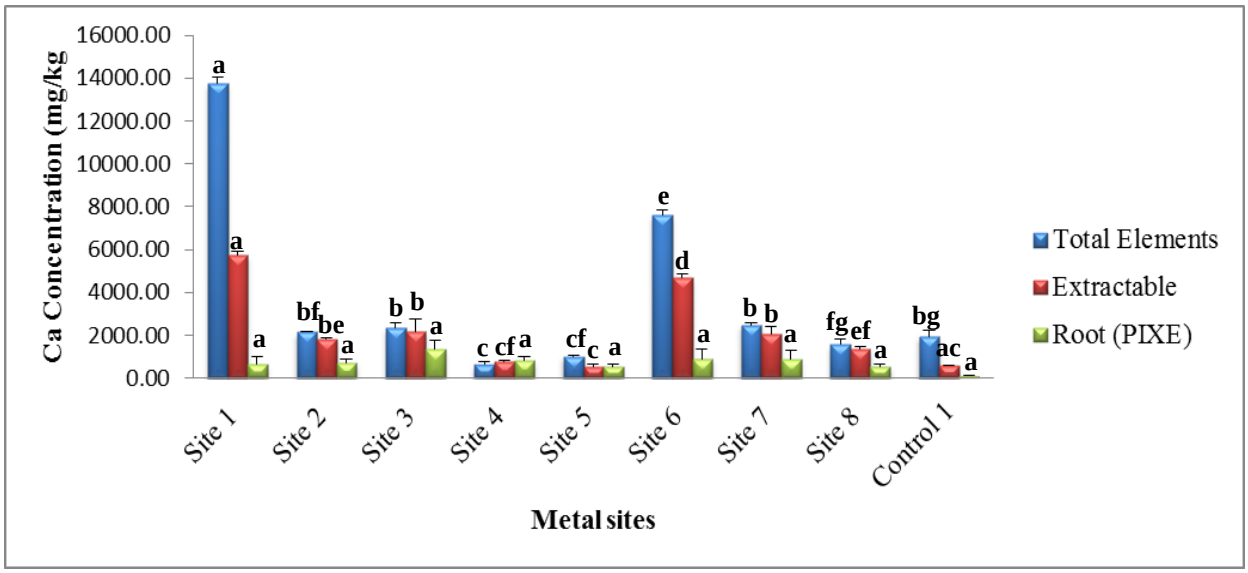
Ca Concentration (mg/kg
16000.00
14000.00
12000.00
10000.00
8000.00
6000.00
4000.00
2000.00
0.00
Site 1
Site 2
Site 3
Site 4
Site 5
Site 6
Site 7
Site 8
Control 1
Metal sites
Total Elements
Extractable
Root (PIXE)

o)

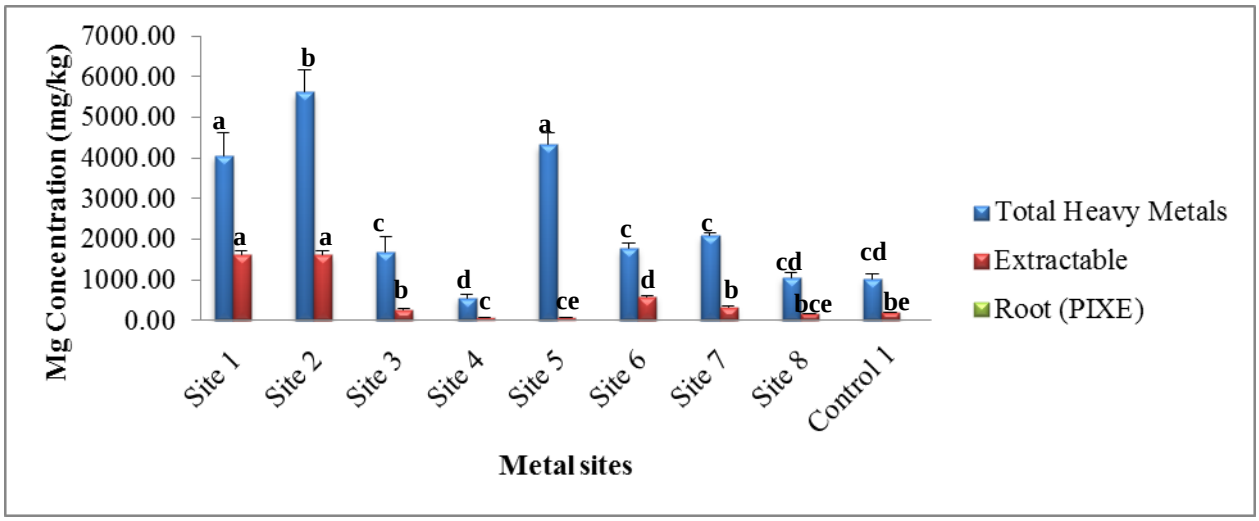
Mg Concentration (mg/kg)
7000.00
6000.00
5000.00
4000.00
3000.00
2000.00
1000.00
0.00
Site 1
Site 2
Site 3
Site 4
Site 5
Site 6
Site 7
Site 8
Control 1
Metal sites
Total Heavy Metals
Extractable
Root (PIXE)

p)

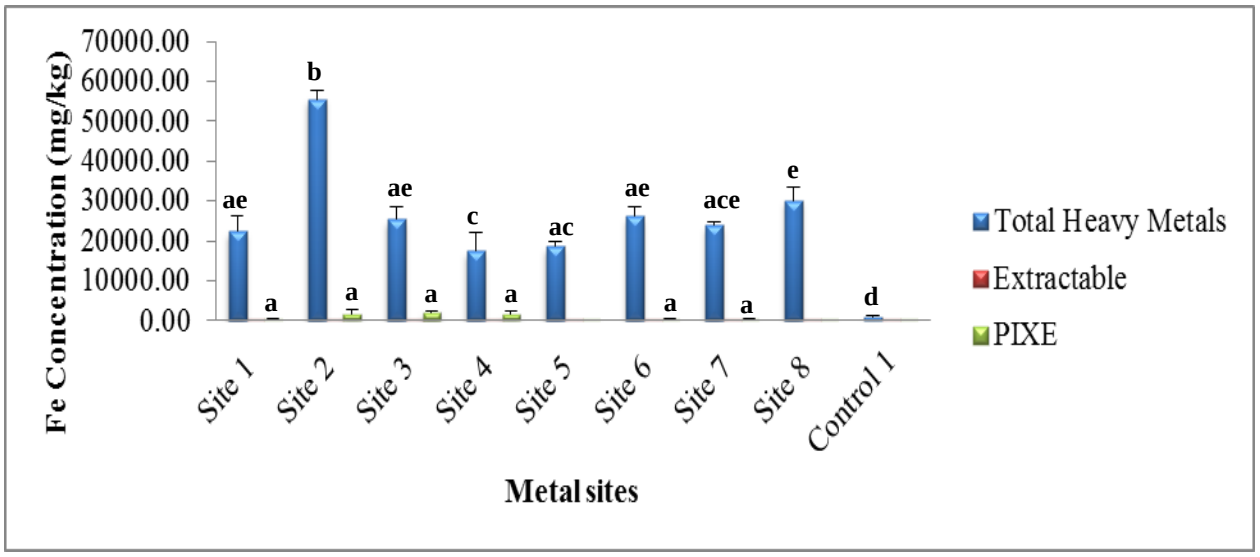
Fe Concentration (mg/kg)
70000.00
60000.00
50000.00
40000.00
30000.00
20000.00
10000.00
0.00
ae a b a ae a c a ac a ae a ace a e d
Site 1
Site 2
Site 3
Site 4
Site 5
Site 6
Site 7
Site 8
Control 1
Metal sites
Total Heavy Metals
Extractable
PIXE

q)

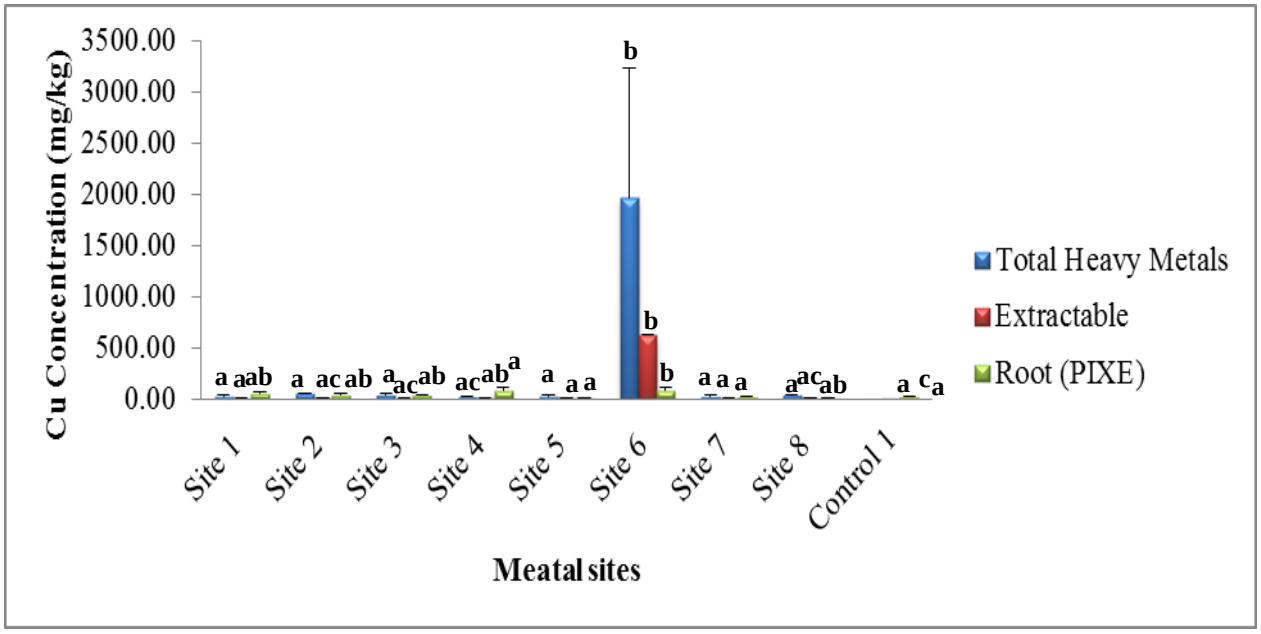
Cu Concentration (mg/kg)
3500.00
3000.00
2500.00
2000.00
1500.00
1000.00
500.00
0.00
a aab a ac ab a ac ab ac ab a a a a b b a a a a ac ab a c a
Site 1
Site 2
Site 3
Site 4
Site 5
Site 6
Site 7
Site 8
Control 1
Meatal sites
Total Heavy Metals
Extractable
Root (PIXE)

r)

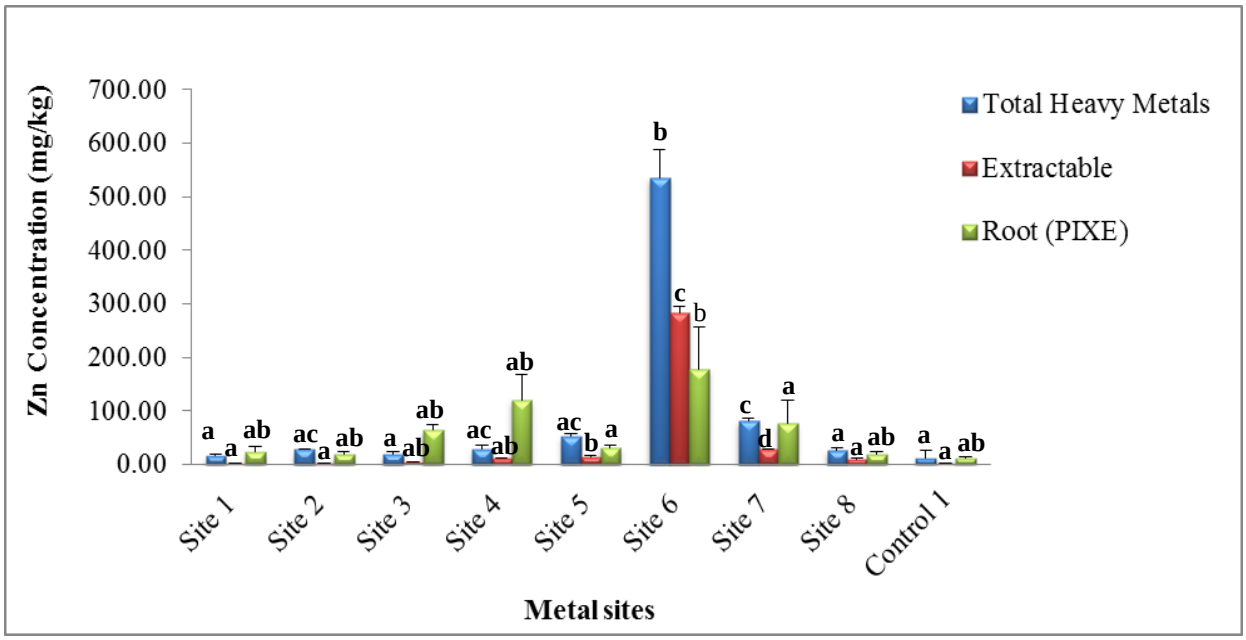

s)

Fig. 6.21 [8]**(a – s)** The elemental concentration results for Total Heavy Metal Content Vs Extractable Heavy Metal concentration & PIXE across eight sites including a control with a) Ti. b) Cr. c) Ni, d) Pt, e) Cd f) Hg, g) Al, h) Si, i) Pb. j) Au, k) U, l) P, m) S, n) K, o) Ca, p) Mg, q) Fe, r) Cu and s) Zn. Common alphabetic letters indicate no significant difference between sites for each element ($p \leq 0.05$).

[8] Pt, Ag, Cd, Hg, Pb, Au and U were measured but they were less than the detection limit thus they could not be included in both table 6.1 and Fig.21 (a – s).

6.5 Discussion

Elemental distribution maps showed that Si, S, Cl and K were localised and detected at maximum concentration in the epi/exodermal-outer cortical root tissues of almost all treatments. Elemental distribution maps also showed that Al, Si, P, S, Cl, K, Ca and Fe were localised and detected at maximum concentration in both the longitudinal and root cross-sections from all the sampling sites (Fig. 6.1 – Fig. 6.19). Ti, V, Cr, Mn, Ni, Cu, Zn, and Br were detected in lower concentrations with As, Se, Sr, Ba, Pb and U present in very low quantities in roots from all the sites often below the detection limit (Table 6.1, Fig. 6.21k, Appendix 3).

The accumulation pattern of all the detected elements in the epi/exodermal-outer cortical root tissues of mycorrhizal plants was not homogeneously distributed (Fig. 6.3 & Fig. 6.8). This is also true for site 3 and control plants in Fig. 6.6, Fig. 6.17, Fig. 6.18 and Fig. 6.19. The accumulation patterns of Al, Si, P, S, Cl, K, Ca and Fe in the epi/exodermal-outer cortical root tissues of control plants were also not homogeneous. This agrees with the studies by Weiersbye *et al.* (1999) and Orlowska *et al.* (2013). Strong accumulation of elements such as Al, Ti, K, Cr, Si, Fe, and Ca within the epi/exodermal-outer cortical layer of mycorrhizal roots and in the selected AM fungi structures (vesicles and hyphae) suggest that fungal structures are the major deposition sites of these elements and are instrumental in plants' detoxification (Orlowska *et al.,* 2011; Orlowska *et al.,* 2013). The spatial distribution of these elements as shown by Micro-PIXE experiments tends to be most concentrated on the edge of the root (epidermis), perhaps reflecting the precipitation of these elements in this location (Fig. 6.2, Fig. 6.11, Fig. 6.12, Fig. 6.13, Fig. 6.14 and Fig. 6.16).

This pattern also indicates that a range of metals and radionuclides can be sequestered in putative AM fungal structures above levels in surrounding host root tissue and demonstrates the potential of PIXE for the resolution of inter-and intracellular AM fungal structures. Thus, distinctive elemental maps have been successfully used to localise sites of colonisation and verification of the symbiotic

nature of the mycorrhizal plant (Weiersbye *et al.,* 1999; Orlowska *et al.,* 2013). This elemental map also indicates that AM fungal structures especially vesicles are most localised on the outer cortex or outer epidermal layer of the root cross-sections, as shown by higher concentration of Si in the vesicles and arbuscules **(**Fig. 6.2b). Since heavy-metal-enriched soils are often not only toxic to plants but also nutrient deficient (Shetty *et al.,* 1994), it is depicted that AM fungi plays a critical role in the early development of plants in such environments by both supplying nutrients as well as protecting the plant from toxicity of heavy metals**.**

Although at trace levels, some of these metals such as Zn, Cu, Fe, Mn, Co and Cr are essential elements for many plants, animals and human beings, at high concentrations, they are all potentially toxic (Nyriagu, 1988; Goyer, 1996). An excessive Fe uptake for example can produce toxic effects in plants growing on soil rich in mobile Fe fractions. Plant injury due to Fe toxicity is most likely to occur on strongly acid soils (Ultisols, Oxisols), on acid sulfate soils, flooded soils, and heavy metal contaminated mine dumps. A high concentration of Fe in the soil solution is almost always related to Fe toxicity. This toxicity is also often associated with salinity and a low phosphorus or base status of soils. This might explain the low phosphorus concentration observed in the Micro-PIXE maps (Fig. 6.1 to Fig. 6.19). Fe is highly available in most mining areas especially in the Witwatersrand tailings due to the oxidation of pyrite (Witkowski and Weiersbye, 1998). Although an indispensable micronutrient, Fe is highly toxic to cells at elevated concentrations and therefore most organisms have sophisticated Fe acquisition and sequestration mechanisms (Gadd, 1993). Vesicle, hyphae and putative arbuscular regions of mycorrhizal roots from almost all the mine tailings examined in this study contained higher concentrations of Fe, than the surrounding host cells. This pattern may be linked to the highly efficient Fe acquisition and sequestration mechanisms characteristic of Glomeromycota fungi.

The higher elemental concentration shown by PIXE at some sites, such as sites 3, 4 and 6 as compared to that of extractable suggests accumulation in the roots. In some cases, some elements such as Pt, Cd, Hg, Pb, Au and U could not be

detected by PIXE. This might indicate that these elements were not assimilated to the root or AM fungal structures.

6.5.1 Statistical interpretation

The correlation between elements and mycorrhizal structures was also conducted using Principal Component Analysis (PCA). According to the results of statistical analysis, large amounts of elements are accumulated in vesicles followed by the arbuscules then hyphae (Fig. 6.20a-j). This agrees with the elemental maps which showed accumulation of elements in the vesicular structures and hyphae especially heavy metals such as Fe, Cu, Mn, Ti, Zn, and alkali metals such as Ca, (Fig. 6.1– Fig. 6.19).

Elemental maps of the root cross-sections demonstrated that AM fungal structures are mostly localised in the outer cortex or outer epidermal layer of the root, as shown by the more significantly enriched Si in the vesicles and arbuscules (Fig. 6.2). Since the roots were freeze dried during sample preparation for the PIXE technique, hyphae could not be visible and as a result, very few elemental maps were obtained in which hyphae and arbuscules were visible. However before freeze drying, the roots were observed for AM fungal colonisation under the light phase microscope and a lot of mycorrhizal structures including hyphae, arbuscules, and vesicles were observed (Fig. 4.1, Fig. 6.5a, 6.6a).

The overall PIXE results demonstrate that most elements are accumulated in vesicles followed by hyphae then arbuscule (Fig. 6.20a to Fig. 6.20j). All the elements observed through PIXE technique in the examined sites have their concentrations above the normal standard required for plants while Al in most sites falls within the normal elemental concentration range required by plants (Table 6.8). Table 6.8 shows standard elements for both above and below the ground (Alloway, 1995; Kabata, 2011; Suruchi and Khanna, 2011). Suruchi and Khanna, (2011) reported high levels of copper and zinc, lead and cadmium ranging from 0.32 to 35.72 $mgkg^{-1}$ for Cu and 0.4 to 63.63 $mgkg^{-1}$ for Zn and 0.018 to 2.57 $mgkg^{-1}$ for both Pb and Cd in various vegetables studies carried out

by different researchers in countries such as Egypt India, Pakistan, Tanzania, Nigeria and Greece. The high concentration range also indicates that the mining sites have higher concentration of elements, thus revealing the high heavy metal contamination of the mining sites and the ability of AM fungi to accumulate and clean up the metal contamination.

Table 6.8 Concentration of heavy metals in soils and plants in mg kg^{-1} both below and above ground. Data are given for the range that can be observed frequently; according to Alloway (1995), Bowen (1979), Adriano (2001), Kabata-Pendias (2000), and own analyses.

No.	Element	Symbol	Soil (mg kg^{-1})	Plant (mg kg^{-1})		
				Low-High	High	Normal (AVR)
1	Antimony	In	0.1 - 2.0	0.01	0.1	0.055
2	Arsenic	As	1.0 – 10	0.1	0.5	0.3
3	Barium	Ba	100 – 1000	10	100	55
4	Berylium	Be	0.1 – 10	0.01	0.1	0.055
5	Boron	B	2.0 – 100	3	90	46.5
6	Cadmium	Cd	0.05 - 1.0	0.05	0.5	0.275
7	Chromium	Cr	10 – 50	0.1	0.5	0.3
8	Cobalt	Co	1.0 – 10	0.02	0.5	0.26
9	Copper	Cu	10 – 40	3	12	7.5
10	Fluorine	F	100 – 500	1	10	5.5
11	Iron	Fe	10000 - 50000	50	200	125
12	Lead	Pb	10 – 30	0.1	0.5	0.3
13	Manganese	Mn	300 – 1000	20	400	210
14	Mercury	Hg	0.05 - 0.5	0.005	0.05	0.0275
15	Molybdenum	Mo	0.5 – 2	0.1	4	2.05
16	Nickel	Ni	10 – 50	0.2	2	1.1
17	Selenium	Se	0.1 - 2.0	0.01	0.5	0.255
18	Thallium	Tl	0.02 – 05	0.005	0.05	0.0275
19	Tin	Sn	0.1 – 10	0.1	1	0.55
20	Vanadium	V	30 – 150	0.2	1	0.6
21	Zinc	Zn	20 -200	20	100	60

Distribution of these metals in the roots and mycorrhizal structures suggests that mycorrhizal plants are able to tolerate high level of heavy metals in contaminated sites. The observed concentrations exceeded the average values for plants grown in non-polluted areas as reported by Markert (1992). The high accumulation

patterns characteristic of *E. curvula* plant has been confirmed in this study. High concentrations of these metals observed in the roots of *E. curvula* species from different metal sites corroborate the findings by Wislocka *et al.* (2006). There were relatively low concentrations of Mn noted in the plant roots ranging from 7 to 150 mg/kg from almost all the sample sites. Similarly for Br, low average concentrations ranging from 0 to 18 mg/kg were also recorded in almost all the sites.

The high concentration of heavy metals observed in the plants is an indication of elevated levels of heavy metals in the soil. High concentration of Fe, Al, Mn, Ti and the presence of U in plants as shown from this study is a useful indicator of soil contamination (Grath, 2000). High concentration of Si, Al and Fe found in this study tallies with the findings indicating Si, as the most abundant element in the earth's crust followed by aluminum and iron. It has also been reported that the relative proportions of metals to aluminum and iron in crustal material are fairly constant (Taylor, 1964; Taylor and Mclennan, 1981). Aluminum, a major component of clay minerals, is usually associated with fine-grained aluminosilicate minerals. These high levels of heavy metals in the soil are toxic to plants, animals and human beings. Thus a serious attention is needed and this research suggests the use of mycorrhizal plants to remediate the toxic metals from the soil mine dumps.

6.5.2 Antagonistic behaviour of each element with other elements

In most elements, an antagonistic relationship was observed where the excess of one element affects the absorption of the other element by plant roots. An example is lower level of copper concentration observed in roots which is attributed to the antagonistic relationship with other trace metals such as Fe, Al and P. Although Cu concentration exceeded the standard concentration levels required by plants, its concentration was very low as compared to the concentration of Fe, Al and P. This then displays the fact that high levels of Fe, Al and P observed in this study lead to the reduced mycorrhizal absorption of Cu

from the soil. In other words the high levels of Fe, Al and P inhibited the absorption of Cu by the mycorrhizas (Reilly and Reilly, 1973).

Furthermore, high levels of Fe concentration recorded in roots are attributed to the antagonistic behaviour of iron with other elements like Ni and Mn. High concentration of Fe in roots inhibits the absorption of other elements such as Ni, and Mn as has been the case in this study. Low levels of Ni and Mn concentration have been observed. The concentration of elements in the sample sites ranged from 0 to 15 000 ppm. Most elemental concentration has been observed to fall between 0 – 1000 mg/kg, with some between 1000 – 4000 mg/kg, and very few with a concentration above 4000 mg/kg (Table 6.1).

Although this concentration seems to be low, most elements had concentrations above the standard limit required for plants. In addition, some of the elements like Gold (Au), Uranium (U), Cobalt (Co), and Platinum (Pt) that were expected to be detected by both ICP-MS and Micro-PIXE could not be measured, as some were far below the detection limit and some were not even detected. This could be attributed to the fact that the pot soil samples were prepared from the soil taken from the rhizosphere of the original plants that were growing on the sample sites. Thus, in the rhizosphere of another plant the nutrients could be limiting and some of the metals available for uptake by *E. curvula* roots could also be quite low as they may be depleted &/or bound by the original plant (Weiersbye *et al.*, 1999).

This study has demonstrated that mycorrhizal fungi have the ability to help plants absorb and tolerate excess amounts of heavy metals in contaminated mine tailings . This emanates from the fact that all the elemental concentrations measured in this study far exceeded the average concentrations levels required by plants (Table 6.8). As indicated above, mycorrhizal structures such as vesicles, hyphae and putative arbuscular regions of mycorrhizal roots from almost all the mine tailings examined had higher elemental concentrations than the surrounding host cells. A mechanism by which AM fungi may prevent metal or radionuclide toxicity to its phytobiont is by sequestering toxic elements in fungal structures (Turnau *et al.*,

1993). Therefore Micro-PIXE has successfully localised HM concentration or accumulation in plant roots and AM fungal structures. This indicates the ability of mycorrhizal plants to be used to remediate contaminated mining sites.

CHAPTER 7

7 General Summary and Conclusions

The study has been able to highlight the potential of AM fungi for inoculation of plants as a prerequisite for successful restoration of heavy metal contaminated soils. It has successfully investigated AM fungal diversity in selected heavy metal (HM) sites in the RSA particularly North West (NW), Mpumalanga and Gauteng (Johannesburg) mining slime dams. Accurate identification of spores from field samples is a complicated process since spores are often old, parasitized, degraded or modified enough in subtle ways that lead to misinterpretations of subcellular characters for species-level identification (Fernández *et al*., 2011). Thus a bait or trap pot cultures of indigenous fungi is recommended which facilitate the isolation and accurate identification of newly formed AM fungal spores (Oehl *et al*., 2009). Spores extracted from bait cultures are much more uniform in their morphologies, and are abundant enough to provide a large sample size to examine the full range of morphological variation in spores (Pfleger and Linderman, 1992).

Through morphological characteristics the following fungal genera were identified for the first time in the studied sites in South Africa. The study identified a total of 14 AM fungal genera and 55 AM fungal species and these are, *Glomus (15), Acaulospora (11), Scutellospora (6), Gigaspora (6), Rhizophagus (3), Funneliformis (3), Archaeospora (2), Claroideoglomus (2), Ambispora (2), Sclerocystis (1), Fuscutata (1), Entrophospora (1), Diversispora (1), Paraglomus (1)* (Table 4.1 to 4.4)**.** *Glomus* has been observed to be the highest occurring genera in the analysed soil samples followed by *Acaulospora, Scutellospora and Gigaspora*. This agrees with the study conducted by Camprubí *et al*. (2010), who found *Glomus* spores as the most abundant species in the direct soil extraction samples. Gunwal *et al.* (2014) also reported *Glomus* as the most abundant species amongst the AM species isolated in their study.

Few studies on AM fungal morphological identification have been conducted in South Africa. Straker *et al*., (2010), in their study on an investigation of AM fungi

associated with cassava in the Limpopo and Mpumalanga provinces identified *Acaulospora mellea* which was also identified in the current study. Five other AM fungal species were identified, including *Claroideoglomus etunicatum* (formerly known as *Glomus etunicatum*) also found in the present study. In another study by Meyer *et al.* (2005), the AM community associated with grapevines in the Western Cape was investigated where in which about 18 AM fungal species were identified including *Sclerocystis sinuosa* (formerly *Glomus sinuosum*). The overlap of AM species identified in these various investigations appears to be small, suggesting that diversity and community composition vary significantly between regions, a trend which has been observed by Öpik *et al.* (2010) from their construction of a SSU rRNA gene virtual taxa database.

The high number of AM fungal spores isolated from all the mining areas sampled is an indication of potential AM fungi to be used to remediate contaminated mining sites. North West Uranium and gold mines (sites 4, 5 and 8) were found to have the highest number of spore counts compared to other areas. Most of the spores counted were observed in 45 µm sieve, these spores were tiny and had different sizes, colour and shapes. Majority of the observed spores were small, brown and oval in shape. Hyphae in root staining were found to be the most abundant in roots followed by vesicles (Fig. 4.1, 4.3 and 4.4). This high mycorrhizal colonisation in almost all the sites is due to the fact that most sites are highly contaminated with various heavy metals such Au, Ti, Al, Fe and U. (Fig. 6.21) and therefore, AM fungi had to multiply in order to survive in these sites. This concurs with the findings by Whitfield *et al*. (2004) and Turnau *et al*. (1996), who noted greater AM vesicle numbers in the roots of *Oxalis acetosella* plants from woodland plots experimentally contaminated with Cd and Zn, compared with control plots.

A high number of AM fungal species were isolated from slime dams and a high Shannon-Weaver index (H) which shows high diversity and presence of the mycorrhizal species in slime dams was recorded (Tables 4.2 - 4.5). The high diversity indicated in Tables 4.2 – 4.5; illustrate the high potential of using AM

fungi to bioremediate toxic heavy metal slime dams in South Africa particularly North West, Mpumalanga and Gauteng gold mining slime dams which are the most mining areas in the RSA. AM fungi diversity is critical to any rhizosphere studies as it provides essential variety link between plants and the soil environments (Timonen and Marschner, 2005). Mycorrhiza formation has been reported to modify the root system metabolism by changing the chemical and mineral composition of root exudates that are released into the soil (Timonen and Marschner, 2005; Azcón-Aguilar and Barea, 1992). Therefore mycorrhizal fungi form a unique part of the rhizosphere and contribute positively to both the plant growth and soil environmental dynamics (Fillion *et al*., 1999). Orlowska *et al*. (2011) also reported in their study that inoculation of *Berkheya coddii* with arbuscular mycorrhizal fungi, especially with the indigenous strains, significantly enhanced plant growth. Some of the positive beneficial effects of AM fungi on plant growth and survival in heavy metal contaminated site include an increased transfer of nutrients such as P which increase plant photosynthesis; an increased uptake of elements to counteract toxicity of some elements such as Ni, Cu, Zn and U; and lastly an increased capture of potentially toxic elements within roots, possibly due to the presence of fungal mycelium and its ability to chelate excess of metals within the mycelium (Turnau *et al*., 2010).

This study has also successfully identified more than three AM fungal genera, through molecular characterisation namely *Acaulospora* (14), *Glomus* (3), *and Scutellospora* (2) using a nested PCR from spores isolated from metal contaminated mining sites. For accurate AM fungal identification, it is very critical to always complement the morphological identification with molecular analysis (Krüger *et al.,* 2012). Almost all the AM fungal genera identified by morphological identification were also confirmed using molecular identification except *Gigaspora*, *Archaeospora*, *Funneliformis*, *Fuscutata* and *Sclerocystis* which were not confirmed by molecular analysis (Fig. 5.5, table 5.1). Both NCBI Genbank Blast and Maarj*AM* Genbank Blast identified *Acaulospora colombiana* (14) followed by *Glomus* (3), and *Scutellospora* (2) species as the most abundant species found in the used AM fungal spores. The molecular identification results

do not only assist in revealing the AM fungal diversity of HM polluted mine tailing environments but also contributes to our knowledge of their diversity in South Africa. This is very vital since in Africa for instance, there is a lack of the understanding of the distribution of AM fungi geographically due to low levels of molecular data from some areas (Öpik *et al*., 2010). Furthermore, new species were identified from Maarj*AM* website replacing the old species, for example, both *Entrophospora* and *Kuklospora*, were replaced by *Acaulospora* (Schüßler and Walker, 2010).

This study further provides a valuable contribution to the database of the Glomeromycota in general especially to that which is found in both South African and African soils. This shows the potential of using mycorrhizas to remediate the toxic heavy metal contaminated sites. To our knowledge, this is the first time these genera have been discovered in heavy metal contaminated sites in South Africa especially *Acaulospora colombiana.* This suggests that both *Glomus* species and *Acaulospora colombiana* are the AM fungal isolates responsible for the survival of plants growing in heavy metal sites and thus they could be useful to solve the heavy metal contamination of the mine dumps (Table 5.1). The study also highlights that AM fungal diversity is very crucial to the maintenance and sustainability of the ecosystem. In addition different primers were employed in this study for PCR application. Some DNA samples were amplified using normal known universal primers, namely, ITS1 & ITS4 or NS31 & AM1. However, the majority of the samples were amplified using primers designed by Lee *et al.* (2008) namely NS1 and NS4 coupled by AML1 and AML2.

PIXE technique was successful in localising elemental concentration in both plant roots and AM fungal structures as well as in indicating the dimensions of large vesicles in root tissue. However, it was less successful in showing areas of both hyphal and arbuscular formations. Although the concentration levels of heavy metals reported in Fig. 6.21(a-k) seem to be low, however, they are far above the acceptable limits required by plants (Table 6.8) (Suruchi and Khanna, 2011; Kabata-Pendias, 2000; Adriano, 2001; and Kabata, 2011). Plant tolerance

response to heavy metal toxicity, is highly variable among genotypes and plant species. It was interesting to observe most AM fungal structures in the outer cortex or outer epidermal layer of the root cross-sections, as shown by the more significantly enriched Si in the vesicles and arbuscules (Fig. 6.2; Fig. 6.3). Previous studies conducted on micro elemental analysis of both mycorrhizal and non-mycorrhizal plants (Weiersbye *et al*., 1999; Alford *et al*., 2010; Turnau and Mesjasz-Przybylowicz, 2003; Vogel-Mikuš *et al*., 2006; Wu *et al*., 2007, 2009; Orlowska *et al.*, 2011; Orlowska *et al.*, 2013), also show that the Micro-PIXE is able to localise the HM concentration in both plant roots and AM fungal structures as well as in indicating the vesicles in root tissues as it is done in this study.

Thus, distinctive elemental maps can be used to localise sites of colonisation and verification of the symbiotic nature of the tissue. This indicates that a range of metals can be sequestered in AM fungal structures above levels in surrounding host root tissue and demonstrates the potential of Micro-PIXE to determine metal accumulation and elemental distribution in mycorrhizal plant roots and inter-and intracellular AM fungal structures. The analysis of soil elemental chemistry compared to plant elemental chemistry (PIXE) showed a high concentration of heavy metal total content as compared to both extractable and PIXE analysis (Fig. 6.21(a-s). However, PIXE showed a higher elemental concentration in some sites such as sites 3, 4 and 6 than extractable, which suggests accumulation in the roots. The lower concentrations of extractable elemental analysis might indicate that mycorrhiza could protect its host plant from the phytotoxicity of excessive metals by changing the speciation from bio-available to the non-bio-available form (Orlowska *et al.*, 2011). The high concentration of heavy metal total content in the soil is the indication of the presence of the heavy metals in the soil above the required amounts.

Although phytoremediation requires a long-term commitment as the process is dependent on plant growth, tolerance to toxicity and bioaccumulation capacity (Suruchi and Khanna, 2011), it has proven to be a good method for cleaning up

soils that have low or intermediate contamination of heavy metals. This is due to its cheapness in comparison with many in-situ methods. Therefore, phytoremediation of mine tailings by mycorrhizal plants seems to be one of the most promising lines of research on mine dumps contamination by heavy metals. The strategies evolved in this project have great potential for phytoremediation of toxic mining sites and thus can help mitigate the environmental problems especially in the mining wastes sites.

Although this study has managed to localise elemental concentration in both plant roots and AM fungal structures in root tissue and also identify both *Glomus* species and *Acaulospora colombiana* species, as the AM fungal isolates responsible for the survival of plants growing in Heavy Metal sites; however, it is highly recommended to further investigate the mechanisms of tolerance and hyperaccumulation of toxic and heavy metals / metalloids / radionuclides in both mycorrhizal structures (HC, AC and VC) and roots of plants growing in the mining waste sites. Thereby investigating how the AM fungi protect the plant from HM toxicity and how the toxic state of the element is reduced to a non toxic state.

REFERENCES

A Training Manual for Mine Rehabilitation for Environment and Health Protection, 1998.

Abbott LK, Robson AD (1991) A quantitative study of the spores and anatomy of mycorrhizas formed by a species of *Glomus*, with reference to its taxonomy. *Aust. J. Bot.* **27**: 363-375.

Adriano DC (1986) Trace elements in terrestrial environments, Springer, Berlin.

Adriano DC (2001) Trace elements in terrestrial environments: Biogeochemistry, Bioavailability, and Risks of Metals. 2nd Edition, Springer, Verlag.

Ahulu EM, Nakata M and Nonaka M (2004) *Arum*- and *Paris*-type arbuscular mycorrhizas in a mixed pine forest on sand dune soil in Niigata Prefecture, central Honshu, Japan, *Myccorrhiza*, Springer Berlin / Heidelberg **15**(2): 129-136.

Alford ÉR, Pilon-Smits EAH, Paschke MW (2010) Metallophytes — a view from the rhizosphere. *Plant Soil* **337**, 33–50.

Alguacil M del Mar, Díaz-Pereira E, Caravaca F, Fernandez DA, and Roldan A (2009a) Increased Diversity of Arbuscular Mycorrhizal Fungi in a Long-Term Field Experiment via Application of Organic Amendments to a Semiarid Degraded Soil. *Appl. Environ. Microbiol*. **75**(13): 4254–4263.

Alguacil MM, Lumini E, Roldán A, Salinas-García JR, Bonfante P, Bianciotto V (2008) The impact of tillage practices on arbuscular mycorrhizal fungal diversity in subtropical crops. *Ecol. Appl.* **18**: 527–536.

Alguacil MM, Rolda´n A, Torres P (2009b) Complexity of semiarid gypsophilous shrub communities mediates the AM fungal biodiversity at the plant species level. *Microb. Ecol*. **57:**718–727.

Alloway BJ (1995) Soil processes and the behaviour of metals. In Alloway, BJ (Ed.), Heavy metals in soils (2nd Edn.), Blackie, Chapman & Hall, London, pp. 11 – 37.

AngloGold Ashanti (2009) Baseline description Vaal River Operations, Chapter 3, pp. 36, 41.

AngloGold Ashanti (2009) introduction to West Wits Operations, Chapter 1, pp. 36, 41.

AngloGold Ashanti Company. AngloGold Ashanti Company Report to Society: Environment (2004). http://www.anglogold.com/subwebs/informationforinvestors/reporttosociety04/values bus principles environment/e cs sa 7 15.htm.

Anhaeusser CR (2012) The history of mining in the Barberton Greenstone Belt, South Africa, with an emphasis on Gold (1868 – 2012) (carl.anhaeusser@wits.ac.za) p. 1- 29 In: Johnson MR., Anhaeusser CR., and Thomas RJ., eds (2006) The Geology of South Africa. Geological Society of South Africa, Johannesburg and Council for Geoscience, Pretoria, pp. 95-134.

Antunes QW (2010) Desktop Study on the Barberton Gold Project, Mpumalanga, South Africa. Prepared by Tala Mineral Services (Pty) Ltd, pp. 1 -15.

Asimi S, Gianinazzi-Pearson V, and Gianinazzi S (1980) Influence of increasing soil phosphorus levels on interactions between vesicular-arbuscular mycorrhizae and Rhizobium in soybeans. *Canadian Journal of Botany* **58**: 2200-2205.

Auge RM (2001) Water relations, drought and vesicular-arbuscular mycorrhizal symbiosis. *Mycorrhiza* **11**(3): 42-45.

Azcón-Aguilar C, Barea J (1992) Interactions between mycorrhizal fungi and other rhizosphere micororganisms. *In* Mycorrhizal Functioning. *Edited by* MF Allen, Chapman and Hall, Inc., New York, USA. pp. 163-198.

Azcón-Aguilar C, Palenzuela J, Roldán A, Bautista S, Vallejo R and Barea JM (2003) Analysis of the mycorrhizal potential in the rhizosphere of representative plant species from desertification- threatened Mediterranean shrublands. *Appl. Soil Ecol*. **22**: 29–37.

Baker AJM, Reeves RD, Mcgrath SP (1991) *In-situ* decontamination of heavy metal polluted soils using crops of metal-accumulating plants: a feasibility study. In: Hinchee RL, and Olfenbuttel RF eds. *In-situ bioreclamation*. Boston, Butterworth - Heinemann, p 600-605.

Barceló J, Poschenrieder C (2003) Phytoremediation: principles and perspectives. *Contributions to Science* **2**(3): 333-334.

Barea JM and Jeffries P (1995) Arbuscular mycorrhizas in sustainable soil plant systems. In *Mycorrhiza: Structure, Function, Molecular Biology and Biotechnology* (Eds. Hock, B. and Varma A) Springer-Verlag, Heidelberg pp. 521–559.

Barea JM, Azco'n-Aguilar C and Azcon R (1997) Interactions between mycorrhizal fungi and rhizosphere microorganism within the context of sustainable soil–plant systems. In: Gange AC and Brown VK (eds.) *Multitrophic Interactions in Terrestrial Systems,* Cambridge, United Kingdom, pp. 65–77.

Bécard G and Pfeffer PE (1993) Status of Nuclear Division in Arbuscular Mycorrhizal Fungi During In-Vitro Development. *Protoplasma* **174:** 62-68.

Benzing DH (1981) Why is Orchidaceae so large, its seeds so small, and its seedlings mycotrophic? *Selbyana* **5:** 241–242.

Berch SM, Fortin JA (1983) Lectotypification of *Glomus macrocarpum* and proposal of new combinations: *Glomus australe, Glomus versiforme*, and *Glomus tenebrosum* (*Endogonaceae*). *Canadian J. of Bot.* **61**: 2608-2617.

Berti, WR, Cunningham SD (2000) Phytostabilization of metals. In: Raskin I, Ensley BD, eds. *Phytoremediation of toxic metals: using plants to clean-up the environment.* New York, John Wiley & Sons, Inc., p. 71-88.

Bever JD (2002) Host-specificity of AM fungal population growth rates can generate feedback on plant growth. *Plant and Soil,* **244**: 281–290.

Bever JD, Morton J, Antonovics J and Schultz PA (1996) Host-dependent sporulation and species diversity of mycorrhizal fungi in mown grassland. *Journal of Ecology* **75,** 1965–1977.

Bhalerao SA (2013) Arbuscular mycorrhizal fungi: a potential biotechnological tool for phytoremediation of heavy metal contaminated soils, *Int. J. of Sci. and Nature* **4**(1): 1-15.

Birhane E, Sterck FJ, Fetene M, Bongers F, Kuyper TW (2012) Arbuscular mycorrhizal fungi enhance photosynthesis, water use efficiency, and growth of frankincense seedlings under pulsed water availability conditions. *Oecologia* **169**: 895-904.

Blaszkowski J (1992) *Scutellospora armeniaca*, a new species in Glomales (Zygomycetes) from Poland. *Mycologia* **84**: 939-944.

Blaszkowski J (1993a) Comparative studies of the occurrence of arbuscular fungi and mycorrhizae (Glomales) in cultivated and uncultivated soils of Poland. *Acta Mycologica*, **28:** 93-140.

Blaszkowski J (1993b) The occurrence of arbuscular fungi and mycorrhizae (Glomales) in plant communities of maritime dunes and shores of Poland. Bulletin of the Polish Academy of Sciences - *Biological Sciences* **41**: 377-392.

Blaszkowski J (1994) Arbuscular fungi and mycorrhizae (Glomales) of the Hel Peninsula, Poland. *Mycorrhiza* **5**: 71-88.

Blaszkowski J, Tadych M, Madej T (2002) Arbuscular mycorrhizal fungi (Glomales, Zygomycota) of the Bledowska Desert, Poland. *Acta Societatis Botanicorum Poloniae* **71**: 71-85.

Blaszkowski J, Tadych, M Madej T, Adamska I, Iwaniuk A (2001) Arbuscular mycorrhizal fungi (Glomales, Zygomycota) of Israeli soils. Mat. II Polsko-Izraelskiej Konf. Nauk. nt. "Gospodarowanie zasobami wodnymi i nawadnianie roslin uprawnych". Przeglad Naukowy Inzynieria I *Ksztaltowanie Srodowiska* **22:** 8-27.

Bolan NS, Park, JE, Robinson B, Naidu R, Huh KY (2011) Phytostabilization: a green approach to contaminant containment. *Adv. Agron.* **112**: 145–204.

Bosch F, El Goresy A, Herth W, Martin W, Nobiling R, Povh B, Reiss HD, and Traxel K (1980), *Nucl. Sci. Appl.* **1:** 35.

Boss CB, and Fredeen KJ (1997) Concepts, Instrumentation and Techniques in Inductively Coupled Plasma Optical Emission Spectrometry, 2nd ed. The Perkin-Elmer Corporation, USA, pp. 1-11, 2-12, 3-13.

Bothe H, Regvar M, Turnau K (2010) Arbuscular mycorrhiza, heavy metal and salt tolerance. In: Sherameti I, Varma A (eds) Soil heavy metals. Springer, Heidelberg, pp 87–111.

Bouamri1 R, Dalpé Y, Serrhini MN, and Bennani A (2006) Arbuscular mycorrhizal fungi species associated with rhizosphere of *Phoenix dactylifera* L. in Morocco, *African Journal of Biotech.* **5**(6): 510-516.

Bowen HJM (1979) Environmental Chemistry of elements. *Acdemic Press London*.

Brundrett MC, Kendrick B (1990b) The roots and mycorrhizas of herbaceous woodland plants. II. Structural aspects of morphology. *New Phytol.* **114**: 469–479.

Cairney JWG (2000) Evolution of mycorrhizal systems. *Naturwissenschaften*, **87**: 467- 475.

Camprubí A, Calvet C, Cabot P, Pitet M and Estaún V (2010) Arbuscular mycorrhizal fungi associated with psammophilic vegetation in Mediterranean coastal sand dunes, *Spanish Journal of Agric. Res.* **8**(S1): S96-S102.

Caproni AL, Franco AA, Berbara RLL, Trufem SB, Granha JRD and Monteiro AB (2003) Arbuscular mycorrhizal fungi occurrence in revegetated areas after bauxite mining at Porto Trombetas, Para state, Brazil. *Pesquisa-Agropecuária-Brasileira* **38**: 1409-1418.

Cardoso IM, Kuyper TW (2006) Mycorrhizas and tropical soil fertility. *Agr Ecosyst Environ.* **116**: 72–84.

Chaney RL (1983) Plant uptake of inorganic waste constitutes. In: Parr JF; Marsh PB, and Kla, JM, eds. *Land treatment of hazardous wastes.* Park Ridge, NJ, Noyes Data Corp., p. 50-76.

Chapman HD, Pratt PF (1961) Methods of analysis for soils, plants and waters. University of California Div. Agr. Sci., Riverside, CA.

Chen B, Christie P, Li L (2001) A modified glass bead compartment cultivation system for studies on nutrient and trace metal uptake by arbuscular mycorrhiza. *Chemosphere* **42**: 185–192.

Chen H, Ganesan S, Jia B (2005) Environmental challenges of post-reform housing development in Beijing. *Habitat International*, **29**(3):571 – 589.

Cole DI (1998) Uranium in Wilson, MGC and Anhaeusser, CR (eds), The mineral resources of South Africa: Handbook. Council for Geoscience, 16, pp. 6422-652.

Cunningham SD, Berti WR, Huang JW (1995) Phytoremediation of contaminated soils. *Trends in Biotechnology* **13** (9):393-397.

Currie LA (1968) Limits for qualitative detection and quantitative determination: application to radiochemistry. *Analytical Chemistry* **40**:586-593.

Dalpé Y, de Souza FA, Declerck S (2005) Life Cycle of *Glomus* Species in Monoxenic Culture. Dans: Biology of arbuscular mycorrhizal fungi under in vitro culture. Eds: Declerck, S, Fortin JA, Strullu, DG, Springer-Verlag, Germany, pp. 49-71.

Dalpé Y, Diop TA, Plenchette C, Gueye M (2000) Glomales species associated with surface and deep rhizosphere of Faidherbia albida in Senegal. *Mycorrhiza* **10:** 125–129.

Daniell TJ, Husband R, Fitter AH, and Young JPW (2001) Molecular diversity of arbuscular mycorrhizal fungi colonising arable crops. *FEMS Microbiology Ecology* **36**: 203-209.

Das M, Maiti SK (2008) Comparison between availability of heavy metals in dry and wetland tailing of an abandoned copper-tailing pond. *Envt. Moni & Assess* **137** (1-3): 343-350.

De Waal SA (1986) The Bon Accord nickel occurrence at Barberton, 287-291. *In:* Anhaeusser, C. R. and Maske, S. eds. Mineral Deposits of Southern Africa, I. *Geological Society of South Africa,* 1020 pp.

del Val C, Barea JM,Azcòn-Aguilar C (1999) Assessing the tolerance to heavy metals of arbuscular mycorrhizal fungi isolated from sewage sludge-contaminated soils. *Appl. Soil Ecol*. **11**: 261–269.

Dickson S (2004) The Arum-Paris continuum of mycorrhizal symbioses. *New Phytol*. **163**:187-200.

Dodd JC, Arias, Koomen I, Hayman DS (1990) The management of populations of vesicular-arbuscular mycorrhizal fungi in acid-infertile soils of a savannah ecosystem. *Plant and Soil* **122**: 241-247.

Dodd JC, Clapp JP, Zhao B (2001) Mycorrhiza manual prepared for the workshop on Arbuscular mycorrhizal fungi in plant production systems: detection, taxonomy, conservation and ecophysiology, laboratory pf Agricultural Microbiology Huazhong Agricultural University, Wuhan, PR. China, pp 14.

Doolittle LR (1986) A semiautomatic algorithm for Rutherford backscattering analysis. *Nucl. Instrum. Methods Phys. Res. Sect. B-Beam Interactions with Materials and Atoms* **15**: 227–231.

Dos Anjos E, Cavalcante U, Correia Gonçalves D, Pedrosa E, Dos Santos J and Costa Maia L (2010) Interactions between an Arbuscular Mycorrhizal Fungus and the Root-knot Nematode. *Brazilian Archives of Biology and Technology* **4**: 801-809.

Douds DD, Schenck NC (1990), Relationship of colonization and sporulation by VA mycorrhizal fungi to plant nutrient and carbohydrate contents. *New Phytol.* **116**: 621-627.

Duffus JH (2002) "Heavy Metals"—A Meaningless Term? *Pure Appl. Chem.* **74** (5): 793–807.

Elias KS, Safir GR (1987) Hyphal elongation of *Glomus fasciculatus* in response to root exudates. *Applied and Environmental Microbiology* **53**: 1928-1933.

Enkhtuya B, Rydlová J, Vosátka M (2002) Effectiveness of indigenous and non-indigenous isolates of arbuscular mycorrhizal fungi in soils from degraded ecosystems and man-made habitats. *Appl. Soil Ecol*. **14**: 201–211.

Ensley BD (2000) Rational for use of phytoremediation. In: Raskin I, and Ensley BD, eds. *Phytoremediation of toxic metals: using plants to clean- up the environment*. New York, John Wiley & Sons, Inc., p. 3-12.

Entry JA, Watrud LS, Reeves M (1999) Accumulation of 137Cs and 90Sr from contaminated soil by three grass species inoculated with mycorrhizal fungi. *Environmental Pollution* **104**: 449-457.

EPA (Environmental Protection Agency) (1997) Electrokinetic laboratory and field processes applicable to radioactive and hazardous mixed waste in soil and groundwater. EPA 402/R- 97/006. Washington, DC.

Evangelou MWH, Ebel M, Schaeffer A, (2007) Chelate assisted phytoextraction of heavy metals from soil. Effect, mechanism, toxicity, and fate of chelating agents,*Chemosphere* **68**: 989–1003.

Feng G, Song YC, Li XL, Christie P (2003) Contribution of arbuscular mycorrhizal fungi to utilization of organic sources of phosphorus by red clover in a calcareous soil. *Appl. Soil Ecol*. **22**: 139–148.

Fernández F, Dell’ Amico JM, Angoa MV, de la Previdencia IE (2011) Use of a liquid inoculum of the arbuscular mycorrhizal fungi *Glomus hoi* in rice plants cultivated in a saline Gleysol: A new alternative to inoculate. *Journal of Plant Breeding and Crop Science* **3**: 24 – 33.

Fillion M, St-Arnaud M, and Fortin JA, (1999) Direct interaction between the arbuscular mycorrhizal fungus *Glomus intraradices* and different rhizosphere microorganisms. *New Phytol.* **141**: 525-533.

Fourie A, Tibett M, Weiersbye I, Dye P (eds) (2008), Mine Closure: proceedings of the third international seminar on mine Closure, 14-17 October 2008|Johannesburg|South Africa, Edited by, page 309 – 318.

Gadd GM (1993) *New Phytol.* **124**: 25.

Gao J, Garrison AW, Hoehamer C, Mazur CS, Wolfe NL (2000) Uptake and Phytotransformation of o,p'-DDT and p,p'-DDT by Axenically Cultivated Aquatic Plants. *J. Ag. and Food Chem.* **48**: 6114-6120.

Garriock ML, Peterson RL, Ackerley CA (1989) Early stages in colonization of *Allium porrum* (leek) roots by the vesicular-arbuscular mycorrhizal fungus, *Glomus versiforme*. *New Phytol.* **112**: 85-92.

Gaur A, Van Greuning JV, Sinclair RC, Eicker A (1999) Arbuscular mycorrhizas of Vangueria infausta Burch. Subsp. Infausta (Rubiaceae) from South Africa. *South African Journal of Botany* **65**: 434–436.

Gaur A, Adholeya A (2004) Prospects of arbuscular mycorrhizal fungi in phytoremediation of heavy metal contaminated soils. *Current Science* **86**(4): 528 – 534.

GDACE (Gauteng Department of Agriculture, Conservation and Environment), 2005. *Information layers and buffer zones for industries, sewage treatment works, landfill sites and mine dumps*, Internal policy document for Gauteng Department of Agriculture, Conservation and Environment, environmental planning section, 36 p.

GDACE (Gauteng Department of Agriculture, Environment and Conservation), (2008) Mining and Environmental Impact Guide. Produced by Staff of Digby Wells and Associates, Growth Lab and the Council For Geoscience, Johannesburg. pp, 1 -1119.

Gerdemann JW, Nicolson TH (1963) Spores of mycorrhizal *Endogone* species extracted from soil by wet sieving and decanting. *Transaction of the British Mycological Society* **46**: 235-244.

Gianinazzi-Pearson V, Branzanti B and Gianinazzi S (1989) *In vitro* enhancement of spore germination and early hyphal growth of a vesicular-arbuscular mycorrhizal fungus by host root exudates and plant flavanoids. *Symbiosis* **7**: 243-255.

Giovannetti M, Avio L, Sbrana C, Citernesi AS (1993b) Factors affecting appressorium development in the vesicular-arbuscular mycorrhizal fungus *Glomus mosseae* (Nicol. & Gerd.) Gerd. and Trappe. *New Phytol.* **123**: 115-122.

Gohre V, Paszkowski U (2006) Contribution of the arbuscular mycorrhizal symbiosis to heavy metal phytoremediation. *Planta* **223**: 1115-1122.

Gollotte A, van Tuinen D, Atkinson D (2004) Diversity of arbuscular mycorrhizal fungi colonizing roots of the grass species *Agrostis capillaries* and *Lolium perenne* in a field experiment, *Mycorrhiza* **14:** 111–117.

Gomez-Morilla I, Simon A, Simon R, Williams CT, Kiss AZ, Grime GW (2006) an evaluation of the accuracy and precision of X-ray microanalysis techniques using BCR-126A glass reference material, *Nucl. Instrum. and Methods B* **267**: 449. P19148.

Gonzini O, Plaza A, Di Palma L, Lobo MC (2010) Electrokinetic remediation of gasoilcontaminated soil enhanced by rhamnolipid, *J. Appl. Electrochem*. **40**: 1239–1248.

Goyer RA (1996) Toxic effects of metals. In: Klaassen CD (ed) *Caserett and Doull's* Toxicology: the basic science of poisons. Fifth edition, McGraw-Hill, *New York*, **5**: 691-736.

Grath MC (2000) Soil and Herbage Heavy Metal/ Trace Element Variability And Relationships At Farm And Regional Level, *Agriculture and Food Development Authority*, Jonstown Castle Research Centre Wexford, pg 13. ISBN No. 1 841701 16 5.

Greipsson S, El-Mayas H (2000) Arbuscular mycorrhizae of Leymus arenarius on coastal sands and reclamation sites in Iceland and response to inoculation. *Restor. Ecol.*, **8**: 144–150.

Gunwal I, Sharma KC, Mago P (2014) Spore density and root colonization by arbuscular mycorrhizal fungi in Heavy-Metal-Contaminated Soils, *IOSR Journal of Pharmacy and Biological Sciences (*IOSR-JPBS) **9**(3): 49-53.

Harrison MJ, Dixon RA (1994) Spatial patterns of expression of flavanoid/isoflavanoid pathway genes during interactions between roots of *Medicago truncatula* and the mycorrhizal fungus *Glomus versiforme. The Plant Journal* **6**: 9-20.

Hartnett DC, Wilson GT (2002) The role of mycorrhizas in plant community structure and dynamics: lessons from grasslands. *Plant and Soil* **244:** 319-331.

Haselwandter K, Bowen GD (1996) Mycorrhizal relations in trees for agroforestry and land rehabilitation. *For. Ecol. Manage*. **81**: 1–17.

Hayat MA (1989) Chemical Fixation, *Principles and Techniques of Electron Microscopy: Biological Applications.* Macmillan and Co; London: Boca Raton, CRC Press: 1-74.

Heggo A, Angle JS, Chaney RL (1990) Effects of vesicular arbuscular mycorrhizal fungi on heavy-metal uptake by soybeans. *Soil Biol. Biochem.* **22**: 865–869.

Helgason T, Daniell TJ, Husband R, Fitter AH (1998) Ploughing up the wood-wide web, *Nature* **394:** 431.

Helgason T, Merryweather JW, Denison J, Wilson P, Young JPW, Fitter AH (2002) Selectivity and functional diversity in arbuscular mycorrhizas of co-occurring fungi and plants from a temperate deciduous woodland. *J. Ecol.* **90:** 371–384.

Hetrick BAD, Wilson GWT, Figge DAH (1994) The influence of mycorrhizal symbiosis and fertilizer amendments on establishment of vegetation in heavy metal mine spoil. *Environ. Pollut***. 86**: 171–17.

Hijri I, Sy´korova Z´, Oehl F, Ineichen K, Ma¨der P, Wiemken A, Redecker D (2006) Communities of arbuscular mycorrhizal fungi in arable soils are not necessarily low in diversity. *Mol. Ecol.* **15**: 2277–2289.

Holley JD, Peterson RL (1979) Development of a vesicular-arbuscular mycorrhiza in bean roots. *Canadian Journal of Botany* **57**: 1960-1978.

Hooda PS, Miller A, Edwards AC (2007) The distribution of automobile catalysts-cast platinum, palladium and rhodium in soils adjacent to roads and their uptake by grass. *Sci. Total Environ.* **384**: 384–392.

Howeler RH, Sieverding E, Saif S (1987) Practical aspects of mycorrhizal technology in some tropical crops and pastures. *Plant and Soil* **100**: 249-283.

INVAM: International Culture Collection of (Vesicular) Arbuscular Mycorrhizal Fungi. (Accessed 21/028/2014). West Virginia University. (Updated 13/07/2013) http://invam.wvu.edu/. http://www.Mycoroot.com.

Husband R, Herre EA, Turner SL, Gallery R & Young JPW (2002a) Molecular diversity of arbuscular mycorrhizal fungi and patterns of host association over time and space in a tropical forest. *Mol Ecol.* **11:** 2669–2678.

Husband R, Herre EA, Young JPW (2002b) Temporal variation in the arbuscular mycorrhizal communities colonising seedlings in a tropical forest. *FEMS Microbiol Ecol.* **42:** 131–136.

Ignatius A, Arunbabu V, Neethu J, Ramasamy EV (2014) Rhizofiltration of lead using an aromatic medicinal plant *Plectranthus amboinicus* cultured in a hydroponic nutrient film technique (NFT) system. *Environ. Sci & Pollut Res*. **21** (22): 13007-13016.

Integrated-report (2013) http://drdgold.integrated-report.com/2013/business/business-model).

Izzo A, Agbowo J, Bruns TD (2005) Detection of plot-level changes in ectomycorrhizal communities across years in an old-growth mixed-conifer forest. *New Phytol.* **166**(2): 619-630.

Jacquot, E, van Tuinen D, Gianinazzi S, Gianinazzi-Pearson V (2000) Monitoring species of arbuscular mycorrhizal fungi in planta and in soil by nested PCR: application to the study of the impact of sewage sludge. *Plant Soil* **226**: 179–188.

Jefwa JM, Sinclair R, Maghembe JA (2006) Diversity of glomale mycorrhizal fungi in maize/sesbania intercrops and maize monocrop systems in southern Malawi. *Agroforestry Systems* **67**: 107-114.

Jamal A, Ayub N, Usman M, Khan AG (2002) Arbuscular mycorrhizal fungi enhance zinc and nickel uptake from contaminated soil by soyabean and lentil. *Int. J. Phytoremed* **4**: 205–221.

James TY, Kauff F, Schoch C, Matheny PB, Hofstetter V, Cox C, Celio G, Gueidan C, Fraker E, Miadlikowska J *et al*., (2006) Reconstructing the early evolution of the Fungi using a six gene phylogeny. *Nature* **443**: 818–822.

Jarup L (2003) Hazards of heavy metal contamination. Br. *Med. Bull.* **68**: 167-182.

Johnson NC, Graham JH, Smith FA (1997) Functioning of mycorrhizal associations along the mutualism-parasitism continuum. *New Phytol.* **135**: 575-585.

Joner EJ, Briones R, Leyval C (2000a) Metal-binding capacity of arbuscular mycorrhizal mycelium. *Plant Soil* **226**: 227–234.

Joner EJ, Leyval C (1997) Uptake of 109 Cd by roots and hyphae of a *Glomus mosseae*/*Trifolium subterraneum* mycorrhiza from soil amended with high and low concentrations of cadmium. *New Phytol*. **135**: 353–360.

Joner EJ, Ravnskov S, Jakobsen I (2000b) Arbuscular mycorrhizal phosphate transport under monoxenic conditions using radiolabelled inorganic and organic phosphate. *Biotechnol. Lett.* **22**: 1705–1708.

Jones DL (2006) A complete guide to native orchids of Australia including the Island Territories. Reed New Holland, Sydney.

Kabata-Pendias A (2000) Trace Elements in Soils and Plants; Academic Press, 3rd edn. CRC Press, Boca Raton.

Kabata-Pendias A (2011) *Trace Elements in Soils and Plants*; *Academic Press*, New York, 4th ed.

Kaixuan Bu, James VC, Lorlyn R (2013) Analysis of herbal supplements for selected dietary minerals and trace elements by laser ablation- and solution-based ICPMS, *Microchemical Journal* **106**: 244–249.

Kaldorf M, Kuhn AJ, Schroder WH, Hildebrandt U, Bothe (1999) Selective element deposits in maize colonised by a heavy metal tolerance conferring arbuscular mycorrhizal fungus. *J. Plant Physiol*. **154**: 718–728.

Khade SW (2008) Morpho-taxonomy of synonyms: Glomus rubiforme and Glomus pachycaulis (Glomeromycota). *Anales de Biologia* **30**: 55–59.

Khan AG, Kuek C, Chaudhry TM, Khoo CS, Hayes WJ (2000) Role of plants, mycorrhizae and phytochelators in heavy metal contaminated land remediation. *Chemosphere* **41**: 197–207.

Kjøller R, Rosendahl S (2000) Detection of arbuscular mycorrhizal fungi (Glomales) in roots by nested PCR and SSCP (Single Stranded Conformation Polymorphism). *Plant and Soil* **226**(2): 189-196.

Koide RT, Mosse B, (2004) A history of research on arbuscular mycorrhizal fungi. *Mycorrhiza* **14**: 145-163.

Koomen I, McGrath SP, Giller KE (1990) Mycorrhizal infection of clover is delayed in soils contaminated with heavy metals from past sewage sludge applications. *Soil Biol. Biochem.* **22**: 871–873.

Koske RE, Gemma JN (1989) A modified procedure for staining roots to detect VA mycorrhizas. *Mycological Research* **92**: 486-505.

Koske RE, Gemma JN (1997) Mycorrhizae and succession in plantings of beach grass in sand dunes. *American Journal of Botany* **84**: 118-130.

Kroopnick PM (1994) Vapor abatement cost analysis methodology for calculating life cycle costs for hydrocarbon vapor extracted during soil venting. In *Remediation of Hazardous Waste* (Eds Wise DL and Trantolo DJ), Marcel Dekker, New York, pp. 779–790.

Krüger M, Krüger C, Walker C, Stockinger H, Schüßler A (2012) Phylogenetic reference data for systematics and phylotaxonomy of arbuscular mycorrhizal fungi from phylum to species level. *New Phytol.* **193**: 970–984.

Kubota M, McGonigle TP, Hyakumachi M (2001) Clethra barbinervis, a member of the order Ericales, forms arbuscular mycorrhizae. *Can J. Bot.* **79**: 300–306.

Kubota M, McGonigle TP, Hyakumachi M (2005) Co-occurrence of Arum- and *Paris*-type morphologies of arbuscular mycorrhizae in cucumber and tomato. *Mycorrhiza* **15**: 73-77.

Kumar PBAN, Dushenkov V, Motto H, Raskin I (1995) Phytoextraction: the use of plants to remove heavy metals from soils. *Environ Sci Technol*. **29**: 1232–1238.

Landberg T and Greger M (1997) Use of willow with high cadmium accumulation properties in soil purification. In: Proceedings of the 3rd international conference on the biogeochemistry of trace elements, 15–20 May 1995, Paris, (in press).

Lanfranco L, Bolchi A, Ros EC, Ottonello S and Bonfante P (2002) Differential expression of a metallothionein gene during the presymbiotic versus the symbiotic phase of an arbuscular mycorrhizal fungus. *Plant Physiol.* **130**: 58–67.

Lanfranco L, Young JPW (2012) Genetic and genomic glimpses of the elusive arbuscular mycorrhizal fungi, Current *Opinion in Plant Biology* **15**: 454–461.

Larsen EH, Lobinski R, Burger-Meÿer K, Hansen M, Ruzik R, Mazurowska L, Rasmussen PH, Sloth JJ, Scholten O, Kik C (2006) Uptake and speciation of selenium in garlic cultivated in soil amended with symbiotic fungi (mycorrhiza) and selenate, *Anal. Bioanal. Chem*. **386** (6): 1098- 1108.

Lee J, Lee S, Young JPW (2008) Improved PCR primers for the detection and identification of arbuscular mycorrhizal fungi. *FEMS Microbiology Ecology* **65**: 339–349.

Lee J, Young JPW (2009) The mitochondrial genome sequence of the arbuscular mycorrhizal fungus *Glomus intraradices* isolate 494 and implications for the phylogenetic placement of *Glomus*. *New Phytol.* **183**: 200–211.

Legge GJF, McKenzie CD, Mazzolini AP (1979) *J. Microsc.* **117** :185.

Leyval C, Singh BR, Joner EJ (1995) Occurrence and infectivity of arbuscular mycorrhizal fungi in some Norwegian soils influenced by heavy metals and soil properties. *Water Air Soil Pollut*. **84**: 203–216.

Leyval C, Turnau K, Haselwandter K (1997) Effect of heavy metal pollution on mycorrhizal colonization and function: physiological, ecological and applied aspects. *Mycorrhiza* **7**: 139–153.

Liebenberg WR (1957) A mineralogical approach to the development of the uranium extraction process practiced on the Witwatersrand. In: Uranium in

South Africa 1946-1956, Vol 1, The Associated Scientific and Technical Societies of South Africa, pp. 219 -274. (Chapter 3 Baseline Description).

Liu Y, Leigh JW, Brinkmann H, Cushion MT, Rodriguez-Ezpeleta N, Philippe H, Lang BF. (2009) Phylogenomic analyses support the monophyly of Taphrinomycotina, including Schizosaccharomyces fission yeasts. *Molecular Biology and Evolution* **26**: 27–34.

Lloyd-Macgilp SA, Chambers SM, Dodd JC, Fitter AH, Walker C, Young J PW (1996) Diversity of the Ribosomal Internal Transcribed Spacers Within and Among Isolates of *Glomus mosseae* and Related Mycorrhizal Fungi *New Phytol.* **133**(1): 103-111.

Lone MI, He Z, Stoffella PJ, Yang X (2008) Phytoremediation of heavy metal polluted soils and water: Progresses and perspectives. *J. Zhejiang Univ. Sci.*, **9**: 210-220.

MADEP (Massachusetts Department of Environmental Protection Publication) (1993). 310 CMR 40.0000: *Massachusetts Contingency Plan (MCP).* Boston.

Magurran AE (2004) *Meausuring Biological Diversity*. Blackwell.

Malcova R, Vosátka M, Gryndler M (2003) Effects of inoculation with *Glomus intraradices* on lead uptake by *Zea mays* L. and *Agrostis capillaris L. Appl. Soil Ecol*. **23**: 55–67.

Mando PA, Przybylowicz WJ (2009) Particle-induced X-ray Emission (PIXE), *Encyclopedia of Analytical Chemistry*, Meyers RA (Ed.), pp 1 -147.

Manian S, Sreenivasaprasad S, Mills PR (2001) (DNA) extraction method for PCR in mycorrhizal fungi. *Applied Microbiology* **33**: 307-310.

Markert B (1992) Presence and significance of naturally occurring chemical elements of the periodic system in the plant organism and consequences for

future investigations on inorganic environmental chemistry in ecosystems. *Vegetation* **103**:1.

Marschner H, Romheld V (1995) Strategies of plants for acquisition of iron. *Plant Soil* **165**: 262–274.

Marx DH, Altman JD (1979) *Pisolithus tinctorius* ectomycorrhiza improve survival and growth of pine seedlings on acid coal spoil in Kentucky and Virginia. In *Mycorrhizal Manual*, Springer, Berlin, pp. 387–399.

Mason PA, Usoko MO, Last FT, (1992) Short-term changes in vesicular–arbuscular mycorrhizal spore population in Terminalia plantations in Cameroon. In: Read DJ, Lewis DH, Fitter AH, Alexander IJ, (Eds.), Mycorrhizas in ecosystems. C.A.B International, Oxon, UK, pp. 261–267.

McCarthy TS, Rubidge B (2005) *The Story of Earth and Life: A Southern African Perspective on a 4.6 Billion-Year Journey*, Struik Publishers, Cape Town, pp. 333.

McCormick MK, Whigham DF, O'Neill J (2004) Mycorrhizal diversity in photosynthetic terrestrial orchids, *New Phytol.* **163**: 425–438.

McGee PA (1986) Mycorrhizal associations of plant species in a semi-arid community. *Aus J Bot*. **34**: 585–593.

McGlasshan ND (2004) Contrasts of cancer rates among black gold miners from Transkei and Lesotho. *South African Journal of Science* **100**: 491 – 497.

Mcgonigle TP, Miller MH, Evans DG, Fairchild GL, Swan JA (1990b) A new method which gives an objective measure of colonization of roots by vesicular-arbuscular mycorrhizal fungi. *New Phytol.* **115**: 495 – 501.

Medina A, Probanza A, Gutierrez Mañero FJ,Azcón R (2003) Interactions of arbuscular-mycorrhizal fungi and *Bacillus* strains and their effects on plant growth, microbial rhizosphere activity (thymidine and leucine incorporation) and fungal biomass (ergosterol and chitin). *Appl. Soil Ecol*. **22**: 15–28.

Meier S, Alvear M, Borie F, Aguilera P, Ginocchio R, Cornejo P (2012) Influence of copper on root exudate patterns in some metallophytes and agricultural plants. *Ecotox. Environ. Saf.* **75**: 8–15.

Meier S, Borie F, Curaqueoa G, Bolan N, Cornejo P (2011). Effects of arbuscular mycorrhizal inoculation on metallophyte and agriculture plants growing at increasing copper levels. *Applied Soil Ecology* pp.1-8.

Mello A, Nosenzo C., Meotto F, Bonfante P (1996) Rapid typing of truffle mycorrhizal roots by PCR amplification of the ribosomal DNA spacers, *Mycorrhiza* **6**: 417–421.

Mendez MO, Maier RM (2008b) Phytoremediation of mine tailings in temperate and arid environments. *Rev Environ Sci Biotechnol*. **7**: 47–59.

Mesjasz-Przybylowicz J, Przybylowicz WJ (2002) Micro-PIXE in plant sciences: Present status and perspectives. *Nucl. Instrum. Methods Phys. Res. Sect. B.* **189**: 470–481.

Meyer AH, Botha A, Valentine AJ, Archer E, Louw PJE (2005) The occurrence and infectivity of arbuscular mycorrhizal fungi in inoculated and uninoculated rhizosphere soils of two-year-old commercial grapevines. *S. Afr. J. Enol. Vitic.* **26**: 90–94.

Miller RM, Jastrow JD (2000) Mycorrhizal fungi influence soil structure. In: Kapulnik Y, Douds DD Jr, eds. Arbuscular mycorrhizas: physiology and function. Dordrecht (The Netherlands): Kluwer Academic Publishers. pp. 3–18.

Mining Weekly (2015) Vested interests, lack of understanding hamper establishment of S African PGMs exchange, 28 March 2015.

Morton JB (1986) Three new species of Acaulospora (Endogonaceae) from high-aluminium, low pH soils in West Virginia. *Mycologia* **78**: 641–648.

Morton JB (1988) Taxonomy of VA mycorrhizal fungi: Classification, nomenclature, and identification. *Mycotaxon* **32:** 267-324.

Morton JB (1995) Taxonomic and phylogenetic divergence among five *Scutellospora* species based on comparative developmental sequences, *Mycologia* **87**; 127–137.

Morton JB, Bentivenga SP, Wheeler WW (1993) Germ plasma in the International Collection of Arbuscular and Vesicular-arbuscular mycorrhizal Fungi (INVAM) and procedures for culture development, documentation and storage. *Mycotaxon* **48**: 491-528.

Morton JB, Redecker D (2001) Two new families of *Glomales*, *Archaeosporaceae* and *Paraglomaceae*, with two new genera *Archaeospora* and *Paraglomus*, based on concordant molecular and morphological characters. *Mycologia* **93**: 181-195.

Mucina L, Rutherford MC (2006) the Vegetation of South Africa, Lesotho and Swaziland, 386, 400, 405, 463.

Mukhopadhyay S. Maiti SK (2010) Phytoremediation of metal mine waste, *applied ecology and environmental research* **8**(3): 207-222.

Mulligan CN, Yong RN, Gibbs BF (2001) Remediation technologies for metal-contaminated soils and groundwater: an evaluation. *Engineering Geology* **60** (1–4): 93–207.

Nielsen KB, Kjøller R, Olsson PA, Schweiger PF, Andersen FO, Rosendahl S (2004) Colonisation and molecular diversity of arbuscular mycorrhizal fungi in the aquatic plants Littorella uniflora and Lobelia dortmana in southern Sweden. *Mycol. Res.* **108**: 616–625.

Nyriagu OJ (1988) A silent epidemic of environmental metal poisoning? *Environ. Pollut.* **50**: 139-161.

Nzengung VA, Wolfe LN, Rennels D, McCutcheon SC (1999) Use of aquatic plants and algae for decontamination of waters polluted with chlorinated alkanes. *Intern. J. Phytorem.* **1**(3): 203 – 226.

Odiyo JO, Bapela HM, Mugwedi R, Chimuka L (2005) Metals in environmental media: A study of trace and platinum group metals in Thohoyandou, South Africa, *Water SA* **31**(4): 581-587.

Oehl F, Sieverding E, Ineichen K, Mäder P, Wiemken A, Boller T (2009) Distinct sporulation dynamics of arbuscular mycorrhizal fungal communities from different agroecosystems in long-term microcosms. *Agriculture, Ecosystems & Environment* **134**: 257 ‑ 68.

Olsson PA, Francis R, Read DJ, Söderström B (1998) Growth of arbuscular mycorrhizal mycelium in calcareous dune sand and its interaction with other soil microorganisms as estimated by measurement of specific fatty acids. *Plant Soil* **201**: 9–16.

Öpik M, Vanatoa A, Vanatoa E, Moora M, Davison J, Kalwij JM, Reier U & Zobel M (2010) The online database Maarj*AM* reveals global and ecosystemic distribution patterns in arbuscular mycorrhizal fungi (Glomeromycota). *New Phytol.* **188**: 223–241.

Orlowska E, Orlowski D, Masjasz-Przbylowicz J, Turnau K (2011) 'Role of Mycorrhizal Colonisation in Plant Establishment on an Alkaline Gold Mine Tailing', *International Journal of Phytoremediation* **13**(2): 185- 205.

Orlowska E, Przybylowicz WJ, Orlowski D, Mongwaketsi NP, Turnau K, Mesjasz-Przybylowicz J (2013) Mycorrhizal colonisation affects the elemental distribution in roots of Ni-hyperaccumulator *Berkheya coddii* Roessler *Environmental Pollution* **175**: 100 – 109.

Pallon J, Wallander H, Hammer E, Arteaga Marrero N, Auzelyte V, Elfman M, Kristiansson P, Nilsson C, Olsson PA, Wegden M (2007) Symbiotic fungi

that are essential for plant nutrient uptake investigated with NMP. *Nucl. Instrum. Methods Phys. Res. Sect. B* **260**: 149-152.

Parker R (1994) Environmental Restoration Technologies. *EMIAA Yearbook*, pp. 169–171.

Pawlowska TB, Blaszkowski J, Rühling A (1996) The mycorrhizal status of plants colonizing a calamine spoil mound in southern Poland. *Mycorrhiza* **6**: 499–505.

Perotto1 S, Girlanda M, Martino E (2002) Ericoid mycorrhizal fungi: some new perspectives on old acquaintances. *Plant and Soil* **244**: 41–53.

Pfleger FL, Linderman RG (ed.) 1992. Mycorrhize and Plant Health. pp. 1 – 344. American Phytopathological Society Press, St. Paul, Minnesota, USA.

Pfleger FL, Stewart EL, Noyd RK (1994) Role of VAM fungi in mine land revegetation. In *Mycorrhizae and Plant Health* (eds Pfleger FL and Linderman RG), *The American Phytopathological Society*, MN, USA, pp. 47–82.

Prasad MNV, Freitas HM (2003) Metal hyperaccumulation in plants – Biodiversity prospecting for phytoremediation technology, *Electronic Journal of Biotechnology* **6**(3): 285-321.

Prozesky VM, Przybylowicz WJ, van Achterbergh E, Churms CL, Pineda CA, Springhorn KA, Pilcher JV, Ryan CG, Kritzinger J, Schmitt H, Swart T (1995) The NAC nuclear microprobe facility. *Nucl. Instrum. Methods Phys. Res. Sect. B* **104**: 36–42.

Przybylowicz WJ, Mesjasz-Przybylowicz J, Migula P, Nakonieczny M, Augustyniak M, Tarnawska M, Turnau K, Ryszka P, Orłowska E, Zubek Sz. and Głowacka E (2005) Micro-PIXE in ecophysiology†, *X-ray Spectrom.* **34**: 285–289.

Ram N, Patrick SAH, Brown H (1997) Techniques for boron determination and their application to the analysis of plant and soil samples, *Plant and Soil* **193:** 15–33.

Raskin I; Kumar PBAN, Dushenkov S, Salt DE (1994) Bioconcentration of heavy metals by plants. *Current Opinion in Biotechnology* **5**(3): 285-290.

Read DJ (1998) Mycorrhiza – the state of the art. In: *Mycorrhiza: structure, function, molecular biology and biotechnology.* (Eds. A Varma & B Hock). Springer-Verlag, Berlin, Germany.

Read DJ, Koucheki HK, Hodgson T (1976) Vesicular-arbuscular mycorrhizae in natural vegetation ecosystems. *New Phytol.* **77**: 641–653.

Redecker D, Hijri I, Wiemken A (2003) Molecular identification of arbuscular mycorrhizal fungi in roots: perspectives and problems. *Folia Geobotanica* **38**: 113-124.

Redecker D, Kodner R, Graham LE (2000) Glomalean fungi from the Ordovician. *Science* **289**: 1920-1921.

Redecker D, Raab P (2006) Phylogeny of the Glomeromycota (arbuscular mycorrhizal fungi): recent developments and new gene markers. *Mycologia* **98**(6): 885-895.

Redecker D, Schüßler A, Stockinger H, Stürmer S, Morton J, Walker C (2013) An evidence-based consensus for the classification of arbuscular mycorrhizal fungi (Glomeromycota). *Mycorrhiza* **23**: 515–531.

Redecker, D (2000) Specific PCR primers to identify arbuscular mycorrhizal fungi within colonised roots. *Mycorrhiza* **10**: 73-80.

Reilly A, and Reilly C (1973) Copper-induced chlorosis in *Becium homblei* (De Wild) Duvig. et Plancke, *Plant Soil* **38**: 671,

Renker C, Weißhuhn K, Kellner H, Buscot F (2006) Rationalizing molecular analysis of field-collected roots for assessing diversity of arbuscular mycorrhizal fungi: to pool, or not to pool, that is the question. *Mycorrhiza* **16**: 525– 531.

Rex HG, Allan K, Human C, Sutton M, Geel C, Grond E, Weiersbye IM, Kotze J, van der Merwe M, Labuschagne P (2009) AngloGold Ashanti Ltd, West Wits Operations, Environmental Management Programme, WSP Project Number, 1919ES, WSP File reference, 1919ES/ EMP, Chapter 1, WW EMPR 2012 pp. (i) – 3.

Rahmanian M, Khodaverdiloo H, Rezaee Danesh Y, Rasouli Sadaghiani MH (2011) Effects of heavy metal resistant soil microbes inoculation and soil cd concentration on growth and metal uptake of millet, couch grass and alfalfa. *Afr. J. Microbiol. Res.* **5**(4): 403-410.

Richaud R, Lachas H, Healey AE, Reed GP, Haines J, Jarvis KE, Herod AA, Dugwell DR, Kandiyoti R (2000) Trace element analysis of gasification plant samples by ICP-MS: validation by comparison of results from two laboratories, *Fuel* **79**: 1077-1087.

Rillig MC, Steinberg PD (2002) Glomalin production by an arbuscular mycorrhizal fungus: a mechanism of habitat modification. *Soil Biol. Biochem*. **34**: 1371–1374.

Robb LJ, Robb VM (1998) Gold in the Witwatersrand basin. In: Wilson MGC., and Anhaeusser CR (eds.), *The Mineral Resources of South Africa*, Handbook 16, Council for Geoscience, pp. 294–349.

Robinson BH, Green SR, Chancerel, B, Mills, TM, Clothier BE (2007) Poplar for the phytomanagement of boron contaminated sites. *Environ. Pollut*. **150**: 225–233.

Roman M De, Claveria V and De Miguel Am (2005) A revision of the descriptions of ectomycorrhizas published since 1961, *Mycol. Res.* **109** (10): 1063–1104.

Rosendahl S, Stukenbrock EH (2004) Community structure of arbuscular mycorrhizal fungi in undisturbed vegetation revealed by analyses of LSU rDNA sequences. *Molecular Ecology* **13**: 3179–3186.

Ryan C (2000) Quantitative trace element imaging using PIXE and the nuclear microprobe. *International Journal of Imaging Systems and Technology* **11**: 219-230.

Ryan C, Cousens D, Sie S, Griffin W, Suter G, Clayton E (1990a) Quantitative PIXE micro analysis of geological material using the CSIRO proton microprobe. *Nuclear Instruments and Methods in Physics Research B* **47**: 55-71.

Ryan C, Jamieson D (1993) Dynamic analysis: on-line quantitative PIXE microanalysis and its use in overlap-resolved elemental mapping. *Nuclear Instruments and Methods in Physics Research B* **77**: 203-214.

Ryan C, Jamieson D, Churms C, Pilcher J (1995) A new method for on-line true-elemental imaging using PIXE and the proton microprobe. *Nuclear Instruments and Methods in Physics Research B* **104**: 157-165.

Ryan CG, Cousens DR, Sie SH, Griffin WL (1990b) Quantitative Analysis of PIXE spectra in geoscience applications. *Nuclear Instruments and Methods in Physics Research B* **49**: 271-276.

Salt DE, Baxter I, Lahner B (2008) Ionomics and the study of the plant ionome. *Annual Review of Plant Biology* **59**: 709–733.

Salt DE, Blaylock M, Kumar NPBA, Dushenkov V, Ensley BD, Chet I, Raskin I (1995) Phytoremediation: a novel strategy for the removal of toxic metals from the environment using plants. *Biotechnology* **13**: 468–474.

Salt DE, Smith RD, Raskin I (1998) Phytoremediation. *Ann. Rev. Plant Mol. Biol.* **49**: 643-668.

Sambrook J, Fritsch EF, Maniatis T (1989) *Molecular Cloning: a Laboratory Manual*, 2nd edn. Cold Spring Harbor, NY: Cold Spring Harbor Laboratory.

Sanders IR (2002) Specificity in the arbuscular mycorrhizal symbiosis. In: van der Heijden MGA, Sanders IE (Eds) Mycorrhizal ecology. *Springer, Heidelberg*, pp. 415–437.

Saito M, Marumoto T (2002) Inoculation with arbuscular mycorrhizal fungi: The status quo in Japan and the future prospects. *Plant Soil* **244**: 273–279.

Saito M, Oba H, Kojima T (2011) Effect of nitrogen on the sporulation of arbuscular mycorrhizal fungi colonizing several gramineous plant species, *Soil Science and Plant Nutrition* **57** (1): 29-34.

Saxton KE, Rawls WJ (2006) Soil Water Characteristic Estimates by Texture and Organic Matter for Hydrologic Solutions. *Soil Sci. Soc. Am. J.* **70**: 1569–1578.

Schenck NC, Péres Y (1990) *Manual for the identification of VA mycorrhizal fungi*, 3rd edition. Synergistic Publications, Gainesville, Florida, USA. pp. 241.

Schultz PA, Bever JD, Morton J (1999) Acaulospora colossica sp. nov. from an old field in North Carolina and morphological comparisons with similar species, A. laevis and A. koskei. *Mycologia* **91**: 676-683.

Schulze RE (1997) South African Atlas of Agrohydrology and Climatology. WRC Report TT82/96. Pretoria: Water Research Commission.

Schüßler A, Krüger M, Walker C (2011) Revealing natural relationships among arbuscular mycorrhizal fungi: culture line BEG47 represents *Diversispora epigaea*, not *Glomus versiforme.* PLoS ONE 6: e23333.

Schüßler A, Schwarzott D, Walker C (2001) A new fungal phylum, the *Glomeromycota*: phylogeny and evolution. *Mycol. Res.* **105** (12): 1413-1421.

Schüßler A, Walker C (2010) The *Glomeromycota*: a species list with new families and genera. Published by A. Schüßler & C. Walker, Gloucester UK, 2010. online available at www.amf-phylogeny.com.

Schwarzott D, Walker C, Schüßler A (2001) *Glomus*, the largest genus of the arbuscular mycorrhizal fungi (Glomales), is non-monophyletic. *Molecular Phylogenetics and Evolution* **21**(2): 190-197.

Sharmah D, Jha DK, Pandey RR (2010) *Molecular* Approaches in Arbuscular Mycorrhizal Research: A Review, *J. of Phytol* **2** (7): 75-90.

Shetty KG, Hetrick BAD, Figge DAH, Schwab AP (1994) Effects of mycorrhizae and other soil microbes on revegetation of heavy metal contaminated mine spoil. *Environ Pollut.* **86**: 181 – 188.

Sieverding E, Oehl F (2006) Revision of Entrophospora and description of Kuklospora and Intraspora, two new genera in the arbuscular mycorrhizal Glomeromycetes. *Journal of Applied Botany and Food Quality* **80**: 69 – 81.

Smith FA, Jakobeson I, Smith SE (2000) Spatial differences in fungi in symbiosis with *medicago truncatula*. *New Phytol.* **147**: 357- 366.

Smith SE, Dickson S (1991) Quantification of active vesicular-arbuscular mycorrhizal infection using image analysis and other techniques. *Australian Journal of Plant Physiology* **18**: 637-648.

Smith SE, Read DJ (1997) *Mycorrhizal symbiosis* 2nd Edn, Academic Press, Horcourt Bruce & Company Publishers. London, pp. 1-3. Smith MR, Charvat I, Jacobson RL (1998) Arbuscular mycorrhizae promote establishment of prairie species in a tallgrass prairie restoration. *Canadian Journal of Botany* **76**: 1947–1954.

Smith SE, Read DJ (2008) *Mycorrhizal symbiosis.* 3rd ed. Academic Press, *San Diego.* pp. 11-187.

Smith SE, Smith FA (2011) Roles of arbuscular mycorrhizas in plant nutrition and growth: new paradigms from cellular to ecosystem scales. *Annu Rev Plant Biol.* **62**: 227-250.

Sommers LE, Nelson DW (1972) Determination of total phosphorus in soils: a rapid perchloric acid digestion procedure. *Proc. Soil Sci. Soc. Am.,* **36** :902-904.

Song W-Y Won-Yong Song[1], Sohn EJ, Martinoia E, Lee YJ, Yang YY, Jasinski M, Forestier C Hwang Inwhan, Lee Y (2003) Engineering tolerance and accumulation of lead and cadmium in transgenic plants. *Nature Biotechnology* **21**(8): 914-919.

South African Weather Service (2006) Climate statistics for the period 1961 to 1990. Climate of South Africa, WB42.

Spruyt A, Buck MT, Mia A, Straker CJ (2014) Arbuscular mycorrhiza (AM) status of rehabilitation plants of mine wastes in South Africa and determination of AM fungal diversity by analysis of the small subunit rRNA gene sequences, *South African Journal of Botany* **94**: 31–237.

Steinberg PD, Rillig MC (2003) Differential decomposition of arbuscular mycorrhizal fungal hyphae and glomalin. *Soil Biol. Biochem.* **35**: 191–194.

Straker CJ, Freeman AJ, Witkowski ETF, Weiersbye IM (2008) Arbuscular mycorrhiza status of gold and uranium tailings and surrounding soils of South Africa's deep level gold mines. II. Infectivity, *South African Journal of Botany* **74**: 197–207.

Straker CJ, Hilditch AJ, Rey MEC (2010) Arbuscular mycorrhizal fungi associated with cassava (*Manihot esculenta* Crantz) in South Africa. *South African Journal of Botany* **76**: 102-111.

Straker CJ, Weiersbye IM, Witkowski ETF (2007) Arbuscular mycorrhiza status of gold and uranium tailings and surrounding soils of South Africa's deep level gold mines: I. Root colonization and spore levels. *South African Journal of Botany* **73**(2): 218-225.

Stürmer SL, Morton JB (1997) Developmental patterns defining morphological characters in spores of species in Glomus (Glomales, Zygomycetes). *Mycologia* **89**:72–81.

Stürmer SL, Morton JB (1999a) Taxonomic reinterpretation of morphological characters in Acaulosporaceae based on developmental patterns. *Mycologia* **91:** 849–857.

Stürmer SL, Morton JB (1999b) *Scutellospora rubra*, a new arbuscular mycorrhizal species from Brazil. *Mycol Res.* **103:** 949–954.

Stürmer SL (2012) A history of the taxonomy and systematics of arbuscular mycorrhizal fungi belonging to the phylum Glomeromycota. *Mycorrhiza* **22**: 247–258.

Stutz JC, Copeman R, Martin CA, Morton JB (2000) Patterns of species composition and distribution of arbuscular mycorrhizal fungi in arid regions of southwestern North America and Namibia, Africa. *Canadian Journal of Botany* **78**: 237–245.

Stutz JC, Morton JB (1996) Successive pot cultures reveal high species richness of arbuscular endomycorrhizal fungi in arid ecosystems. *Canadian Journal of Botany* **74**: 1883-1889.

Suruchi and Pankaj Khanna (2011) Assessment of Heavy Metal Contamination in Different Vegetables Grown in and Around Urban Areas. *Research Journal of Environmental Toxicology* **5**: 162-179.

Sutton MW (2012) Use of remote sensing and GIS in a risk assessment of gold and uranium mine residue deposits and identification of vulnerable land use, MSc Thesis, pp. 56.

Sylvia DM, Williams SE (1992) Vesicular–arbuscular mycorrhizae and environmental stresses. In: Bethlenfalvay GJ and Linderman RG) (eds), *Mycorrhizae in Sustainable Agriculture* ASA No. 54, Madison, USA, pp. 101–124.

Tabachnick BG, Fidell LS (2001) *Using multivariate statistics* (4th ed.). Needham Heights, MA: Allyn & Bacon (from Appendix 2)

Tao G, Liu ZY, Hyde KD, Lui XZ, Yu ZN (2008) Whole rDNA analysis reveals novel and endophytic fungi in *Bletilla ochracea* (Orchidaceae). Fungal Diversity **33**: 101-122.

Taylor S, McLennan S (1981) The Composition And Evolution Of The Continental Crust: Rare Earth Element Evidence From Sedimentary Rocks. *Philosophical Transactions of the Royal Society of London* **301A**: 381 - 399.

Taylor SR (1964) Abundance of Chemical Elements in the Continental Crust: A New Table. *Geochimica et Cosmochimica Acta* **28**: 1273 - 1286.

The Non-Affiliated Soil Analyses Work Committee, (1990) Handbook of standard soil testing methods for advisory purposes. Soil Sci. Soc. S.A., P.O. Box 30030, Sunnyside, Pretoria.

Timonen S, Marschner P (2005) Mycorrhizosphere concept. *In* Microbial activity in the rhizosphere. *Edited by* K.G. Mukerji, C. Manoharachary and J. Singh. Springer Verlag, Berlin.

Toro M, Azcon R Barea J (1997) Improvement of arbuscular mycorrhizae development by inoculation of soil with phosphate-solubilizing rhizobacteria to improve rock phosphate bioavailability (32P) and nutrient cycling. *Applied and Environmental Microbiology* 4408 - 4412.

Trevor TG (1920) Nickel. Notes on the occurrence in the Barberton district. *South African Journal of Industries* **3**: 532-533.

Tullio M, Pierandrei F, Salerno A, Rea E (2003) Tolerance to cadmium of vesicular arbuscular mycorrhizae spores isolated from a cadmium-polluted and unpolluted soil. *Biol. Fertil. Soils* **37**: 211–214.

Turnau K, Kottke I, Oberwinkler F (1993) *New Phytol.* **123**: 313.

Turnau K, Mesjasz-Przybylowicz J (2003) Arbuscular mycorrhiza of *Berkheya coddii* and other Ni-hyperaccumulating members of Asteraceae from ultramafic soils in South Africa. *Mycorrhiza* **13**: 185–190.

Turnau K, Miszalski Z, Trouvelot, A, Bonfante P, Gianinazzi S (1996) *Oxalis acetosella* as a monitoring plant on highly polluted soils. In: Azc_n-Aguilar C, Barea JM (Eds) Mycorrhizas in integrated systems from genes to plant development. European Commission, Brussels, pp. 483–486.

Turnau K, Ryszka K, Wojtczak G (2010) Metal tolerant mycorrhizal plants: a review from the perspective on industrial waste in temperate regions. In: Koltai, H., Kapulnik, Y. (Eds.), Arbuscular Mycorrhizas: Physiology and Function. Springer Science þ Business Media B.V, Heidelberg, Germany, pp. 257-276.

Urcelay C, Diaz S, (2003) The mycorrhizal dependence of subordintes determines the effects of arbuscular mycorrhizal fungi on plant diversity, – *Ecology Letters* **6**: 388-391.

Vallino M, Massa N, Lumini E, Bianciotto V, Berta G, Bonfante P (2006) Assessment of arbuscular mycorrhizal fungal diversity in roots of *Solidago gigantea* growing on a polluted soil in northern Italy. Environ. *Microbiol.* **8**: 971-983.

van Achterbergh E, Ryan CG, Gurney JJ, le Roex AP (1995) PIXE profiling, imaging and analysis using the NAC proton microprobe: Unraveling mantle eclogites. *Nuclear Instruments and Methods in Physics Research Section B* **104**: 415-426.

van Tichelen KK, Colpaert JV, Van Assche JA (1996) Development of arbuscular mycorrhizas in a heavy metal-contaminated soil amended with a metal immobilizing substance. In: Azcon-Aguilar C, Barea JM (eds) Mycorrhizas in integrated systems: from genes to plant development. European Commission, EUR 16728, Luxembourg, pp. 479–482.

van Tuinen D, Trouvelot S, Hijri M, Gianinazzi-Pearson V (1998) Visualization of ribosomal DNA loci in spore interphasic nuclei of glomalean fungi by fluorescence in-situ hybridization. *Mycorrhiza* **8**: 203–206.

Vandenkoornhuyse P, Husband R, Daniell TJ, Watson IJ, Duck JM, Fitter AH, Young JPW (2002) Arbuscular mycorrhizal community composition associated with two plant species in a grassland ecosystem. *Molecular Ecology* **11**: 1555-1564.

Vandenkoornhuyse P, Ridgway KP, Watson IJ, Fitter AH and Young JPW (2003) Co-existing grass species have distinctive arbuscular mycorrhizal communities. *Molecular Ecology* **12**: 3085–3095.

Vestbery M (1995) Occurrence of some Glomalesin Finland. *Mycorrhiza* **5**: 329- 336.

Vivas A, Marulanda A, Gómez M, Barea JM, Azcón R (2003) Physiological characteristics (SDH and ALP activities) of arbuscular mycorrhizal colonization as affected by *Bacillus thuringiensis* inoculation under two phosphorus levels. *Soil Biol. Biochem.* **35**: 987–996.

Vogel-Mikuš K, Arčon I, Kodre A (2010) Complexation of cadmium in seeds and vegetative tissues of the cadmium hyperaccumulator Thlaspi praecox as studied by X-ray absorption spectroscopy, *Plant Soil.*

Vogel-Mikuš K, Pongrac P, Kump P, Necěmer M, Regvar M (2006) Colonisation of a Zn, Cd and Pb hyperaccumulator *Thlaspi praecox* Wulfen with indigenous arbuscular mycorrhizal fungal mixture induces changes in heavy metal and nutrient uptake, *Environmental Pollution* **139**: 362-371.

Waaland ME, Allen EB (1987) Relationships between VA mycorrhizal fungi and plant cover following surface mining in Wyoming. *J. Range Manage* **40**: 271–276.

Walker C (1983) Taxonomic concepts in the Endogonaceae: spore wall characteristics in species descriptions. *Mycotaxon* **18**: 443-455.

Walker C, Blaszkowski J, Schüßler A (2004) *Gerdemannia* gen. nov., a genus separated from *Glomus*, and *Gerdemanniaceae fam*. nov., a new family in the Glomeromycota. *Mycological Research* **108**: 707-718.

Walker C, Cuenca G, Sánchez F. 1998. Scutellospora spinosissima sp. nov. a newly described Glomalean fungus from low nutrient communities in Venezuela. *Annals of Botany* **82**: 721–725.

Walker C, Koske RE (1987) Taxonomic concepts in the Endogonaceae. IV. *Glomus fasciculatum* redescribed. *Mycotaxon* **30**: 253-262.

Walker C, Mize CW, McNabb Jr HS (1982) Populations of endogonaceous fungi at two locations in central Iowa. *Canadian Journal of Botany* **60**: 2518-2529.

Walker C, Pfeiffer CM, Bloss HE (1986) *Acaulospora delicate* sp. Nov. – An endomycorhizal fungus from Arizona. *Mycotaxon*. **XXV/25** (2): 621-628.

Walker C, Vestberg M (1998) Synonymy Amongst the Arbuscular Mycorrhizal Fungi: *Claroideoglomus claroideum, G. maculosum, G. multisubstenum* and *G. stulosum*. *Annals of Botany* **82**: 601-624.

Wang CL, JSM Tschen, and CL Wang (1997) Factors on the spore germination of arbuscular mycorrhizal fungi, *Glomus* spp. *Fungal Science* **12**: 3–4.

Wang FY, Tong RJ, Shi ZY, Xu XF, He XH (2011) Inoculations with Arbuscular Mycorrhizal Fungi Increase Vegetable Yields and Decrease

Phoxim Concentrations in Carrot and Green Onion and Their Soils. *PLoS ONE* **6** (2): e16949. doi:10.1371/journal.pone.0016949.

Ward JHW (1999) The metallogeny of the Barberton greenstone belt, South Africa and Swaziland. Memoir, *Council for Geosciences* **86**: 108.

Weiersbye IM, Witkowski EM (1998) Plant ecology and Conservation, Series 8, AngloGold Ltd.

Weiersbye IM, Cukrowska EM (2007) Phytoremediation at the Lonmin Marikana Base Metal Refinery: Pollution control & carbon sequestration measures. (unpublished data) page (1- 75).

Weiersbye IM, Straker CJ, Przybylowicz WJ (1999) Micro-PIXE mapping of elemental distribution in arbuscular mycorrhizal roots of the grass, *Cynodon dactylon*, from gold and uranium mine tailings. *Nuclear Instruments and Methods in Physics Research Section B: Beam Interactions with Materials and Atoms* **158**: 335–343.

Weiersbye IM, Witkowski ETF (2003) Acid rock drainage (ARD) from gold tailings dams on the Witwatersrand Basin impacts on tree seed fate, inorganic content and seedling morphology. In: D. Armstrong, A.B. de Villiers, R.L.P. Kleinmann, T.S. McCarthy and P.J. Norton (eds.), *Mine Water and the Environment, Proceedings of the 8th International Mine Water Association (IMWA) Congress*, Johannesburg, pp. 311–328.

Weiersbye IM, Witkowski ETF, Reichardt M (2006) Floristic composition of uranium tailings dams, and adjacent polluted areas on South Africa's deep level mines. *Bothalia* **36**: 101–127.

West Wits Mining, (2008) Geology of Leases. Available at: www.westwitsmining.com/projects/geology (As accessed on 23 September 2008).

White TJ, Bruns T, Lee S, Taylor J (1990) Amplification and direct sequencing of fungal ribosomal RNA genes for phylogenetics. In: Innis MA,

Gelfand DH, Shinsky JJ, White TJ, (eds). *PCR Protocols: A Guide to Methods and Applications*, Academic Press, San Diego. pp. 315–322.

Whitfield L, Richards AJ, Rimmer DL (2004) Relationships between soil heavy metal concentration and mycorrhizal colonization in Thymus polytrichus in northern England. *Mycorrhiza* **14**: 55–62.

Whitten DGA, Brooks JRV (1972) The Penguin dictionary of geology. Penguin Books, Harmondsworth, UK.

Williams GM (1998) Integrated studies into ground water pollution by hazardous wastes. In *Land Disposal of Hazardous Waste, Engineering and Environmental Issues* (eds Gronow JR, Schofield AN and Jain RK, Horwood Ltd, *Chichester*, UK.

Wilson GWT, Hetrick BAD Schwab AP (1991) Reclamation effects on mycorrhizae and productive capacity of flue gas desulfurization sludge. *J. Environ. Qual*. **20**: 777–783.

Wirsel SGR **(**2004) Homogenous stands of a wetland grass harbour diverse consortia of arbuscular mycorrhizal fungi. *FEMS Microbiol*. *Ecol.* **48**: 129–138.

Wislocka M, Krawczyk J, Klink A, Morrison L (2006) Bioaccumulation of Heavy Metals by selected Plant Species from Uranium Mining Dumps in the Sudety Mts, Poland, *Polish J. of Environ. Stud.* **15**(5): 811 -818.

Witkowski ETF, Weiersbye IM (1998) Plant Ecology and Conservation, Series 5, *Anglogold Ltd.*

Wu FY, Ye ZH, Wu SC, Wong MH (2007) Metal accumulation and arbuscular mycorrhizal status in metallicolous and non-metallicolous populations of *Pteris vittata* L. and *Sedum alfredii* Hance. *Planta* **226**: 1363–1378.

Wu, FY, Ye ZH, Wong MH (2009) Intraspecific differences of arbuscular mycorrhizal fungi in their impacts on arsenic accumulation by *Pteris vittata L*. *Chemosphere* **76**: 1258–1264.

Xavier IJ, and Boyetchko SM (2002) Arbuscular mycorrhizal fungi as biostimulants and bioprotectants of crops, *In*: Khachatourians GG, Arora DK (Eds.), *App. Mycol. And Biotechnol. Agriculture and Food Production*, Elsevier, Amsterdam **2**: 311-330.

Yao Q, Li X, Weidang A Christie P (2003) Bi-directional transfer of phosphorus between red clover and perennial ryegrass via arbuscular mycorrhizal hyphal links. *Eur. J. Soil Biol.* **39**: 47–54.

Yonghwang Ha, Olga G, Tsay, David G Churchill (2011) A tutorial and mini-review of the ICP-MS technique for determinations of transition metal ion and main group element concentration in the neurodegenerative and brain sciences, *Monatsh Chem*. **142**: 385–398.

Young JPW (2012) A molecular guide to the taxonomy of arbuscular mycorrhizal fungi; Commentary; *New Phytol.* **193**: 823–826.

Zak JC, Parkinson D (1982) Initial vesicular-arbuscular mycorrhizal development of the slender wheatgrass on two amended mine soils. *Can. J. Bot*. **60**: 2241–2248.

Zettler LW, Sharma J, Rasmussen F (2004) Mycorrhizal diversity. In: Dixon, K, Cribb, P, Kell, S, Barrett, R, eds. Orchid Conservation. Kota Kinabalu, Sabah, Malaysia: *Natural History Publications*, 185–203.

Zhang Z, Schwartz S, Wagner L, Miller W (2000) A greedy algorithm for aligning DNA sequence. *J. Comput. Biol.* **7**: 203–214.

Zhu YG, Christie P, Laidlaw AS (2001) Uptake of Zn by arbuscular mycorrhizal white clover from Zn-contaminated soil. *Chemospher*, **42**: 193–199.

APPENDICES

Appendix 1 : Elemental Maps presented as HTML.

See it in the attached CD.

Appendix 2: Variance in the concentration of elements in roots from different metal sites.

Table 9.1 below indicates first, for final average in sample sites that five factors accounted for about 92 % of the total variance. The second group for total concentration of elements in roots from different metal sites accounted for about 95% of the total variance. In practice, a robust solution should account for at least 50% of the variance (Tabachnick & Fidell, 2001b).

Table 9.1a Final average in sample sites that five factors accounted for about 92% of the total variance. Total Variance Explained

Component		Initial Eigenvalues			Extraction Sums of Squared Loadings			Rotation Sums of Squared Loadings		
		Total	% of Variance	Cumulative %	Total	% of Variance	Cumulative %	Total	% of Variance	Cumulative %
	1	5.589	34.934	34.934	5.589	34.934	34.934	4.897	30.609	30.609
	2	3.165	19.779	54.714	3.165	19.779	54.714	3.068	19.177	49.786
	3	2.449	15.309	70.022	2.449	15.309	70.022	2.851	17.821	67.607
	4	2.017	12.603	82.626	2.017	12.603	82.626	2.189	13.679	81.285
	5	1.462	9.136	91.761	1.462	9.136	91.761	1.676	10.476	91.761
	6	.986	6.161	97.922						
Dimension0	7	.194	1.210	99.132						
	8	.099	.620	99.752						
	9	.040	.248	100.000						
	1 0	2.995E-16	1.872E-15	100.000						
	1 1	2.140E-16	1.338E-15	100.000						

1	7.277E-17	4.548E-16	100.000						
2									
1	-3.235E-18	-2.022E-17	100.000						
3									
1	-8.665E-17	-5.416E-16	100.000						
4									
1	-1.344E-16	-8.399E-16	100.000						
5									
1	-2.352E-16	-1.470E-15	100.000						
6									

Extraction Method: Principal Component Analysis.

Table 9.1b Total concentration of elements in roots from different metal sites accounted for about **95%** of the total variance.

Total Variance Explained

Component		Initial Eigenvalues			Extraction Sums of Squared Loadings			Rotation Sums of Squared Loadings		
		Total	% of Variance	Cumulative %	Total	% of Variance	Cumulative %	Total	% of Variance	Cumulative %
Dimension0	1	8.117	81.167	81.167	8.117	81.167	81.167	6.932	69.315	69.315
	2	1.395	13.951	95.118	1.395	13.951	95.118	2.580	25.803	95.118
	3	.296	2.964	98.082						
	4	.135	1.350	99.432						
	5	.042	.420	99.852						
	6	.012	.123	99.975						
	7	.002	.022	99.996						
	8	.000	.003	100.000						
	9	1.657E-5	.000	100.000						
	10	5.515E-6	5.515E-5	100.000						

Extraction Method: Principal Component Analysis.

Appendix 3: Limits of detection Table 1-WP-18 Aug 2012 (06 July 13).

See it in the attached CD.

Appendix 4: Nutrient Solution

Table 9.2. Nutrient supplements for pot cultures grown in fertile sandy soil using clover or sorghum as host plants

Compound	**Added to pot (mg/kg soil)**		**Stock solution for sorghum**	
	Cover[1]	**Sorghum[2]**	**(g/L)[3]**	**No.**
KH2PO4	36	36	10.8	A
K2SO4	71	150	45	A
NH4NO3/2weeks		50	15	A
CaCl2.2H2O	94	150	45	**B**
MgSO4.7H2O	20	20	6	C
MnSO4.7H2O	10	10	3	C
ZnSO4.7H2O	5	10	3	C
CuSO4.7H2O	2.1	5	1.5	C
H3BO3	0.8	0.8	0.24	C
CoSO4.7H2O	0.36	0.4	0.12	C
NH4MO7(Na2MoO4.2H2O)	0.18	0.3	0.09	C
Total	**239.44**	**432.5**	**129.75**	

Source: M.C. Brundrett & G. Murase, unpublished data

Notes:

1. P Level adjusted to provide 60% of maximum clover growth, while other nutrients are optimal for a very infertile sandy soil (Gazey *et al.*, 1992). Clover seedlings are inoculated with an appropriate strain of rhizobium so they do not require nitrogen supplements.
2. Based on the nutrition requirements of cereals grown in a very infertile sandy soil (Snowball & Robson 1984). This P level has been adjusted to limit plant growth. While promoting VAM fungus formation and

sporulation. **Fe EDTA (25mg/kg** – Fe EDTA 0.09g/L Stock) may be required for some soils.

3. These nutrients are dissolved in water to form stock solutions (A, B, C) which are further diluted into a nutrient solution (by adding 33 mL of each stock/L final volume). This solution is applied to soil by watering it to field capacity (i.e. add 100 mL solution/kg of dry sand to get 10% water content). The values have to be adjusted for soils with other field capacities. This method of applying fertilizers works very well for sandy soils that have a limited capacity to fix nutrients. For other soils, nutrients may have to be applied in a dry form and mixed through the soil (see section 6.2).

Commercial Multi – nutrient

Dilution of multi- Nutrient Medium for Plants.

About 10 – 20 ml of the multi-nutrient was added to the 100g of soil every week until the control plants were harvested. Conversion of units was done as follows:

P 82g/kg = 0.082g/g
= 82 mg/g
= 82 000 µg/g

5g/2L – weekly
1g/400ml

Change units from ppm = µg/g

82000 = µg/g
205 = µg/g
205 µg/g
0.5g per 2L
Add 10 – 20 ml

Appendix 5: Mthuthu Stats Correction last data analysis (26 Jan 15) final.

See it in the attached CD.

Appendix 6: Analysis of Bemlab results (Total HM Vs Extractable HV & PIXE)

See it in the attached CD.

Appendix 7: The ligation for bacterial transformation (DNA).

A. Transformation of competent *E.coli* cells prepared with TransformAid™ Bacterial Transformation Kit (#K2710)
    1. Prepare LB-ampicillin agar plates (*see* p.11). Pre-warm the plates at 37°C for at least 20 min.
    2. Prepare competent *E.coli* cells as described in the protocol provided with the
    3. TransformAid™ Bacterial Transformation Kit.
    4. Transfer 2.5 µl of the ligation mixture into a new microcentrifuge tube. Chill 2 min on ice.
    5. Add 50 µl of the prepared competent *E.coli* cells. Incubate on ice for 5 min.
    6. Plate immediately on pre-warmed LB-ampicillin agar plates. Incubate overnight at 37°C.

B. P 11

    Reagents

    a. Ampicillin stock solution (50 mg/ml)

    b. Dissolve 2.5 g ampicillin sodium salt in 50 ml of deionized water. Filter sterilize and store in aliquots at 4°C.

    c. LB-ampicillin plates

    d. Prepare LB-agar Medium (1 liter), weigh out:

    e. Bacto Tryptone® 10 g,

    f. Bacto Yeast extract® 5 g,

    g. NaCl 5 g.

h. Dissolve in 800 ml of water, adjust pH to 7.0 with NaOH and adjust the volume with water to 1000 ml. Add 15 g of agar and autoclave.

i. Before pouring LB-ampicillin agar plates, allow the medium to cool to 55°C. Add 2 ml ofampicillin stock solution (50 mg/ml) to a final concentration of 100 μg/ml. Mix gently and pour plates.

j. For fast and easy preparation of LB medium and LB agar plates supplemented with ampicillin, use pre-mixed and pre-sterilized microwaveable FastMedia™ LB Liquid Amp (#M0011)

Appendix 8: Mycorrhiza Manual mounting PVLG.

Making a permanent slide mount for reference or beg registration

a. After extracting spores from a fresh pot culture. Isolate a minimum of 10-20 spores.

b. On two clean microscope slides place one drop each of the mountant PVLG (Polyvinyllactoglycerol) and Melzer's PVLG see annex 2. Transfer half the spores to the first drop of mountant and the second half to the second drop using fine tip forceps (e.g. VOMM forceps No. 999220: HWC 118-10 Hammacher Instruments, P. O. Box 120209, D-42677 Solingen, Germany)

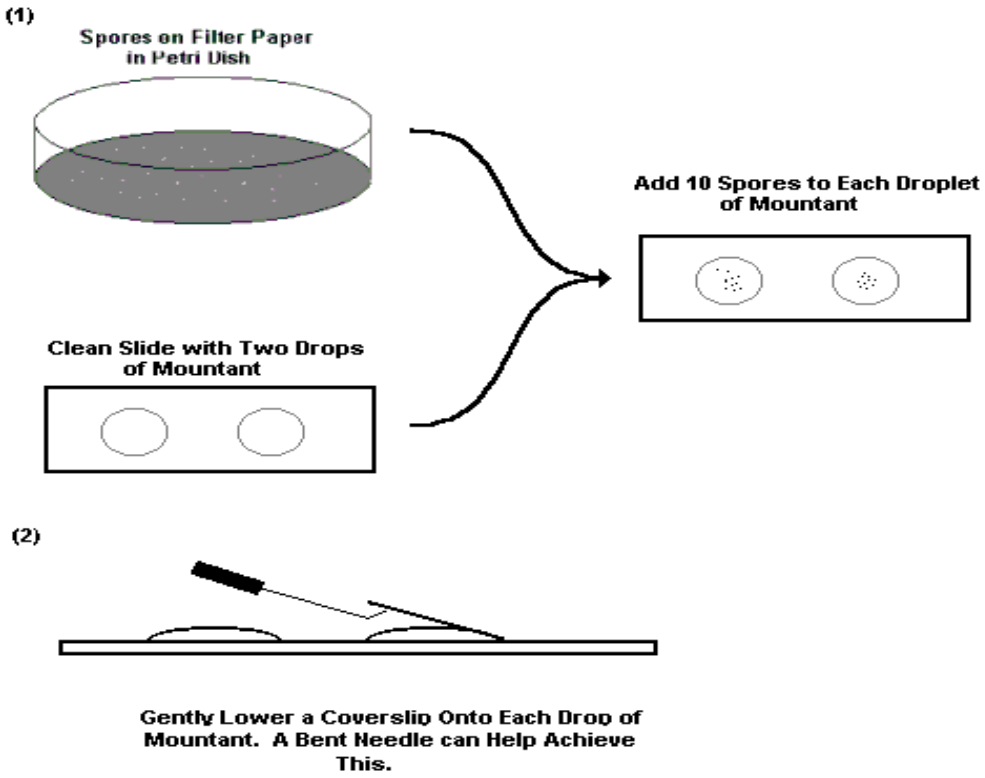

c. Try to orientate the spores so that distinguishing features will be apparent once the coverslip is added.

d. Carefully place a clean coverslip over each drop, making sure to lower the coverslip at an angle to prevent air bubbles being trapped.

e. Gently apply a pressure to the coverslips of one of the slides to break open the spores. Wait 30 seconds and then apply gentle pressure in a circular motion with a soft (B) pencil to break spore walls open further (The pressure will depend on the species of AM fungi). This should be done under a stereomicroscope.

f. If using PVLG, remember to allow the mountant to polymerise and top it up as necessary before sealing with clear nail varnish or white/silver car paint.

g. Label the slide at one end with the species name and reference code, date, your name, and the mountant used.

Annex 2 Reagents

Polyvinyl-Lacto-Glycerol (PVLG)

PVLG is used to permanently mount whole or broken spores on glass slides. For best results, mounted specimens should not be studied for 2-3 days after they were mounted to give time for spore contents to clear. Whole spores will change colour, generally darkening to varying degrees, and shrink or collapse with plasmolysis of spore contents. Discrete layers of the spore wall or flexible inner walls of broken spores will swell to varying degrees and appear fused after long storage in some instances.

Ingredient Quantity
Distilled water 100 ml
Lactic acid 100 ml
Polyvinyl alcohol (PVA) 16.6 g
It is most important to mix all ingredients in a dark bottle BEFORE adding polyvinyl alcohol. The PVA should have the following properties: 50 - 75% hydrolyside, and a viscosity of 20 - 25 centipoise in a 4% aqueous solution at 20 C. The PVA is added as a powder to the other mixed ingredients and then placed in a hot water bath to dissolve (70 - 80 C), which takes between 4-6 hours. PVLG stores well in dark bottles for approximately one year.

Melzer's Reagent
Ingredient Quantity
Chloral hydrate 100 g
Distilled water 100 ml
Iodine 1.5 g
Potassium iodide 5.0 g
Melzer's reagent can be used alone to mount spores and look for diagnostic iodine staining reactions (to hydrophobic regions of structures), but the mounts are temporary and subject to drying out within 1-2 years of storage. For permanence, Melzer's reagent is mixed in equal proportions with PVLG in a separate dark bottle. There is no diminishing of a staining reaction with the 1:1 dilution. However, the reaction will fade (or disappear in lightly staining structures) in prepared slides after a year or longer of storage.

Sodium Azide

Sodium azide is a respiratory inhibitor and therefore should be handled with care (wearing gloves) in the preparation of stock solutions (2.5 g in 50 ml of distilled water). A one ml aliquot of the stock is added to 90 ml of distilled water for a 0.05% working solution. For vial vouchers, spores are collected and added to 2 ml vials in a minimum of water. The vial is then filled with the sodium azide working solution and labelled. Solutions and vials are stored at 4 C as an added precaution to optimise safety of the workplace.

Spores will darken and contents become cloudy after long term storage, but subcellular structural properties retain their integrity to a great extent. Other preservative solutions such as FAA (Formalin + Acetic Acid + Alcohol) and lactophenol (lactic acid + phenol) have been used extensively in the past, but evidence from type specimens indicates they can cause major changes or degradation of subcellular structure of spores.

Appendix 9: Table 9.3, ICP-MS analysis performed on root samples for bulk elemental concentration.

Table 9.3 ICP-MS analysis performed on root samples for bulk elemental concentration. Values are the means of 3 technical replicates ± SD. Results for site 3, 4 and 6 could not be obtained because the root sample mass was less than the required amount for ICP-MS analysis.

Sites		Concentrations of elements (mg kg^{-1})										
		Cr	**Fe**	**Ni**	**P**	**K**	**Pt**	**Ti**	**Mn**	**Cu**	**Zn**	**U**
Site 1	**NW (L)**	26.1 ± 1.7	850.0 ± 0.9	30.7 ± 1.6	1685.0 ± 0.4	3750.0 ± 0.5	nd	28.8 ± 2.9	57.9 ± 0.4	57.4 ± 1.7	55.8 ± 1.8	nd
Site 2	**AGM**	69.1 ±2.5	2450.0 ± 0.5	87.2 ± 1.0	1710.0 ± 0.7	3490.0 ± 1.5	nd	55.5 ± 6.8	79.9 ± 4.9	15.9 ± 3.9	59.4 ± 1.3	nd
Site 5	**WW**	22.1 ±1.4	1640.0 ± 0.9	19.6 ± 1.3	1920.0 ± 0.9	4770.0 ± 1.7	nd	50.9 ± 3.4	129 ± 2.9	35.7 ± 1.2	105.9 ± 1.5	nd
Site 7	**ER2 D, MP**	21.7 ± 1.2	1900.0 ± 1.6	21.3 ± 1.6	2130.0 ± 3.1	5700.0 ± 1.9	nd	110.1 ± 6.8	85.8 ± 1.9	22.8 ± 1.0	140.7 ± 0.2	nd
Site 8	**VRM**	15.2 ± 2.2	835.0 ± 0.5	14.5 ± 1.8	1840.0 ± 0.3	3995.0 ± 1.8	nd	30.4 ± 5.0	109.7 ± 0.2	14.7 ± 2.5	66.9 ± 2.7	nd
Control 1	**CTRL 1 & Nu**	14.8 ± 1.1	490.0 ± 0.4	11.1 ± 1.5	1705.0 ± 0.2	3170.0 ± 1.3	nd	40.1 ± 1.3	94.5 ± 0.3	32.9 ± 1.8	78.4 ± 1.5	nd
Control 2	**CTRL 2 & Myco**	22.2 ± 0.9	510.0 ± 0.5	13.2 ± 0.2	1950.0 ± 0.8	6020.0 ± 0.5	nd	43.5 ± 2.8	192.9 ± 2.1	82.1 ± 0.7	146.6 ± 2.3	nd

- **nd** : Not detected

Appendix 10: Communalities.

Table 9.4 (b) Displays communalities indicating the degree to which each variable

Communalities

	Initial	***Extraction***
Al	*1.000*	*.970*
Si	*1.000*	*.990*
P	*1.000*	*.968*
S	*1.000*	*.985*
Cl	*1.000*	*.907*
K	*1.000*	*.971*
Ca	*1.000*	*.918*
Ti	*1.000*	*.990*
V	*1.000*	*.930*
Cr	*1.000*	*.890*
Mn	*1.000*	*.980*
Fe	*1.000*	*.980*
Ni	*1.000*	*.975*
Cu	*1.000*	*.751*
Zn	*1.000*	*.984*
Br	*1.000*	*.493*

Extraction Method: Principal Component Analysis.

Communalities

	Initial	***Extraction***
Gauteng WW (West Wits) Au+ U	*1.000*	*.980*
North West**,** Vaal reefs (VRS),	*1.000*	*.983*
North West, Vaal reefs (VRM)	*1.000*	*.974*
North West Lonmin Platinum Mine (L)	*1.000*	*.967*
East Rand, Metallurgical plant (ER2D MP)	*1.000*	*.958*
East Rand, Brakpan (ER1),	*1.000*	*.846*
East Rand, Metallurgical plant (MP)(ER2A)	*1.000*	*.973*
Agnes Serpentine Mine (AGM), Mpumalanga (AGM)	*1.000*	*.994*
Grown in Zeolite Ctr + MyCo 8 R1 (Control 2)	*1.000*	*.857*
Grown in Zeolite Ctr + NuR2 (Control 1)	*1.000*	*.980*

Extraction Method: Principal Component Analysis.

Appendix 11: Correlation in part 1, The total concentration of elements in roots from different metals sites.

Correlation in part 1: The total concentration of elements in roots from different metal sites

The mechanisms of tolerance to metals associations between total elements in roots from different metals could be seen related to concentrations of biogenic metals (Substances produced by living organisms or biological processes). It can also be defined as substances necessary for the maintenance of life processes such as trace elements in plants as presented in Table 9.5 below. The highest correlation could be attributed to the highest concentration of the elements which were detected in almost all the sites. A good example of metal association is demonstrated by the following elements namely, iron (Fe), manganese (Mn), Vanadium (V), and Zinc (Zn). There is a strong correlation between, Fe and Al (R= 0.94), Fe and Ti (R = 0.95), Fe and V (R = 0.77) and Fe and Mn (R = 0.72) (Table 9.5). The effects of certain metals are seen pinpointing certain circumstances where particular elements were concentrated at higher levels when correlated with other elements. Iron (Fe), showed a strong relationship or correlation with aluminium (Al), Ti, V and Mn. This indicates that high proportions of detrital bonds (loose fragments or grains that have been worn away from the rock) are assumed. Correlation relationships for Fe and Ti showed very high correlation coefficients (R,) of 0.95 for concentration in plants.

There is also a strong correlation between, the following elements, Cl and P (R= 0.80), K and P (R = 0.86), K and Cl (R = 0.68), Ca and S (R = 0.57); Ti and Al (R = 0.92); V and Al (R= 0.72); V and Ca (R = 0.69); V = Ti (R =0.87); Mn and Al (R =0.75), Mn and Ca (R = 0.68) Mn and Ti (R = 0.84); Mn and V (R = 0.94); Ni and Cr (R= 0.83); Cu and P (R = 0.67); Cu and K (R = 56) lastly, Zn and S (R = 0.53), Zn and Ca (R = 0.83), Zn and V (R = 0.54) and Zn and Mn (R = 0.52) (Table 9.5).

Table 9.5. Shows the correlation matrix of element association between elements examined in roots from different metal sites.

	Al	Si	P	S	Cl	K	Ca	Ti	V	Cr	Mn	Fe	Ni	Cu	Zn
Al	1.00														
Si		1.00													
P			1.00												
S	-0.51			1.00											
Cl		-0.52	0.80		1.00										
K			0.86		0.68	1.00									
Ca				0.57			1.00								
Ti	0.92							1.00							
V	0.72						0.69	0.87	1.00						
Cr										1.00					
Mn	0.75						0.68	0.84	0.94		1.00				
Fe	0.94							0.95	0.77		0.72	1.00			
Ni										0.83			1.00		
Cu			0.67			0.56								1.00	
Zn				0.53			0.83		0.54		0.52				1.00

This matrix is not positive definite.

LIST OF PUBLICATIONS AND CONFERENCE PRESENTATIONS

Publications to be submitted

1. Zamxaka M, Straker CJ, Weiersbye IM (2016) Spore morphological identification and diversity of arbuscular mycorrhizal fungi (AM fungi) in different South African contaminated mining sites.
2. Zamxaka M, Straker CJ (2016) The application of nested PCR to identify arbuscular mycorrhzal (AM) fungi from spores isolated from heavy metal contaminated mining sites, in South Africa.
3. Zamxaka M, Straker CJ, Weiersbye IM (2016) The application of micro-pixe in analysing the mechanisms of tolerance to metals and metalloids in arbuscular mycorrhizas.

Conference/Seminar presentations and posters

1. Zamxaka M, Straker CJ (2009) Comparison of AM fungal diversity in selected high heavy metal sites in South Africa particularly North West and Johannesburg gold mining slime dams, The 46th congress of the Southern African Society for Plant Pathology (SASPP) held at Villa Via Hotel, Gordon's Bay, Cape Town, South Africa from the 25th to the 28th of January 2009. Poster.

2. Zamxaka M: Scientific research collaboration at Elettra Synchrotron, Trieste, Italy from 26 November 2011 to 10 January 2012. This collaboration seeks to create a pool of Mentor-Mentee relationship between the two countries.

3. Zamxaka M: participated in an International BioCamp, which took place at Novartis Institute for Biomedical Research in Cambridge, Boston (Massachusetts) in 26-31 Oct 09.

4. Zamxaka M: Participated in Italian-Mediterranean Conference for the Development of Economic Cooperation that show-cased the new developments in both biotechnology and nanotechnology fields in Rome, on 27 - 29 May 2010.

5. Zamxaka M (2010) Metal accumulation in arbuscular mycorrhizal (AM) fungi and their role in phytoremediation of mine tailings, Materials Research Department, iThemba LABS, Cape Town, South Africa biennial Users Meeting on the 3rd of September 2010. Oral presentation.

6. Zamxaka M (2008) Mine closure, proceedings of the Third International Seminar on Mine Closure 14 -17 October 2008, Johannesburg, South Africa, Conference.

7. Zamxaka M, Przybylowicz WJ, Jan Pallon, Sechogela P (2010) performing parallel PIXE measurements on AM fungal root specimens and data processing in Lund University (Sweden) on the 31 July to 08 August 2010. Collaboration visit.